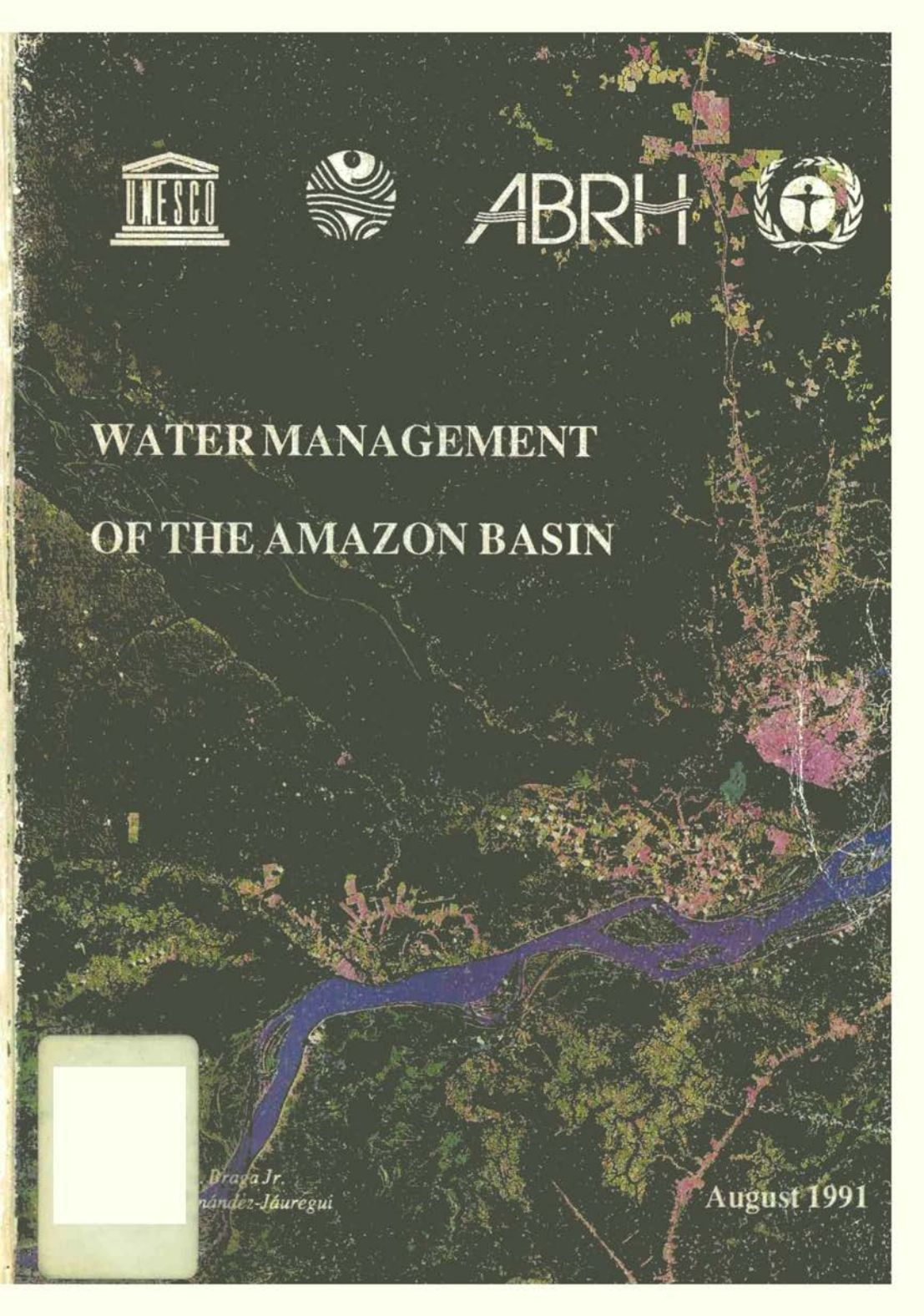

WATER MANAGEMENT OF THE AMAZON BASIN

Braga Jr.
nández-Jáuregui

August 1991

WATER MANAGEMENT

OF THE AMAZON BASIN

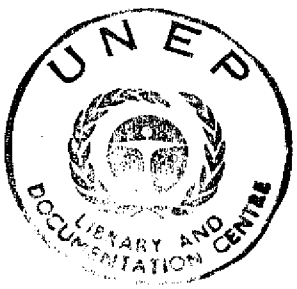

Edited by
Benedito P. F. Braga Jr.
Carlos A. Fernández-Jáuregui

August 1991

Edited by: Benedito P. F. Braga Jr. -
Carlos A. Fernández-Jáuregui

Text revision: Angélica Obes de Lussich
Entry of information in micro-computer
and layout: Silvia Diez de Garicoïts
Preparation of masters: Jorge Pérez
Printing: Andrés Barreiro

Published and printed in 1991 at the UNESCO Regional Office for Science and Technology for Latin America and the Caribbean - ROSTLAC - Montevideo - Uruguay

ISBN 92-9089-017-7

Cover:
Satellite image transmitted by Landsat received and processed by the Instituto Nacional de Pesquisas Espaciais (INPE). Image obtained by Landsat 5 TM (Thematic Mapper) sensor with around 30 m spatial resolution. Photograph of the Amazon region showing the Negro and Amazon rivers, Manaus, the confluence of both rivers near Manaus and the forest.

PREFACE

The International Seminar on Hydrology and Water Management of the Amazon Basin was held in Manaus, Brazil from 5 to 9 August 1990, under the sponsoring of the International Water Resources Association (IWRA), the Brazilian Water Resources Association (ABRH), UNESCO, UNEP and other national and international organizations related to hydrology and water resources.

After the meeting an assessment of the different papers presented and discussed in Manaus was carried out by the president of the ABRH and the UNESCO regional hydrologist, upon which it was decided that in addition to the publication of all the papers distributed during the seminar a book would be edited containing the papers of scientific relevance which warranted inclusion in a bibliography for future activities in the framework of the UNESCO Humid Tropics programme.

The Editors wish to thank FINEP for their sponsoring of the Brazilian authors and to all national and international institutions which facilitated research work and preparation of the papers presented by scientists from each participating country. Last but not least our thanks go to the UNESCO secretarial and publications team for their painstaking work and for all the suggestions received during the preparation of this book.

The Editors

CONTENTS

ANALYSIS OF ANNUAL MAXIMUM PRECIPITATION SERIES FOR XINGU AND TAPAJOS BASINS USING PROBABILITY WEIGHTED MOMENTS

Fernanda Da Serra Costa and Jorge Machado Damázio *

ABSTRACT

This paper analyzes annual maximum precipitation series for the Xingu and Tapajos basins located both in the Amazon basin. The analysis has the objective of indicating a probability distribution function that can be used in design flood calculations for spillways of large dams in the region. Due to the short length of the records in the region and the robustness of the estimates of population descriptors (ex: variation and skewness coefficients) based on probability weighted moments, this approach is adopted as the main methodology.

1. INTRODUCTION

Streamflow and precipitation extreme frequency analysis are very important parts of the design of hydraulic structures like spillways. In the Amazon region these studies face low gauge densities and short records lengths. In this situation the hydrologist should not only use information spatial transfer techniques, [1] and [2], but also use estimators that are less sensitive to sampling errors.

In this paper, the results of a frequency analysis of annual maximum precipitation series of the Tapajos and Xingu basins are presented. The study aimed at the choice of the probability model to use in 10000-year precipitation calculations for the design of spillways for hydroelectric dams located in these basins. The two basins will be considered as one homogeneous region for the sake of the analysis of the occurrence of extreme precipitation. In order to minimize sampling errors problems, the probability weighted moments theory was used.

2. PRELIMINARY DATA ANALYSIS

Data of 86 raingauges from the Xingu and Tapajos basins were available. The beginning of the records for the majority of the raingauges was 1970. In general, the records were available up to 1987.

* *Electrical Power Research Center - CEPEL - P. O. Box 2754 - CEP 20001 - Rio de Janeiro, Brazil*

Calculation of the Annual Maximum Series - First, all the data of years which presented missing values were eliminated. For each of the remaining years (449 years) annual maximum values for eight durations (1, 2, 3, 5, 10, 15, 30, 60 days) were calculated and the month of the begining of the maximum identified. Table 1 shows the frequency of beginning of maximum for each month and duration where it can be noted that for any duration more than 92% of the years had beginning of its maximum between October and April. Accordingly, it was decided to use a hydrological year starting in October and not to consider the data between May and September. Data of gauges with less than four hydrological years were abandoned. After all this, the number of raingauges dropped to 55 (yielding a station-density of 1 station for 18000 km^2). Figure 1 shows location of these gauges. For each duration, it was obtained 403 hydrological years, yielding a mean record length of 7,33 "years".

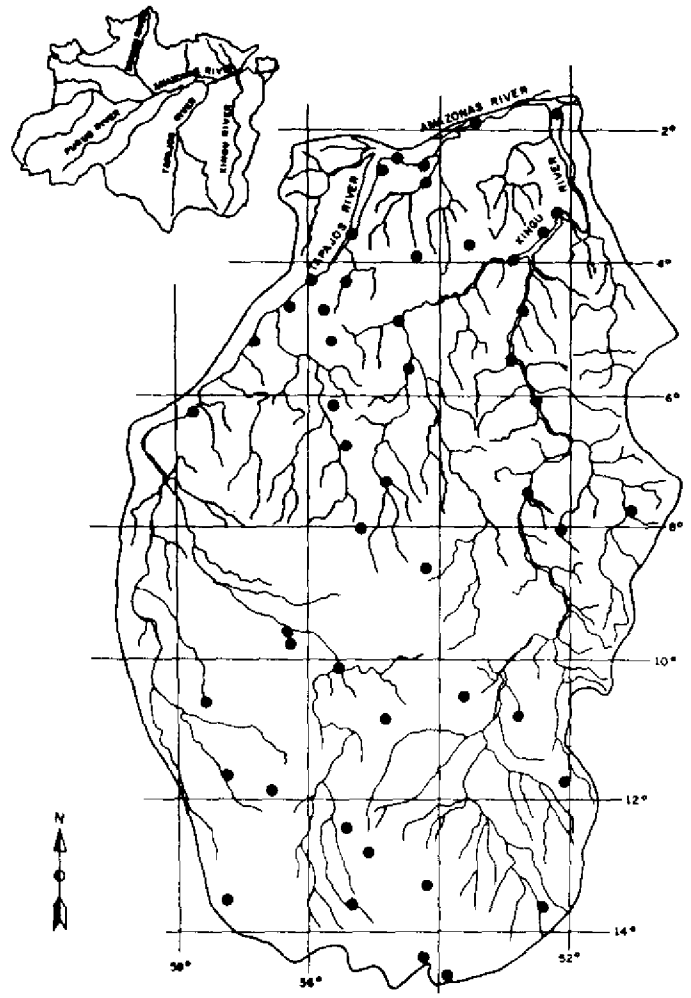

Figure 1 - Raingauge localization

Table 1 - Begining of annual maximum frequency

DURATION (Days)	MONTH											
	JAN	FEB	MAR	APR	MAY	JUN	JUL	AUG	SEP	OCT	NOV	DEC
1	0.15	0.15	0.20	0.12	0.03	0.01	0.01	0.01	0.03	0.08	0.10	0.13
2	0.17	0.20	0.19	0.12	0.03	0.00	0.00	0.01	0.01	0.06	0.09	0.12
3	0.17	0.20	0.02	0.10	0.03	0.00	0.01	0.01	0.01	0.07	0.07	0.13
5	0.22	0.22	0.17	0.11	0.03	0.00	0.01	0.00	0.01	0.05	0.07	0.11
10	0.27	0.21	0.15	0.11	0.03	0.00	0.00	0.01	0.01	0.04	0.06	0.11
15	0.27	0.25	0.16	0.11	0.02	0.00	0.00	0.01	0.01	0.05	0.05	0.09
30	0.38	0.23	0.14	0.09	0.01	0.00	0.00	0.00	0.01	0.04	0.08	0.03
60	0.53	0.18	0.11	0.02	0.00	0.00	0.00	0.01	0.02	0.09	0.05	0.00

Stationarity Tests - The check of stationarity of these annual maximum series was verified before the frequency studies. Each series was split in two which frequency curves were compared using Smirnov test. The significance levels of 1%, 5% and 10% werre used. Table 2 presents for each duration the number of rejections for each significance level, and between brackets the probability of having this number of rejections or more under the hypothesis of stationarity and mutual independence. It can be concluded, for all the durations, that the set of series is stationary.

Table 2 - Number of rejections for each duration and significance level

	DURATION (days)							
Signf. Level	1	2	3	5	10	15	30	60
1%	0 (100)	0 (100)	0 (100)	0 (100)	0 (100)	0 (100)	0 (100)	0 (100)
5%	0 (100)	1 (94.3)	1 (94.3)	2 (77.7)	1 (94.3)	0 (100)	0 (100)	0 (100)
10%	0 (100)	2 (98.0)	3 (92.8)	6 (49.3)	5 (67.1)	6 (49.3)	1 (99.7)	3 (92.8)

3. FREQUENCY ANALYSIS

In this study the region shown in figure 1, Tapajos and Xingu basins, was considered as one homgeneous region in terms of extreme precipitation frequencies. On the other hand, the variability of the mean values of the extremes distributions is recognized, not only because of the duration, but also because of local conditions variations as latitude and altitude.

The above considerations imply for each duration the homogeneity of the dimensionless maximum precipitation, that is the maximum values divided by the mean probability distributions. This permits the joint use of all the records in the region in order to infer dimensionless coefficients valid for all the region. This type of study traditionally uses conventional variation, skewness and kurtosis coefficients, [3]. Nevertheless the estimation of skewness and kurtosis with extreme short length records as those available for this study, is susceptible to great errors. In order to minimize this problem L-Coefficients derived from the Probability Weighted Moments Theory were used [4]. The main advantages of using L-Coefficients instead of conventional ones is that its estimations are more robust and less sensitive to ocurrences.

PWM, L-Moments and L-Coefficients - Let Z be a random variable with cdf given by F(z). The PWM of Z are defined by [5]:

$$M_{p,r,s} = E\{z^p\{F_{(z)}\}^r\{1-F_{(z)}\}^s\} \qquad (1)$$

where p, r and s are real values.

The conventional moments, $E[z^p]$, are obtained by (1) making p=1,2,... and r and s always equal to zero. The complete set of conventional moments totally describe F(z), the use of the first three or four moments being natural to describe the main characteristics.

Another possibility is to work with p=1, s=0 and r=0,1,... to obtain:

$$B_r = M_{1,r,s} = E[\, z\, \{F(z)\}^r\,] \tag{2}$$

Just as with the conventional moments, the complete set B_r, r=0,1,2,... totally describes F(z) and the first three or four values can be used to describe the main characteristics. Note that $B_0 = E[z]$. Just as the description of characteristics like locations, scale and form of F(z) is better done by using combinations of the $E[z^p]$ so that central moments are obtained, there are B_r combinations which are similar with the advantage of being linear. These combinations, called L-Moments are defined in [4] by;

$$L_{r+1} = \sum_{K=0}^{r} p_{r.k}\, B_k,\ r = 0,1,... \tag{3}$$

where:

$$P_{r.k} = (-1)^{r-k} \binom{r}{k} \binom{r+k}{k} \tag{4}$$

In particular we have:

$$L_1 = B_0 \tag{5}$$

$$L_2 = 2B_1 - B_0 \tag{6}$$

$$L_3 = 6B_2 - 6B_1 + B_0 \tag{7}$$

$$L_4 = 20B_3 - 30B_2 + 12B_1 - B_0 \tag{8}$$

From (5), $L_1 = E[z]$. [4] showed that L_2 is a measure of scale similar to the standard deviation and the L-Coefficient of variation is defined by:

$$\text{L-CV} = L_2 / L_1 \tag{9}$$

[4] showed that L_3 is a measure of skewness and L_4 of kurtosis. Dividing L_3 and L_4 by L_2 we obtain the L-Coefficients:

$$\text{L-SKEW} = L_3 / L_2 \tag{10}$$

$$\text{L-KUR} = L_4 / L_2 \tag{11}$$

The coefficient L-SKEW can only assume values between -1 and 1 and for symmetric distributions it is zero. Coefficient L-KUR assumes values between -0,25 and 1, and for the uniform distribution it is zero.

L-Coefficients Calculation - For each of the maximum annual series the PWM B_r, r=0,1,2,3 were estimated using [4]:

$$B_r = n^{-1} \sum_{i=1}^{n} \binom{i-1}{r} Z_i / \binom{n-1}{r} \tag{12}$$

where n is the length of the series and z_i, i=1,...,n are the ordered series values ($z_i \leq z_{i+1}$). The third order PWM was calculated only for series of more than four values. The L-Moments, L_1,L_2,L_3 and L_4 were estimated by substituting B_r in (5) to (8) by its estimatives. These estimates were standardized by dividing by L_1. Then, for each duration regional values for L_2, L_3 and L_4 were obtained by:

$$L_r \text{ regional} = \frac{\sum_{k=1}^{55} n_k L_r^k}{\sum_{k=1}^{55} n_k} \quad r = 2,3,4,- \tag{13}$$

where n_k is the record length of the series k.

Table 3a and 3b show the obtained regional L-Moments and their corresponding L-Coefficients. These tables also show between brackets minimum and maximum local estimates. In part, the found variability can be explained by the short length of the records and by the possible heterogenity in the region.

Table 3a - Region L-Moments for annual maximum precipitation in Xingu and Tapajos basins

DURATION (Days)			
1	2	3	5
	L_1		
(0.1661 -0.0562;0.4936)	0.1574 (-0.0842;0.4545)	0.1502 (-0.0415;0.3889)	0.1442 (-0.0743;0.3648)
	L_3		
0.0305 (-0.0664;0.1986)	0.0215 (-0.0985;0.1136)	0.0222 (-0.0693;0.1055)	0.0162 (-0.0943;0.1054)
	L_4		
0.0233 (-0.1145;0.1785)	0.0224 (-0.1026;0.1434)	0.0234 (-0.0343;0.1568)	0.0269 (-0.0308;0.1386)
	L-CV		
0.1661 (-0.0562;0.4936)	0.1574 (0.0842;0.4545)	0.1502 (0.0415;0.3889)	0.1442 (0.0743;0.3648)
	L-SKEW		
0.1835 (-0.4754;0.6113)	0.1367 (-0.5909;0.5478)	0.1476 (-0.4161;0.6508)	0.1123 (-0.2766;0.6863)
	L-KUR		
0.1404 (-0.4807;0.6649)	0.1425 (-0.5138;0.6957)	0.1558 (-0.3068;0.7670)	0.1864 (-0.3740;0.9020)

In order to verify the second hypothesis it was investigated if there is a relationship between latitude and local L-Coefficients values by grouping the stations in classes of 2° latitudes and in less or more than the regional value. Table 4 presents for each coefficient and duration the obtained test statistics. There was no rejection at the 5% level indicating homogenity.

Table 3b - Region L-Moments for annual maximum precipitation in Xingu and Tapajos basins

DURATION (Days)			
10	15	30	60
	L_2		
0.1437 (-0.0301;0.3766)	0.1446 (-0.0444;0.3433)	0.1429 (-0.0164;0.3462)	0.1450 (-0.6638;0.3333)
	L_3		
0.0167 (-0.1948;0.0957)	0.0182 (-0.2239;0.1158)	0.0123 (-0.1923;0.0886)	0.0089 (-0.2432;0.0880)
	L_4		
0.0241 (-0.0549;0.1167)	0.0293 (-0.0313;0.1250)	0.0244 (-0.0430;0.1765)	0.0164 (-0.0678;0.2182)
	L-CV		
0.1437 (-0.0301;0.3766)	0.1446 (0.0444;0.3433)	0.1429 (0.0164;0.3462)	0.1450 (0.0638;0.3333)
	L-SKEW		
0.1162 (-0.5172;0.6078)	0.1255 (-0.4540;0.6774)	0.8586 (-0.5556;0.5185)	0.0614 (-0.7297;1.000)
	L-KUR		
0.1679 (-0.4474;0.8485)	0.2025 (-0.2903;0.8387)	0.1710 (-0.2553;0.7059)	0.1129 (-0.3529;0.8276)

Table 4 - Statistics of the contingency test for independence between latitude and L-Coefficients

	DURATION (Days)							
L-COEF	1	2	3	5	10	15	30	60
L-CV	5.82	6.62	3.78	3.46	1.05	3.19	8.01	2.69
L-SKEW	5.60	3.78	3.10	4.35	1.55	6.04	1.54	7.51
L-KUR	8.86	1.32	2.58	1.91	4.01	5.24	5.68	6.71

Regional Distribution - For each duration a general extreme value distribution defined by (14) was fitted using the L-Moments in tables 3a and 3b.

$$F_z(z) = \begin{cases} \exp\{-[1-k((z-e)/a)]^{1/k}\} & ,k \neq 0 \\ \exp\{-\exp[-((z-e)/a)]\} & ,k = 0 \end{cases}$$

$a > 0$ e

$e + a/k < z < \infty$ se $k < 0$

$-\infty < z < e + a/k$ se $k > 0$

$-\infty < z < \infty$ se $k = 0$

The used estimation equations were:

$$k = 7.8590\,c + 2.9554\,c^2 \tag{15}$$

$$a = \frac{KL_2}{\Gamma(1+k)(1-2)^{-k}} \tag{16}$$

$$e = L_1 + \frac{a}{k}\left[\Gamma(1+\kappa) - 1\right] \tag{17}$$

where:

$$c = \frac{2L_2}{L_3 + 3L_2} - \frac{Ln(2)}{Ln(3)} \tag{18}$$

Table 5 presents the obtained parameters and coefficients of variation and skewness. A Kolmogorov-Smirnov test was done with all the series assuming as null hypothesis the regional distribution. This hypothesis was never rejected for the 10% level, indicating the homogenity in the region.

Table 5 - GEV parameters and coefficients

	DURATION (Days)							
PARAMETERS								
a	0.235	0.238	0.224	0.225	0.223	0.222	0.231	0.240
k	-0.021	0.053	0.035	0.092	0.086	0.071	0.136	0.177
e	0.859	0.875	0.878	0.889	0.889	0.887	0.895	0.898
CV	0.310	0.290	0.270	0.260	0.260	0.260	0.260	0.260
SKEW	1.310	0.840	0.920	0.670	0.700	0.760	0.490	0.330

4. CONCLUSIONS

The results of a frequency analysis for annual maximum precipitation series of Xingu and Tapajos basins are presented. Records of 86 raingauges were available, but because missing values and record lengths of less than four years it was only possible to analyze data from 55 raingauges. The mean record length for these 55 raingauges was 7,33 "years". It was proved that these series are stationary. In spite of the great span of latitude the set of series could be considered as homogeneous based on tests of correlation between L-Coefficients and latitude and on regional dimensionless distribution tests.

Finally, the obtained regional skewness indicated a decreasing tendency with the duration, starting from 1.31 for the daily duration. According to the robust tests made in CEPEL [7], these values of skewness indicate the use of the Gumbel distribution to calculate the 10000-year precipitation.

5. REFERENCES

[1] Madeira, E. F.; Ferreira, L. C.; Lafore, D. P.; Maranhão, N Considerações sobre a Metodologia Adotada nos Estudos Hidrologicos da Bacia do Tapajos, VIII Simposio Brasileiro de Recursos Hídricos, Foz de Iguaçu,1989 (In Portuguese).

[2] Barbosa, C. S.; Moreira, J. O. S.; Pfastetter, O.; Coimbra, A. R.; Araújo, A. L.; Café, F. ; Lopes, M. L. Avaliação da Vazão de Projeto de um Vertedor de Grande Porte com Carência de Dados - Caso do Rio Trombetas. VIII Simposio Brasileiro de Recursos Hídricos, Foz do Iguaçu, 1989 (In Portuguese).

[3] Natural Environmental Research Council, Flood Studies Report, London, 1975 .

[4] Hosking, J. R. M. The Theory of Probability Weighted Moments, Research Report RC 12210, IBM Research, Yorktown Heights, New York, 1986.

[5] Greenwood, J. A.; Landwehr, J. M.; Matalas, N. C.; Wallis, J. R. Probability Weighted Moments: Definition and Relation to Parameters of Several Distributions Expressable in Inverse Form, Water Resources Research, 15, 1049-1054, 1979.

[6] Mood, M. A.; Graybill, F. A.; Boes, D. C. Introduction to the Theory of Statistics, McGraw Hill, New York, 1963.

[7] Damázio, J. M. Estimação Robusta de Vazões Milenares, Relatorio Técnico CEPEL N° 002/84 - CEPEL, Rio de Janeiro,1984 (In Portuguese).

AN ION BUDGET FOR A "TERRA FIRME" RAINFOREST IN CENTRAL AMAZONIA

M. Cristina Forti*
Lycia M. Moreira-Nordemann**

ABSTRACT

This work discusses the ion budget for a "terra firme" rainforest ecosystem in Central Amazonia, during two periods of contrasting rainfall. The samples (rainwater, throughfall, litter solution, soil solution and river water), were collected during April-May and August-September 1987, at Reserva Ducke (2°57'S, 59°58'W), near Manaus. The budget indicates that the ionic species (Na^+, K^+, Mg^{2+}, NH^+_4, Cl^- and SO^{2-}_4) are found mainly in the portions of the hydrological cycles which cross the aerial phytomass and percolate throughout the root zone, showing the existence of a closed mineral cycle.

INTRODUCTION

In an ecosystem the cycling of nutrients as well as the processes through which they are lost/ retained are important mechanisms to analyze and understand their behavior. Integrated studies on cycling and budget of nutrients in small hydrographic basins in the Brazilian Amazonia are few [1, 2, 3]. These information are necessary to orient preservation or agricultural exploitation in those areas.

It is presented an estimation of ion budget for Na^+, K^+, Mg^{2+}, Ca^{2+}, NH^+_4, Cl^- and SO^{2-}_4 that are present in the hydrological part of the nutrients cycle during a wet and a dry season. The samples were collected at Reserva Ducke (2°57'S, 59°58'W) during April-May and August-September 1987. For that purpose, samples of rainwater, throughfall, soil solution (20 cm and 2 m deep), litter solution and river water at Barro Branco Igarapé were collected (Figure 1).

* *Assistant Researcher - Instituto de Pesquisas Espaciais (INPE) - C.P. 515 -12201 São José dos Campos, SP, Brazil*

** *Senior Researcher - Instituto de Pesquisas Espaciais (INPE) - C.P. 515 -12201 São José dos Campos, SP, Brazil*

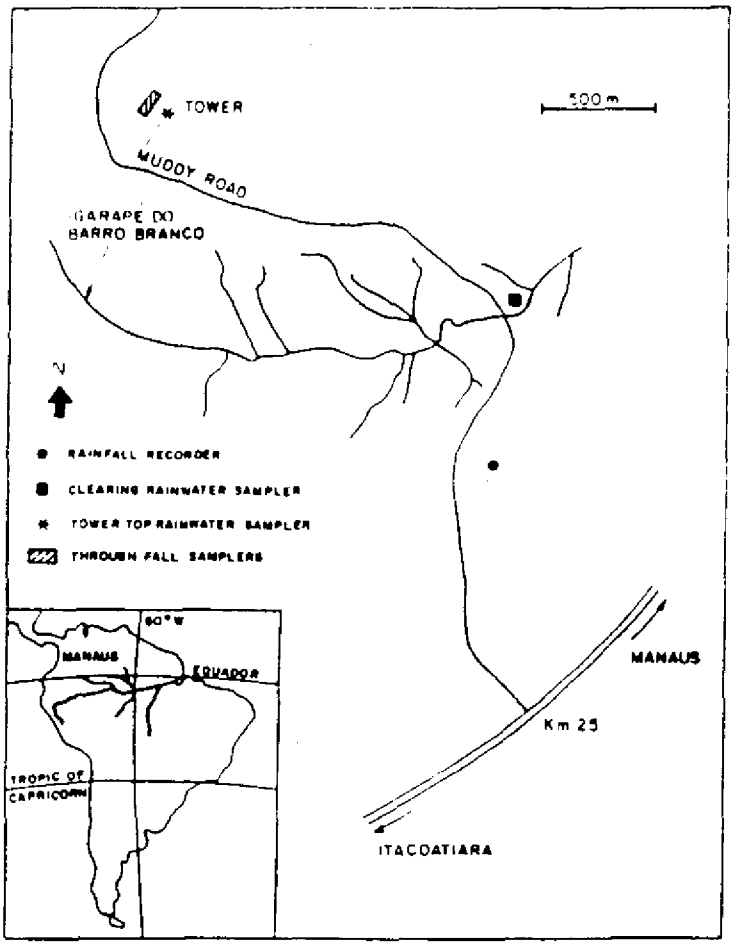

Figure 1 - Map showing the Reserva Ducke area and sampling places

The cations Na^+, K^+, Mg^{2+} and Ca^{2+} were analyzed by atomic absorption spectroscopy, NH^+_4 by potenciometry and the anions (Cl^- e SO^{2-}_4) by ion liquid chromatography [4].

RESULTS AND DISCUSSION

The amount of transferred ions in hydrological cycle was obtained from the elemental concentration [4] and from the measured or estimated volumes. The rainfall and the river discharge were measured. The amount of percolated water in soil was estimated, based on the humidity profile

[5]. It was considered that all precipitated water percolated the first 20 cm of soil, and that at 2 m deep the volume were 40% of the total incoming. The litter solution was obtained by washing the litter with deionized water and the total amount (kg/ha) was estimated from literature [6]. The throughfall ion budgets are expressed in gross content (Table 1).

In the soil ion budget, the salution's residence time, lateral fluxes and mixture with resident waters were not considered. Golley et al [7] estimated a period of 8 hours for residence time of the water from the litter solution layer. Leopoldo et al [8] pointed out that even though there was no mixture with resident waters in the first 30 cm of soil, around 1 m the mixture spent up to 3 weeks to be completed. According to Vitousek [9], in flat regions with forest cover the water flow in the root region is mostly vertical. Therefore, the estimated amount of water that percolates through litter layer and the first 20 cm of soil, must be close to true value. However, as the soils are deeper [10], the determined amount of ions in the soil solution, gives only an indication of ions retention throughout the soil profile.

It is noted that the ion budget presents significant differences between the two periods. During the rain period, a larger ionic deposition occurs due to high rainfall totals. The water flow through the ecosystem is larger too, what makes the leaching more efficient. These two factors are responsible for the larger amount of ions in the wet period.

The throughfall ion budget shows the importance, related to rainwater, of the species transference from the vegetation cover to the soil. It is noted that the nutrients which return to the soil, via throughfall, in the two periods are given by: 90% K^+ and Mg^{2+}, 70% for Na^+, between 60% and 70% for Ca^{2+}, between 25% and 40% for Cl^- and 40% for SO^{2}_{4}. Around 50% of NH^{+}_{4} returns via throughfall during the wet period; during the dry period this ion seems to be absorbed.

The litter solution and the soil solution (20 cm) are responsible for the major amount of ions. It is through the litter solution that happens the main process of nutrients transference from the vegetation to the ground [11]. The soil solution from 20 cm has larger amounts of ions than that found in the others analyzed sections of the hydrological cycle; this variation can be attributed to the decomposition and leaching of the litter, which is more effective during the wet period. It is observed that the amount of ion species in the soil solution, from 2 m deep, is smaller than that found in the first 20 cm of soil, what shows clearly that the species were absorbed/retained in the soil superior zone. Around 80% of the vegetation radicular system are on the soil's first 40 cm [3].

The outputs via Igarapé are smaller than the inputs through rainwater, which means that the system must retain the ions. However, the amounts of elements found either in the rainwater or in the Igarapé water are an order of magnitude smaller than those found in the internal sections of the hydrological cycle. This behavior indicates that the ionic balance for this ecosystem is less important than its internal cycling.

CONCLUSIONS

The variation pattern of the ion species in the different sections of the hydrological cycle shows that there exists a storage of these ions during the wet period. Probably this nutrient surplus is important for the ecosystem maintenance during the periods with lower rainfall. It is possible to conclude that there exists a short period recycling of nutrients that accompanies the annual variation of the hydrological cycle.

Table 1

Elements budget in the different segments of the hydrological cycle in kg/hax10^{-2}. The values in boldface are normalized for rainwater.

Rainwater (C) Throughfall (T) Litter solution (SE)
Soil solution (SSS: 20 cm; SSI: 2 m) River water (R) Volume (V) in l/ha

	Na^+	K^+	Mg^{2+}	Ca^{2+}	NH^+_4	Cl^-	SO^{2-}_4	$Vx10^5$
RAIN PERIOD				Kg ha x 10^{-2}				Liters
C	**100** 12.3	**100** 3.88	**100** 1.29	**100** 16.4	**100** 7.44	**100** 46.9	**100** 49.4	17.1
T	**328** 40.3	**1147** 44.5	**1140** 14.7	**207** 33.9	**187** 13.9	**129** 60.6	**148** 74.0	16.6
SE	**241** 29.6	**1165** 45.2	**992** 12.8	**89** 14.6	**1398** 104	**42** 19.9	**153** 19.9	3.3*
SSS	**4252** 523	**11288** 438	**11163** 144	**2073** 340	**246** 18.3	**1154** 541	**2575** 1285	16.6
SSI	**537** 66.0	**2041** 79.2	**1078** 13.9	**237** 38.9	**177** 13.2	**155** 72.6	**98** 48.8	6.6
R	**111** 13.7	**42** 161	**16** 0.82	**27** 4.38	**19** 1.39	**56** 26.3	**1** 0.47	5.88
DRY PERIOD								
C	**100** 28.8	**100** 18.3	**100** 2.42	**100** 16.1	**100** 20.3	**100** 54.8	**100** 91.0	13.1
T	**276** 79.6	**628** 115	**1277** 30.9	**296** 47.7	**64** 13.0	**159** 87.2	**146** 133	11.7
SE	**160** 46.2	**461** 84.3	**1525** 36.9	**158** 25.5	**1266** 257	**76** 41.7	**207** 188	4.9*
SSS	**420** 121	**243** 44.5	**822** 19.9	**102** 16.4	**12** 2.34	**141** 77.2	**225** 205	11.7
SSI	**129** 37.1	**69** 12.7	**117** 2.82	**38** 6.11	**8** 1.69	**62** 33.8	**10** 9.40	4.7
R	**36** 10.3	**15** 2.73	**31** 0.75	**30** 4.81	**2** 0.44	**38** 20.8	**7** 6.59	4.92

* t/ha [6]

The results show that the ions are found mostly in the solution that crosses the aerial phytomass and in that which percolates throughout the root zone. The ion budget variation in the different sections of the hydrological cycle shows that this kind of ecosystem is self-sustained; so it cannot be subtituted.

REFERENCES

[1] Franken, W.; Leopoldo, P. R.; Bergamin, H. Nutrient flow through natural waters in "Terra Firme" forest Central Amazonia, Turrialba, Vol. 35, No. 4, 1985, p. 383-393.

[2] Nortcliff, S.; Thornes, J. B.; Waylen, M. J. Tropical forest systems: a hydrological approach, Amazoniana, Vol. 6, No. 4, 1979, p. 557-568.

[3] Brinkmann, W. L. F. Studies on hydrobiogeochemistry of a tropical lowland forest system, GeoJournal, Vol. 11, No. 1, 1985, p. 89-101.

[4] Forti, M. C. Hidroquímica das soluções na interface atmosfera-solo num ecossistema de terra firma (Amazônia Central), Tese de Doutorado, Dept. de Geofísica, Inst. Astr. e Geof., Univ. de São Paulo, Dezembro 1989.

[5] Cabral, O. M. R. Dados não publicados, 1989.

[6] Luizão, F. T. Litter production and mineral element input to forest floor in a Central Amazonia Forest, submetido ao GeoJournal, 1989.

[7] Golley, F. B.; McGinnis, J. T.; Clements, R. G.; Child, G. I.; Duever, M. J. Ciclagem de minerais em un ecossistema de floresta tropical úmida (EDUSP, São Paulo, 1975).

[8] Leopoldo, P. R.; Matsui, E.; Salati, E.; Franken, W.; Ribeiro, M. N. G. Composição isotópica da água do solo em floresta Amazônica do tipo terra firme, região de Manaus, Suplemento da Acta Amazônica, Vol. 12, No. 3, 1982, p. 7-13.

[9] Vitousek, P. M. Litterfall nutrient cycling and nutrient limitation in tropical forests, Ecology, Vol. 65, No. 1, 1984, p. 285-298.

[10] Melfi, A. J.; Queiroz Netto, J. P. Solos da Amazônia. Estudos setoriais e levantamento de dados da Amazônia (SUDAM, Manaus, 1972).

[11] Vitousek, P. M.; Sanford Jr., R. L. Nutrient cycling in moist tropical forest, Ann. Rev. Ecol. Syst., Vol. 17, 1986, p. 137-167.

ANALYSIS OF THE STREAMFLOW RECORD EXTENSION FOR THE XINGU RIVER AT BABAQUARA

María Elvira Pineiro Maceira and Jorge Machado Damázio *

ABSTRACT

The planning of the development of the Amazon Basin hydropower resources is being done in a situation of scarcity of riverflow data. The majority of the records do not cover more than two decades. The more commonly used methodology is the extrapolation (extension) of the riverflow records through the use of precipitation data. The hydropower-plant of Babaquara is an example. A series with eighteen years of recorded riverfow data has been extended to cover fifty-six years. This paper compares the two series (Non-extended and Extended) from the point-of-view of the productibility of the plant.

1. INTRODUCTION

The growth of the Brazilian electrical energy demand for the next decades will be supplied by the development of the Amazon Basin hydroelectrical potential. The planning studies considers beyond building costs, the productivity of the projects, expressed by the firm energy generation capability. For hydro-power plants, the firm energy depends on stochastic properties of the streamflow process. For example, high mean streamflow indicates high generation capability. Variability and temporal persistence are another important factors.

The identification of these properties is based on the streamflow record, and it is always subjected to sampling error, which is higher for short length records. In the Amazon Basin these studies face scarcity of data, due to the very recent installation of the gages and existence of energy important sub-basins without any installed gage. The more commonly used methodology to face the problem is to extend the historical records using precipitation data with conceptual or regression models, [1]. The obtained extended series are considered as historical and its stochastic properties define the energy generation capability of the projects.

ELETROBRAS (the Brazilian Government Holding Company for the public electrical sector) planning studies consider, for the Babaquara project, a monthly streamflow record spanning the years from 1931 to 1986, [2]. The data corresponding to the 1969-1986 period results from riverflow measures done in Altamira, a gage near the project. The data for 1931 to 1968 were obtained by regression riverflow and basin precipitation.

* *Electrical Power Research Center - CEPEL - P. O. Box 2754 - CEP 20001 Rio de Janeiro, Brazil*

Table 1 compares sample mean, standard deviation and lag-one autocorrelation annual statistics of the extended and non-extended series. It is clearly seen that the annual correlation structure has been modified by the extension process.

Table 1 - Annual statistics for non-extended and extended historicals records - Babaquara project

HISTORICAL RECORDS	MEAN (m^3/s)	STANDARD DEVIATION	CORRELATION (m^3/s)
Non-extended	8213.	1827.	0.23
Extended	8030.	1632.	0.00

The purpose of this paper is to present the consequences of this difference in the assessment of the Babaquara project energy potential. This is done using the periodic auto-regressive model (PAR (p_1, ...,p_s), [3], described by:

$$\Phi^m(B)\left[\frac{Z_t - \mu_m}{\sigma_m}\right] = a_t \qquad (1)$$

where:

Z_t is a seasonal series of period S

t is the time indice t=1,2,...,SN, a function of the year T (T=1,2,...,N) and season m (m=1,2,...S)

s is the number of seasons (S=12 for monthly series)

N is the number of years

μ_m is the seasonal mean

σ_m is the seasonal standard deviation

$\Phi^m(B)$ is the auto-regressive operator of order p_m

$\Phi^m(B) = (1 - \phi_1^m B - \phi_2^m B^2 - ... - \phi_{pm}^m B^{pm})$

B^i operated on Z_t yields Z_{t-i} ($B^i.Z_t=Z_{t-i}$)

p_m is the order of the auto-regressive operator of season m

a_t is a Gaussian white noise series, with zero mean and variance $\sigma_a^2(m)$.

2. PAR (p_1, p_2,..., p_{12}) MODEL FIT TO THE EXTENDED HISTORICAL RECORD

The methodology presented in [3] was used for model fitting. Previously, data of each month was transformed using the Box-Cox equation, [4]:

$$Z_t^{\lambda m} = \frac{(Z_t + 1)^{\lambda m}}{\lambda m} \quad \lambda m \neq 0 \tag{2a}$$

$$Z_t^{\lambda m} = \ln Z_t \quad \lambda m \neq 0 \tag{2b}$$

where λ_m was chosen to turn out the sample skewness null. The order of the AR operator of each month was obtained by the analysis of the monthly partial autocorrelation function and the ϕ parameters were estimated using an adaptation of the Yule - Walker equations [3]. The model adequacy was verified by testing the randomness and normality of the residuals, using Pormanteau [6], and sample skewness [5], tests. Table 2 shows λ_m values, p_m values, the Portmanteau statistics ($Q_{m,l}$) and the sample skewness (γ_m) of the residuals, for each month. For all the months the residuals can be considered free of temporal dependence and only for the months of June and December the residuals presented significant skewness.

The fitted model was used to produce a synthetic trace of 1120 years. Table 3 presents monthly and annual means, standard-deviations and lag-one autocorrelations for the extended historical and synthetic series. This table indicates that the fitted model can well represent the main moments of the extended historical series. Only this does not imply that the fitted model can be used in the electric sector planning studies. The model assessment should also include a comparison between the historical and the synthetic frequency distributions for random variables related with drought.

Table 2 - PAR (p) model fitted to the extended historical record - Babaquara Project. The asterisks indicate rejection at 1% level.

MONTH	λ_m	p_m	$Q_{m,l}$	γ_m
JAN	-0.1143	6	6.13	0.429
FEB	-0.0489	1	15.48	-0.818
MAR	0.0454	1	20.43	-0.001
APR	0.5130	7	4.70	-0.103
MAY	0.4197	7	9.21	0.754
JUN	0.2753	1	20.68	-1.830*
JUL	-1.5000	5	13.23	-0.254
AUG	-1.9084	10	6.18	-0.393
SEP	-1.3225	2	15.30	0.699
OCT	-0.7605	6	6.46	-0.129
NOV	-0.3070	12	2.89	0.405
DEC	0.2051	4	14.31	1.390*

Table 3 - Main moments of the streamflow record - Babaquara Project. Historic: Extended; synthetic: produced by the model fitted to the extended historic.

MONTH	MEAN (m^3/s)		STANDARD DEVIATION (m^3/s)		LAG-ONE AUTOCORRELATION	
	HISTORIC	SYNTHETIC	HISTORIC	SYNTHETIC	HISTORIC	SYNTHETIC
JAN	7134.	7169.	2836.	2963.	0.58	0.59
FEB	13301.	13333.	4567.	4767.	0.85	0.92
MAR	18816.	18933.	5283.	5436.	0.86	0.86
APR	20654.	20626.	5250.	5079.	0.37	0.40
MAY	16643.	16512.	5436.	5352.	0.90	0.88
JUN	7859.	7836.	2669.	2690.	0.98	0.98
JUL	2753.	2778.	661.	868.	0.18	0.19
AGO	1521.	1526.	324.	379.	0.95	0.88
SEP	1101.	1103.	215.	240.	0.92	0.94
OCT	1176.	1183.	307.	330.	0.47	0.38
NOV	1921.	1919.	588.	597.	0.83	0.85
DEC	3479.	3498.	1024.	1025.	0.73	0.79
ANNUAL	8030.	8041.	1632.	1690.	0.00	0.07

A drought can be characterized using the concept of negative run, that is, a time sequence of values less than pre-specified levels (for example, the monthly means) preceded and followed by values greater than these levels, as shown in figure 1.

There are variables related to a negative run which are of special interest: sum, length and intensity.

Obtaining these values for each negative run in the historical series yields a sample for each variable. The same calculations performed with the synthetic traces result in three other samples and the hypothesis that their historical counterpart sample was sampled from the same population can be tested.

Another random variable which was considered in the model assessment is the partial sum, S_t

$$S_t = \sum_{j=1}^{t} (Z_j - \beta\mu) \qquad (3)$$

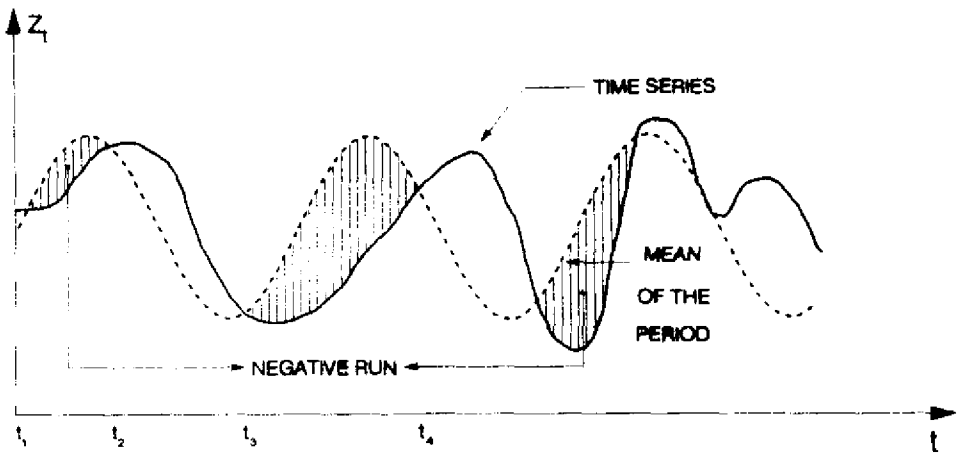

Figure 1 - Negative Run

where:

μ is the long *term* mean

β is a constant, $0 < \beta \leq 1$

In figure 2 the values d_1, d_2,.... are observations of a random variable called deficit. Rippl proposed to use the maximum deficit observed in the historical series as the design capacity for a regulation reservoir. A model oriented for energy sector studies should produce synthetic traces that yields maximum deficit sample frequency distribution in agreement with the historical value.

Tables 4 and 5 compare historical and synthetic values for drought related variables, showing the compatibility between the extended historical series and the series produced by the model fitted to it. It is interesting to verify if this compatibility also occurs if historical values are obtained from the only actualy measured record. Tables 6 and 7 show that, with the exception of the run length, this compatibility exists.

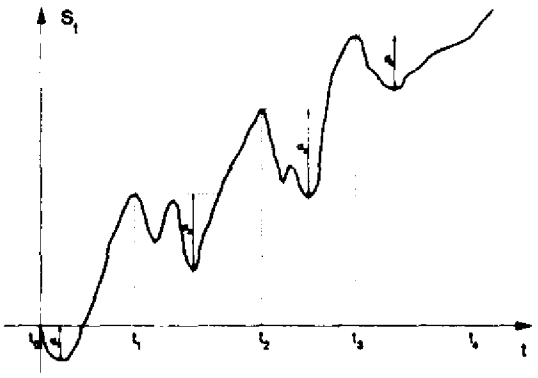

Figure 2 - Partial sums

Table 4 - Main moments and Kolmogorov-Smirnov tests for drought variables. Historical record: Extended; synthetic series: generated by the model fitted to the extended historical record. The critical value for a 5% test is between brackets.

SERIES	MEAN	STANDARD DEVIATION	SAMPLE	MAXIMUM	MINIMUM	TEST STATISTIC
			NEGATIVE RUN SUM			
HISTORICAL	11876.	14794.	56	81722.	0.861	-
SYNTHETIC	9020.	12777.	1414	85541.	0.043	0.160 (0.185)
			NEGATIVE RUN LENGTH			
HISTORICAL	6.9	6.0	56	33	1	-
SYNTHETIC	5.4	5.3	1414	38	1	6.220 (9.490)
			NEGATIVE RUN INTENSITY			
HISTORICAL	1429.	1177.	56	4821.	0.861	-
SYNTHETIC	1322.	1335.	1414	9280.	0.430	0.111 (0.185)

Table 5 - Maximum values of drought variables. Historical record: Extended; synthetic series: generated by the model fitted to the extended historical record.

SERIES	MEAN	STANDARD DEVIATION	NUMBER OF SEGMENTS	P [SYNT. < HIST.]
		NEGATIVE RUN SUM		
HISTORICAL	81722.	-	1	-
SYNTHETIC	60425.	12919.	20	0.95
		NEGATIVE RUN LENGTH		
HISTORICAL	33.0	-	1	-
SYNTHETIC	25.4	6.2	20	0.80
		NEGATIVE RUN INTENSITY		
HISTORICAL	4821.	-	1	-
SYNTHETIC	5954.	1552.	20	0.25
		MAXIMUM DEFICIT (= 0.70)		
HISTORICAL	30479.	-	1	-
SYNTHETIC	36824.	5558.	20	0.15

Table 6 - Main moments and Kolmogorov-Smirnov tests for drought variables. Historical record: Non-Extended; synthetic series: generated by the model fitted to the extended historical record. The critical value for a 5% test is between brackets.

SERIES	MEAN	STANDARD DEVIATION	SAMPLE	MAXIMUM	MINIMUM	TEST STATISTIC
			NEGATIVE RUN SUM			
HISTORICAL	11705.	20221.	19	87283.	100.540	-
SYNTHETIC	11165.	14858.	1248	96135.	1.633	0.244 (0.314)
			NEGATIVE RUN LENGTH			
HISTORICAL	5.9	7.9	19	34	1	-
SYNTHETIC	6.7	6.2	1248	45	1	9.374 (3.840)
			NNEGATIVE RUN INTENSITY			
HISTORICAL	1275.	1022.	19	4044.	96.620	-
SYNTHETIC	1359.	1260.	1248	8577.	1.633	0.093 (0.314)

Table 7 - Maximum values of drought variables. Historical record: Non-Extended; synthetic series: generated by the model fitted to the extended historical record.

SERIES	MEAN	STANDARD DEVIATION	NUMBER OF SEGMENTS	P [SYNT. < HIST.]
		NEGATIVE RUN SUM		
HISTORICAL	87283.	-	1	-
SYNTHETIC	52666.	18116.	60	0.93
		NEGATIVE RUN LENGTH		
HISTORICAL	34.0	-	1	-
SYNTHETIC	23.1	7.0	60	0.93
		NEGATIVE RUN INTENSITY		
HISTORICAL	4044.	-	1	-
SYNTHETIC	4596.	1395.	60	0.40
		MAXIMUM DEFICIT (= 0.70)		
HISTORICAL	33046.	-	1	-
SYNTHETIC	32486.	6454.	60	0.68

3. PAR (p_1, p_2,..., p_{12}) MODEL FIT TO THE NON-EXTENDED HISTORICAL RECORD

The PAR (p_1,...,p_{12}) was fitted to the non-extended historical record in the same way as was done with the extended historical record.

Table 8 presents λ_m values, pm values, the Portmanteau statistics and the sample skewness of the residuals, for each month. For all the months the residuals can be considered free of temporal

dependence and only the July residuals presents significant skewness.

The fitted model was used to produce a synthetic trace of 1080 years.

Table 9 presents monthly and annual means, standard deviations and lag-one autocorrelations for the non-extended historical record and synthetic series. Tables 10 and 11 compares the historic and synthetic values for the drought variables.

Tables 9 to 11 indicate that, considering the non-extended historical record, this model can be used in the assessment of the Babaquara project energy potential.

Table 8 - PAR (p) model fitted to the non-extended historical record - Babaquara Project. The asterisks indicate rejection at 1% level.

MONTH	λ_m	p_m	$Q_{m,1}$	γ_m
JAN	0.2997	3	13.24	0.429
FEB	0.6854	1	18.94	0.590
MAR	0.1834	1	13.11	0.310
APR	-0.8453	2	13.84	0.771
MAY	-0.0307	2	17.97	-0.816
JUN	-0.5283	1	19.36	-0.377
JUL	0.0933	1	15.14	-1.670*
AUG	0.1690	2	16.23	-0.140
SEP	1.8025	1	15.92	1.080
OCT	0.1127	4	8.80	0.229
NOV	0.2796	2	15.06	-0.274
DEC	0.8963	5	8.88	0.896

Table 9 - Main moments of the streamflow record - Babaquara Project. Historical record: Non-Extended; synthetic series: produced by the model fitted to the Non-Extended historical record.

MONTH	MEAN (m^3/s)		STANDARD DEVIATION (m^3/s)		LAG-ONE AUTOCORRELATION	
	HISTORIC	SYNTHETIC	HISTORIC	SYNTHETIC	HISTORIC	SYNTHETIC
JAN	8290.	8181.	3564.	3520.	0.78	0.79
FEB	14583.	14543.	4905.	4859.	0.70	0.76
MAR	19859.	19978.	6222.	6095.	0.77	0.78
APR	19515.	19508.	3796.	3854.	0.63	0.65
MAY	15604.	15706.	5016.	5194.	0.74	0.64
JUN	7046.	7187.	2466.	2931.	0.94	0.91
JUL	3128.	3151.	865.	906.	0.93	0.91
AUG	1737.	1741.	370.	377.	0.92	0.92
SEP	1245.	1245.	223.	230.	0.80	0.78
OCT	1351.	1360.	400.	431.	0.80	0.80
NOV	2217.	2218.	834.	866.	0.72	0.75
DEC	3982.	3969.	1450.	1392.	0.63	0.67
ANNUAL	8213.	8232.	1827.	1794.	0.23	0.16

Table 10 - Main moments and Kolmogorov-Smirnov tests for drought variables. Historical record: Non-Extended; synthetical series: generated by the model fitted to the Non-Extended historical record. The critical value for a 5% test is between brackts.

SERIES	MEAN	STANDARD DEVIATION	SAMPLE	MAXIMUM	MINIMUM	TEST STATISTIC
			NEGATIVE RUN SUM			
HISTORICAL	11705.	20221.	19	87283.	100.540	-
SYNTHETIC	9613.	14856.	1300	121333.	0.065	0.188 (0.314)
			NEGATIVE RUN LENGTH			
HISTORICAL	5.9	7.9	19	34	1	-
SYNTHETIC	5.3	5.8	1300	41	1	0.768 (3.840)
			NEGATIVE RUN INTENSITY			
HISTORICAL	1275.	1022.	19	4044.	92.620	-
SYNTHETIC	1361.	1133.	1300	6417.	0.065	0.082 (0.314)

Table 11 - Maximum values of drought variables. Historical record: Non-Extended; synthetic series: generated by the model fitted to the extended historical record.

SERIES	MEAN	STANDARD DEVIATION	NUMBER OF SEGMENTS	P [SYNT. < HIST.]
		NEGATIVE RUN SUM		
HISTORICAL	87283.	-	1	-
SYNTHETIC	52954.	23148.	60	0.92
		NEGATIVE RUN LENGTH		
HISTORICAL	34.0	-	1	-
SYNTHETIC	21.9	7.1	60	0.90
		NEGATIVE RUN INTENSITY		
HISTORICAL	4044.	-	1	-
SYNTHETIC	4014	1011.	60	0.58
		MAXIMUM DEFICIT (= 0.70)		
HISTORICAL	33046.	-	1	-
SYNTHETIC	33120.	7357.	60	0.63

4. ENERGY ASSESSMENT OF THE BABAQUARA PROJECT

The assessment of the Babaquara project energy potential was done in this work based on the relationship between the energy demand and the annual probability of load not supplied (deficit). The probability of deficit is obtained by simulating the operation of the reservoir when submitted to the synthetic series generated by the two models developed in the last sections. The operation rule adopted in the simulations was such that, when possible, the turbined flow at each month is always made sufficient to supply the energy demand defined by M. In months for which the stored water plus the inflow are not sufficient to supply the demand, the reservoir is complete emptied. The probability of

deficit for a demand M is calculated by the frequency of years with at least one month in which the demand was not completely supplied.

It was considered a constant hydraulic head of 61m, given by the difference between reservoir and tailrace mean levels. It was also adopted a constant turbine-generator efficiency (0,81). For the reservoir volume it was considered 51,94 x 10^9 m^3.

Figure 3 presents, for each model, the relationship between annual probability of load not supplied and energy demand. It can be seen that for low demand levels the probability of deficit obtained with the non-extended model is greater than that obtained with the extended model. The opposite occurs with high demand levels, with the equilibrium point occurring for a probability of deficit of 5%. As 5% is, by coincidence, the planning criterium adopted by the Brazilian electric sector, the energy potential of the Babaquara project can be estimated to be 3250 Mw, whichever model is considered.

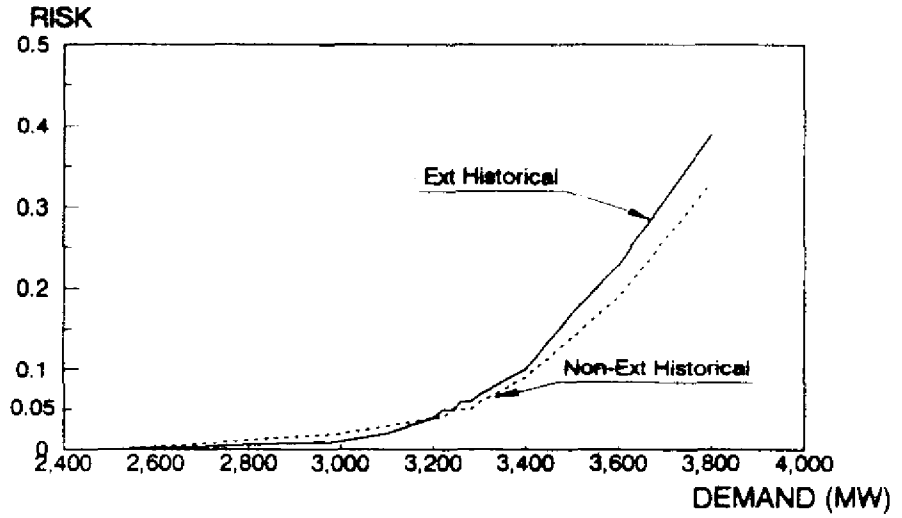

Figure 3 - Annual probability of deficit for the Babaquara Project

5. CONCLUSIONS

The Babaquara project case gives a good opportunity to verify precipitation data based riverflow record extension methods when applied in the Amazon Basin, as for this case an actual measured flow record with eighteen years permits some inference.

The main difficulties faced by extrapolation (extension) process in the Amazon Basin are the low precipitation network density and the scarce knowledge about the basin process of storing water.

It can be speculated that the last factor determined that the extended historical series presented lower annual persistence than the non-extended historical series. In spite of this, the analysis presented in this paper showed that this difference does not yield practical effect on the energy assessment of the Babaquara project.

6. REFERENCES

[1] Madeira, E. F.; Ferreira, L. C. H.; Lorafe, D. P.; Maranhão, N. Considerações sobre a Metodologia Adotada nos Estudos Hidrológicos da Bacia do Tapajós, VIII Simpósio Brasileiro de Recursos Hídricos, ABRH, Foz do Iguaçú, 1989 (in portuguese).

[2] ELETROBRAS. Metodologia Utilizada para Obtenção das Séries de Vazões Naturais Médias Mensais, Departamento de Recursos Energéticos, Diretoria de Planejamento e Engenharia, 1985 (in portuguese).

[3] Maceira, M. E. P. Operação Ôtima de Reservatórios com Previsão de Afluências, Tese de Mestrado, COPPE, Universidade Federal do Rio de Janeiro, 1989 (in portuguese).

[4] Box, G. E. P.; Cox, D. R. An Analysis of Transformations, Journal of The Royal Statistical Society, A127, 211-252, 1964.

[5] Snedecor, G. W.; Cochran, W. G. Statistical Methods, The Iowa State University Press, Iowa, 1967.

[6] Noakes, D. J.; McLeod, A. I.; Hipel, K. W. Forecasting Seasonal Hydrological Time Series, Technical Report, Dept. of Statistical and Actuarial Sciences, University of Waterloo, Waterloo, Ontario, Canada, 1983.

A NEW APPROACH TO RAINFALL RECORDING AND ANALYSIS

S. K. Tan and Y. M. Chiew *

ABSTRACT

The conventional method of recording rainfall has the disadvantage of masking high intensity but short duration tropical rainfall. Also, both rain and non-rain events have to be recorded. The authors' new approach requires the recording of time of occurrence when an equivalent of 0.2 mm rainfall depth is collected. This arrangement yields results of temporal resolution of better than 5 seconds while the conventional one yields, at best, a resolution of 5 minutes. Non-rain event, though not recorded, can be deduced from the record of rain event. The time intervals between rain events can be immediately sorted and ranked to establish a sort of statistical 'rainfall-arrival-time' relationship, not dissimilar to that commonly used in Transportation Engineering or Operations Research. The results obtained over a 9-month period show that gamma distribution functions of appropriate shape and rate parameter can be used to fit the recorded data and suggested that the functions could be extrapolated to include statistically probable but as yet unrecorded extreme events.

INTRODUCTION

Sophisticated techniques of measuring areal rainfall by using radar (for example Grayman & Eagleson, 1971; Collier, 1989) or satellite pictures, (for example Oliver & Scofield, 1976) are already available. However, in most parts of the world, analysis involving areal distributions of rainfall is still based on data derived from a network of point rainfall records. The prospect of such analysis is usually less than glamorous. It is firstly a mammoth task to gather all the necessary data from various sources and secondly, a tedious process of sorting, grouping and double checking the relevant sets of data. The daunting task of entering the data into a computer system which follows usually frustrates the researchers. In comparison, the numbers crunching process by a digital computer becomes one of the least time consuming and problematic part of the work.

A well-planned network of rainfall gauges and standardized recording procedures would simplify the data collection processes. It is better still if the data can be directly routed to digital computers. Then again, one still has to deal with reels and reels of magnetic tapes. This is perhaps unavoidable, but any measure that will reduce the amount of data storage not only enhances the efficiency of the work involved, but also saves valuable resources such as time, computer hardwares and storage space required.

* *School of Civil & Structural Engineering, Nanyang Technological Institute, Singapore 2263*

A REVIEW OF THE TRADITIONAL APPROACH

The traditional procedures are very much dictated by the type of raingauge and recording devices available at the earlier times. Descriptions of most of the devices and procedures can be found in Hydrological Practices Manual, WMO (1981). The tradition is so strong that even when one uses modern electronics-based data-logging devices, one is still conditioned to express rainfall in terms of the total quantity of rainfall collected during a pre-set period. The recording devices are also designed to do just that. This method of quantifying rainfall is suitable for design purposes but could have been modified to take full advantage of the available technology to gain more information on the rainfall. In other words, despite the advancement in modern data-logging techniques, the same 'obsolete' procedures of recording data are still being used.

Another disadvantage of this method of recording is that zero-rainfall events also have to be faithfully recorded and archived. In terms of recording on paper or charts, there will soon be mountains of records of which zero-rainfall records form a substantial bulk. In terms of digital data storage, a lot of valuable spaces are devoted to storing zeros.

These problems are compounded when one realizes that, because of the discrete nature of the event and the difficulty in the treatment of the logarithm of zero, one would need to organize the data into rainfall and non-rainfall series, perform statistical analysis on each, and later, recombine the two series when one generates synthetic rainfall series.

All of these wasted storage resources and double work could have been avoided if one takes a fresh look at the system of recording and analyzing rainfall data.

PROPOSED ALTERNATIVE APPROACH

Rainfall is but one of many 'random' events one encounters. A quick survey of the methods used by other researchers in random processes reveals that, in some cases, one needs not look at the 'quantity' of an event during a prescribed period. Instead, one could look at the time-intervals between consecutive 'quantity' of a prescribed event. In the case of recording point rainfall, one would be looking at the time intervals between successive events when a fixed quantity of rainfall, say 0.2 mm or 0.5 mm are collected. The selected quantity is dependent on the size of the receptacle used. The authors use one with 0.2 mm receptacle.

In short, one shifts from the emphasis of a fixed-time domain to one of a fixed-event domain. In the former, one records the quantity of the event; in the latter, one records the time when the event takes place. While in the former method, a null event must also be recorded, in the latter, the null event is already accounted for by simply not recording it. The question of whether the zero-rainfall event and rainfall event are statistically mutually exclusive would not invalidate this approach.

The advantages of the latter method are many:

1. One needs to record and store only the time when the event occurs. No resources are wasted in storing null data.
2. Consequently, one needs only to deal with a series of data statistically, namely, the time-interval between consecutive events.

3. Regardless of the intensity of a rainfall, there will definitely be a finite time interval between each tipping of the tipping-bucket. As such, the traditional problems of having to deal with discontinuous function and logarithm of zeros are avoided.

4. Data with fine temporal resolutions could be obtained. The accuracy of timing is dependent on the clock maintained by the micro-processor. The accuracy of this clock is usually in the order of better than milliseconds. This accuracy in timing will not be a restricting factor in capturing the desired event. Mechanically based rainfall collection receptacles could not be operated in such time frame.

5. Synthetically generated sequence of the events is more straight forward as only one series is involved.

All of these advantages could be realized by taking full advantage of modern data-logging facilities through simple reorganization of the method of recording rainfall data. A traditional autographic raingauge could be used after a simple modification. The tipping of the bucket and the mercury switches in the raingauge, instead of activating an event recorder or a digital/mechanical counter, interrupts a dedicated microprocessor equipped with a real-time clock. The actual time of interruption is recorded. The quantity of the event is known since an interruption represents a tip of the bucket, which usually represents 0.2 or 0.5 mm of rainfall depth.

The size of data storage required in the proposed method is much less than that required by the traditional method. Singapore typically receive 2300 mm of rain a year. If a raingauge of 0.2 mm bucket is used, then one will have 2300/0.2 = 11,500 records. If it is established at a 15-minutes recording period, the traditional method of recording would have required 365 * 24 * 4 = 35,040 records. The size of the records required is more if one requires records based on a finer resolution of time.

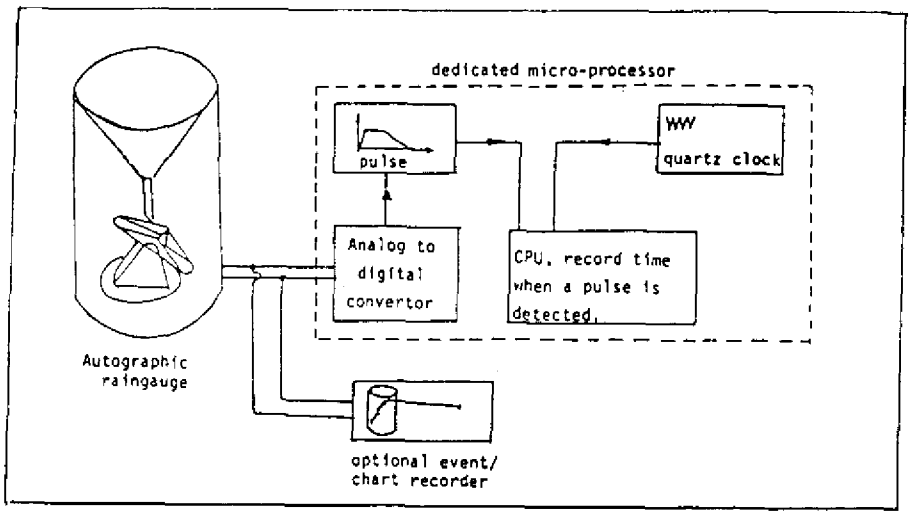

Figure 1 - A schematic representation of the pilot rainfall monitoring station.

SET-UP OF THE RECORDING FACILITY

Figure 1 shows the schematic representation of a pilot station, located in NTI campus, which utilizes the alternative approach of recording. As the time-interval between each tip of a 0.2 mm bucket is not expected to be less than 1 second, (which corresponds to a very high rainfall intensity of 7200 mm hr^{-1}), a small 8-bit technical computer equipped with a time clock and an analog to digital converter (ADC) would be sufficient to monitor the raingauge. The on-board memory requirement is low as well. A computer with 128 kbyte RAM is capable of supporting at least a single array of 7000 elements. This number is arrived at assuming that 56 kbyte of stack memory is available and it requires 8 bytes to store a number. Eight thousand records would have corresponded to 1400 mm of rainfall. Therefore, one may not even need to install a disk drive to store the data were it not for the purpose of providing a back-up or permanent storage facility.

The detection of the tipping event is straight forward. The tipping process temporarily closes a circuit connected to a specified channel in the analog-to-digital (ADC) interface. That the circuit is closed for a fraction of a second is sufficient to send a pulse to the ADC. Upon detecting the pulse, the program then records the current time and set the pointer to the next array element. If the next pulse is not detected within an hour of the occurrence of the last pulse, the current file is closed.

The array is reinitialized and the next pulse will toggle the creation of a new file.

The principle of operation is simple. However, provision must be given to allow for the possibility of double detection of the same signal, error recovery and power interruption, failure or rebooting of the system.

RESULTS

Expression of rainfall records in the traditional manner of maximum rainfall in a period of time can be obtained quickly from the sequence of rainfall recorded in this manner. The period specified could be from 5 seconds to 4 weeks or more, depending on the length of the record. This is the normal way of presenting rainfall data.

One can extract much more information from rainfall data recorded in this alternative approach. Figure 2 shows the result obtained from rainfall record at the pilot station from 1 August 1989 to 30 April 1990. It is presented in terms of relative frequency of occurrence (density) against selected categories of time-interval. The range of time-interval is large, ranging from a few seconds to a few days, which is why they are expressed in terms of logarithm to the base of 10. It can be seen that the distribution is skew to the left.

This type of function is classified as a gamma distribution function in the field of hydrology, (Raudkivi, 1979) or Erlang's distribution function in the field of Operations Research (Winston, 1987):

$$f(t) = R\,\{Rt_c)^{k-1} \exp(-Rt_c) / (k-1)\} \qquad (1)$$

where k and R are shape and rates parameter, respectively. t_e is $\log_{10}$ (time interval) in this application. The first and second Moment of the function are k/R and k/R^2, respectively. k is a positive integer and the term in , respectively. k is a positive integer and the term in is the well known Poisson probability function. Reference to the function can be found in most standard textbooks on statistics.

By approximating the sample mean, μ, and sample standard deviation, σ, to the first and second moment of the function correspondingly, one could estimate the values of k and R:

$$1/R = \sigma^2/m$$

and (2)

$$k = \mu^2/\sigma^2$$

However, this treatment will lead to non-integer value of k. A more successful approach is to treat the product of the moments as whole, whereby

$$k^2/R^3 = \mu s^2 \quad (3)$$

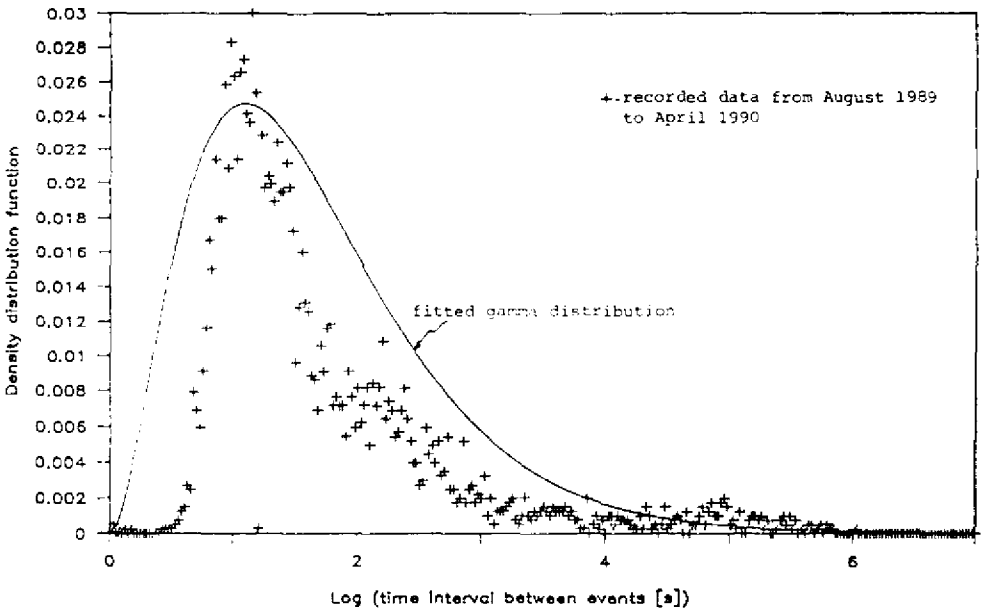

Figure 2 - Distribution of the time intervals (log base 10) between consecutive events equivalent to 0.2 mm of rainfall depth.

By following an approach similar to Kolmologrov-Smirnov method for testing the goodness of fit of cumulative density function, (Kottegoda, 1980), several integer-values of k (and the corresponding R, from eqn. 3) could be used and superimposed on the cumulative density curve of the sample, Fig. 3. It can be seen that the case of k = 3 best fitted the sample distribution (r^2 = 0.99 from regression analysis).

One needs not be restricted to long period of record to obtain sufficient data to utilize gamma distribution function. Figure 4 shows the fitted gamma distribution function for each month of the 9-month period. In all cases, the goodness of fit are 0.98 or better.

In fact, one needs not stop at selected period of one year, one season or one year. One can even venture into the temporal distribution of rainfall intensity of a storm. The result, no doubt, would interest a climatologist.

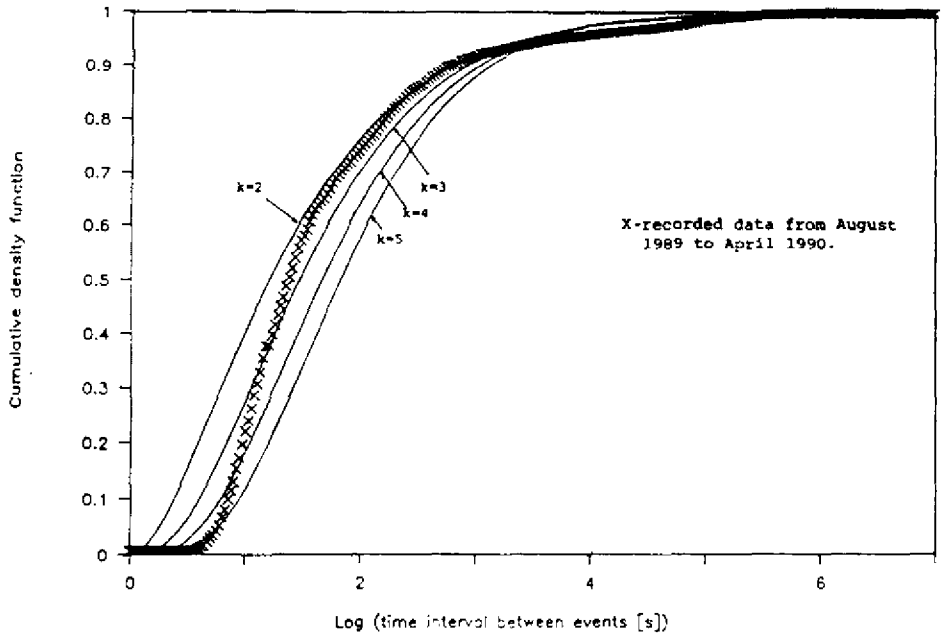

Figure 3 - A comparison of the recorded field data with gamma distribution functions of various shape and rate parameters.

DISCUSSION

It can be seen from Table 1 that there is a narrow band of k and R values. Records of the first four months and April 1990 depicted the same k value while those of the other two months showed larger k values. For those of the same k-value, R increases with total rainfall. Since the mean of the population is k/R, the larger the R-value for the same k means that the average time interval between successive events are shorter, hence more occurrence of the event or larger quantity of rainfall over the same period of time.

These observations reflected some of the properties of the gamma distribution function. Of K and R-value of the same magnitude, the same k-value means that the relative frequency of occurrence of the time intervals are the same. This is very indicative of the similar nature of rainfall taking place during the period, (thunder storms at dawn and in the afternoon). For the same values of k, the larger the value of R, the larger is the total quantity of rainfall, as explained earlier.

Table 1 - The shape, k, and rate parameters, R of the fitted gamma distribution functions for the 9-month data

Month	k	R(s^{-1})	Total rainfall (mm)
August 1989	3	1.64	94.0
September	3	2.09	179.0
October	3	2.17	226.6
November	3	1.82	113.8
December	4	1.78	62.4
January 1990	4	1.99	56.8
February	4	1.66	15.4
March	4	2.66	72.6
April	3	2.07	109.2

The distribution function for December 1989 to March 1990 depicted larger values of k which mean that the time-intervals are skewed towards larger value of time-interval, hence less occurrences. The field records showed that these are associated with less total rainfall recorded.

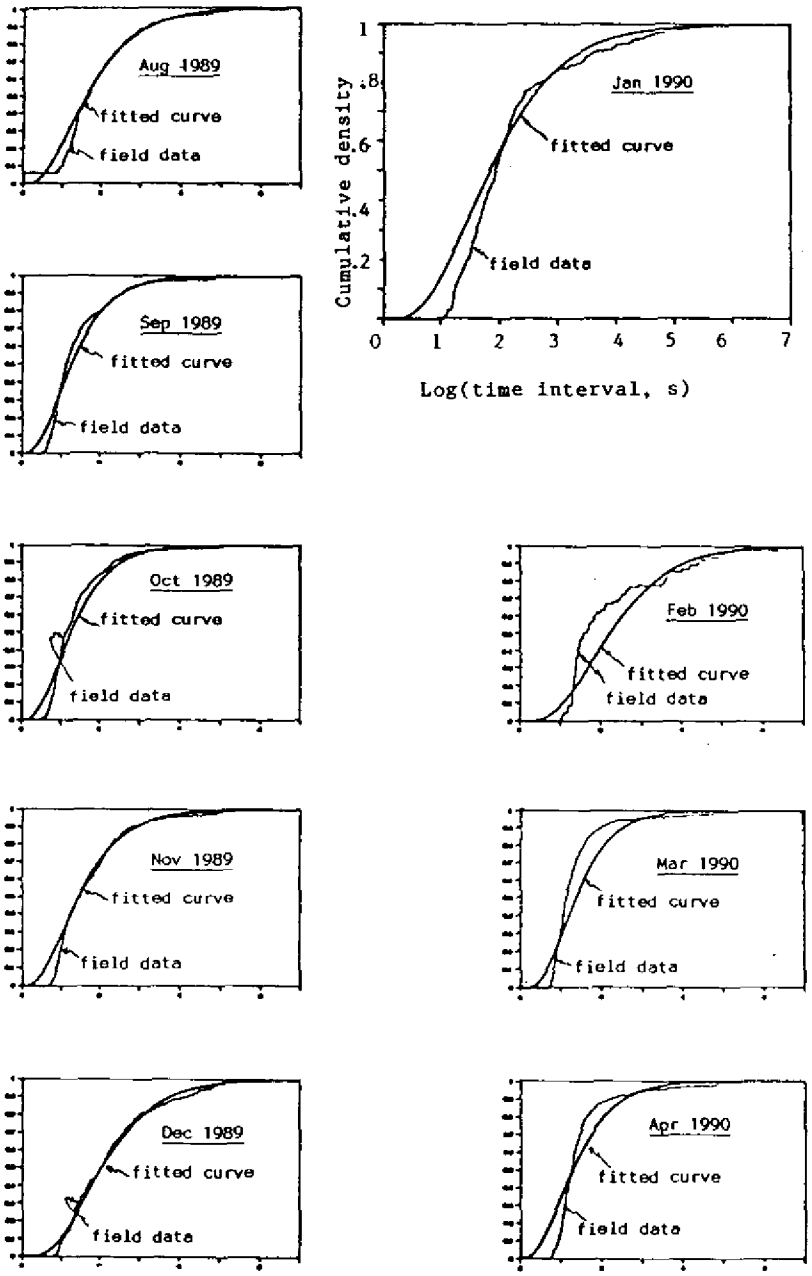

Figure 4 - A comparison of monthly field data with individually fitted gamma distribution curve. The scale and axes are as shown in the larger picture on the top right.

The goodness of fits of the gamma distribution function to the data ordered and the encouraging results obtained imply that:

1. Perhaps if one record the rainfall in this approach, a single well defined gamma distribution function could be established for every distinct hydrological periods of a year;

2. The well-defined curve suggested that the more frequent components of a rainfall event could have been approximated even without a reasonably long record of rainfall. The results shown in Figures 3 and 4 show that the main core of the distribution curve may have been established.

3. It follows from the above, then, the time interval between successive events during an extremely wet period may have already been recorded during a less severe event, except that the number of such occurrences are much less.

4. A longer period of records would confirm the established-core of the distribution curve and modify the two limbs of the curve. However, it is plain to deduce from Figures 3 and 4 that it is already not difficult to establish the left limb from the mere 9-month data. The right limb which corresponds prolonged periods of drought may be harder to establish.

5. If we are more interested in how large the rainfall is rather than in how long the drought lasted, the distribution curves may be considered established.

It appears, then, one could immediately re-plot the distribution function in the form of a cumulative density function and couple with a pseudo-random number generation routine to synthetically generate artificial rainfall sequences. The plot is in fact, already shown in Figures 3 and 4. However, this approach assumed that the occurrence of successive 0.2 mm of rainfall is statistically independent of one another. This assumption may not be too unreasonable an assumption since unlike stream flow or other phenomena with 'memory' effects, rainfall event, treated in the fashion described, is a true-false phenomenon. The 'true' event needs not depend on the previous 'true' or 'false'.

CONCLUSION

An alternative approach to record and analyze point rainfall data was presented. The results showed that the time-interval records can be described by an Gamma Distribution function with suitable shape and rate parameters. The well defined function also presented a direct means towards synthetic generation of rainfall series.

LIST OF SYMBOLS

k shape parameter in a Gamma distribution function

t_* $\log_{10}$ (time interval)

R rate parameter in a Gamma distribution function

μ sample mean

σ sample variance

REFERENCES

1. Collier, C. G. Application of weather radar systems: a guide to uses of radar data in meteorology and hydrology. Ellis Horwood, 1989.

2. Grayman, W. M. and Eagleson, P. S. A Review of the Accuracy of Radar and Raingauges for Precipitation Measurements. Cambridge, Mass.: MIT Department of Civil Engineering, Ralph M. Parson Laboratory, 1970. (Technical Report No. 119).

3. Kottegoda, N. R. Stochastic Water Resources Technology. The MacMillan Press, London and Basingstoke, 1970.

4. Oliver, V. J. and Scofield, R. A. Estimation of Rainfall from Satellite Imagery. Proceeding of the Sixth AMS Conference on Weather Forecasting and Analysis, May 10-13, 1976, Albany, N.Y.

5. Raudkivi, A. J. Hydrology. An Advanced Introduction to Hydrological Processes and Modelling. Pergamon Press, 1979.

6. Winston, W. L. Operations Research: Applications and Algorithms. PWS Publication, Boston, Massachusetts, 1987.

APPLICATIONS OF HILLSLOPE PROCESS HYDROLOGY IN FOREST LAND MANAGEMENT ISSUES: THE TROPICAL NORTH-EAST AUSTRALIAN EXPERIENCE

Mike Bonell *

ABSTRACT

There has been an upsurge in publicity regarding the hydrological consequences related to large-scale conversion of tropical forests to other land uses. Many of the conclusions drawn from hydrological experiments (both in temperate and tropical areas) are based on only input-output studies, with the scale of enquiry within the drainage basin either limited or non-existent. The role of process hydrology is two-fold, *viz*:

i) to assist in our understanding of the stores and fluxes of water transfer so that simplified water balance results are better interpreted, and

ii) to test the application of physically-based theory to field environments as part of the long term goal for using physically-based models in ungauged drainage basins.

The paper will first set out the conflicting notions concerning the delivery mechanisms of storm runoff due to land use conversions. With the aid of research findings from two major projects in contrasting humid and semi-arid tropical environments in north-east Queensland, *viz* tropical rainforest and open eucalypt woodland, the paper will address the dichotomy of views concerning such changes in storm runoff. During the course of the presentation particular attention will be given to methodology and the problems of integrating process hydrology results through different scales of investigation.

The interaction between synoptic climatology —rainfall intensities— soil hydraulic properties will be a strong emphasis throughout the paper for explaining differences in runoff generation observed in north-east Australia and other parts of the tropics. Both tropical rainforest and open eucalypt woodland generate large volumes of overland flow in the summer wet season, with the former environment presenting the paradox of high surface infiltration rates typical of forested environments but a runoff response that is not typical of these environments. There is however a parallel between these contrasting environments in that each has a 'throttle' layer to the prevailing rain intensities, *viz* at the surface in the semi-arid study to produce Hortonian overland flow and in the subsoil in the rainforest to produce saturation overland flow. This is caused by opposite trends in the order of magnitude change in field saturated hydraulic conductivity, K* down the soil profiles. It is shown that K* is a significant hydraulic property in both environments, where temporal as well as spatial variability has to be considered, especially in the semi-arid study.

The paper finally provides possible explanations for the varying hydrological responses related to hillslope hydrology in other tropical environments.

* *Director - Institute for Tropical Rainforest Studies and Reader in Physical Geography - Department of Geography - James Cook University of North Queensland - Townsville - Queensland 4811, Australia*

Paper prepared for the UNESCO Regional Seminar on Tropical Forest Hydrology, 4-9 September 1989, Kuala Lumpur, Malaysia

INTRODUCTION

In the 1980s there has been upsurge in publicity regarding the hydrological (and climatic) consequences related to large-scale conversion of tropical forests to other land uses. In response to this concern, several rigorous reviews on the hydrological effects of land use conversion have emerged (eg.: Bosch and Hewlett, 1982; Bruijnzeel, 1987a, b, 1989; Cassells *et al*, 1987; Hamilton, 1986, 1987; Hamilton with King, 1983) which essentially concentrate on the end-product, *viz* changes in water yield, based mostly on controlled experiments.

Many of the conclusions drawn from such experiments are based only on input-output studies, with the scale of enquiry through process hydrology studies within the drainage basin either limited or non-existent. The role of process hydrology within a drainage basin is two-fold, *viz*: i) to assist in an understanding of the stores and fluxes of water transfer so that simplified water balance results are better interpreted, and ii) to assist in the development of physically-based models which are intended to have application to ungauged drainage basins. One of the aims of this paper is to highlight the need for greater expansion of process hydrology studies in hydrological land management issues within the humid tropics, with a particular focus on hillslope hydrology. In fact there are significant voids in our understanding of hydrological processes in such areas. Resort to transposing findings from temperate experiments to address land management problems in the humid tropics is more common, without the opportunity for field verification (eg.: Hamilton with King, 1983).

Despite considerable progress in hillslope hydrology since Hewlett (1961) first proposed the variable source area concept of runoff generation, the momentum of research continues because many details concerning process mechanisms of storm runoff are still not fully understood (Dunne, 1983). The temporal and spatial variability of storm runoff whether it be Hortonion overland flow (Horton, 1933, defined by Kirkby, 1978, p. 368), saturation overland flow (defined by Kirkby, 1978, p. 371) or subsurface stormflow (defined by Kirkby, 1978, p. 373) have important applications in the continuing debate on the hydrological effects of land conversion. To date most work has been undertaken in the higher latitudes focussing in particular on the humid temperate areas of the eastern United States and western Europe (Dunne, 1978; Hewlett *et al*, 1984). Research in tropical areas has been more sparse (Douglas and Spencer, 1985; Walsh, 1980). Recently Dunne (1983, p. 44) called for "...field research... to be pursued vigorously in a wider range of environments..." such as "... tropical rainforest".

During the course of evaluating wet/dry canopy evaporation differences between forest and grassland in the Amazonas, Shuttleworth (1988, p. 344) pitched a commonly held notion by stating "... a poorly managed land-use change would exacerbate this difference. Soil compaction and destruction of surface macropores during deforestation could dramatically reduce infiltration and increase surface runoff, thereby generating soil erosion and nutrient loss and reaching the resilience and persistence of the ensuing grassland in dry months...". An additional implication in this statement is also one of reduced recharge to the soil water/groundwater stores and their subsequent effect on water yield. As Bruijnzeel (1987a, p. 12) noted "... the general experience in the tropics is unfortunately much more unfavourable (concerning dry-season flow): decreasing infiltration properties generally result in increased direct runoff during rainy periods. The water thus lost cannot contribute to deep percolation, with diminished dry-season flows as the real results". Conversely, the idea of forests being 'sponges' which can absorb most rainfall because of their superior infiltration properties and that deforestation increases flooding from infrequent, large storms, is still widely prevalent, despite available evidence indicating the contrary (Cassells *et al*, 1987; Hamilton, 1987).

In addition, controlled experiments have shown that the conversion of forests to grasslands usually increases delayed flow (dry-weather flow) (Bosch and Hewlett, 1982; Cassells *et al*, 1987). During extended dry periods when the shallow rooted, herbaceous cover is under stress; the deeper rooted trees continue to access soil moisture or even groundwater. Thus removal of trees prevents additional water losses at these times and allows unsaturated/saturated flow to continue transmission to streams. In turn, groundwater levels rise in response to the decreased evapotranspiration (Bosh and Hewlett, 1982; Peck and Williamson, 1987). Another factor which contributes to these changes in water yield revolves around wet/dry canopy evaporation differences between forests and low crops. Where soil water is non-limiting, McNaughton and Jarvis (1983) noted that whilst the canopy resistance (or bulk surface resistance, representing stomatal control, r_s; Shuttleworth, 1988) of forests was higher than grasses, therefore causing dry canopy evaporation over forests to be lower; the rate of evaporation of intercepted water over forests (wet canopy evaporation) was higher than the herbaceous cover. In climates where the canopy is wet for a significant proportion of time, then the combined wet canopy/dry canopy evaporation from forests can approach or even exceed the potential evapotranspiration rates of short crops (McNaughton and Jarvis, 1983; Morton, 1984). This particularly applies to locations near the edge of continents or on islands where it appears the energy attracted from the ocean is capable of enhancing the evaporation of intercepted water; and net time-average water loss exceeds the potential rate (Calder, 1985; Morton, 1985; Shuttleworth, 1989). The fewer studies undertaken in continental interiors indicate the the time-average total evaporation reverts to almost the potential rate (Shuttleworth, 1989). In the case of central Amazonas, evaporation losses were within 5 percent of the potential rate (time-averaged over 25 months), but as Shuttleworth (1988, p. 342) noted 'the time-average behaviour is therefore a balance between less than potential rate, with a dry canopy, and greater rate with a wet canopy. The near equality between average evaporation and potential evaporation in central Amazonas is ... in part fortuitous...' and continues '... it is, for instance, very probable that Amazonas regions with higher rainfall, where the forests spend a greater proportion of the time wet, will tend to have average evaporation rates greater than the potential rate'.

The conflict then in water yield changes in the humid tropics revolves around the delicate balance between the complexities of the evapotranspiration process and changes in soil hydraulic properties connected with infiltration, a relationship also emphasized by Bruijnzeel (1989) and Chang (1989). If the net gains in groundwater accretion from lower evapotranspiration are more than offset by much-reduced percolation, and therefore reducing groundwater accession, then the depth of the water table may decline causing springs and stream flow discharges to reduce in dry seasons.

In spite of these assertions, there is a dearth of supporting evidence concerning changes in hillslope storm runoff and soil hydraulic properties. There are additional factors which confound these widely held ideas, *viz* scale of investigation, controlled or uncontrolled drainage basin comparisons and the prospect of drainage basin leakages, all of which are closely interrelated (Bruijnzeel, 1989; Shuttleworth, 1988). As Morton (1984, p. 385) noted "... in a large basin the difference between the groundwater and topographic divide is negligible and the river has eroded into channel deep enough to intercept all significant groundwater flow systems. In a small basin this is not necessarily so". The underlying geology and different scales of investigation are particularly appropriate to the Amazon Basin where a review of the deforestation controversy showed that annual runoff coefficients ranged from 0.19 to 0.57 (Salati, 1987, p. 288) from different water balance studies. Shuttleworth (1988, p. 322) commented "... water balance experiments are prone to the uncertainty that ungauged, subterranean leakage forms a significant part of the total movement, a problem of considerable relevance in the free-draining soils of this region. Underestimation of drainage easily leads to a (proportionately

enhanced) overestimation of evaporation...". Furthermore possible misleading conclusions emanate from *uncontrolled* experiments (no prior calibration between pairs of drainage before disturbance) as noted by Bruijnzeel (1989) in the case of work reported from central Java (Hardjono, 1980).

The development of process-hydrology studies however, are not devoid of their own problems. In a recent commentary on the state of physically-based models, Beven (1987, 1989) highlighted the critical issues facing process hydrology and the inadequacies of such models. These included the problems of applying small scale physics of homogeneous systems to large scale drainage basins, eg. infiltration equations derived from laboratory experiments. As Beven (1989, p. 161) noted "... it is not possible to use small scale physics equations (such as the application of infiltration theory in runoff generation studies) at the grid scale (eg. 250 x 250 m in the case of the Système Hydrologique Européen, SHE model, Abbott, 1986a, b: Bathurst, 1986a, b); and that we should be developing more complex equations that account for the effects of such heterogeneity". These concerns also applied to temporal heterogeneity at a point within a drainage basin as well as spatial heterogeneity. Amongst several developments required, Beven (1989, p. 170) outlined the need for closer correspondence between model equations and field processes at different scales.

It was in recognition of the preceding issues that major programmes initiated between the Department of Geography of James Cook University and the Queensland Department of Forestry in 1974 in the tropical rainforest of north-east Queensland, and in 1980 with CSIRO Division of Soils, Townsville, in an open eucalypt woodland within the semi-arid area of central-north Queensland.

Both programmes were initiated to seek baseline information on the mechanisms of storm runoff for the development of rigorous land management guidelines in connection with disturbance by logging and clearing of tropical rainforest, and the future introduction of improved pasture species and more intensive grazing in the semi-arid area. These research programmes are still continuing and this paper will briefly review the published literature to date in each study and outline possible future developments. Special emphasis will be placed on the interaction of synoptic climatology with the runoff process in both studies. As this is a review, only a brief description of the physical background, and experimental and analytical methods for each study will be given. Further details are obtainable from the literature cited.

THE WET TROPICAL COAST

The problem

Work in this area has focussed on paired experimental catchments in lowland tropical rainforest near Babinda (Fig. 1) (17°20'S, 145°58'E). They were originally installed by the Queensland Department of Forestry in 1969. The earlier objective was to develop a water balance for both catchments (North Creek, 18.3 ha; South Creek, 25.7 ha) to determine the hydrological impact of land use change. Some 67% of North Creek was subsequently logged and cleared between June 1971 and July 1973 in preparation for the establishment of tropical pastures (Fig. 2). This was never achieved, because of economic problems in the beef cattle industry, and the drainage basin remained largely bare for over two years before complete recolonisation by volunteer grasses and regrowth forest.

The results up to the end of 1974 were presented in detail by Gilmour (1975) and in summary by Gilmour (1977). After logging and clearing in North Creek, there was no detectable change in quickflow volume, quickflow duration and time to peak and only weak statistical evidence for a small increase in peak discharge. These characteristics implied that there were only minor changes in the storm runoff process in the wet season (December to mid-June), when 85% of the annual rainfall is recorded (mean annual rainfall, 4009 mm, 1970-1983 incl, median 3630 mm, range 2654 mm (1980) — 5496 mm (1973). Also noted was the rapidity with which both North and South Creek responded to heavy rain with frequently more than 45% of gross storm rain appearing as quickflow. It was these factors which provided the initial interest and prompted a more detailed investigation of the runoff process.

Physical background

South Creek is characterised by steep slopes (average 19°) (Fig. 1) and underlain by deep, kaolin-dominated silty clay loam to clay soils which may continue to 6 m in depth (Red Podzolic, Stace *et al*, 1968; intergrade Ultisol-Inceptisol, Soil Survey Staff, 1975; detailed descriptions are given by Bonell *et al*, 1981, 1983a, b), formed from basic metamorphic rocks, the Babalangee Amphibolite of de Keyser (1964).

The combination of high root density in the top 0.2 m and the rapid incorporation of organic matter from the surface layer of rotting leaf and twig litter, causes a marked decline in soil permeability (field saturated hydraulic conductivity, K*), and an increase in bulk density with depth using the methods of Talsma (1969) and Talsma and Hallam 1980. This means that the surface soils (0-0.1 m) are highly transmissive (log mean K* = 20.22 m day^{-1}, n = 65 > 800 mm hr^{-1}), even to peak monsoon rain intensities. The next 0.10 m is a transitional layer in terms of transmissivity (log mean K* = 1.44 m day^{-1}, n = 60,60 mm hr^{-1}). It is the subsoil below 0.2 m in particular which controls the runoff process and therefore the magnitude of the lateral and vertical stormflow components.

The runoff process

The most outstanding feature was the frequent occurrence of saturation overland flow in the monsoon season monitored at three detailed study sites (Fig. 1: see Bonell *et al*, 1981 and Gilmour *et al*, 1980 for experimental details). Furthermore the quickflow component (Lyne and Hollick, 1979; Moore *et al*, 1986) of the stream hydrograph very closely mirrored the time of occurrence of saturation overland flow and subsurface stormflow above 0.25 m depth (Bonell *et al*, 1986). Cross-correlation analysis for 38 major storms between January and mid-June, 1976 and 1977 (Bonell *et al*, 1986) indicated that the frequency distribution of maximum coefficients had modal response times of 12 min for saturation overland flow and 24 min for stream discharge despite differing storm lengths and intensities. This highlighted the importance of rainfall intensity and enabled the development of simple lagged regression models (Bonell *et al*, 1979, 1981).

The interaction between the prevailing rain intensities and the hydraulic properties of the subsoil below 0.2 m largely explains these responses. On considering the rainfall frequency-intensity-duration analysis (using RRUMS, Littleboy *et al*, 1986), the 0.1 hr equivalent hourly intensities range from 95 to 247 mm hr^{-1} and even absolute hourly intensities lie between 46 and 104 mm hr^{-1} for return periods ranging from 1 to 14 years (Fig. 3). These figures emphasize the high short term intensities

which occur during the summer months. But what makes this area outstanding is the long duration of rainfall events which is shown by the 24 hour amounts which range between 8 and 27.5 mm hr^{-1}. Clearly this subsoil layer impedes the vertical transmission of rain water during storms, leading to saturation overland flow and subsurface stormflow particularly in the root layer.

The significance of rain intensity in differentiating between this area and equatorial rainforest areas is well demonstrated by data presented by Griffiths (1972) for the Lower Congo and west Malaysia by Lockwood (1967).

When comparing Kinshasa (Lower Congo) with Babinda (Table 1), it is evident that the equatorial location records much lower longer duration rainfalls. Shorter term amounts (say, less than 1 hour) however, are not greatly different. It is significant that the return period for amounts exceeded once every 10 years in West Malaysia, occur at least once every two years in Babinda (see Lockwood, 1967).

The hydraulic status of the Babinda soils is also very important. During the wet season the matric potentials (¥) are only marginally below atmospheric pressure (¥,0 to -1 m). During the early part of storms rain quickly occupies most of the remaining air-filled pores and positive matric potentials develop (¥ > 0 m), which allows widespread saturation and runoff to redevelop almost instantaneously. A similar process has been described elsewhere (O'Brien, 1982; Abdul and Gillham, 1984, Gillham, 1984). Furthermore, the use of tritiated water as a tracer indicates that both interstitial piston flow (Foster and Smith-Carrington, 1980) and macropore or preferential flow, operate simultaneously in the soil-water recharge process (Bonell *et al*, 1982, 1983a).

In summary, the quick response of the various stormflow components is a function of several factors including high rainfall intensities, sparsely littered forest floor, large volume of biopores in the top soil, high antecedent soil moisture, steep slopes and the addition of numerous linear, shallow swales which add to the dendritic drainage density (0.23 $m.m^{-1}$). This network is able to tap a substantial amount of the saturation overland flow and to a lesser extent subsurface stormflow. It is these characteristics which can give peak stream discharges in excess of 5000 l/s^{-1} (70 mm hr^{-1}) from South Creek (see the example of January, 1981, described in Bonell *et al*, 1986).

Despite the varying contributions by volume of saturation overland flow and subsurface stormflow (especially in the top 0.25 m) at the three study sites, the close relationship between these components and rainfall and in turn with stream discharge could be argued as typical responses over large areas of the catchment (for example Bonell *et al*, 1981; Cassells *et al*, 1985). However, Gilmour *et al*, (1980) acknowledged the need for a more detailed survey of hydraulic properties across the catchment to check the representativeness of the runoff plots. Work commenced in 1985 (with D. Cassells) measuring the spatial variability of field saturated hydraulic conductivity, K* (Talsma and Hallam, 1980; Reynolds *et al*, 1983) of the 'impeding layer' 0.2-0.5 m at several points over North and South Creek (Figs. 4 and 5). From a sample of 5 holes at each site, the log mean was calculated.

Preliminary results for South Creek (Bonell *et al*, 1987) suggest that the runoff characteristics previously described for the runoff plots (Bonell *et al*, 1981) apply to a large proportion of the catchment so far investigated. The log mean K* for South Creek based on a sample size, n = 219 (0.2 - 0.5 m depth) is 3.5 mm hr^{-1} (unpublished data) (*) which is frequently exceeded by the high

(*) Note the increase in sample size from that reported by Bonell et al, 1987 causes K to increase from 1.4 to 3.5 mm hr^{-1}.*

prevailing intensities. During intense monsoon rainfall, saturation overland flow is expected to occur at all sites, other than limited areas similar to site 5. However, on this basis for runoff plots in Ia and Ib, subsurface stormflow would become more significant over large areas of the catchment when rain intensities decline in the post-monsoon season (April to mid-June, 21.5% of mean annual rainfall, max 6 min storm intensities, 25 - 80 mm hr^{-1}). The lithology becomes important here. For example the metamorphic rock exhibits strong schistosity with a coarse grained texture (Richards, 1977; Arnold and Fawckner, 1980) which is commonly found preserved in sections of the soil profile as at plots Ia and Ib. Differential weathering results in localized pathways of higher hydraulic conductivity, up to 4 m day^{-1}, which are up to two orders of magnitude higher than the surrounding soil matrix. This encourages greater volumes of subsurface stormflow. At the bulk of sites sampled, saturation overland flow would be restricted to peak rainfall intensities during the post-monsoon season, though it would continue to monopolize the hillslope discharge of the sites directly comparable to study site 2.

THE SEMI-ARID OPEN EUCALYPT WOODLAND

The problem

Little is known of the runoff processes in the eucalypt woodlands of the 'smooth plainlands' in the semi-arid and tropics of Australia, which are characterized by low topographic relief and the lack of an integrated stream network (Gifford, 1978; Pilgrim *et al*,1979). Previous water balance work by Williams and Coventry (1979, 1981) near the experimental site (20°45'S, 145°10'E) implied runoff to be very small. Strong evidence suggested water losses were by evapotranspiration and deep drainage alone. Such areas are also similar to parts of the 'Sahel' of West Africa (Williams *et al*, 1985) and need to be investigated to provide a baseline against which to evaluate the impact of land use change in these environments on the landscape hydrology.

Physical background

The work was carried out to the east of Torrens Creek on a slope of 1.5% (0.8°) under an open eucalypt woodland on a deep (5-36 m+) red earth soil (Stace *et al*, 1968; Oxic Paleustulff, Soil Survey Staff, 1975). These deep loamy soils have a massive structure.

Other details concerning the geology, pedology and hydrology of the area are described elsewhere (Coventry and Williams, 1984; Williams and Coventry, 1979).

The rainfall has a high index of variability (Brudekin Project Committee, 1976) and is strongly seasonal with 71% of the mean annual rainfall of 552 mm (median 497 mm) occurring in the summer wet season, December to March (Comm Aust, Bur Met, 1977).

Rain commonly results from thunderstorms which produce high intensity falls of short-duration (< 1 hr). Maximum 1 minute intensities frequently occur in the range 36-72 mm hr^{-1}, although peak intensities over 1 minute intervals of up to 360 mm hr^{-1} have been recorded in our experiments. Individual storm totals are low and only occasionally exceed 30 mm. Daily totals can however be very much higher when more than one event occurs.

The low, open woodlands are dominated by Eucalyptus and/or Acacia species and support a discontinuous ground cover of spinifex (*Heteropogon contortus*) and white spear grass (*Aristida leptopoda*).

Scattered throughout the grass understorey are low termite mounds dominated by *Drepanotermes rubriceps* (Holt, 1985, pers. comm.) and bare areas whose surfaces are either smooth and crusted (Mott *et al*, 1979) or covered with a thin layer of fine sand deposited by the erosion process of rainflow transportation (Moss *et al*, 1979). There is no evidence of scour by flowing water such as rills or gullies. Soil fauna such as ants produce macropores which are significant in this environment. The openings of such channels are temporarily or permanently blocked by inwashing of splashed material from raindrop impact especially where a low protective vegetation cover is absent (McIntyre, 1958a, b).

The experimental methods

Details of the experimental methods have been discussed elsewhere (Bonell and Williams, 1986b, 1987; Williams and Bonell, 1987, 1988). The principal focus was a cascade system of five troughs, 10 m long and offset at 25 m intervals, which monitored a 100 m section of slope (Fig. 6) located 2.5 km from a subdued topographic divide. This design is based on the assumption that the overland flow observed on the upslope trough is an estimate of the runon to a 250 m^2 plot and that the runoff from the plot is monitored by the downslope trough. Unlike bounded plots, the continuous systems allows the outputs and inputs of both water and sediment to be estimated without interference to the natural processes.

The runoff-runon (mm) for the plots between the troughs for a given period is given by X = Qd = Qu where Qu is the upslope and Qd is the downslope overland flow. Infiltration, i (mm) for a given period is calculated by i = R - X - dS - dV where R is the rainfall in the given period, and change in surface detention store and depth in surface water is given by dS while dV represents the change in water interception by vegetation.

It follows that X is positive for runoff and negative for runon. Where runon prevails, this adds to rainfall and contributes to infiltration. For the time intervals of 1 min used in the analysis it is assumed that dS and dV are zero. Consequently the plots behave as a constant head infiltration device in which ponded infiltration theory is applied to determine cumulative infiltration using rainfall and overland flow only, [dS = 0], from the commencement of overland flow.

The runoff process

The time to commencement of runoff, t_r could be as short as 1 min when average rain intensities were high (equivalent hourly rate up to 84 mm hr^{-1}) and inferred incipient ponding (Rubin, 1966) occurs even earlier. Rain intensities that generate Horton-type overland flow (Horton, 1945; Dunne, 1983) also showed a marked variability over time above 10 mm hr^{-1} due to the temporal variability of soil hydraulic properties (Bonell and Williams, 1986a, b). Such variability reflects in part the change in soil fabric from biological activity, raindrop compaction and dessication cracks of the surface crust.

The trend of runoff-runon is not consistent in the storms shown in Table 2. For most events Plots 2 and 3 are runoff areas, but the volumes generated remain small and are less than 19% of total rain. Plot 1 changes from a runoff to a runon area from 23.1.82 whilst Plot 4 is a consistent runon area.

acting as a sink for excess runoff generated by the preceding plots. This internal redistribution causes only a small amount of overland flow (≤ 1 mm) to be exported downslope out of this 100 m transect, and it is less than 4% of total rain.

Infiltration parameters

The infiltration parameter sorptivity, S and transmission, A of Philip (1969) and *in situ* field saturated hydraulic conductivity K* were determined over time from infiltration rings (0,3 m dia, 0.15 m deep driven into the soil 0.10 m), using analytical techniques described by Bonell and Williams (1986a). The same hydraulic properties at the scale of the plot were determined from cumulative infiltration as a function of time (Bonell and Williams, 1986b; Williams and Bonell, 1987, 1988), using the simple analysis described above.

The range and magnitude of the sorptivity parameter (Philip, 1969) in the infiltration rings were small (grand mean, 0.097 mm $s^{-1/2}$ Bonell and Williams, 1986a) and were consistent with the low storage capacity (only 8-12% by volume of water held between matric potentials - 10 kpa and - 1500 kpa). The conditions of 'profile at infinity' (Philip, 1969) were quickly attained under ponded infiltration such that the transmission parameter, A in Philip's truncated equation, approximated K* (Bonell and Williams, 1986a) and cumulative infiltration (I) = K* t, where t is time from ponding.

A similar behaviour was observed for the runoff plots during ponding under natural rainfall (Bonell and Williams, 1986b; Williams and Bonell, 1987, 1988). Under a mature ground cover before fire, the same order of magnitude of K* was determined for the infiltration rings in non-vegetated surfaces (log mean K* = 65.8 mm hr^{-1}) and for the runoff plots (log mean K* = 42.1 mm hr^{-1}). This contrasts with K* determined from rings enclosing spinifex tussocks (289.6 mm hr^{-1}). These findings are supported by partial correlation analysis (Bonell and Williams, 1986b), which showed that 1 minute rainfalls with an equivalent hourly intensity of 60 mm hr^{-1} or greater were highly correlated with measured overland flow where the largest volumes are produced.

Away from the surface, the subsoil K* (Talsma and Hallam, 1980) is higher (log mean K* = 100.4 mm hr^{-1}) than the non-vegetated soil, but less than the surface soils associated with spinifex tussocks. The effects of raindrop impact are then evident at the surface.

Scale of measurement and soil variability

Williams and Bonell (1988) later analyzed over thirty storms ranging from 5 to 55 mm in magnitude and to date all storms provided remarkably linear cumulative infiltration-time relations, including records collected over a two year period following fire. The analysis assumed that once the surface detention store was filled (approximately 3-4 mm), the flow depth remained constant with time and the infiltration process could be described by I = K* t.

The spatial variability of the 0.7 m^2 ring estimates of K* was approximately 4-10 times greater than that for the large 250 m^2 plots. This is consistent with Sisson and Wieringa (1981) who noted a substantial reduction in spatial variability upon increasing the diameter of infiltration rings. With respect to temporal variability of K*, the plot estimates of K* were again much less variable in time than those of the rings, although the differences were less than for spatial variability. In addition rings enclosing bare soil appeared to undergo less variation with time than the part-vegetated rings.

A comparison of the combined spatial and temporal variability of K* for ring and plot estimates is set out in Table 3. For K* the plots provide a 3-4 fold reduction in variability over the infiltration rings located in bare surfaces and a 10-12 fold reduction compared to rings located in tussock vegetation. More important, the mean values of K* for 4 rings located in bare soil between tussocks were approximately twice that of the plots whilst those rings located in soil associated with grass tussock was some six or seven times larger than that estimated from the plot. Apart from differences in the scale of measurement, the fact the bare ring estimates are of the same order of magnitude to those from the plots is encouraging particularly when it is recognized that the rings and plot measurements were not made at exactly the same time.

This leads to the concept of the 'representative elementary volume' (REV) as applied to soil physical measurements (Youngs, 1983; Baveye and Sposito, 1984). To incorporate the macroscale variability, the sampling scale must exceed the REV of the system. This leads to the additional concept 'repetitive unit' which is intended at regarding the behaviour of an inhomogeneous material equivalent homogeneous material if the length scale of observation is much larger than the characteristic length of the repetitive unit (Fig. 7). From mapping of the understory, it would appear that the repetitive unit has characteristic lengths of approximately 1 to 2 m. It follows that the plot or infiltration ring dimensions would need to be at least this size before a reduction of spatial variability would be observed and it indicates why the spatial variability of the 250 m^2 plots is so small.

The problem of 'scaling-up' measurements made by rings to a plot level, disregarding a larger pixel scale as discussed by Beven (1989), are demonstrated by Williams and Bonell (1988). Whilst Youngs (1983) noted that there was no general solution for recombining hydraulic properties, Williams and Bonell (1988) weighed the K* values for each of the strata according to their relative area as follows. The area of soil associated with tussock grasses is 6 percent, the area associated with termite mounds is 1 percent, with the remaining 93 percent consisting of bare soil. Using the values of these strata and a value of 0.128 m d^{-1} for the termite mounds (Bonell and Williams, 1986b), results in an arithmetic mean K* for the soil system to be 2.82 m d^{-1}. This figure is still considerably greater than the mean for the plots of 1.06 m d^{-1}. A possible explanation is that the tussock areas are slightly higher in elevation than the bare soil surface and may not be ponded, in such areas infiltration would be determined by the rainfall rate only. The effect would be to reduce the estimates of K* for the plots biassed towards the bare soil. The fact that the arithmetic mean yields much larger values than the large plot estimates does serve to illustrate the intractable position if measurements are made at a scale smaller than the characteristics length of the repetitive unit.

The same work showed that the temporal variability in infiltration parameters that arise as a consequence of biological activity or the impact of rainfall cannot be removed by changing the scale of measurement. The temporal effect can however, be reduced at an increased scale of measurement through the influences of numerous compensating processes that influence soil hydraulic properties.

It is clear that the advantages of using bulk properties of the whole system are more useful than point soil physical properties (Youngs, 1983). The merit of measuring infiltration parameters from a hydrograph of a large unbounded plot or small catchment (eg: Burch *et al*, 1987) is that these soil parameters refer to a scale that appears to be representative of that landscape element.

It is apparent that this is a relatively simple environment for the testing of scale problems, physically-based infiltration theory and possible future application of physical process models.

HYDROLOGICAL IMPLICATIONS FOR LAND MANAGEMENT

The wet tropical coast — the impact of logging and clearing of tropical rainforest on storm runoff hydrology erosion

It became apparent by the 1960s that unconstrained logging was causing spectacular gully erosion up to 12 m deep (Gilmour, 1977a), especially on logging or 'snig' tracks. This instigated two separate investigations within the Freshwater Creek basin near Cairns (Gilmour, 1971) and in the Babinda catchments (Gilmour, 1977b).

The Babinda work followed the classes approach of calibration of undisturbed, paired catchments (North and South Creek), followed by monitoring the impact of logging and later clearing of North Creek. Statistical details of the work were presented by Gilmour (1977) and further interpreted in Gilmour *et al* (1982), in the light of process studies concerning runoff generation. Particularly outstanding was no detectable change in quickflow volume, quickflow duration or time to peak after logging and clearing in North Creek. These characteristics imply that there was only minor changes in the storm runoff, in terms of process and source areas despite a significant increase in soil moisture content (Gilmour *et al*, 1982) and an order of magnitude decline in the surface (0-0.1 m depth) log mean K*. For example, Gilmour (1975) showed that when the soils were in their driest condition after clearing in 1973, South Creek required 291 mm of rain for the soils in the surface three metres to attain 'field capacity', whereas the treated North Creek catchment required only 94 mm for the soils to reach the same condition.

Determinations undertaken between 1984-1986 (over 10 years since logging and clearing followed by forest regeneration) showed that the surface 0-0.1 m depth K* (log mean = 184.0 mm hr^{-1}, n = 34) was in the same order of magnitude as the corresponding K* for South Creek (log mean 842.5 mm h^{-1}), but obviously the absolute value is a lot lower and more towards the log mean K* for the 0.1 to 0.2 m depth (60.0 mm hr^{-1}, n = 60) in South Creek. In addition, there was no significant difference between the drainage basins at the depth intervals, 0.1-0.2 m and 0.2-0.5 m(*). It is not clear whether the significant decline in surface K* of North Creek is the result of either compaction from earlier logging and clearing coupled with a reduction in soil biological activity and raindrop compaction of the newly exposed soil; or erosion of the original top 0.1 m exposing part of the former 0.1-0.2 m layer in the undisturbed soil. Current work detecting Caesium-137 levels in the soil profile will assist in this interpretation. The fact that the subsoil K* for both North and South Creek, 0.1-0.2 m layer are comparable encourages the idea that compaction and reduction in biological activity maybe the more likely explanation. In this context it is interesting that the few determinations of K* for the surface 0-0.1 m layer in the remaining undisturbed area of the upper reaches of North Creek (log mean K* = 1144.8 mm hr^{-1}, n = 10) are not much higher than the larger sample measurements in South Creek.

Despite these surface changes of K* in North Creek, it is evident that the subsoil K*, continue to act as the 'throttle' or impeding layer in the storm runoff process in a similar manner to that occurring in undisturbed South Creek. Consequently determination of just this one parameter helps considerable to interpret Gilmour's (1975) earlier water balance results.

(*) *0.1 - 0.2 log mean K*, North Creek, 57.3 mm hr^{-1}, n = 28; South Creek, 60.0 mm hr^{-1}, n = 60 / 0.2 - 0.5 m log mean K*, North Creek, 3.3 mm hr^{-1}, n = 155; South Creek, 3.5 mm hr^{-1}, n = 219.*

Major changes however, were evident in the water quality of North Creek after the change in land use. Peak suspended sediment concentrations rose from 180 mg L^{-1} before logging to about 520 mg L^{-1} in the two years after logging.

Clearing brought a much more dramatic change in suspended sediment concentrations in North Creek reaching values as high as 400 mg L^{-1} despite dilution from peak discharges. From the data on stream sediment levels in North Creek, Capelin and Prove (1983) estimated that annual suspended levels rose from 4.8 tonnes ha^{-1} before disturbance to 10.9 tonnes ha^{-1} after logging and 59.6 tonnes ha^{-1} after clearing. Bedload was not measured, but Douglas (1967) suggested this factor may be as high as 50 percent of the suspended load which raises the total loss to about 90 tonnes ha^{-1}.

When the erodibility of various rainforest soil types is considered, the quoted erosion losses from the Babinda catchments are likely to be conservative if the same activity had been undertaken on other catchments of the same morphometry. Using the dispersion index of Middleton (1930), the most stable soils are those derived from basalt, basic metamorphic (Babinda catchments), colluvium and some of the granite members (Bonell *et al*, 1986). The remaining soils derived from granite and acid metamorphics were erodible below the surface layer where organic matter is not incorporated. Exposure of these subsoils by log haulage causes them to disperse easily from raindrop impact and concentrated overland flow especially on logging tracks. Thus overland flow can be a mixture of both saturation overland flow and Hortonian overland flow due to soil compaction.

Apparent from this Babinda study, is that the amount of vegetation and the conditions of the top 0.2 m of soil are relatively unimportant in terms of quickflow generation. But the same two factors are of great importance in controlling erosion. The frequency of widespread saturation overland flow in undisturbed rainforest due to the prevailing rainfall intensities and shallow impeding subsoil, ensures little change in the storm runoff hydrology even after varying degrees of soil compaction from logging and clearing.

The need for the development of watershed management controls was initially advances by the Freshwater Creek study. Gilmour (1971) presented evidence to show that the principal sources of sediment in the creek were from poorly located undrained roads and 'snig' tracks, and from earth and log filled crossings. In the light of these findings, several guidelines were put into operation and included:

1) Snigging and hauling through streams was prohibited.
2) The use of streamside buffer strips at least 20 m from the stream were adopted to reduce the supply of sediment from 'snig' tracks, roads and logging ramps. These strips also ensured stream bank stability from the high discharges resulting from monsoon storms.
3) Earth and log fill crossings were prohibited. The alternative was the construction of girder bridges.

Following the implementation of these guidelines, significant reductions in suspended load were evident. For example, the highest measured concentration was 188 mg L^{-1} after a 262 mm rainfall compared with c 780 mg L^{-1} after 66 mm storm before these initiatives (Gilmour, 1971).

Further refinements to Gilmour's management controls were subsequently developed in the light of understanding of regional hydrological processes developed in the Babinda Research Programme, and these have been routinely applied to all forest harvesting operations since 1981. The nature of these controls and the social and technical considerations were described in detail by Cassells *et al* (1984). Amongst the technical improvements were:

1) The allotment of specifications for buffer strip width based on watercourse width, soil type and catchment size.
2) Maximum spacing of cross drains along 'snig' tracks and roads for different slope angles and soil erodibilities to reduce concentration of overland flow.
3) Design and location of haulage roads, 'snig' tracks, stream crossings, landings and the general logging direction and methodology.

It is interesting to compare these findings with the controlled experimental study described by Nik (1987) and Law and Cheong (1987) referring to the Sungai Tekem Experimental Basin in Peninsular Malaysia. No soil hydraulic properties are reported, but Law and Cheong (1987) indicate the soils have high surface infiltration capacities. Following clearing, no significant change was observed in quickflow volumes, but peak specific discharges increased up to 65 percent more than that in the calibration period and time to peak decreased considerably. Following the complete establishment of cover crops, peak specific discharge reduced but still remained 30 percent higher than that in the calibration period. Significantly, suspended sediment loads of one of the partially deforested basins rose from 0.3 t ha^{-1} yr^{-1} to 4.1 t ha^{-1} yr^{-1} following initial clearing, before a decrease after establishment of a cover crop to 1.6 t $ha^{-1}yr^{-1}$. These losses are very low compared with Babinda and highlight the differences in rainfall characteristics, topography and soils between the two areas. For example, Law and Cheong report annual maximum rain intensities of 24 hr duration (range 64.5 to 149.5 mm) much lower then those experienced in Babinda (Table 1, Fig. 3).

The semi-arid open eucalypt woodland

Table 4 shows the aggregate fluxes in overland flow and sediment between field visits, rather than for specific storms (Table 2), before a severe fire passed through the experimental site. Aggregate erosion from rainflow transportation (Moss *et al*, 1979) along the 100 m segment of slope remains small (approx. 0.02 tonnes ha^{-1}) considering the amount of overland flow being exchanged between plots and even deposition is indicated, as shown by the negative change, is indicated during period 6. Following the fire, equipment malfunction caused some loss of data, but that available showed no statistical significant difference (Bonell and Williams, 1987) in terms of sediment transfer. Following a combination of all records from the plots 1 to 4, a good relation was developed (Fig. 8) between runon-deposition and runoff-erosion and the nonsignificant regression intercept is particularly notable. From a conceptual understanding of the erosion process (eg: Kirkby and Morgan, 1980) such a result can be expected, but to our knowledge has not been demonstrated from field experiments using natural rainfall. The commonly used bounded runoff plots in hillslope hydrology prohibit this type of analysis.

Clearly on these low relief landscapes where the soil infiltration properties are in near-equilibrium with the prevailing rain intensities, the amounts of erosion are small in the undisturbed landscape. Any disturbance by way of soil compaction from cattle or tracks induced by vehicles, has the potential to reduce infiltration and increase overland flow, and in turn erosion judging by field evidence of degradation in these landscapes.

DISCUSSION

The dominance of overland flow

In both the humid and semi-arid environment overland flow is the major delivery component, but the process of generation is quite different in undisturbed conditions. Hortonian overland flow prevails in the semi-arid area, where the lowest K* occurs at the soil surface due to raindrop compaction. Perhaps the occurrence of this flow type is not surprising as it is associated with arid and semi-arid landscapes where vegetation densities are low (Dunne, 1983), and the Torrens Creek experiment provides a classic example. But the temporal variability of surface K* requires different rain intensities and in turn different times to runoff to exceed infiltration and depression storage. Therefore factors such as biological activity and raindrop compaction continually altering the surface soil fabric cannot be ignored.

By contrast, the highly transmissive surface soils make Hortonian overland flow impossible in undisturbed rainforest, and the 'throttle' to vertical transmission of rainwater occurs below 0.2 m depth, away from the dense surface root mat. High rain intensities, long duration of storms and low prevailing soil matric potentials (¥) result in the rapid emergence of subsurface stormflow, especially in the top 0.25 m, and in turn widespread saturation overland flow in the monsoon season. This vindicates Burt's (1985: 582) observation for humid environments that ' ... amongst the various conclusions reached is the agreed dominance of subsurface (storm) flow as *the* major contributor to stormflow in its own right...'. Both flow components are significant contributors to quickflow, but saturation overland flow dominates in the monsoon (December-March) which is a remarkable response for a forested environment, and in areas of South Creek comparable with study site 2 in the post-monsoon (April-mid-June). Subsurface stormflow becomes a more significant contributor to streamflow over remaining areas of the catchment in the latter season, with saturation overland flow restricted to the highest rain intensities in storms. In terms of peak runoff volumes and lag times between rainfall and stream discharge, South Creek has a hydrological response more akin to an environment where Hortonian overland flow is the dominant contributor to stormflow rather than subsurface stormflow generally associated with humid forested lands, particularly in temperate areas. For the same catchment area of 0.257 km^2, Dunne (1978, [Figure 7.18 and Figure 7,19]) estimated a peak runoff rate of 0.6 mm hr^{-1} and a lag time of 12.99 hours from experience in humid temperate catchments (some of which are forested) where subsurface stormflow is claimed to be the dominant contributor to stormflow. This rainforest catchment has recorded peak flows up to 74 mm hr^{-1} and average lag response times of 0.4 hrs (mode 0.3 hr, range 0.2-0.9 hr) during monsoon storms (January to March, 1976 and 1977). These responses are more towards response patterns of environments dominated by Hortonian overland flow, where a similar-sized catchment can be expected to produce peak runoff rates of 150 mm hr^{-1}, with lag times of 0.32 hrs (Dunne, 1978 [Figures 7.7 and 7.8]). This highlights the significance of saturation overland flow as a contributor to stream flow in this environment and contributes to the high annual and individual storm runoff coefficients. About 65% (2515 mm) of the annual rainfall (4009 mm) appears as runoff and 47% of this amount appears as quickflow, mostly between December-May (Gilmour, 1975), thus incorporating the monsoon and the bulk of the post-monsoon season.

The disturbed North Creek would still favour saturation overland flow, but the lower surface K* could also produce infiltration-excess, Hortonian overland flow during the most highest short-term

rain intensities, especially in the summer monsoon season. A saturation overland flow is also capable of developing almost instantaneously following commencement of storms in the undisturbed rainforest, so there should be little difference in the timing of both overland flow mechanisms which explains why only minor changes in the storm runoff response occurred between the two drainage basins.

By contrast, Nortcliff and Thornes (1981) noted the occurrence of overland flow was rare in a hillslope study located in the Amazonas, near Manaus. The possible reasons will be discussed later. In the same area, Salati and Vose (1984) reported only 19 to 26 percent of the annual rainfall (c 2000 mm) appearing as total runoff (quickflow and delayed flow) from Amazon rainforest basins near Manaus. Elsewhere in undisturbed equatorial rainforest, Nik (1987) reported low annual runoff coefficients ranging between 9.0 and 14.3 percent across three drainage basins in the Sungai Tekem Experimental Basin Project in Pahang, Peninsular Malaysia where mean annual rainfall was 1722 mm. Law and Cheong (1987) noted quickflow accounted for only 21 percent of annual runoff due to the high infiltration capacities of these drainage basin soils. No data was presented on the hillslope hydrology, but the work was reviewed by Bruijnzeel (1989) who suggested that the relative absence of increased stormflows even following forest clearance, indicated that significant overland flow along hillslopes still did not occur. Other separate studies in lowland or highland equatorial rainforest for example, in Tanzania by Edwards (1979) and Lundgren (1980), and in the reviews by Lal (1981), Walsh (1980) and Douglas and Spencer (1985) all point to saturation overland flow being relatively unimportant except in highly localized areas in some of these environments.

The significance of rain intensity

The significance of rain intensity is central to the description of runoff generation in these studies, and was shown statistically by cross-correlation and lagged regression analysis referring to the rainforest (Bonell *et al*, 1979; 1981), and by simple regression and partial correlation analysis in connection with times to runoff and overland flow volumes in the semi-arid area (Bonell and Williams, 1986b). By definition, the role of rain intensity in producing Hortonian overland flow makes this conclusion perhaps predictable, although the temporal variability of rain amounts required for ponding between discrete events adds another perspective due to soil fabric changes. The evidence from the rainforest, however, differs from other environments. For example, the comprehensive studies by Hewlett and co-workers (Hewlett *et al*, 1977, 1985; Hewlett and Bosh, 1984) statistically showed that rain intensity had no appreciable effect on quickflow volumes and only a small effect on peak flows. The data base for that work was drawn from temperate areas where reported rain intensities, for example max 1 hr, and response ratios (quickflow/gross storm rainfall) are low compared with South Creek. The much lower rain intensities experienced in the Coweeta Experimental Forest project in the southern Appalachians are reinforced by the later summary of 40 years of rainfall data by Swift *et al* (1988). They noted that the reason why Hewlett *et al* (1984) strongly questioned the value of intensity in that environment was because '... nearly three-quarters of Coweeta's precipitation falls with an intensity of less than 10 mm hr^{-1}, and only 10 percent of storms have maximum intensities over 50 mm hr^{-1} (Swift *et al*, 1988, p. 43).

It is our intention to analyze the long-term rainfall records for both North and South Creek in the same way as Hewlett *et al* (1984), but based on the meteorological seasons, monsoon (December-March), post-monsoon (April-mid-June), winter (mid-June-September) and pre-monsoon (October-

November) (Bonell and Gilmour, 1980) rather than lumping all the storms together. Much of the discussion in this paper has concentrated on the first two seasons when 85 percent of annual rainfall occurs.

Soil hydraulic properties

The measurement of soil hydraulic properties and the use of elementary soil physics has been fundamental to both studies in the interpretation of runoff process on the lines called for by Burt (1985). The establishment of field saturated hydraulic conductivity as the dominant parameter in both studies holds significance for extrapolation to other 'similar' areas. A preliminary assessment of other geological and soil types has already been made on the wet tropical coast (Bonell *et al*, 1983b). In the meantime work has just been completed measuring K* on a 75 m^2 grid in both North and South Creeks to assist interpretation of the long-term rainfall-runoff records and for use in O'Loughlin's (1986) topography-catchment wetness model.

Despite the subsoil (> 0.2 m) of the rainforest impeding most of the rain, the transitional 0.1 to 0.2 m layer is capable of causing ponding during the highest short-term rains. It is ironic that the K* of this horizon is in the same order of magnitude as that of the non-vegetated areas in the semi-arid eucalypt woodland, and that maximum 1 minute rain amounts between the two environments are not too dissimilar (unpublished data). There are some parallels then in that each layer can act as a 'throttle' to downward movement of rainwater and this in turn produces overland flow. The point of genesis, however, makes this component hydrologically different between each environment.

The variable source area concept

The occurrence of widespread saturation overland flow and subsurface stormflow in rainforest, particularly in the summer monsoon, represents part of the extreme 'wet' hydrological situation in the context of Hewlett's variable source area concept. The proportion of South Creek contribution to quickflow depends on the transit distance saturation overland flow has to take before it is tapped by organized drainage lines, either perennial or ephemeral. The soil hydraulic properties, the intensity and long duration of monsoon storms, the high drainage density and the steep catchment slopes favour widespread contributing areas to quickflow. There is pedological evidence for natural erosion by saturation overland flow on the steeper slopes with only remants of the A^2 and A^3 horizons surviving. Research on hillslope erosion coupled with statistical (Hewlett *et al*, 1984) and topography-wetness modelling (O'Loughlin, 1986) will further check this conclusion. Furthermore new initiatives during the 1989-90 wet season will attempt to reconcile the earlier hydrometric study with the stream hydrographs utilizing the environmental isotopes deuterium, oxygen-18 and radon-222 to identify runoff sources (eg.: hydrograph separation into 'old' and 'new' water) on the lines described elsewhere (Bonell *et al*, 1989; Rodhe, 1987; Pearce *et al*, 1986; Sklash and Farvolden, 1979).

In the semi-arid study, the soil hydraulic properties and short-term rain intensities favour the classical Horton view of widespread areas of a catchment contributing to flood peaks. However, only a very small proportion of rain is transferred downslope to organized drainage and most overland flow is redistributed. This area differs from the Babinda study in that the storm durations are too short to maintain surface saturation for long periods, the slopes are too shallow for rapid transfer of overland flow, and the drainage network too poorly developed to capture most of it. Following the variable

source area concept, the contributing area to flood peaks would be dependent on such factors as the duration as well as the intensity of storms. For most rain events, this area would seem limited to the valley bottoms.

A synoptic climatology perspective

Much emphasis has been placed on rain intensity and how it makes these environments hydrologically active in comparison with other areas, especially with regard to the tropical rainforest. There is a link here between hillslope hydrology and synoptic climatology. Bonell *et al* (1986) reviewed the principal rain-producing systems affecting the wet tropical coast, but such descriptions have some relevance to the Torrens Creek area as well. In that review it was noted that north-east Queensland is located on the southern rim of what Ramage (1968) termed 'the maritime continent'. This area extends across from the Indo-Malayan archipelago, through Papua New Guinea to the scattered islands of the west Pacific, and incorporates a broad region of sea temperature maximum and large scale release of energy from convective activity. As McAlpine *et al* (1983, p. 1) commented, the maritime continent ' ...acts as an important global heat engine driving not only its own internal atmospheric circulation but extensive regional circulations to the north and south as well'. The geographical position of north-east Queensland in relation to this 'continent' makes it one of the most meteorologically active areas of the tropics. There is a marked concentration of high intensity rain in a few months of the year associated with the inter-hemisphere monsoon exchange of air (as represented by the monsoon trough and defined by Sadler and Harris, 1970); and the poleward draining of latent heat energy and moisture liberated from convective activity in the maritime continent by low pressure troughs in the upper westerly circulation (as defined by McAlpine *et al*, 1983). All four rain generating mechanisms of WMO (1983) are represented on the wet tropical coast (convection, convergence, orographic and cyclonic) (Bonell *et al*, 1986), but what makes this area outstanding is that circular disturbances can be almost stationary for several days, embedded in the monsoon trough over the warm waters of the Gulf of Carpentaria or western Coral Sea. Such disturbances are more commonly tropical depressions (as defined by Lourensz, 1981) rather than tropical cyclones (as defined by Bureau of Meteorology, 1978), and the nature of this activity means that rain occurring on a few days makes up a large proportion of the annual total. For example, 48 percent of the annual 1981 rainfall total of 5324.5 mm occurred between January 3-17, inclusive.

As discussed elsewhere (Bonell *et al*, 1986) a significant proportion of tropical rainforest, for example in Indonesia, Malaysia and the Congo basin, is associated with the maximum cloud zone (as defined by Davidson *et al*, 1983; Sadler, 1974) of the summer equatorial westerlies (Atkinson and Sadler, 1970), or orographic uplift of winter easterlies where rain occurs from deep convective cells and not from well organized circular systems in either season. The Amazon is different, with the main influx of atmospheric moisture coming into the basin only as easterlies from the Northern Hemisphere trade winds (Atkinson and Sadler, 1970; Salati and Vose, 1984). However, the geographical location of the area prevents the formation of tropical cyclone or depressions, and convective cells are once again the rainfall source as in the equatorial westerlies. Differences, then, can be expected solely on meteorological grounds between the hydrological response of these non-tropical cyclonic areas and the hydrological response for the wet tropics of north-east Queensland based on rainfall intensity (Bonell *et al*, 1986). In a survey of tropical rainfall, Jackson (1988a, p. 112) noted that ' ... lack of data for tropical areas, particularly in the case of conditions for periods less than 24 hrs makes it impossible to give indications of highest falls and intensities experienced'. However, he concurred with the view

that thunderstorms may produce the highest falls for periods of 1 hr or less, especially identified with the low latitude areas like the Amazon. In turn Jackson (1988a, p. 112) noted that 'for longer time periods, high totals will be associated with major organized disturbances of which the most extreme case is the hurricane — especially a slow moving, declining system. Since hurricanes in particular do not usually occur within about 5° of the equator, it follows that maximum totals are found in higher latitudes'. When comparing daily rainfall over northern Australia with other tropical areas, Jackson (1988b) noted that northern Australia rainfall stations (including some on the wet tropical coast of NE Queensland) tended to record most concentrated rainfall, i.e. fewer raindays and higher mean daily intensities, compared with most other areas of the tropics, thus emphasising northern Australia as a highly energetic environment. However the simple distinction between tropical cyclonic and non-cyclonic areas maybe inadequate, because an earlier study (Jackson, 1986) showed stations in central Africa having the closest rainfall characteristics to those found in northern Australia. Other factors such as orographic uplift over high topography may be as significant and need further investigation.

The more remote position of Torrens Creek, in relation to well-organized maritime disturbances, means that scattered thunderstorms are the most common source of rain. This contrasts with the wet tropical coast where thunderstorms are less frequent. The Gulf of Carpentaria is a major source of moisture into central-north Queensland induced by the eastward passage of upper meridional troughs, or more occasionally from the equatorial westerlies associated with the southward movement of the monsoon trough.

Do forests act like 'Sponges'? The NE Queensland tropical rainforest experience

The clearing of forests in tropical uplands has often been misconceived as the major source of severe flooding, despite recent scientific reviews showing that there is no strong evidence for this belief (Hamilton, 1987; Bruijnzeel, 1987). Perhaps the commonly quoted example is just outside the tropics, concerning deforestation in the Middle Hills of Nepal being blamed for increased flooding in the lower Indo-Gangetic plain (eg: Nautiyal and Babor, 1985) even though preliminary studies have argued the contrary (Gilmour *et al*, 1987).

The process hydrology studies described here have shown that widespread saturation overland flow can occur within tropical rainforest where prevailing rain intensities are high and subsoil K* are very low, away from the surface horizons containing biological activity. Under these circumstances, floods can occur from pristine forested drainage basins on the same scale as from disturbed areas. For example, Bonell *et al* (1986) describe in detail the storm runoff generated from 2560 mm of rain between 3-17 January, 1981 in the Babinda drainage basins. During this period daily rain exceeded 200 mm on 6 days, with a maximum total of 433 mm on 12 January 1981. Total discharge for North Creek (disturbed) and South Creek (undisturbed) was respectively 2096 mm and 1880 mm and so did not differ greatly. In more detail, seven hydrograph consecutive separations were analyzed over this 14 day period and quickflow percentages of total rain ranged from 10 to 75 percent for North Creek and 18 to 64 percent for South Creek. The small difference between these treatments confirm that pristine forests do not act as infinite 'sponges', but can generate flood-producing runoff.

Discussion so far has concentrated on the effect of rainfall on lowland tropical rainforest. Further west on the mountain range, more impressive rain amounts are recorded. A rain gauge on Mt Bellenden Ker Top (1561 m), immediately to the west of Babinda, has a mean annual rainfall of 7664 mm, 1974-84 incl. (median 7210 mm, range 6305 mm (1974) to 11,346 mm (1977)). It is from such

mountain areas covered in 'pristine' forests that a major contribution to the recurrent disastrous flooding is made by affecting the lower reaches of the Mulgrave, North and South Johnstone, Tully and Murry Rivers (Bonell, 1983). Annual runoff coefficients can also range between 0.58 and 0.90 (Bonell, 1988).

When the K* results presented by Herwitz (1986) are examined for a sample plot on the Mt Bellenden Ker range, it is evident that a similar trend exists as that described for the Babinda study in the order of magnitude decline in K* down the profile, despite differences in parent materials. The soil horizons below 0.20 m are once again the persistent impeding layer (K* range 2 to 7 mm hr^{-1}), although the 0.05-0.20 m layer also would be impeding to maximum short term intensities in excess of 100 mm hr^{-1} (K* = 108 mm hr^{-1}, 0.05 -0.20 m layer). Consequently, widespread saturation overland flow would occur during the summer monsoon season, but Herwitz produced results to show that a combination of high intensity rainfall and the funnelling effect of trees would produce 'localized', based stemflow fluxes capable of exceeding the surface K* and thus producing Hortonian overland flow.

Under these wet conditions, it can be concluded that forests respond to extremely high rainfalls similar to other land use conversions and do not act as infinite 'sponges'. One of the critical differences between tropical rainforests in say, the Amazonas, and NE Queensland concerns the vertical changes in K* down the soil profile. The results presented here show that the transmissive layer is very shallow and confined to the top 0.2 m of soil. Irrespective of any reductions in surface K* from compaction, the chief 'throttle' controlling the disposition of soil/rain water remains in the shallow subsoil ($\geq$ 0.2 m depth). Good quality soil K* from other rainforest environments is scarce, but Nortcliff and Thornes (1981) presented K* for Amazonas Oxisols near Manaus which showed that those soils had a deeper transmissive layer down to 0.90 m depth (K* range 61.3 to 156.7 mm hr^{-1}) before K* lowered to 21.7 mm hr^{-1} (0.90-1.15 depth) which is in the range of the more permeable soils of NE Queensland, eg. derived from basalts and colluvium (Bonell *et al,* 1983). The K* of the top 0.15 m of the Amazonas soils (K* = 921,3 mm hr^{-1}) differed little from those reported from NE Queensland. The effects of surface compaction, however, in the Amazonas might have greater ramifications on the runoff process because the predisturbance subsoil 'throttle' is more remote from the surface (unlike in the Babinda study), and the upper transmissive layer is much deeper which acts as a buffer to overland flow. Nortcliff and Thornes' (1981) had noted that the occurrence of overland flow was rare. Consequently, the effect of transferring the 'throttle' layer to the surface in relation to short term rain intensities on disturbance, might be more significant in causing changes in the delivery mechanisms and magnitudes of storm runoff. The need for detailed K* measurements on the lines described in the Babinda study is highlighted to substantiate this argument.

CONCLUSION

The tropical rainforest presents the paradox of high surface infiltration rates typical of humid forest environments but a runoff response that is not typical of those environments. Given the high field saturated hydraulic conductivity of the surface rainforest soils, Hortonian overland flow is clearly not possible. But the high prevailing rain intensities and the low K* subsurface values ensure the frequent presence of widespread saturation overland flow in the summer, and cause this catchment to be highly responsive to rainfall inputs. Similarly, the surface permeability of the open eucalypt woodland soils is comparatively high despite raindrop compaction producing sealed areas. Ponding and subsequent Hortonian overland flow only occur because short-term rain intensities are high. There

is a parallel between these contrasting environments in that each has a 'throttle' layer to the prevailing inputs, *viz* at the surface in the semi-arid study and the subsoil in the rainforest. This is caused by opposite trends in the order of magnitude of change in K* down the respective soil profiles. Field saturated hydraulic conductivity is a significant hydraulic property in both environments, where temporal as well as spatial variability has to be considered, especially in the semi-arid study.

In contrast to the rainforest example, most overland flow is redistributed within the semi-arid study because of the very shallow slopes. Such redistribution, however, is sufficient to provide a high erosion potential through rain-flow transportation (Moss *et al.*, 1979) following disturbance of these landscapes. The runoff characteristics on the wet tropical coast cause disastrous erosion to occur on disturbance as shown by the Babinda study. In addition, average annual losses of 100 tonnes ha^{-1} have been estimated for 11,000 ha of sugar canelands on various soils north of Cardwell (Capelin and Prove, 1983).

There are, then, close links between storm drainage and synoptic climatology in north-east Queensland. Such links have been largely ignored in other runoff processes studies because most research has been undertaken in humid temperate areas of western Europe and the eastern United States where rain intensities are much lower in magnitude (examples: Hewlett *et al*, 1977; Weyman, 1973) and where streams have a lower responsiveness to storms. The tropical rainforest study, in particular, emphasize this link. This means that, when considering synoptic climatology in addition to soil and slope factors, differences between this area and other rainforests can be expected. In a review of runoff process and models in the humid tropics, Walsh (1980: 181) noted that of all the tropical rainforest areas so far investigated, the Babinda catchments have '... the only *distinctively tropical* runoff process pattern'. Clearly the high rainfalls in the Babinda catchments outweigh the lithologic influences. Otherwise the soil hydraulic properties would have suggested a localized saturation overland flow and subsurface stormflow model found elsewhere in humid tropical and temperate areas (Kirkby, 1978; Walsh, 1980). Detailed knowledge of the interaction between synoptic climatology and runoff hydrology is clearly required.

Finally the Australian experience has emphasized the need for detailed measurements of soil hydraulic properties, notably K*, at different scales of investigation in line with Beven's (1989) comments and the need for an open, cascade trough system to monitor overland flow rather than the commonly used bounded plot studies. This new design forms the basis for future investigations concerning the possibilities of extrapolation of measured parameters to other ungauged areas. Future research on these lines is suggested to resolve the continuous debate whether conversion of forests increases storm runoff or not in a wide variety of humid tropical environments. In the meantime an explanation is offered for the dichotomy of views in terms of the effect of land use conversion on the runoff process.

ACKNOWLEDGEMENTS

These research programmes have been supported by the Australian Research Grants Scheme, Australian Water Resources Council, National Soils Conservation Program, CSIRO (Division of Soils), James Cook University (Special Research Grant and University Research Grant Schemes), and the Queensland Department of Forestry.

REFERENCES

Abbott, M. B.; Bathurst, J. C.; Cunge, J. A.; O'Connell, P. E. and Rasmussen, J. An introduction to the European Hydrological System — Système Hydrologique Européen, 'SHE', 1. History and philosophy of a physically-based, distributed modelling system. *Journal of Hydrology*, 87, 45-59, 1986a.

Abbott, M. B.; Bathurst, J. C.; Cunge, J. A.; O'Connell, P. E. and Rasmussen, J. An introduction to the European Hydrological System — Système Hydrologique Européen, 'SHE', 2. Structure of a physically-based, distributed modelling system. *Journal of Hydrology*, 87, 61-77, 1986b.

Abdul, A. S. and Gillham, R. W. Laboratory studies of the effects of the capillary fringe on stream flow generation, *Water Resources Research*, 20(6), 691-698, 1984.

Arnold, G. O. and Fawckner, J. F. The Broken River and Hodgkinson Provinces. In: Henderson, R. A. and Stephenson, B. J. (eds.), *The Geology and Geophysics of North-east Australia*, Geol. Soc. Aust. Inc., Qld. Div. July 1980, 175-189, 1980.

Atkinson, G. D. and Sadler, J. C. Mean-cloudiness and gradient-level-wind charts over the tropics. Vol. II, Charts, *Technical Report 215*, Air Weather Service (MAC), USAF, 1970.

Baveye, P. and Sposito, G. The operational significance of the continuum hypothesis in the theory of water movement through soils and aquifers. *Water Resources Research*, 20, 521-530, 1984.

Bathurst, J. C. Physically-based distributed modelling of an upland catchment using the Système Hydrologique Européen. *Journal of Hydrology*, 87, 79-102, 1986a.

Bathurst, J. C. Sensitivity analysis of the Système Hydrologique Européen for an upland catchment. *Journal of Hydrology*, 87, 103-123, 1986b.

Bear, J. *Hydraulics of Groundwater*, McGraw-Hill, New York, pp. 28-33, 1979.

Beven, K. J. Towards a new paradigm in hydrology. *International Association of Hydrological Sciences, Water for the Future — Hydrology in Perspective*, (Ed. J. C. Rodda and N. C. Matelas), Publication N° 164, pp. 393-403, 1987.

Beven, K. J. Changing ideas in hydrology — the case of physically-based models *Journal of Hydrology*, 105, 157-172, 1989.

Bonell, M. Hydrological processes and implications for land management in forests and agricultural areas of the wet tropical coast of north-east Queensland. In: *Fluvial Geomorphology of Australia* (Ed. R. F. Warner), Academic Press, 41-68, 1988.

Bonell, M.; Cassells, D. S. and Gilmour, D. A. Vertical and lateral soil water movement in a tropical rainforest catchment. In: O'Loughlin, E. M. and Bren, L. (Eds.), *National Symposium on Forest Hydrology*, (Proc. Melbourne Symp. May 1982), Canberra, Institution of Engineers, Australia/ Forest Hydrology Working Group Australian Forestry Council, 30-38, 1982.

Bonell, M.; Cassells, D. S. and Gilmour, D. A. Vertical soil water movement in a tropical rainforest catchment in northeast Queensland, *Earth Surface Processes and Landforms*, 8(3), 253-272, 1983a.

Bonell, M.; Cassells, D. S. and Gilmour, D. A. Spatial variations in soil hydraulic properties under tropical rainforest in north-eastern Australia, *International Conference on Infiltration, Development and Application*, (Ed. Yu-si Fok), University of Hawaii, Water Resources Center, January 1987, 153-165, 1987.

Bonell, M. and Gilmour, D. A. Variations in short-term rainfall intensity in relation to synoptic climatological aspects of the humid tropical north-east Queensland coast, *Singapore Journal of Tropical Geography*, 1(2), 16-30, 1980.

Bonell, M.; Gilmour, D. A. and Cassells, D. S. A preliminary survey of the hydraulic properties of rainforest soils in tropical northeast Queensland and their implications for the runoff process. In: the Ploey, J. (Ed.), *Rainfall Simulation, Runoff and Soil Erosion*, Catena Supplement 4, 57-78.

Bonell, M.; Gilmour, D. A. and Cassells, D. S. The storm runoff response to various rainfall systems on the wet tropical cost of northeast Queensland. *East-West Center, Environment and Policy Institute Working Paper*, Honolulu, Hawaii, 96848, 48 pp. Presented in modified form in: *Australian National Rainforests-Study Report*, vol. 2, Australian Heritage Commission (P. A. Kershaw and G. Werran, eds.), 1989 (in press).

Bonell, M.; Gilmour, D. S. and Sinclair, D. F. A statistical method for modelling the fate of rainfall in a tropical rainforest catchment, *Journal of Hydrology*, 42, 241-257, 1979.

Bonell, M.; Gilmour, D. A. and Sinclair, D. F. Soil hydraulic properties and their effect on surface and subsurface water transfer in a tropical rainforest catchment, *Hydrological Sciences Bulletin*, 26, 1-18, 1981.

Bonell, M.; Pearce, A. J. and Stewart, M. K. The identification of runoff-production mechanisms using environmental isotopes in a tussock grassland catchment, eastern Otago, New Zealand, *Hydrological Processes*, 3, 1989 (in press).

Bonell, M. and Williams, J. The two parameters of the Philip infiltration equation: their properties and spatial and temporal heterogeneity in a Red Earth of tropical semi-arid Queensland, *Journal of Hydrology*, 87, 9-31, 1986a.

Bonell, M. and Williams, J. The generation and redistribution of overland flow in a massive oxic soil in a eucalypt woodland within the semi-arid tropics in north Australia, *Hydrological Processes*, 1, 31-46, 1986b.

Bonell, M. and Williams, J. Infiltration and redistribution of overland flow and sediment on a low relief landscape of semi-arid, tropical Queensland. *International Association of Hydrological Sciences, Forest Hydrology and Watershed Management*, Publication N° 167, pp. 199-211, 1987.

Bosch, J. M. and Hewlett, J. D. A review of catchment experiments to determine the effect of vegetation changes on water yield and evapotranspiration. *Journal of Hydrology*, 55, 3-23, 1982.

Bruijnzeel, L. A. Environmental impacts of (de)forestation in the humid tropics. A watershed perspective *MURS* Programme 1986-87. *Water for Mankind in the Years 2000*, Paris, France, Seminar 25-26 April 1987, 33 pp., 1987a.

Bruijnzeel, L. A. On the hydrology of moist tropical forests: with special reference to the study of nutrient cycling. Paper presented at British Ecological Society Symposium on mineral nutrients in tropical forest and savanna ecosystems, Stirling, 9-11 September 1987, 45 pp. 1987b.

Bruijnzeel, L. A. Review Paper. (De)forestation and dry season flow in the tropics: A closer look. *Journal of Tropical Forest Science*, 1989 (in press).

Burch, G. J.; Bath, R. K.; Moore, I. D. and O'Loughlin, E. M. Comparative hydrological behaviour of forested and cleared catchments in south eastern Australia. *Journal of Hydrology*, 90, 19-42, 1987.

Burdekin Project Committee. *Resources and Potential of the Burdekin River Basin, Queensland Appendix 2a: Land and Associated Features*, Canberra, Australian Government Publishing Service, 1976.

Bureau of Meteorology. *Australian Tropical Cyclone Forecasting Manual*, Australian Bureau of Meteorology, 1978.

Burt, T. P. Slopes and slope processes, *Progress in Physical Geography*, 9, 582-599, 1985

Capelin, M. A. and Prove, B. G.. Soil conservation problems of the humid coastal tropics of north Queensland, *Proceedings of Australian Society of Sugar Cane Technologists*, 87-93, 1983.

Calder, I. R. What are the limits on forest evaporation? Comment, *Journal of Hydrology*, 82, 179-184, 1985.

Cassells, D. S.; Gilmour, D. A. and Bonell, M. Watershed forest management practices in the tropical rainforests of north-eastern Australian. In: O'Loughlin, C. L. and Pearce, A. J. (Eds.), *Proc. IUFRO Symp. on Effects of Forest Land Use on Erosion and Slope Stability*, East-West Center, Honolulu, NZ Forest Research Institute Publication, 289-298, 1984.

Cassells, D. S.; Bonell, M.; Hamilton, L. S. and Gilmour, D. A. The protective role of tropical forests: A state of knowledge review. In: *Agroforestry in the Humid Tropics — its protective and ameliorative roles to enhance productivity and sustainability*. (Eds. N. T. Vergara and N. C. Briones), Environment and Policy Institute, East-West Center, Honolulu, Hawaii, Southeast Asian Regional Center for Graduate Study and Research in Agriculture, College, Laguna, Philippines, pp. 31-58, 1987.

Chang, J. Hydrology in humid tropical Asia. Paper presented at the UNESCO *International Colloquium on the Development of Hydrologic and Water Management Strategies in the Humid Tropics*, Townsville, 15-22 July, 1989, Australia, 21 pp. 1989.

Commonwealth of Australia, Bureau of Meteorology. *Rainfall Statistics — Australia*, Metric Edition, Australian Government Publishing Service, 1977.

Coventry, R. J. and Williams, J. Quantitative relationships between morphology and current soil hydrology in some Alfisols in semi-arid tropical Australia, *Geoderma*, 33, 191-218, 1984.

Davidson, N. E.; McBride, J. L. and McAvaney, B. J. The onset of the Australian monsoon during Winter MONEX: Synoptic Aspects, *Monthly Weather Review*, 111, 496-516, 1983.

DeKeyser, F. *Explanatory Notes on the Innisfail, Qld Sheet SE/55-6*, Department of National Development, Bureau of Mineral Resources, Geology and Geophysics, Commonwealth of Australia, 1964.

Douglas, I. and Spencer, T. (Eds.). *Environmental Change and Tropical Geomorphology*, London, Allen and Unwin, 1985.

Dunne, T. Field studies of hillslope processes. In: Kirkby, M. J. (Ed.), *Hillslope Hydrology*, Chichester, Wiley, 227-293, 1978.

Dunne, T. Relation of field studies and modelling in the prediction of storm runoff. *Journal of Hydrology*, 65, 25-48, 1983.

Edwards, K. A. The water balance of the Mbeya experimental catchments. *East African Agricultural and Forestry Journal*, 43, 231-247, 1979.

Foster, S. S. D. and Smith-Carrington, A. The interpretation of tritium in the chalk unsaturated zone. *Journal of Hydrology*, 46, 343-364, 1980.

Gillham, R. W. The capillary fringe and its effect on water table response. *Journal of Hydrology*, 67, 307-324, 1984.

Gilmour, D. A. Catchment water balance studies on the wet tropical coast of north Queensland. Unpublished PhD Thesis, Department of Geography, James Cook University of North Queensland, 1975.

Gilmour, D. A. Effects of logging and clearing on water yield and quality in a high rainfall zone of northeast Queensland. In *The Hydrology of Northern Australia* (Proc. Brisbane Hydrol. Symp., June 1977), Canberra, Institution of Engineers Australia, Nat. Conf. Publ., 775, 156-160, 1977.

Gilmour, D. A.; Bonell, M. and Sinclair, D. F. An investigation of storm drainage processes in a tropical rainforest catchment. *Australian Water Processes Council Technical Paper* 56. Canberra, Australian Government Publishing Service, 1980.

Gilmour, D. A.; Bonell, M. and Cassells, D. S. The effects of forestation on soil hydraulic properties in the middle hills of Nepal: a preliminary assessment. *Mountain Research and Development*, 7, 239-249, 1987.

Gilmour, D. A.; Cassells, D. S. and Bonell, M. Hydrological research in the tropical rainforests of north Queensland: Some implications for land use management. In: *First National Symposium on Forest Hydrology* (Eds. E. M. O'Loughlin and L. J. Bren), Melbourne, May 1982, Instit. Engrs. Australia, Nat. Conf. Public, N° 82/6, pp. 145-152, 1982.

Gifford, G. F. Infiltrometer studies in rangeland plant communities of the Northern Territory, *Aust. Range J.* 1(2), 142-149, 1978.

Griffiths, J. F. *Climates of Africa*, Elsevier, Amsterdam, 1972.

Hamilton, L. S. Overcoming myths about soil and water impacts of tropical forest land uses. In: *Soil Erosion and Conservation* (Eds. by S A. El-Saify, W. C. Moldenhauer and A. Lo). Akeny, Soil Conservation Society of America, pp. 680-690, 1986.

Hamilton, L. S. The environmental influences of forests and forestry in enhancing food production and food security. FAO, Rome (1987). Presented at *Expert Consultation on Forestry and Food Production/Security*, Bangalore, India, 14-20 February, 1988, 69 pp, 1988.

Hamilton, L. S. (with P. N. King). *Tropical Forested Watersheds: Hydrology and Soils Response to Major Uses or Conversions*, Boulder, Westview Press, 1983.

Hardjono, H. W. Influence of a permanent vegetation cover on streamflow. In: *Proceedings Seminar on Watershed Management, Development and Hydrology*, Solo, 3-5 June 1980, pp. 280-297 (in Indonesia reported by L. A. Bruijnzeel, 1989), 1980.

Herwitz, S. R. Infiltration-excess caused by stemflow in a cyclone-prone tropical rainforest. *Earth Surface Processes and Landforms*, 11, 401-412, 1986.

Hewlett, J. D. Watershed managements. In: *Report for 1961 Southeastern Forest Experiment Station*, Asherville, North Carolina, US Forest Service, 1961.

Hewlett, J. D. and Bosch, J. M. The dependence of storm flows on rainfall intensity and vegetal cover in South Africa, *Journal of Hydrology*, 75, 365-381, 1984.

Hewlett, J. D.; Fortson, J. C. and Cunningham, G. B. Additional tests on the effect of rainfall intensity on stormflow and peak flow wild-land basins, *Water Resources Research*, 20, 985-989, 1984.

Horton, R. E. The role of infiltration in the hydrologic cycle, *Transactions of American Geophysical Union*, 14, 446-460, 1933.

Horton, R. E. Erosional development of streams and their drainage basins: hydrological approach to quantitative morphology. *Bull. Geol. Soc. Amer.*, 56, 275-370, 1945.

Jackson, I. J. Relationships between raindays, mean daily intensity and monthly rainfall in the tropics. *Journal of Climatology*, 6, 117-134, 1986.

Jackson, I. J. *Climate, Water and Agriculture in the Tropics*. Longman, Second Edition, 1988a.

Jackson, I. J. Daily rainfall over northern Australia: Deviations from the world pattern. *Journal of Climatology*, 8, 463-476, 1988b.

Kirkby, M. J. (Ed.). *Hillslope Hydrology*, Chichester, Wiley, 1978.

Kirkby, M. J. and Morgan, R. P. C. *Soil Erosion*, Wiley, Chichester, 1980.

Lal, R. Deforestation of tropical rainforest and hydrological problems. In: *Tropical Agricultural Hydrology —Watershed Management and Land Use* (Eds. by R. Lal and E. W. Russell), Wiley, Chichester, pp. 131-140, 1981.

Law, K. F. and Cheong, C. W. Effects of land use changes on the hydrological characteristics of Sungai Tekam Experimental Basin. Paper presented at UNESCO/MRP workshop on *Impact of Operations in Natural and Plantation Forest on Conservation of Soil and Water Resources*, 23-26 June 1987, Universiti Pertanian Malaysia, 50 pp., 1987.

Littleboy, M.; Silburn, M. and Rosenthal, K. RRUMS Version 3.0 User Manual. Qld. Dept. Primary Industries, Brisbane, 1986.

Lockwood, J. G. Probable maximum 24 hour precipitation over Malaya by statistical methods. *Meteorological Magazine*, 96, 11-19, 1967.

Lourensz, R. S. *Tropical Cyclones in the Australian Region, July 1909 to June 1980*, Canberra, Australian Government Publishing Service, 1981.

Lundgren, L. Comparison of surface runoff and soil loss from runoff plots in forests and small scale agriculture in the Usambera Mts, Tanzania. Geografiska Annaler, 62, 113-148, 1980.

Lyne, V. and Hollick, M. Stochastic time-variable rainfall-runoff modelling. In: *Hydrology and Water Resources Symposium, Perth 1979*, Canberra, Institute of Engineers, 89-92, 1979.

McAlpine, J. R. and Keig, G. with Falls, R. *Climate of Papua New Guinea*, Canberra, Commonwealth Scientific and Industrial Research Organization in association with Australian National University Press, 11-38, 1983.

McIntyre, D. S. Permeability measurements of soil crusts formed by raindrop impact. *Soil Science*, 85, 185-189, 1958a.

McIntyre, D. S. Soil splash and the formation of surface crusts by raindrop impact. *Soil Science*, 85, 261-266, 1958b.

McNaughton, K. G. and Jarvis, P. G. Predicting effects of vegetation changes on transpiration and evaporation. In: *Water Deficits and Plant Growth* (T. T. Kozlowski, Ed.), Academic Press, vol. 7, pp. 1-47, 1983.

Middleton, H. e. Properties of soils which influence soil erosion. *USDA Technical Bulletin*, pp. 1-16, 1930.

Moore, J. D.; Mackay, S. M.; Wallbrink, P. J.; Burch, G.J. and O'Loughlin, E. M. Hydrologic characteristics and modelling of a small forested catchment in southeastern New South Wales, Pre-logging condition, *Journal of Hydrology*, 83, 307-335, 1986.

Morton, F. I. What are the limits on forest evaporation? *Journal of Hydrology*, 74, 373-398, 1984.

Morton, F. I. What are the limits on forest evaporation? Reply *Journal of Hydrology*, 82, 184-192, 1985.

Moss, A. J.; Walker, P. H. and Hutka, J. Raindrop-stimulated transportation in shallow water flows: an experimental study. *Sedim. Geol.*, 22, 165-184, 1979.

Mott, J.; Bridge, B. J. and Arndt, W. Soil seals in tropical tall grass pastures of northern Australia, *Aus. J. Soil. Res*, 17, 483-494, 1979.

Nautiyal, J. C. and Babor, P. S. Forestry in the Himalayas — How to avert an environment disaster. *Interdisciplinary Science Reviews*, 10, 27-41, 1985.

Nik, A. R. Impact of forest conversion on water yield in peninsular Malaysia. Paper presented at the Workshop on *Impact of Operations in Natural and Plantation Forests on Conservation of Soil and Water Resources*, held at Universiti Pertanian, Malaysia, Serdan, 23-26 June 1987, 17 pp., 1987.

Nortcliff, S. and Thornes, J. B. Seasonal variations in the hydrology of a small forested catchment near Manaus, Amazonas, and the implications for its management. In: *Tropical Agricultural Hydrology — Watershed Management and Land Use* (Eds. by R. Lal and E. W. Russell), Wiley, Chichester, pp. 37-57, 1981.

O'Brien, A. L. Rapid water table rise, *Water Resources Bulletin*, American Water Resources Association, 18(4), 713-715, 1982.

O'Loughlin, E. M. A method for analyzing catchment topography for applications to hydrology and land conservation, *Water Resources Research*, 22, 794-804, 1986.

Pearce, A. J.; Stewart, M. K. and Sklash, M. G. Storm runoff generation in humid headwater catchments 1. Where does the water come from? *Water Resources Research*, 22, 1263-1272, 1986.

Peck, A. J. and Williamson, D. R. Effects of forest clearing on groundwater. *Journal of Hydrology*, 11, 147-66, 1987.

Philip, J. R. Theory of infiltration, *Advances in Hydroscience*, 5, 215-296, 1969.

Pilgrim, D. H.; Cordery, I. and Doran, D. G. Assessment of runoff characteristics in arid western New South Wales, Australia. In: *The Hydrology of Areas of Low Precipitation*. Proceedings of the Canberra Symposium, International Association of Hydrological Sciences, Publication 128, 141-150, 1979.

Ramage, C. S. Role of a tropical 'maritime continent' in the atmospheric circulation, *Monthly Weather Review*, 96, 365-370, 1968.

Reynolds, W. D.; Elrick, D. E. and Topp, G. C. A re-examination of the constant head well permeameter method for measuring saturated hydraulic conductivity above the water table. *Soil Science*, 136-250-268, 1983.

Richards, T. H. The Geological History of the Frankland Island Region, Coastal North Queensland, Unpublished Honours Thesis, Department of Geology, James Cook University of North Queensland, 1977.

Rodhe, A. *The Origin of Streamwater Traced by Oxygen-18*, Uppsala University, Department of Physical Geography, Division of Hydrology (Doctoral Thesis), Report Series A, N° 41, 260, pp. 1987.

Rubin, J. Theory of rainfall uptake by soils initially drier than their field capacity and its application. *Water Resources Research*, 2, 739-749, 1966.

Sadler, J. C. *The Monsoon Circulation and Cloudiness Over the GATE Area*, Department of Meteorology, University of Hawaii.

Sadler, J. C. and Harris, B. E. *The Mean Tropospheric Circulation and Cloudiness Over South-east Asia and Neighbouring Areas*, Hawaii Institute of Geophysics, University of Hawaii, 1970.

Salati, E. The forest and the hydrological cycle. In: *The Geophysiology of Amazonia — Vegetation and Climate Interactions* (Ed. by R. E. Dickinson), Wiley/UNU, pp. 273-296, 1987.

Salati, E. and Vose, P. B. Amazon Basin? A system in equilibrium, *Science*, 225 (4658) 129-138, 1984.

Shuttleworth, W. J. Evaporation from Amazonian rainforest. *Proceedings of the Royal Society of London*, Series B, 233, 321-346, 1988.

Shuttleworth, W. J. *Priorities in Climate — Related Hydrological Research in Amazonia*, Institute of Hydrology, Unpublished Report, 16 pp. 1989.

Sisson, J. B. and Wieringa, P. J. Spatial variability of steady-state infiltration rates as a stochastic process. *Soil Science Society of America Journal*, 46, 20-26, 1981.

Sklash, M. G. and Farvolden, R. N. The role of groundwater in storm runoff. *Journal of Hydrology*, 43, 45-65, 1979.

Soil Survey Staff. *Soil Taxonomy, A Basic System of Soil Classification for Making and Interpreting Soil Surveys*, US Department of Agriculture Handbook 436, 1975.

Stace, H. C. T.; Hubble, G. D.; Brewer, R.; Northcote, K. H.; Sleeman, R. Jr.; Mulcahy, M. J. and Hallsworth, E. G. *A Handbook of Australian Soils*, Glenside, Rellim Technical Publications, 1968.

Swift, L. W.; Cunningham, G. B. and Douglas, J. E. Climatology and Hydrology. In: *Forest Hydrology and Ecology at Coweeta* (Eds. W. T. Swank, D. A. Crossley), Springer-Verlag, New York, pp. 35-55, 1988.

Talsma, T. and Hallam, P. M. Hydraulic conductivity measurement of forest catchments, *Australian Journal of Soil Research*, 18, 139-148, 180.

Walsh, R. P. D. Runoff processes and models in the humid tropics, *Zeitschrift fur Geomorphologie*, NF Supplement-Band 36, 176-202, 1980.

Weyman, D. R. Measurements of the downslope flow of water in a soil. *Journal of Hydrology*, 20, 267-288, 1973.

Williams, J. and Bonell, M. Computation of soil infiltration properties from the surface hydrology of large field plots. *International Conference on Infiltration, Development and Application* (Ed. Yu-Si Fok), University of Hawaii, Water Resources Center, pp. 272-281, 1987.

Williams, J. and Bonell, M. The influence of scale of measurement on the spatial and temporal variability of the Philip infiltration parameters — an experimental study in an Australian savannah woodland. *Journal of Hydrology*, 104, 33-51, 1988.

Williams, J. and Coventry, R. J. The contrasting hydrology of red and yellow earths in a landscape of low relief. In: *The Hydrology of Areas of Low Precipitation*, Proceedings of the Canberra Symposium, International Association of Hydrological Sciences, Publication 128, 385-395, 1979.

Williams, J. and Coventry, R. J. The potential for groundwater recharge through red, yellow and grey earth profiles in central north Queensland. In: *Groundwater Recharge*. Australian Water Resources Council, Conference Series 3, 169-181.

Williams, J.; Day, K. G.; Isbell, R. F. and Reddy, S. J. Soils and Climate. In: Muchow, R. C. (Ed.), *Agro-Research for the Semi-Arid Tropics: North-West Australia*. St. Lucia University of Queensland Press, 31-92, 1985.

World Meteorological Organization (WMO). *Operational Hydrology in the Humid Tropical Regions*. Final Report, Geneva, 1983.

Youngs, E. G. Soil physical theory and heterogeneity. *Agricultural Water Management*, 6, 145-159, 1983.

Table 1 — a — Lower Congo (Kinshasa) rainfalls (mm) for various durations and return periods (after Griffiths, 1972).

Return period (years)	Duration (min)									
	10	20	30	40	50	60	70	80	90	24hr
2	23.3	37.5	46.5	56.2	62.0	66.1	67.3	69.5	69.8	
10	30.6	49.3	61.2	74.4	82.4	87.9	89.5	92.5	92.7	117
25										132
50										143

b — Babinda rainfalls (mm) for selected durations and return periods for a comparison with Kinshasa

Return period (years)	Duration (min)						
	6	12	18	30	60	3hr	24hr
2	12.7	23.1	29.3	42.2	67.5	120.9	335.8
7	20.5	28.3	40.3	58.5	90.7	209.3	497.0
14	24.7	32.0	45.5	64.5	103.9	244.0	660.9

Table 2 — Runoff-runon for Individual Storms for Plots 1 and 4

Date	Total rain	DIFFERENCES IN OVERLAND FLOW (mm)				NET CHANGE BETWEEN PLOTS
		Plot 1 Trough 2-Trough 1	Plot 2 Trough 3-Trough 2	Plot 3 Trough 4-Trough 3	Plot 4 Trough 5-Trough 4	
21.1.87	14.8	0.14	-0.14	0.20	-0.12	0.08
20.1.82	9.8	0.04	0.12	0.45	-0.44	0.17
21.1.87 (Storm A)	10.8	0.05	0.14	1.05	-0.94	0.30
21.1.82 (Storm B)	12.0	0.04	-0.09	0.04	-0.03	-0.04
23.1.82	16.4	-0.63	2.24	1.20	-2.53	0.28
2.2.82	34.0	-2.86	6.36	1.82	-4.54	0.78
18.2.82	23.6	-0.97	4.04	1.37	-3.44	1.00

Source: Bonell and Williams, 1986b.

Table 3 — Comparison of combined spatial and temporal variability in the Philip parameters and saturated hydraulic conductivity (K*) between large plots and infiltration rings

	N	Mean	Median	Max	Min	Stdev
A parameter ($m\ d^{-1}$)						
Plot	21	1.08	0.95	2.16	0.35	0.59
Ring, bare	24	2.78	2.76	10.02	0.52	2.04
Ring, vegetation	26	7.06	4.45	22.03	0.52	6.70
S parameter ($mm\ s^{-1/2}$)						
Plot	21	0.0070	0.0170	0.0860	-0.0740	0.0452
Ring, bare	24	0.0455	0.0316	0.3430	-0.0450	0.0666
Ring, vegetation	26	0.0391	0.0280	0.1940	-0.1490	0.0885
K* (md^{-1})						
Plot	21	1.08	0.86	1.90	0.52	0.52
Ring, bare	24	2.63	2.42	7.69	0.86	1.53
Ring, vegetation	26	6.19	4.45	15.29	1.64	4.67

Source: Williams and Bonell, 1988.

Table 4 — Fluxes in overland flow (mm) and sediment (g m^{-2}) [1, 2]

N°	Sampling period date	Total rain (mm)	Plot 1 Trough 2-Trough 1	Plot 2 Trough 3-Trough 2	Plot 3 Trough 4-Trough 3	Plot 4 Trough 5-Trough 4	Net change between plots
1	17/12/81-	47.60	1.28	-2.46	-0.57	1.80	0.06
	5/1/82		*0.782*	*-0.69*	*0.434*	*1.810*	*2.327*
2	6/1/82-	19.80	0.12	-0.14	0.20	-0.12	0.06
	19/1/82		*0.109*	*0.175*	*-0.010*	*0.137*	*0.411*
3	20/1/82-	106.60	-3.41	8.80	4.56	-8.48	1.47
	3/2/82		*-0.814*	*9.488*	*0.150*	*0.975*	*9.799*
4	4/2/82-	28.60	-0.97	4.04	1.37	-3.44	0.99
	2/3/82		*0.012*	*1.318*	*-0.430*	*-0.031*	*0.869*
5	3/3/82-	40.20	-0.01	-0.07	0.21	-0.10	0.04
	16/3/82		*0.315*	*-0.032*	*0.09*	*-0.21*	*0.163*
6	17/3/82-	12.60	0.10	-0.01	0.06	-0.09	0.05
	6/4/82		*-0.203*	*-0.043*	*-0.011*	*0.074*	*-0.183*
7	7/4/82-	11.80	0	0	0	0	0
	14/5/82		*0*	*0.145*	*-0.157*	*0.055*	*0.043*
			FIRE				
8	10/12/82-	11.20	-0.06	1.32	0.06	-1.02	0.30
	21/12/82		*-0.401*	*1.725*	*(-1.159)*	*(0.330)*	*NR*
9	22/12/82-	86.25	-1.52	NR	NR	-8.32	NR
	5/1/83		*-0.289*	*(5.163)*	*(-2.062)*	*-1.48*	*NR*
10	6/1/83-	26.75	-0.28	1.26	-0.41	-0.84	-0.27
	3/2/83		*-0.406*	*0.029*	*1.843*	*NR*	*NR*
11	4/2/83-	29.75	-1.24	4.89	-1.35	-2.93	-0.63
	1/3/83		*-1.102*	*4.594*	*0.057*	*-2.361*	*1.188*
12	2/3/83-	25.00	-0.23	2.07	-0.66	-1.24	-0.06
	22/3/83		*-0.034*	*0.960*	*-0.958*	*-0.043*	*-0.075*
13	21/4/83-	222.60	-27.11	81.38	-26.01	-22.77	5.49
	30/4/83		*-11.618*	*55.979*	*(5.226)*	*(-0.400)*	*NR*
14	1/5/83-	93.20	-44.60	65.45	-24.63	-17.47	-21.25
	13/5/83		*(1.709)*	*(6.851)*	*(-5.364)*	*(1.006)*	*NR*
15	14/5/83-	58.25	-12.33	27.00	-6.19	-7.01	1.47
	22/5/83		*-0.068*	*7.277*	*-1.641*	*-3.693*	*1.875*
16	9/12/83-	169.20	-14.21	39.12	-13.34	NR	NR
	12/1/84		*-0.533*	*10.643*	*-4.672*	*(-5.093)*	*NR*
17	13/1/84-	42.75	-3.41	5.83	-1.98	-2.37	-1.92
	19/1/84		*0.008*	*4.403*	*-2.114*	*-1.798*	*0.499*
18	20/1/84-	67.50	-4.67	14.83	-5.96	-6.03	-1.83
	2/2/84		*-2.791*	*9.679*	*-5.395*	*-3.022*	*-1.529*
19	3/2/84-	74.50	-0.24	1.96	-0.86	0.90	-0.03
	23/2/84		*-0.639*	*2.031*	*-1.210*	*-0.312*	*-0.130*

[1] Figures shown as italics and underlined refer to sediment transport. Where the suspended load sampler malfunctioned, the bedload collected from froughs shown in brackets. NR denotes no result available.

[2] Overland flow is positive for runoff and negative for runon and sediment flux is positive for erosion and negative for deposition.

Source: Bonell and Williams, 1987.

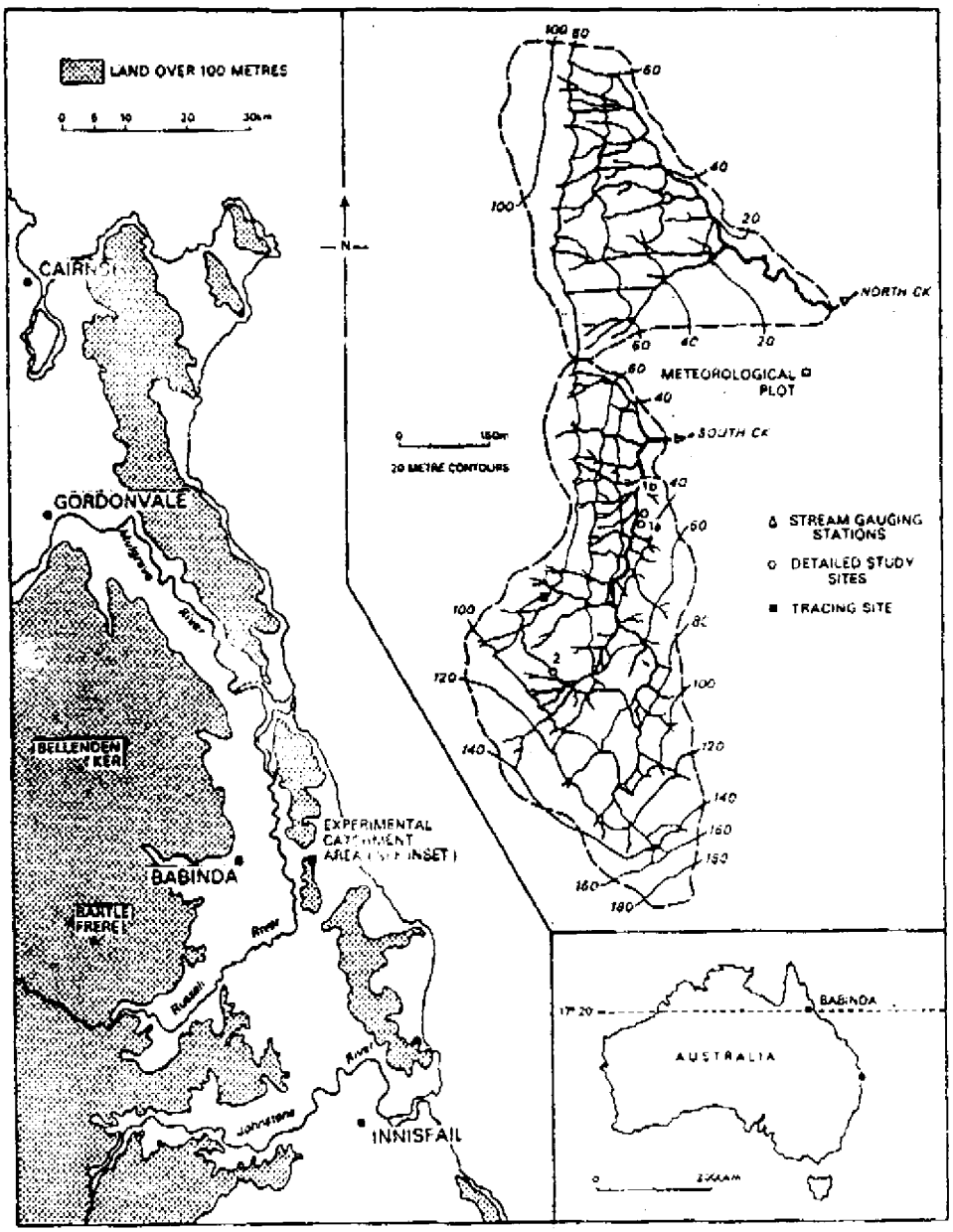

Fig. 1 — The location, experimental sites and physiographic features of the Babinda catchments.

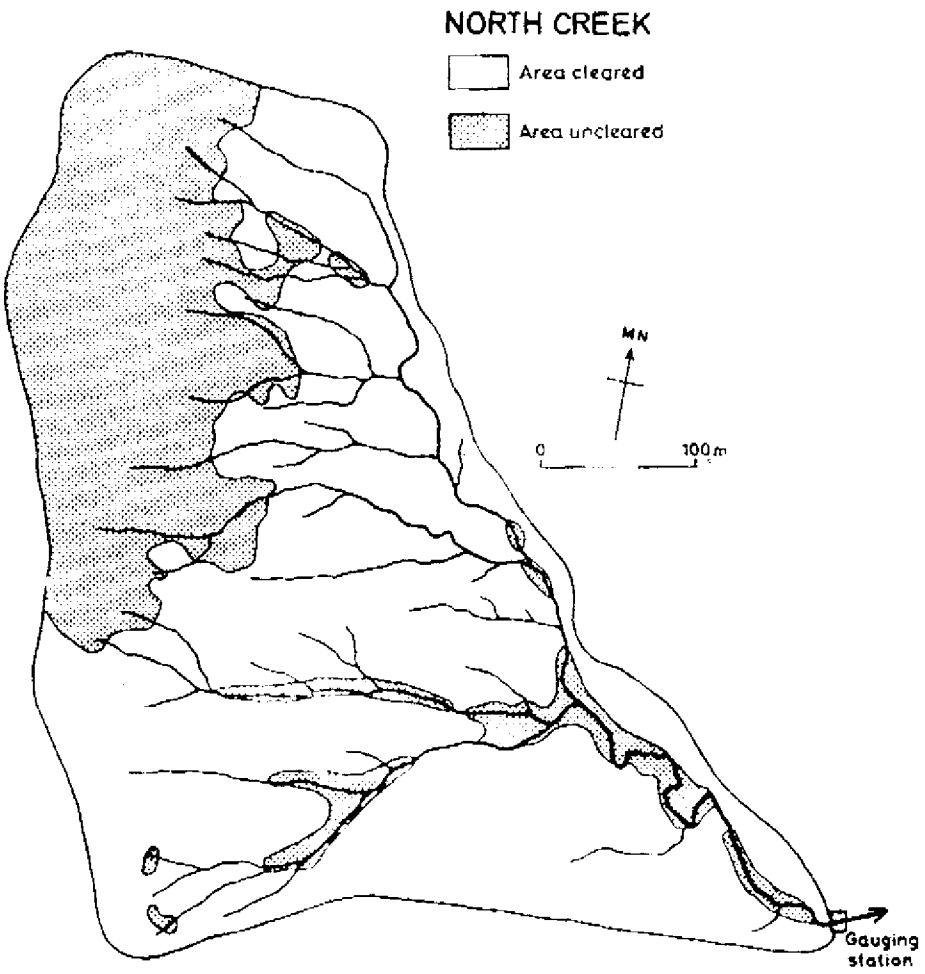

Fig. 2 — The distribution undisturbed/disturbed tropical rainforest in North Creek.

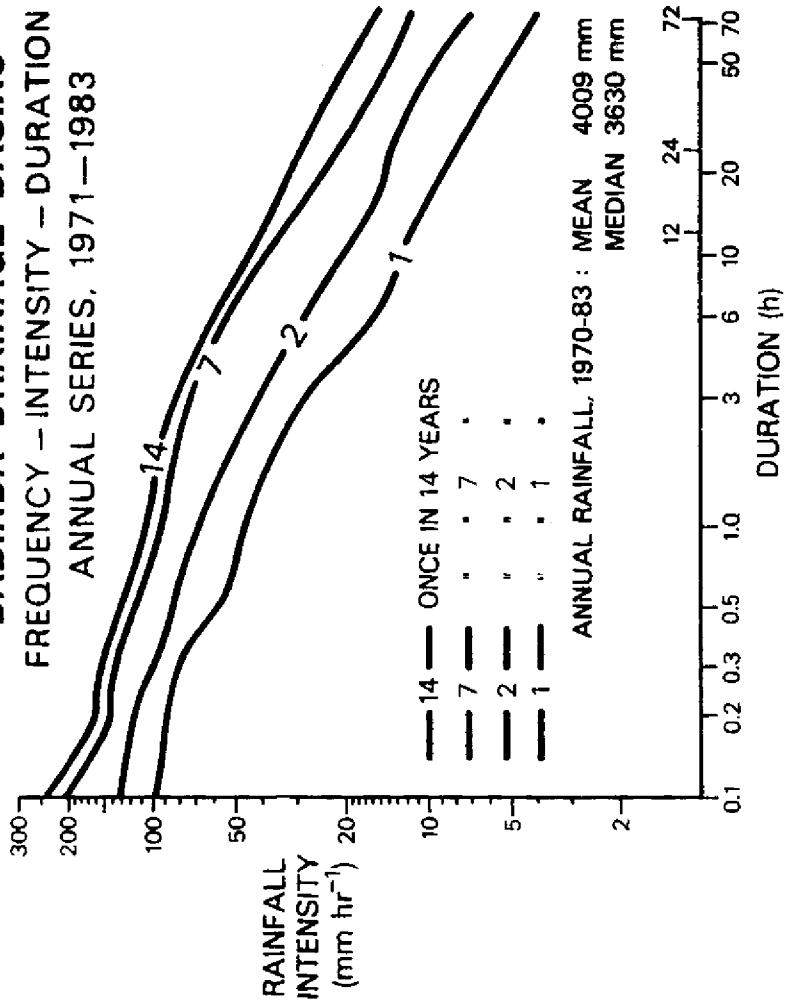

Fig. 3 — Rainfall intensity - frequency - duration analysis for the Babinda experimental drainage basins (1971-83)

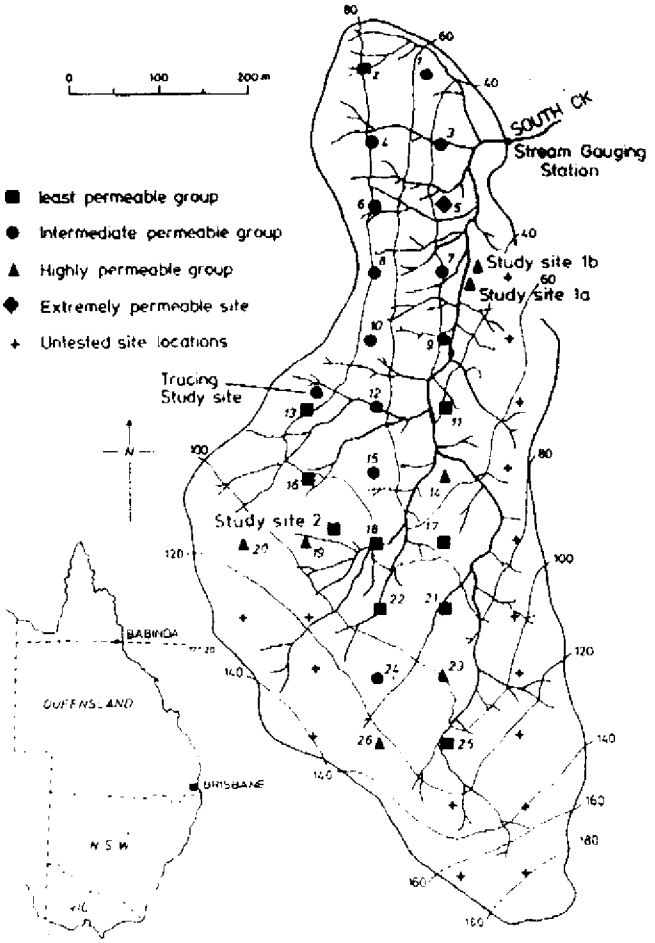

PERMEABILITY GROUP	RANGE OF K (mm hr⁻¹)	NO. OF SITES	SUGGESTED DOMINANT FLOWPATHS	
LEAST PERMEABLE	0.2 - 2.1	4	MONSOON POST-MONSOON	SOF SOF
INTERMEDIATE PERMEABLE	2.9 - 3.2 5.5 - 5.9	4 2	MONSOON POST-MONSOON	SOF SSF
HIGHLY PERMEABLE	17 - 18	3	MONSOON POST-MONSOON	SOF SSF
EXTREMELY PERMEABLE	315	1	VERTICAL TRANSMISSION	

SOF - SATURATION OVERLAND FLOW
SSF - SUBSURFACE STORMFLOW ESPECIALLY ABOVE 0.25m DEPTH

Fig. 4 — The location of sampling points for K* determination for the impeding layer 0.02-0.5 m depth in South Creek and preliminary permeability.

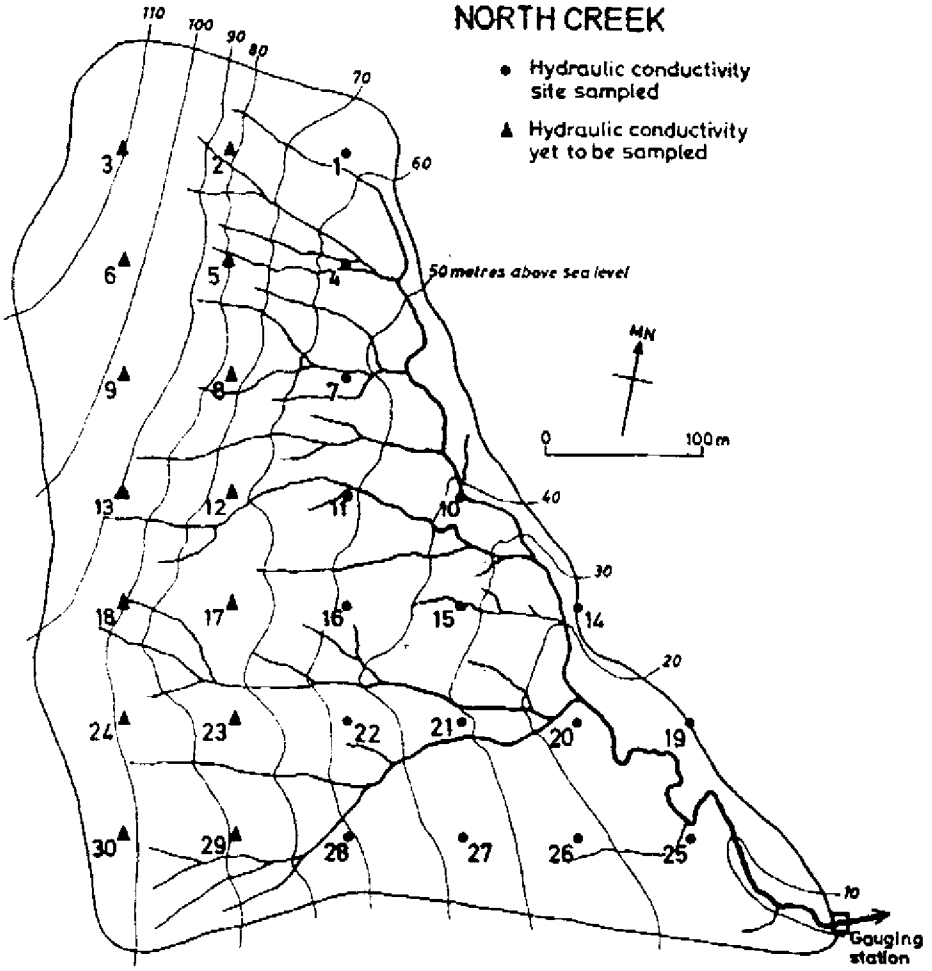

Fig. 5 — The location of sampling points for K* determination for the impeding layer 0.02-0.5 m depth in North Creek

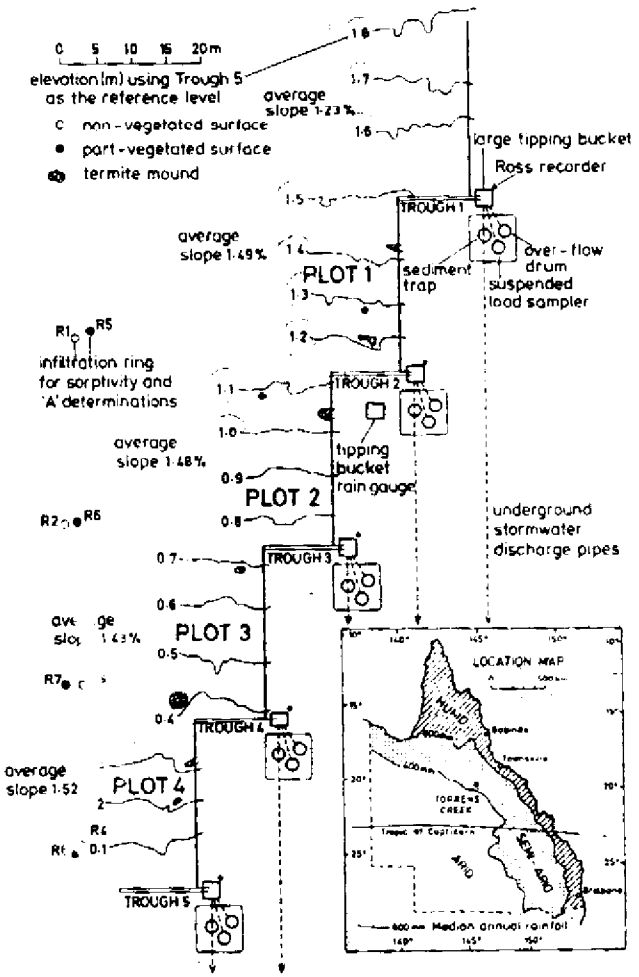

Fig. 6 — The experimental layout at the instrumented slope near Torrens Creek in central north Queensland, Australia

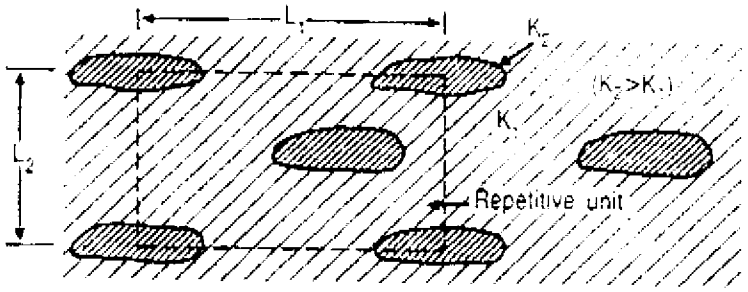

Fig. 7 — Diagram to illustrate the concept of the 'repetitive unit' which is aimed at regarding the behaviour of an inhomogeneous material as an equivalent homogeneous material if the length scale of observation exceeds the characteristic length (L_1 and L_2) of the repetitive unit (after Bear, 1979).

Source: Williams and Bonell, 1988.

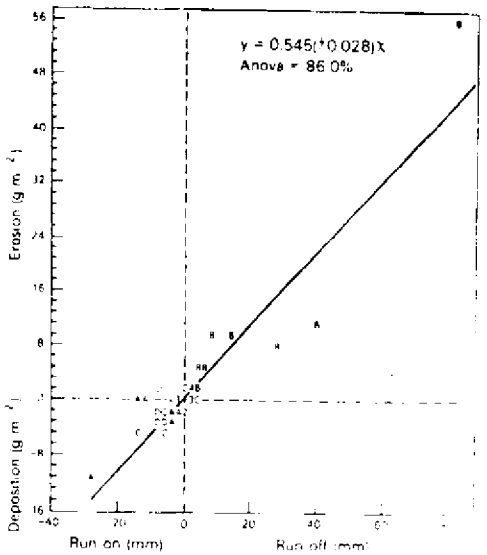

Fig. 8 — Eorsion-deposition versus runoff-runon for the pre- and post-fire periods. The equation shown is for a zero intercept. The constant for the fitted equation ($y = 0.4543x + 0.546$) was not significantly different from zero ($p > 0.05$). The ANOVA percentage variance accounted for is defined as 100 x (total mean square minus residual mean square)/(total mean square). The symbols A to D represent individual observations from plots 1 to 4 respectively. Where more than one observation is coincident this is shown numerically. The + symbol close to the origin indicates 28 almost coincident points.

Source: Bonell and Williams, 1987.

WATER AND SALT BALANCES OF THE BOLIVIAN AMAZON

M. A. Roche *
C. Fernández-Jáuregui **
A. Aliaga ***
J. Bourges *
J. Cortes ****
J.-L. Guyot *
J. Peña ***
N. Rocha ****

ABSTRACT

The Bolivian Amazon region lies in the upper middle part of the Madeira River basin (850,000 km²), a portion of which extends in the Andes (24%), and also in Peru and Brazil. The water and salt balances of the main sub-basins and the entire basin of the upper Madeira River are established for the interannual period 1968/1970 to 1982.

The mean interannual precipitations on the great basins vary from 750 to 3000 mm, the entire upper Madeira basin receiving 1705 mm yr^{-1}. The biggest extremes of the rainfall reach 490 and more than 7000 mm. At its head, the Madeira River is yet one of the largest rivers of the world, with a mean interannual discharge of 17,000 $m^3 s^{-1}$, i.e. 536 x 10^9 m^3 yr^{-1}, approximately half the discharge of the Congo River. The mean interannual contribution of the Bolivian Andes is 4170 $m^3 s^{-1}$, i.e. 132 x 10^9 m^3 yr^{-1}, representing 25% of the discharge of the entire upper Madeira basin. The values of actual evapotranspiration vary from 615 mm in the driest Andean basin to 1520 mm yr^{-1} in a forest and low drainage basin. Global ionic contents, with values of 59 mg l^{-1}, 61 mg l^{-1}, and 57 mg l^{-1} for the Madeira, the Beni and the Mamoré Rivers respectively, out of any contamination, are somewhat higher than for the Amazon River. Interannual dissolved ionic transport is evaluated to 32 x 10^6 t at the begining of the Madeira River, i. e. 1 t s^{-1}.

The contribution of the upper Madeira River to the Amazon system, at the ocean, is evaluated to 9.7% of the water and 10.9% of the ions, whereas the surface represents 12.1%.

* *Institut Français de la Recherche Scientifique pour le Développement en Coopération (ORSTOM) - P. O. Box 9214 - La Paz, Bolivia*

** *UNESCO/ROSTLAC - P. O. Box 859 - Montevideo, Uruguay*

*** *Instituto de Hidráulica e Hidrología (IHH de la UMSA) - P. O. Box 699 - La Paz, Bolivia*

**** *Servicio Nacional de Meteorología e Hidrología (SENAMHI) - Ed. La Urbana - La Paz, Bolivia*

INTRODUCTION

The Bolivian Amazon region lies in the upper middle part of the Madeira River basin (Sioli, 1984), a portion of which also is in Peru and Brazil. The basin extends through the Eastern Cordillera of the Andes, the adjoining Plain, and the Brazilian Shield. Mean drainage axes are constituted by the Madre de Dios, Beni, Mamoré and Itenez Rivers which join to become the Madeira River, the more important south affluent of the Amazon. At the confluence of the Beni and Mamoré Rivers, the Madeira River drains a basin of 850,000 km^2, 24% of which lies in the Andes. The water flows through varied zones of relief, lithology, climate and vegetation which determine diverse hydrological and hydrochemical characteristics.

The international Project PHICAB, conducted by ORSTOM, IHH and SENAMHI, under agreement with the International Hydrological Programme of UNESCO, studies climate, hydrology, hydrochemistry and sediment transport in Bolivia, in particular the Amazon part (Roche, 1982; Roche and Canedo, 1984). Thanks to measurements and the compilation of other available data, the PHICAB has established the water and salt balances of the main sub-basins and the entire basin of the upper Madeira River (Espinoza, 1985; García, 1985; Abasto, 1987; Cruz, 1987; Roche and Fernández-Jaúregui, 1988). In the Amazonian region of Bolivia, climatological data is available since 1945 at many stations. The hydrometric measurements have been made in the Andes since the 1970's but, in the plain, they began in 1982. However, three hydrometric stations, among a PHICAB network of 15 stations, have been observed there before over a 15 to 20 years period. Then, the values obtained over the whole basin are adjusted for a first evaluation to the interannual period 1968/1970 to 1982, according to the UNESCO recommendations for the water balance of South America.

Differents periods have also been considered in other studies for sub-basins (Bourges et al., 1987, 1990; Guyot et al., 1987, 1990; Roche et al., 1989). Details of the water and salt balances for an hydrological division in 16 sub-watersheds are presented in Tables I and II.

PHYSICAL AND BIOLOGICAL CONDITIONS

The surface of the whole basin is 850,000 km^2 of which one third is represented by the Beni basin and two thirds correspond to the Mamoré basin. The Andes occupy 205,000 km^2, i. e. one fourth of the surface.

Between the glaciers of the andean crests and the tropical rainy forest of the piedmont, the rivers drain frequently semi-arid areas of high altitude, particularly in the south west of the Beni basin and in the Rio Grande basin. In the center of the eastern plain of Bolivia, the forest is interrupted by savanna with forest gallery but resumes in the Brazilian Shield and to the north where the great amazon forest begins.

The andean rocks are of all geological times: Paleozoic, Mesozoic, Tertiary and Quaternary. They were affected by Pliocene folding, with locally upper Cretaceous and Eocene folding. Intrusive rocks constitute the highest mountains of the head-watersheds. The Permian and Cretaceous sections contain gypsiferous red clays where the gypse is locally exploited. White exudations in the dry periods cover diverse terrains in the semi-arid areas, especially the black Paleozoic schists.

RAINFALL

The spatial rainfall distribution over all Bolivia and the parts of the basin situated in the border countries has been displayed on maps at 1/4,000,000 scale (Roche and Rocha, 1985) and for each of the four main basins at 1/1,000,000 scale. The Figure 1 is a simplification of maps drawn at 1/5,000,000 scale. This distribution of the precipitation differs greatly according to the regions, the dynamics of air masses and orographic phenomena. However, the monthly distribution in the course of the year presents a similar pattern over the entire Bolivian Amazon basin, showing that it is part of a same pluviometric regime (Roche et al., 1990).

The Madre de Dios basin receives yearly heavy rainfall from 2500 mm to more than 7000 mm on the andean flank, and from 1800 to 2500 mm on the plain, with an average of 2380 mm.

The Beni River basin, in its andean part, receives between some 800 and 1000 mm on the summit, and more than 4000 mm in the upper part of the hot valleys (Yungas). The most protected zones due to its western situation behind the upper summits of the Cordillera, such as the valleys of La Paz and Luribay, have rainfall in the range of 350 to 500 mm. The main rainfall in the andean basin is estimated at 1720 mm. Rainfall in the plain ranges from 1650 to 2000 mm, with a mean precipitation evaluated at 1810 mm, and at 1755 mm in the entire Beni basin, at the confluence with the Madre de Dios river.

The mean precipitation in the Beni and the Madre de Dios basins, as a whole, is 2060 mm.

The Mamoré andean basin, with extrem values of 480 mm in the most semi-arid zone to 6000 mm at the foot of the Andes, receives a mean rainfall of 750 mm in the Río Grande basin and 3000 mm on the oriental watersheds. The Amazon plain has rainfall between 800 mm in the Río Grande basin, 3000 mm in the Ichilo basin and 1900 mm at the head of the Madeira river. The increase in rainfall is remarkable toward the north (800 to 1900 mm) and to the west (1000-1900 mm to 2000-4000 mm). The mean rainfall on the basin is estimated at 1850 mm and 1520 mm over the entire Mamoré basin.

The Itenez River basin receives rainfall as follows: 900 mm in the south, 1800 mm in the east and 1900 mm in the north east, with a mean value estimated at 1375 mm.

The mean precipitation on the upper Madeira basin is 1705 mm.

EVAPOTRANSPIRATION

Evapotranspiration has been evaluated in two ways: the water balance, by the difference between precipitation and discharge, furnishes a value of the actual evapotranspiration that has been compared to that obtained by formulas (Figure 2). According to the recommendations of UNESCO for the water balance of South America, the formula of Thornthwaite or Turc has been used for land, and of Penman for free-water.

Interannual values vary from 610 mm, in the semi-arid Río Grande basin where the water deficit is high, to 1520 mm in the Orthon River basin, characterized by a very flat relief, low drainage and rainy forest covering. The andean part of the Beni River basin shows a value of evapotranspiration of 780 mm, just a little higher than that of the previous basin. The evaluation of 1220 mm, made for

the rainy oriental basins of the Mamoré River, increases the global value of evapotranspiration in the Bolivian andean part of the upper the Madeira River basin, where it is estimated at 800 mm.

The actual evapotranspiration in the plain, varies from 1075 mm to 1520 mm and tends to increase from South to North. This highest value is similar to that evaluated at 1470 mm for the Amazonian forest in French Guiana (Roche, 1982 a, b).

The comparison of the evaluations obtained by the two methods, shows differences included between zero and 14%. Evapotranspiration remains the most difficult evaluation of the water balance, compared to the other terms that can be more easily measured.

RUNOFF

The annual rain distribution, conditioned by the alternation of a rainy season and a dry season, determines in the Andes and its piedmont, hydrographs of multi-peaked floods which fuse dowstream to originate the large annual flood of tropical type, preceded or followed by small well-differentiated floods. The annual flood seems more and more defined from upstream to downstream of the large drainage axis. It is more regulated and flattened in the Mamoré and Itenez Rivers mainly because of longer courses and above all because of lateral extension of broad flooded areas. This also explains the delay of the floods of the Mamoré and Itenez Rivers versus those of the Beni and Madre de Dios Rivers. This can represent a two-month difference of phase (Roche and Fernández-Jaúregui, 1986; Bourges et al., 1988).

These floods of a remarkable magnitude, extend over surfaces in the order of 100,000-150,000 km², particularly in the Mamoré and Itenez River basins. These are mainly produced starting at the confluence of the Chapare, Ichilo and Grande Rivers, and extending up to the Mamoré and Itenez Rivers.

During the flooding period, it appears that the whitish and turbid water of the upstream tributaries is sufficient to fill the bed of the Mamoré River which, having very slight slope, does not allow the prompt discharge of water of the upstream tributaries and rainfall from the lateral plain. Floods on the plains, originating from local rains, are transparent and reddish-black. The mixture of "white" and "brownish-black" water seems to take place gradually but the color difference makes it possible to distinguish lateral trails, which indicate a longitudinal component of the drainage of the flood water. The Itenez River, which does not descend from high mountains, also drains large flooded areas carrying clear water. These floods take place from January to May-June, their decay toward the main axis being delayed downstream.

The Madeira at its head is one of the world largest rivers, with a mean interannual volume of 536×10^9 m³, i.e. 17,000 $m^3 s^{-1}$, 52% of which is contributed by the Beni River and 48% by the Mamoré River (Figure 3). The Mean interannual contribution of the Bolivian Andes represents 132×10^9 m³, i.e. 1170 $m^3 s^{-1}$, i.e. 25% of the total discharge of the Madeira. In Bolivia the Andean basin of the Beni River exports the greatest amount (72×10^9 m³ i.e. 13%), followed by the eastern basin (evaluated to 51×10^9 m³). The Andean basin of the Río Grande, with semi-arid regime in its largest part, supplies 8×10^9 m³, only 1.5% of water of the Madeira. To these inputs have to be added those of the Peruvian Andes which feed the upper Madre de Dios River.

Like the Madeira, the Beni and the Mamoré (both of same discharge) are also classified as large rivers, greater than the Volga River, the largest in Europe, and the Niger River, the second largest in Africa. The Madeira represents almost half the discharge of the Congo River.

SALINITY

The low salinity observed at the limit of the glaciers, covering intrusive rocks of the crest, increases quickly dowstream due to the dissolution of altered or evaporitic varied rocks. Often, high contents of sulphate comes from gypsum dissolution as well as from the leaching of whitish pellicular efflorescences exuded by capillarity from different formations, especially from black schists (alteration of sulphure). The pollution by La Paz city is locally strong but disappears some hundreds of kilometers downstream.

In the Amazon plain, the effects of the climatohydrological regimes and of the vegetation prevail over those of lithology. It occurs a continuous dilution of the andean inputs by the abundant and less mineralized water of the lateral yields, on Quaternary detrital sediments. The extreme type of water of the savanna and forest has salinity among the lowest in the world (13-20 uS at 25 C). Filtered by vegetation, without turbulence, it shows great transparency. A prolonged contact with herbaceous thick vegetation, or with the forest that it soaks in the shallow flatlands, as well as with humus-bearing and often hydromorphic soils, gives a brown-reddish coloration with a black gleam, originating thus the name of "black water". With low pH, they show high relative contents in potassium due to interaction with vegetation (Roche et al., 1986; Guyot et al., 1988).

The global salinity of the Madeira River at its begining has been measured and evaluated at 59 mg l^{-1} (Figure 3). It is a value higher than that of the Amazon, Orinoco, and Congo Rivers evaluated at 53 mg l^{-1}, 52 mg l^{-1}, and 31 mg l^{-1}, respectively (*in* Gac, 1980). The interannual salinity of the Beni (61 mg l^{-1}) and Mamoré (57 mg l^{-1}) are both similar.

The mean annual dissolved transport, at the head of the Madeira, reaches 32 x 10^6 t, i. e. 1 t s^{-1}. The Beni and Mamoré River yield, each one, 17 x 10^6 t and 15 x 10^6 t. An estimation made for another period (1983-1987) by Guyot (1988), leads for the Madeira River to 41 x 10^6 t of dissolved ions and silica. These values can be compared to those of the Amazon River (290 x 10^6 t), Orinoco (50 x 10^6 t), Congo (37 x 10^6 t). It represents 10.9% of the total load of the Amazon.

In the Beni River basin at its confluence with the Madre de Dios, the Andes (60% of the surface) exports yearly 5.2 x 10^6 t of ions, whereas the plain yields 1.6 x 10^6 t. The total input of the Madre de Dios River is evaluated at 7.1 x 10^6 t of dissolved ions. At the confluence of the Madre de Dios and Beni Rivers, 60% of the water inflow arises from the first river, while the dissolved contributions are better balanced, closer to 50% for each river.

The contribution of the Bolivian Andes is evaluated at 12.9 x 10^6 t (i.e. 80 t km^{-2}), with a mean salinity of 98 mg l^{-1}, and respective yields of 40% by the Beni River, 30% by the Grande River, and 30% by the eastern watershed.

The Upper Madeira water carries in solution mainly bicarbonates (61%), sulphate (14%), sodium (5%), magnesium (5%), and potassium (4%).

CONCLUSION

The upper Madeira River, in its Andean and plain basins, has yet an important role for the yield of water and dissolved matter through the Amazon and the Atlantic Ocean. The contribution to Amazon River transport (175,000 $m^3 s^{-1}$ and 9.2 $t s^{-1}$) is 9.7% for water, and 10.9% for dissolved ions, while the surface involved represents 12.1% of the entire hydrological system. These evaluations are the first made in the basin as a whole.

In this large basin, evapotranspiration removes 1075 to 1155 mm (according to the way of evaluation), i. e. 63 to 68% of the 1705 mm of the precipitation. Then, runoff as complement, evacuates 33 to 37%, according to the two ways of evaluation of actual evapotranspiration. The losses are assumed at two thirds by evapotranspiration. The region includes high and cold mountains, semi-arid zones, and flooded savannas and forest over tens of thousands of square kilometers for many months in the year. Taking in account this great variety of factors, the global value is compatible with those of the Amazon, Orinoco, Paraná, and San Francisco Rivers, estimated at 49%, 48%, 72% and 70% (UNESCO, 1980) or that on the continents of the planet for which authors agree for values between 60% and 65%. This term of the water balance emphasizes the important phenomenon of recycling of water vapor in the Amazon basin, even in the absence of thick forest.

Complementary new data are soon ready to be published by the PHICAB staff in climatology, hydrology, hydrochemistry and sediment transport. But beyond these results and the necessity to lengthen the series of data, the difficulties and incertitudes of evaluating regional evapotranspiration remain. They justify to continue to carry out, by classical and up-to-date technics, thorough studies of this so important term of the water and energy balances. The regionalization should be the guide-line of a new state of such studies.

REFERENCES

Abasto, N. Balance hídrico superficial de la cuenca del Río Madre de Dios, Amazonia, Bolivia-Perú. PHICAB, 1987, 259 p.

Bourges, J.; Cortés, J.; Hoorelbecke, R. Estudio de los caudales del Mamoré en Guayaramerin. PHICAB, 1987, 29 p.

Bourges, J.; Guyot, J. L.; Carrasco, M.; Barragán, M. C.; Cortés, J. Evolution spatio-temporelle des débits et des matières particulaires sur un bassin des Andes boliviennes: Le Rio Beni. Conf. Int. sur les ressources en eaux des régions montagneuses. Aih-aihs, Lausanne, 1990, 7 p.

Cruz, C. Balance hídrico superficial de la cuenca del Río Itenez, Amazonia, Bolivia-Brasil. PHICAB, 1987, 218 p.

Espinoza, O. Balance hídrico superficial de la cuenca del Río Beni, Amazonia, Bolivia. PHICAB, 1985, 199 p.

Gac, J. Y. Géochimie du bassin du Lac Tchad. Bilan de l'érosion et de la sédimentation. ORSTOM, 1980, 251 p.

García, W. A. Balance hídrico superficial de la cuenca del Río Mamoré, Amazonia, Bolivia. PHICAB, 1985, 110 p.

Guyot, J. L.; Roche, M. A.; Bourges, J. Etude de la physicochimie et des suspensions des cours d'eau de l'Amazonie bolivienne: l'exemple du Río Beni. Journées hydrol. de l'ORSTOM, Montpellier, 1988.

Roche, M. A. Evapotranspiration réelle de la forêt amazonienne en Guyane. Cah. ORSTOM, Sér. Hydrol., 1982a, XVI (1): pp.37-44.

Roche, M. A. Comportements hydrologiques comparés et érosion de l'écosystème tropical humide à Ecerex, en Guyane. Cah. ORSTOM, Sér. Hydrol., 1982b, pp. 81-114.

Roche, M. A. Les conditions d'une étude hydrologique en Amazonie bolivienne. PHICAB, ORSTOM, 1982, 31 p.

Roche, M. A. and Canedo, M. Programa Hidrológico y Climatológico de la Cuenca Amazónica de Bolivia. Folleto de presentación del PHICAB, offset color, 1984, 4 p.

Roche, M. A.; Abasto, N.; Tolede, M.; Cordier, J. P.; Pointillart, C. Mapas de las salinidades iónicas de los Ríos de la Cuenca Amazónica de Bolivia. PHICAB, 1986a, 3 hojas offset.

Roche, M. A. and Fernández-Jaúregui, C. Water Resources, Salinity and Salt Exportations of the Rivers of the Bolivian Amazon. J. of Hydrol., Elsevier, 1988, No. 101, pp. 305-331.

Roche, M. A. Las aplicaciones del Proyecto PHICAB al Desarrollo de Bolivia. Segundo Simposio de la Investigación Francesa en Bolivia, La Paz., 1988, pp. 77-88.

Roche, M. A.; Bourges, J. and Guyot, J. L. Hydrology, Hydrochemistry and Sediment Yields in the Bolivian Amazon Drainage Basin. Poster and extended abstract. Third IAHS Scientific Assembly, Baltimore, 1989, 5 p.

Roche, M. A.; Aliaga, A.; Campos, J.; Cortés, J.; Peña, J.; Rocha, N. Héterogénéité des précipitations sur la cordillère des Andes boliviennes. Int. Conf. on Water Resources in mountaneous regions, AIH-AIHS, Lausanne, 1990, 8 p.

Sioli, H. The Amazon, Junk, 1984, 672 p.

UNESCO. Balance hídrico mundial y recursos hidráulicos de la tierra. Instituto de Hidrología, UNESCO, 1980, 925 p.

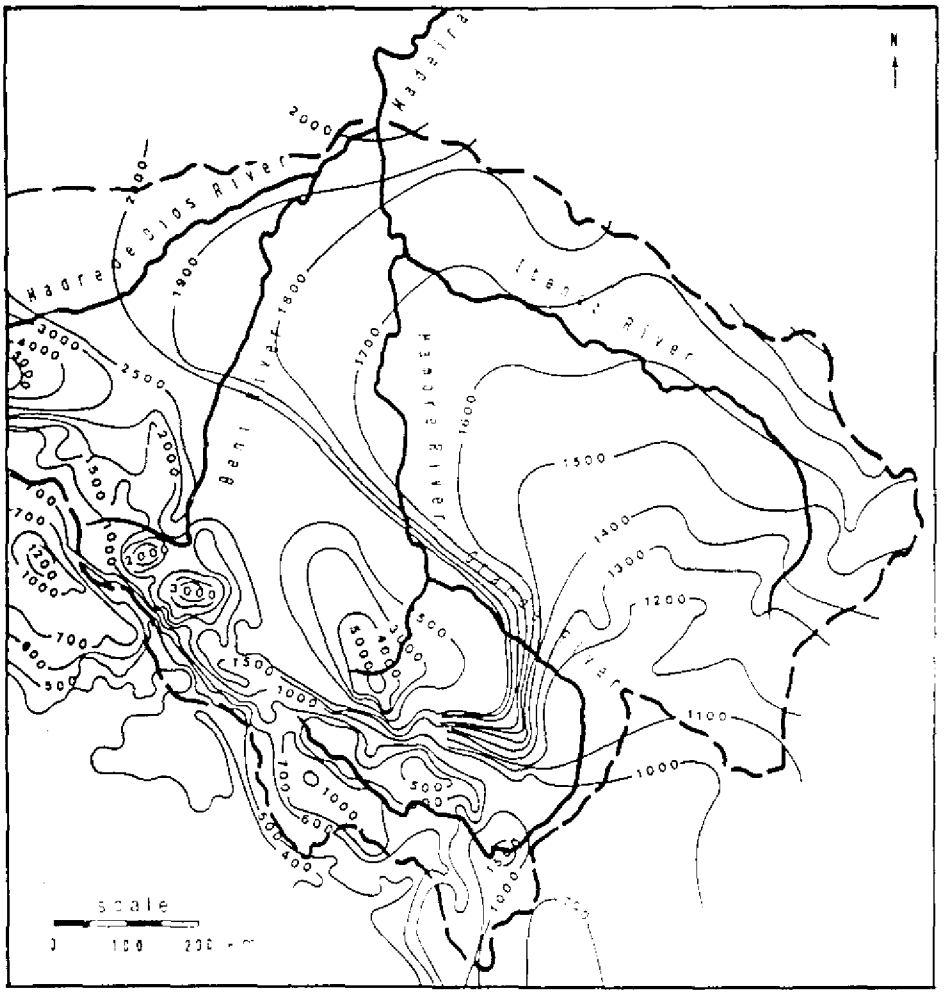

Figure 1 - Map of interannual rainfall in the upper Madeira River basin, in mm yr^{-1} (period 1968-1982).

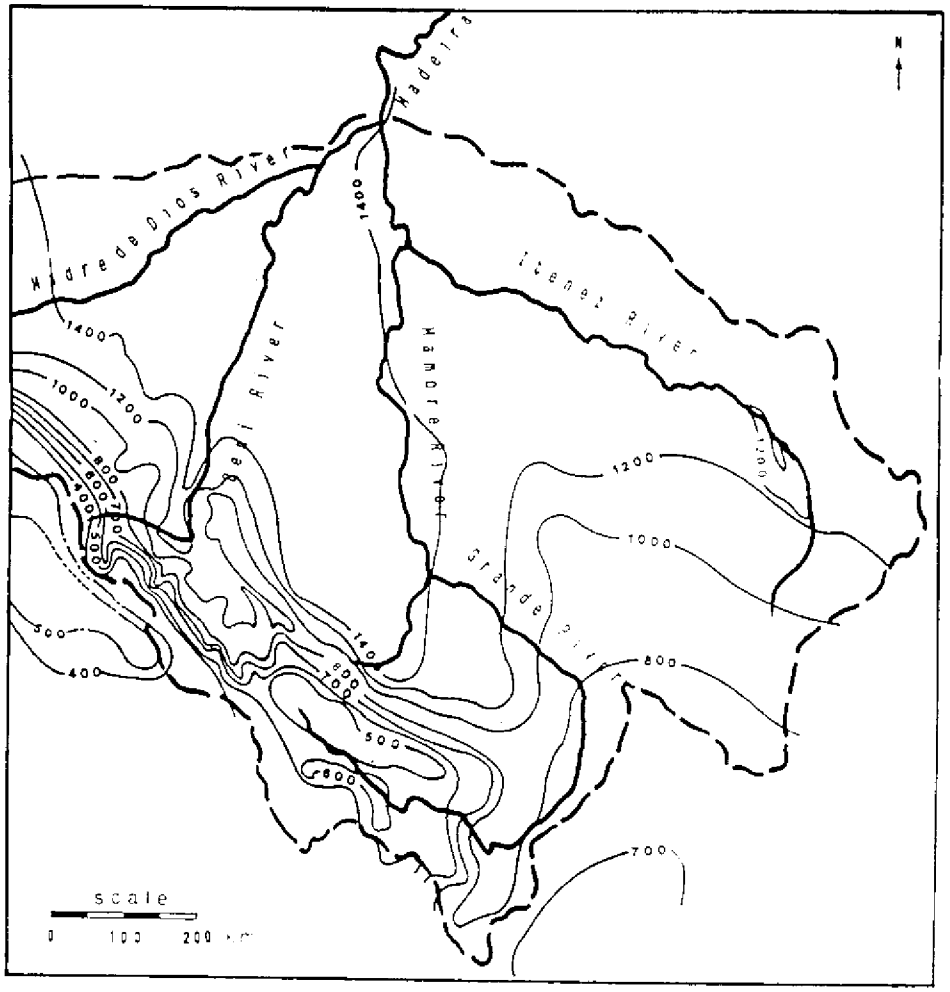

Figure 2 - Map of interannual actual evapotranspiration in the upper Madeira River basin, in mm yr^{-1}, evaluated by Turc and Thornthwaite formulas

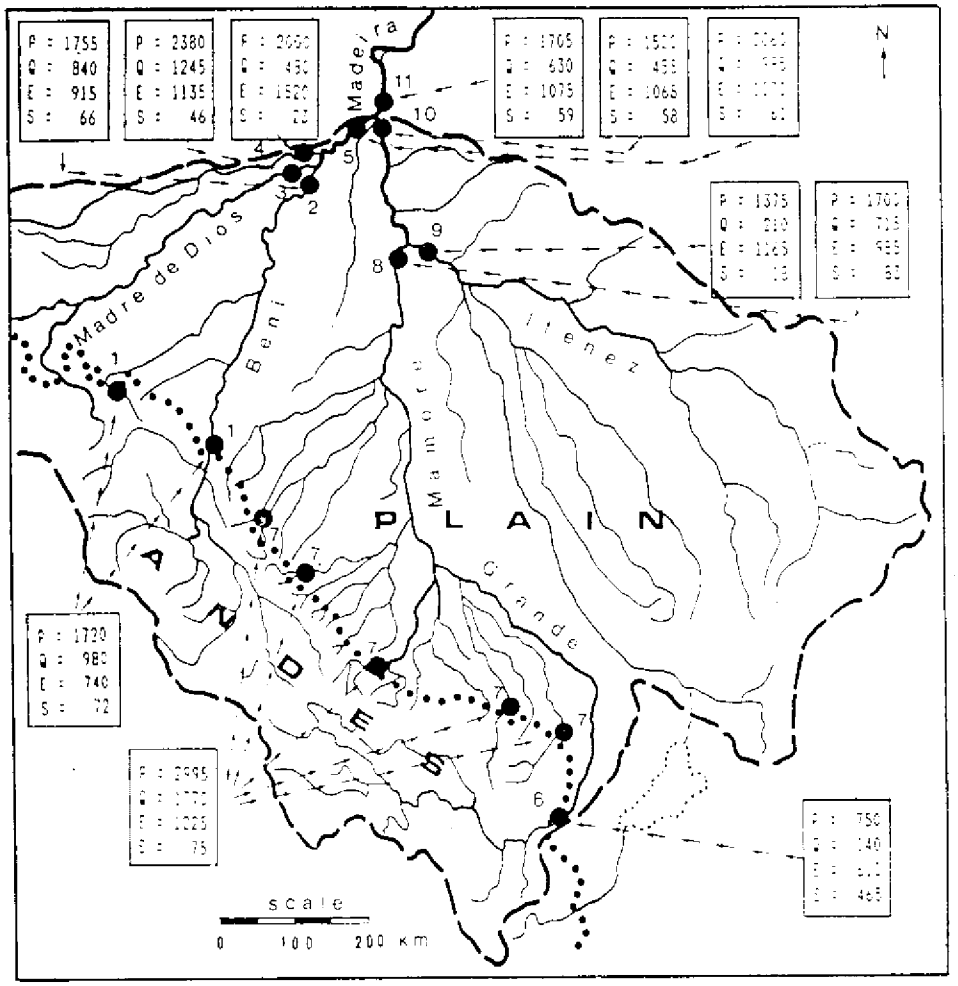

Figure 3 - Water balance: Rainfall (P); Depth of runoff (Q); and Evapotranspiration (E), in mm yr^{-1}, and salinity (S), in mg l^{-1}, in the basins of the Upper Madeira River (period 1968-1982). 1: Beni River at the limit of the Andes. 2: Beni River at the confluence with the Madre de Dios River. 3: Madre de Dios River. 4: Orthon River. 5: Beni River at the confluence with the Mamoré River. 6: Río Grande at the limit of the Andes. 7: Oriental Watersheds at the limit of the Andes. 8: Mamoré River at the confluence with Itenez River. 9: Itenez River. 10: Mamoré at the confluence with the Beni River. 11: Madeira River at its head.

Table I - Interannual Salinity, Water and Ionic Yields of the Upper Amazonian Basin of Bolivia (period 1968/70-1982).

ENTIRE MADEIRA RIVER UPPER BASIN		S U R F A C.	WATER										SALT						
			CLIMATOLOGY			RUNOFF							SALINITY		EXPORTATION				
Period 1968/70-82			Rain mm	Actual Evapot. mm Balance formula		mm	10^9 m^3	%	%	Module m^3s^{-1}	Module sp $ls^{-1}km^{-2}$		Cond. pond. µS	Salin. pond. mgl^{-1}	Exp.sal. 10^6t	%	%	Mod. ion kgs^{-1}	Mod.ion. sp. tkm^2
Beni	Andes	73670	1719	739	781	980	72.2	13.5	25.7	2228	31.1		102	72	5.2	16.4	30.4	165	71
Beni	Plain	48710	1806	1180		626	30.5	5.7	10.9	966	19.8		79	53	1.6	5	9.4	52	33
Beni	s/total	122380	1754	915	1043	839	102.9	19.2	36.7	3261	26.6		95	66	6.8	21.5	39.8	217	56
Madre de Dios	total	125000	2378	1136		1242	155.1	28.9	55.3	4915	39.6		68.8	45.5	7.1	22.3	41.3	224	57
Orthon	total	32360	2000	1518		482	15.6	2.9	5.6	494	15.3		41.2	23.4	0.37	1.2	2.2	11.6	11.3
Beni s.l.	total	283350	2061	1069	1140	993	280.4	52.3	100	8865	31.5		88.1	60.9	17.1	53.9	100	542	60.3
Grande	Andes	59840	751	612	614	139	8.3	1.5	3.2	264	4.4		595	464	3.9	12.3	26.7	123	65
Eastern Basins	Andes	29000	2992		1225	1767	51	9.5	19.9	1617	55.7		106	75	3.8	12	26	121	132
Andes	s/total	88840	1480	812	813	669	59.3	11.1	23.2	1880	21.2		175	130	7.7	24.3	52.7	244	87
Mamore	Plain	133230	1847	1100	1211	747	99.6	18.6	39	3155	23.7		80	54.2	5.4	17	37	171	40
Mamore	s/total	222070	1700	984	1052	716	158.9	29.6	62.1	5033	22.7		115	82.5	13.1	41.3	89.7	415	59
Itenez	total	303280	1373	1162	1223	211	63.9	11.9	25	2021	6.7		34	17.6	1.1	3.5	7.5	35.3	2.8
Mamore	Guayaramerin	547060	1519	1064	1155	455	248.7	46.5	97.4	7880	14.4		84.6	58.1	14.5	45.7	99.3	459	26.5
Yata + B.Brazil	Llanos	20770	1690	1350		340	7	1.3	2.7	222	10.7		37	20	0.14	0.4	0.9	4.4	6.7
Mamore s.l.	total	567830	1525	-1075	1162	450	255.7	47.7	100	8105	14.3		83.4	57.2	14.6	46.1	100	463	25.7
Madeira	Confluence	851180	1704	-1073	1154	631	536	100	-	17000	20		86	59	31.7	100	-	1005	37

Table II - Interannual Salinity, Water and Ionic Yields of the Andean Upper Basins in Bolivia, for the period 1968/70-1982.

Bolivian Amazon, Andes	SURFACE	WATER							SALT					
		Rainfall	Actual evapot.	Runoff					Salinity	Exportation				
	km^2	mm	mm	mm	$10^9\ m^3$	%	m^3s^{-1}	$ls^{-1}km^{-2}$	μS	mgl^{-1}	10^6t	%	kgs^{-1}	tkm^2
Rio Beni	73670	1719	781	980 938	72.2	54.9	2288	31.1	102	72	5.2	40.3	165	71
Eastern basins	28870	2984	1224	1767	51	38.8	11617	56	106	75	3.8	29.5	121	132
Rio Grande	59840	751	614	137	8.32	6.3	264	4.44	595	464	3.9	30.2	123	65
Total Amazon Andes in Bolivia	162280	1587	798	810	131.5	100	4169	25.7	135	98.1	12.9	100	409	80

WATER RESOURCES MANAGEMENT FOR ENERGY GENERATION PURPOSES IN STREAMS PRESENTING STRONG SEASONAL FLOW VARIATIONS - PLANNING ASPECTS -

Bela Petry *
Doron Grull **

ABSTRACT

Important streams of the Amazon region clearly present a huge seasonal variation of discharges. Ratios between the long term mean values of flowrates for the wettest and driest month reach values of 20 in this region while such ratios are only about 3 for rivers such as the Paraná and the São Francisco. Therefore the use of water resources based on river regulation in the Amazon region requires large storage capacities and large flooded areas. The paper deals with this subject in the context of hydropower generation and presents a discussion of criteria related to the value of firm energy, guaranteed energy and mean primary energy as well as their importance as decision parameters for planning purposes. The evaluation of hydrothermal generation systems which may economically justify the construction of Hydroelectric Powerplants having considerably smaller reservoirs is also suggested.

1. INTRODUCTION

The use of water resources for electric power generation purposes had a decisive role in the development of the Brazilian energy mix until the present date.

This general trend is expected to continue during the next decades in view of the still unexplored water resources which can efficiently be utilized considering all technical, economical and environmental aspects involved.

Table 1.1 presents the regional forecast of electric energy demand in Brazil and the regional hydropower potential. It is clear that future hidropower sources to be explored are mainly concentrated in the Northern (Amazon) Region which, due to its particular characteristics, requires a large and general program of natural resources management, as well as carefully selected specific criteria and guidelines, with scarce equivalent precedents to consider in the international or the Brazilian experience.

* *Technical Director* - THEMAG *Engenharia, Brazil.*

** *Consultant* - CASTOR *Planejamento de Sistemas Hídricos , Brazil.*

Table 1.1 - Regional Forecast of Demand of Electric Energy
(Based on Official data from Eletrobras and Brazilian Committee of the World Energy Council)

REGION	INSTALLED CAPACITY IN 1985 (MW)		ELECTRIC ENERGY DEMAND (MW)			HYDROPOWER POTENTIAL	
	HYDRO	THERMAL	1985	2000	2010	(MW)	(%)
North	1370	600	530	3950	7000	48400	45
Northeast	5600	580	2580	8000 *	13500 *	8200	8
Southeast/ Center	23600	2000	13600	33200 *	50200 *	33200	31
South	5630	1160	2700	8900	15220	16800	16
Total	36200	4340	19410	54050	85920	106700	100

(*) Demand exceeds regional offer; supply includes inter-regional flow (from the North)

Three fundamental questions correspond to important challenges to be met:

— First of all the need to provide adequate river regulation and favorable installed capacities of Hydropower Developments to be constructed along important streams characterized by large seasonal discharge variations, without causing excessive environmental impacts. Although several high priority hydrographic basins of Northern Brazil (e.g. the 800.000 km² area Tocantins basin) are not located in the Amazon rain forest, the question of Reservoir Storage capacities and flooded areas becomes very important.

Therefore the design of such Reservoirs must result from a detailed planning activity including an exhaustive search of alternatives, the preference being given to smaller size Reservoirs which cause moderate impacts.

— A second major problem is the distance over 2000 km to be covered by the energy transmission system connecting these powerplants with the major centres of consumption located in the Southeastern and Northeastern regions of the Country.

In addition to the usual power transmission problems such as high cost, UHV technology and operation of the resulting system, the environmental impacts caused by the implementation of these lines and their supporting infrastructure have to be coped with.

— Finally the inter-regional exchange of energy and the differences in hydrologic cycles between drainage basins in different regions of the Country require to certain extent a revision of presently used planning practices and criteria in order to incorporate in detail the variation

of energy generation capabilities, their time patterns, the possibilities of thermal complementation, pumped storage schemes, development of use of secondary energy, etc.

Based on specific cases encountered in Northern Brazil, this paper focuses on the question of seasonal flow variations in the context of energy planning.

2. SEASONALITY AND ENERGETIC CONCEPTS

The planning of energy resources, in Brazil, has been up to now concentrated in the use of hydraulic resources from large basins. This has been the main reason for the intense activity carried out in the last 20 years on the study and development of models, mechanisms and auxiliary tools that could help those that plan the Brazilian energetic system. All of them have been thought, directed and applied to the Brazilian Southeast and Northeast sceneries, considering mainly the Parana, São Francisco and Uruguay rivers and their main tributaries. Therefore most of the existing planning parameters and decision criteria have been strongly influenced by these sceneries.

The proposed question is whether and how a different hydrological behaviour affects those concepts and how to review them. It is noticeable the difference on the seasonality of the Xingu River when compared to the Parana, São Francisco or Tocantins rivers.

To analize and exemplify the influences of a new hydrological scenery, the North-Northeast electrical system has been used, represented by the hydroelectric enterprises on the São Francisco, Tocantins and Xingu rivers.

The simulation of this system on a monthly basis, was processed using the historical inflow series (1931 - 1982) and tried to reach the highest level of energy generation for the biggest demand, with no deficit.

For the Tocantins and São Francisco rivers, the considered dams are those proposed for the year 2005. For the Xingu basin a hypotetical hydropower plant named UHE AMAZ has been considered. The study did not take into consideration neither thermoelectricity generation nor any restrictions from transmission lines.

Tables 2.1 and 2.2 present some of the results, and clearly demonstrate two aspects:

1 — The general guaranteed energy of the system is very sensitive to the regulation capacity of the UHE AMAZ power plant.

Considering the lowest and highest levels of regulation at AMAZ only, while it increases its firm energy to 560 MW the correspondent increment in the system capacity able to handle the demand is increased by 1300 MW. (The firm energy corresponds to the average generation during the system's critical period - July/49 to November/56).

The importance of the regulation can also be observed through the reduction that it causes in the secondary energy (from 24% to 16%). For regulation volumes smaller then 35 km^3 (Ravg), the rate of secondary energy is similar to the rate of the system without the AMAZ powerplant; this energy can be economically "fixed" by using an adequate thermoelectrical generation, as will be shown later.

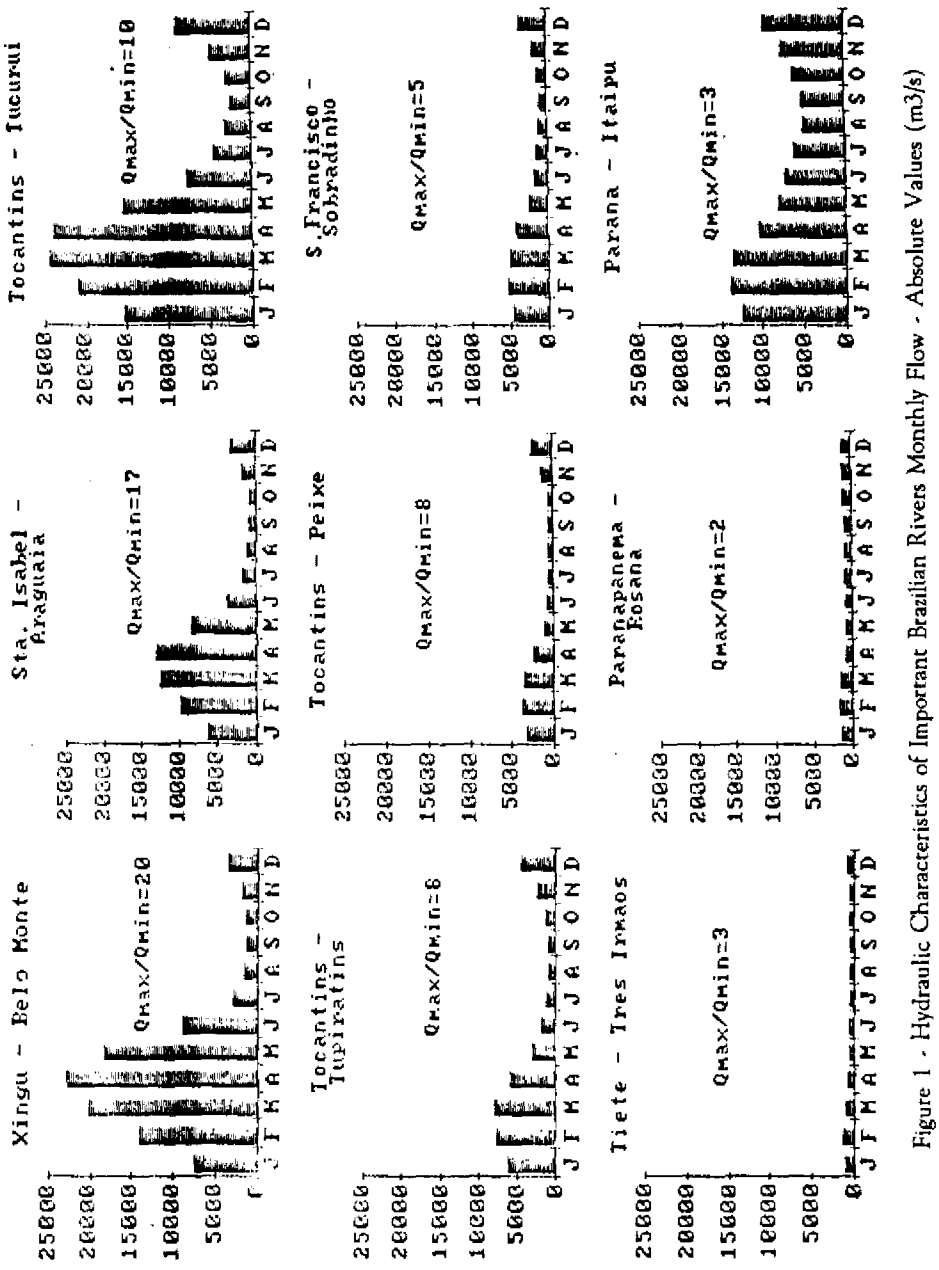

Figure 1 - Hydraulic Characteristics of Important Brazilian Rivers Monthly Flow - Absolute Values (m3/s)

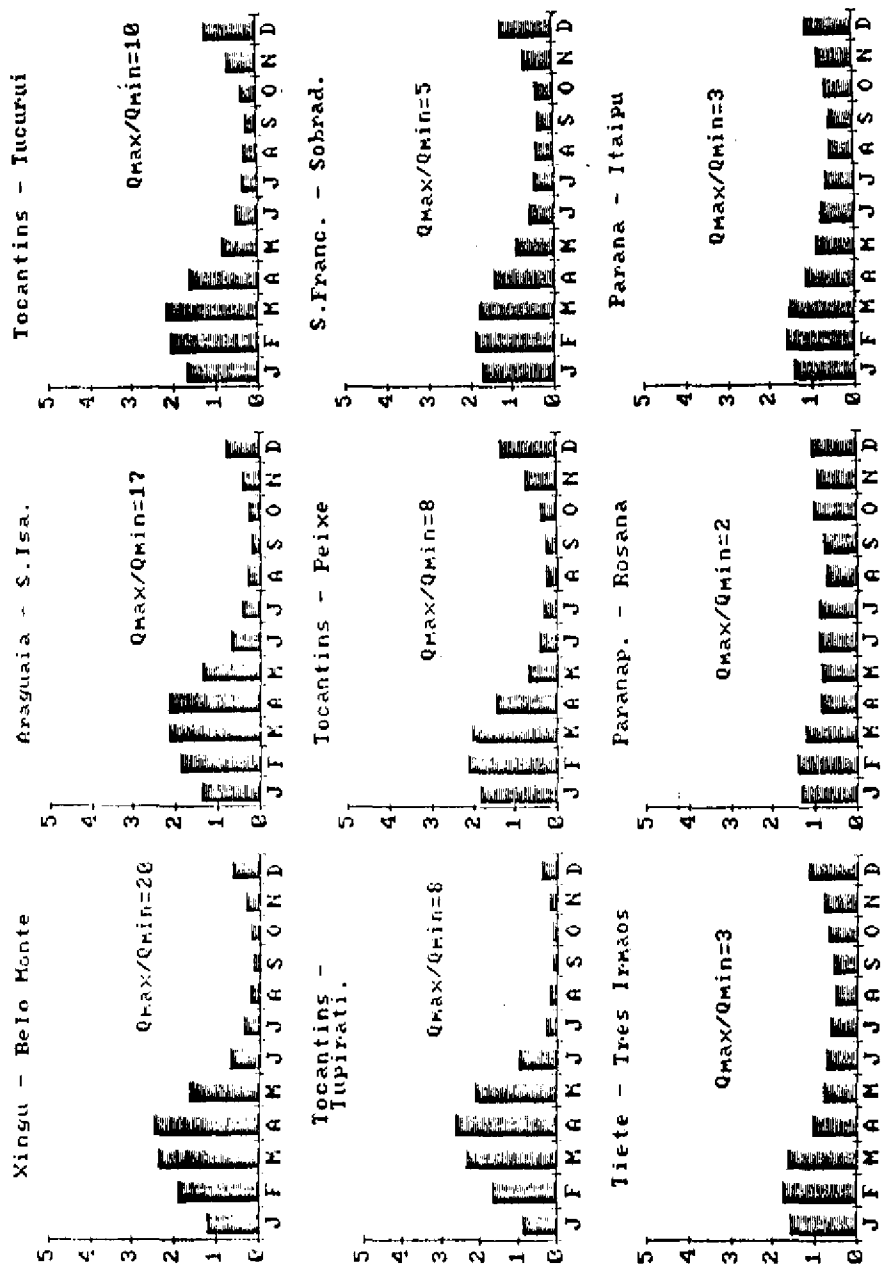

Figure 2 - Hydraulic Characteristics of Important Brazilian Rivers - Values Related to the Average

2 — Although having high hydraulicity in some months and the huge installed capacity at UHE AMAZ, the real energetic content added to the system, as measured by the primary energy, is relatively low when compared to other powerplants from the system.

Therefore, for a UHE AMAZ powerplant without any regulation capacity, primary energy corresponds to about 2230 MW; that means only 43% of the 5130 MW average generation capability.

It is also possible to see that the firm energy at AMAZ is much higher then the real guaranteed energy increment produced by the powerplant; this aspect is important because for the existing dimensioning criteria the opposite would be expected.

The assurance of an increment of 3850 MW brought by the AMAZ powerplant to the system is the sum of AMAZ primary energy of 2230 MW and of 1620 MW produced by the other powerplants of the system due to a synergic effect obtained when the existing reservoirs are better used.

Therefore, the concept and value of primary energy should be taken into account in the procedures used to evaluate the feasibility of hydropower enterprises.

Table 2.1 - System Simulation Results (MW)

	CASE ---->>	WITHOUT AMAZ	AMAZ WITH NO REGULATION	LOW REGULATION (20 km³)	AVERAGE REGULATION (35 km³)	HIGH REGULATION (50 km³)
	Demand	12800	16650	17150	17600	17930
	Average Energy	15166	20561	20700	20786	20866
Nort-East	Superavit	2375	3919	3557	3199	2945
System	Critical Period Energy	13235	17925	18161	18324	18520
	Critical Period Superavit	445	1285	1019	759	611
AMAZON	Average Energy	---	5133	5223	5269	5319
	Firm Energy	---	4852	5066	5214	5412
Powerplant	Primary Energy	---	2234	2541	2819	3051
Paulo Afonso	Average Energy	2145	2180	2186	2194	2198
	Firm Energy	1980	1954	1964	1978	1981
Powerplant	Primary Energy	1220	1344	1397	1457	1491
Xingo	Average Energy	2078	2155	2169	2184	2189
	Firm Energy	2044	2027	2047	2070	2074
Powerplant	Primary Energy	1278	1407	1462	1525	1559
Peixe	Average Energy	604	594	595	595	595
	Firm Energy	430	410	407	406	406
Powerplant	Primary Energy	383	404	413	423	430
Serra	Average Energy	943	975	980	985	988
Quebrada	Firm Energy	864	854	854	856	855
Powerplant	Primary Energy	589	608	631	660	679
Tucurui	Average Energy	4970	5036	5046	5050	5057
	Firm Energy	3905	3919	3907	3877	3865
Powerplant	Primary Energy	3092	2718	2909	3090	3220

Cases

— Without AMAZ	— system without UHE AMAZ
— AMAZ without Regulation	— system with UHE type runoff river
— Low Regulation	— system with UHE AMAZ and reservoir having 20 km³ of useful volume
— Average Regulation	— system with UHE AMAZ and reservoir having 35 km³ of useful volume
— High Regulation	— system with UHE AMAZ and reservoir of 52 km³ of useful volume

Table 2 - Comparative Analysis of Primary Energy Content

Table 2.2.A

			PRIMARY ENERGY/FIRM ENERGY			
CASE —>>	INSTALLED CAPACITY	WITHOUT AMAZ	AMAZ WITH NO REGULATION	LOW REGULATION	AVERAGE REGULATION	HIGH REGULATION
Paulo Afonso Powerplant	4436	0.62	0.69	0.71	0.74	0.75
Xingo Powerplant	3210	0.63	0.69	0.71	0.74	0.75
Peixe Powerplant	1294	0.89	0.99	1.01	1.04	1.06
Serra Quebrada Powerplant	1362	0.68	0.71	0.74	0.77	0.79
Tucurui Powerplant	7920	0.79	0.69	0.74	0.80	0.83
AMAZ Powerplant	11000	—	0.46	0.50	0.54	0.56

Table 2 - Comparative Analysis of Primary Energy Content

Table 2.2.B

			PRIMARY ENERGY/FIRM ENERGY			
CASE ----->>	INSTALLED CAPACITY	WITHOUT AMAZ	AMAZ WITH NO REGULATION	LOW REGULATION	AVERAGE REGULATION	HIGH REGULATION
Paulo Afonso Powerplant	4436	0.28	0.30	0.31	0.33	0.34
Xingo Powerplant	3210	0.40	0.44	0.46	0.48	0.49
Peixe Powerplant	1294	0.30	0.31	0.32	0.33	0.33
Serra Quebrada Powerplant	1362	0.43	0.45	0.46	0.48	0.50
Tucurui Powerplant	7920	0.39	0.34	0.37	0.39	0.41
System (*)	25112+AMAZ	0.51	0.46	0.47	0.49	0.50
AMAZ Powerplant	11000	---	0.20	0.23	0.26	0.28

(*) Demand/Installed Capacity

3. SEASONALITY AND THERMOELECTRICAL COMPLEMENT

Studies performed regarding the Tucurui Hydroelectric Powerplant on the Tocantins river, have demonstrated that for the original proposed installed capacity of 7260 MW there was not only a very meaningful secondary energy of over 1000 MW (longterm average) but also a more impressive amount of spilled seasonal energy: 2300 MW

There are many ways to assure part of this seasonal energy: one of them is the introduction of thermo electric powerplants that our studies have shown to be economically interesting.

The analyzed scenery considered the North - Northeast Interconected System in the year 2005, as foreseen scenery in the "Plano 2010" of ELETROBRAS.

Studies have shown that the guaranteed energy produced by the hydroelectric powerplants is 10000 MW, considering risk of deficit about 3% and supposing that there are no transmission capacity restrictions.

The operation criteria adopted for the analysis were similar to those used by the GCOI/ELB (Interconected Operation Coordination Group/ELETROBRAS) considering monthly revised storage level targets.

The thermoelectric powerplants were added to the system with the same capacity as the generation capacity added to Tucurui powerplant.

The simulation tried to establish the best added firm energy to the system with the minimum use of the thermoelectric powerplant.

An increase of about 80% of the added thermoelectric generation capacity was obtained for an operation time of only 42%.

In other words, for each increment of 1000 MW added to the already "existing" 7260 MW at Tucurui Powerplant an equivalent 1000 MW of thermoelectric generation capacity was added to the system. This mix increased the guaranteed energy of the system in about 800 MW, activating the "thermo" powerplant only 42% of the time.

The simple operation rule that produced this result was to activate the thermoelectric powerplant only when the useful volume of Tucurui was under 45%.

Table 3.1 presents the cost-index for the incremental guaranteed energy obtained for an added generation capacity at Tucurui of 2800 MW, and various types of thermoelectric powerplants.

The results show the feasibility of using the secondary and seasonal energies available at Tucurui powerplant, being an excellent alternative for the regional system by the end of the century.

The added capacity values and operation rules can be optimized as well as the geographical distribution of the thermoelectric powerplants.

It is important to point out that the results obtained for Tucurui powerplant are not necessarily suitable to all other powerplants of the North region. An extremely strong hydrologic seasonality like that occurring at the Xingu river will certainly demand a more intensive and frequent thermoelectric complementation, therefore turning its feasibility. more difficult. In this case the correct amount of regulation capacity must be determined in order to optimize the system.

Table 3.1 - Thermo Electric complementation cost-index for the use of seasonal energy at Tucurui Powerplant

THERMO TYPE	ANUAL COSTS			
	THERMOELECTRIC POWERPLANT		POWERPLANT	COMBINED HYDROTERMIC POWERPLANT
	FIX COST/YEAR US$/kW	VARIABLE COST/YEAR US$/kW	FIX COST/YEAR US$/kW	UNITARY COST US$/MWh
gas-simple cycle burning gas	59	26	33	24
gas-simple cycle burning oil	59	45	33	32
gas-combined cycle burning gas	87	17	33	24
gas-combined cycle burning oil	87	28	33	29
steam burning oil	96	28	33	30
steam burning charcoal	116	26	33	32

4. CONCLUSIONS AND SUGESTIONS

The mentioned cases can be considered as typical examples for the Brazilian North region. Of course not all hydroenergetic related problems are presented, but some important aspects have arisen demanding a special care from the planner:

— A wider and more intensive use of the North Region hydroenergetic resources and its linking to the Northeast and Southeast consumer market brings to the planning scenery the marking difference of huge seasonal variation discharges.

  This new scenery demands the consideration of new decision parameters and the revision of the existing planning tools and models. More flexible and adaptable simulation systems - like CASTOR, for instance, - should be used in order to allow the modeling of real operation and energy transmission problems.

— Transmission costs from the North region to the consumer market are very high, being approximately of the same order of magnitude of the generation costs. Besides, the worries related to the environmental impact are similar.

For these reasons, regulation, transmission and installed capacities are related problems with an stronger interdependence than in hydroenergetic planning in other regions.

— Specifically, the size of the reservoirs should be optimized taking into account the primary energy offered by the powerplant to the system and the possibilities of thermoelectric complementation improving the efectiveness of the seasonaly available energy.

Also, a seasonal consumer market can be very interesting, and it is advisable to look for it for future sceneries.

WORTH OF HYDROLOGICAL DATA IN WATER RESOURCES PROJECTS. APPLICATION: BOLIVIANS AMAZONES ZONE

*Edgar Salas Rada**
Gert A. Schultz **

ABSTRACT

If water projects are planned and designed on the basis of rather short time series of observed hydrological data the danger of inefficient solutions is high. Therefore the knowledge of the value of additional information is of great interest. The Bayesian theory allows the introduction of so called "prior information" into the decision process. Prior information may stem from regional hydrological data or from other sources of knowledge on geophysical processes. In this paper Bayes theory is used to quantify the value of additional information in a planning process expressed by the Bayes risk parameter.

In order to do this a simulation model is used which consists of three components:

— Bayesian submodel for generation of hydrological time series.
— Submodel simulating the operation of a water resources system (hydropower/flood protection resp.) on the basis of the synthetic data.
— Submodel for the evaluation of the system performance expressed by the minimum Bayes risk.

The latter submodel allows analysis and comparison of results obtained from different information-decision systems. The technique was applied to the ENDE hydropower system and to the flood Trinidad Protection System in Bolivia. The Bayes risk values were computed for all simulated alternatives, including different lengths of available hydrological data series. The results obtained show that the losses -or risk- due to incomplete information decrease with increasing amount of data or in other words: the value of additional information decreases with time. This is expressed in terms of the dimensionless Bayes risk or in monetary terms. The value of prior information is high, if only short observation periods of hydrological data exist. It also decreases with observation time.

1. THE PROBLEM

Many failures of water projects -particularly in developing countries- are due to project planning on the basis of inadequate hydrological data. By inadequate we mean two properties:

— data which are not accurately measured;

— too short time series of observed data not allowing reliable estimates of system performance

In the latter case some scientists suggest to postpone the project until more adequate data are observed. Although this suggestion is theoretically sound it lacks a feeling for the needs of practice.

* *Universidad Mayor de San Andrés - La Paz, Bolivia*
** *Ruhr University - Bochum, Germany*

A better way to alleviate the problem may be the use of other available information ("prior information") which -in combination with inadequate measured data- may improve the planning results. The Bayesian theory uses this approach.

By "prior information" we mean knowledge on comparable processes, e.g. hydrological data from other comparable river basins or even from other geophysical processes.

The primary aim of this paper is to demonstrate the value of additional information for the efficiency of water projects. This value is expressed either by a monetary gain due to more (or better) information or by the reduction of the so-called Bayes risk of the project.

The theoretical approach is verified along with the planning process of a hydropower project and a flood-protection project in Bolivia.

In these cases the available information consists in observed hydrological data of a river in the high mountains, resp. in the plain of Bolivia. Prior information is obtained from river gauges in a larger region around the project area.

The planning purpose is the optimum design of a hydropower plant. Inadequate hydrological data may lead to over -or under- design of the power plant. Bayesian theory is applied in order to minimize the risk of such over- or underdesign.

In this context we have to distinguish between two types of hydrological uncertainty.

The natural uncertainty is due to the random variation of hydrometeorological processes, which is unavoidable, i.e. it exists always, even if all possible information on that process were known. In this context runoff, for example, in a river has to be considered as a random variable. Its random variability is due not only to the stochasticity of the causative rainfall process but also due to interception, infiltration, snow melt, evapotranspiration, etc. These combined uncertainties may be expressed mathematically by a probability distribution function (pdf) of the population, i.e. the process in nature.

The information uncertainty is due to the effect that data observed from nature represent always only samples of a unknown population. This leads to the fact that the knowledge on such processes -expressed by pdf's- yields only sample parameters but never population parameters (e.g. means, variances, correlations). While classical probability approaches assume sample statistics to be identical with population statistics, Bayes theory accepts that each sample produces it own set of parameters. Thus also each sample parameter has its own pdf being the reason for the information (samples) uncertainty.

It is the aim of this paper to show that planning results can be improved (by reduction of sample uncertainty, i.e. reduction of planning risk) with the aid of Bayes theory. This is done along with a case study representing planning of a hydropower (resp. flood-protection) system in Bolivia. For the solution of this problem within the framework of Bayes theory (Zellner, 1971; Berger, 1980), models were developed allowing to estimate the worth of information expressed by a special type of risk (Bayes risk). Various informations -partially observed discharge data at project site, partially discharge values from other gauges within the region (prior information) are combined by the Bayes theorem. The concept of an information decision system (Krzystofowicz, 1983) is applied in order to investigate the interdependencies between available information, models applied, evaluation criteria

and decisions to be taken. For this purpose the Bayes risk for various information-decision systems is computed and results are compared.

A further source of uncertainty -model uncertainty- will not be discussed in this paper.

2. THEORY

The theoretical derivations which were necessary in order to fulfill the task discussed above, were rather extensive and are published elsewhere (Sales, 1989). Therefore they are sketched here only briefly.

In the Bayes approach the pdf's of a process are combined with the pdf's of the parameters of such processes. In order to express the pdf of a process in nature (e.g. runoff) considering natural and parameter uncertainty, Bayes pdf can be used:

$$f(x) = \int_{\theta} \int_{x} f(x \mid \theta) \; f(\theta) \, dx \, d\theta \tag{1}$$

where $\varnothing$ represents parameters of the pdf (e.g. mean, variance, correlation coefficient) and $f(\varnothing)$ is the pdf of such parameters.

f(x) = pdf of a process of interest.

Each parameter set $\varnothing$ is obtained from different prior information (e.g. discharges observed at neighbouring river gauges). Equation (1) thus represents a Bayesian pdf which may be interpreted as conditional pdf of the process variable weighted by the probabilities of the parameter vector $\varnothing$. Based on the observed (too short) sample data and prior information the posterior distribution of the parameters can be computed with the aid of Bayes Theorem (Fig. 1).

$$f''(\theta \mid x) = \frac{p(x \mid \theta) \, f'(\theta)}{\int_{\theta} p(x \mid \theta) \, f'(\theta) \, d\theta} \tag{2}$$

with

$f''(\theta \mid x)$	Posterior pdf of variable
$f'(\theta)$	Prior density of $\varnothing$
$p(x \mid \theta) = L(\theta)$	Likelihood-function

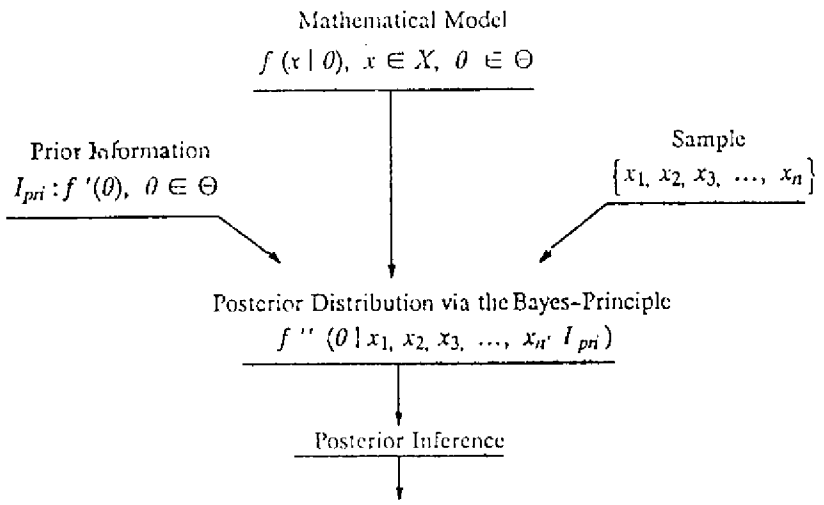

Fig. 1 - Prior Information, Sample and Posterior Distribution

A basic component in Bayes' theory is the risk concept which requires the definition of a risk function. The risk function R represents the expected value of a goal function g quantifying the consequences (e.g. losses L) which occur if a decision d_i is made process x is realized and $\varnothing$ is the true parameter:

$$g(d_i, x) = \int_x L(x, d_i)\ f(x \mid \theta)\ dx \tag{3}$$

$$R(d_i) = \int_\theta g(d_i, x)\ f(\theta)\ d\theta \tag{4}$$

Following Bayes' rule from all possible decision d_i the optimum decision d* is selected which minimizes the Bayes risk:

$$R_B(d^*) = \min_{d_i} R(d_i) \tag{5}$$

For design purposes decision d* is the alternative to choose.

If the true values of $\varnothing$ (i.e. of the population) were known, the pdf of $\varnothing$ could be replaced by one value $\varnothing t$. In this case the optimum value of the risk and thus the optimum decision could be specified. Compared to this value a decision made on the basis of equation (5) would lead to an

opportunity loss. Since $\varnothing$ t is unknown it is replaced by the prior information. For purposes of comparison of two alternatives (e.g. availability of different quantities of information) the evaluation criteria would be the reduction in expected opportunity loss. Later it will be shown that an increase in information leads to a reduction in Bayes' risk as well as in opportunity loss.

In order to prove this along with the example of the hydropower project in Bolivia a numerical technique has to be chosen since an explicit mathematical representation of the planning process as required here is not possible. Therefore a simulation technique will be chosen using synthetic input data computed with the aid of a Bayesian data generation model.

3. ESTIMATION OF BAYES' RISK WITH THE AID OF A SIMULATION MODEL

The computation of all relevant values of Bayes risk for many alternatives of information-decision systems and the evaluation and comparison of results is carried out on the basis of a simulation model containing three submodels:

— Bayesian submodel for the generation of synthetic hydrological time series (discharges);

— Submodel simulating the process occurring in the water resources system including hydropower plants (flood-protection system);

— Submodel for the evaluation of the system's performance for the given (synthetic) input time series.

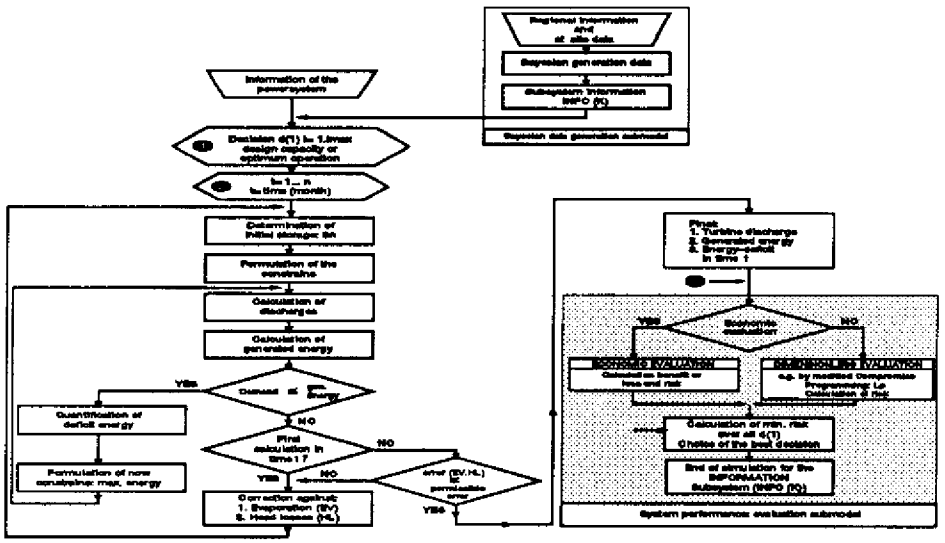

Figure 2 - Simulation model for hydropower system including submodels

3.1 Bayesian Synthetic Data Generation Model

Classical stochastic models for the generation of synthetic hydrological time series consider only the natural uncertainty of the process but not the information uncertainty. Models taking into account both natural and information uncertainty become rather complex which may be the reason why only few such models are "on the market". As can be seen from Figure 2 in the context of the work presented in this paper such a Bayesian data generation submodel is applied, which takes into account the natural uncertainty as well as the sample uncertainty. Monthly runoff time series are generated at a project site by the model which considers the model parameters as random variables using the "Bayesian predictive function". Figure 3 show the flow chart of this model.

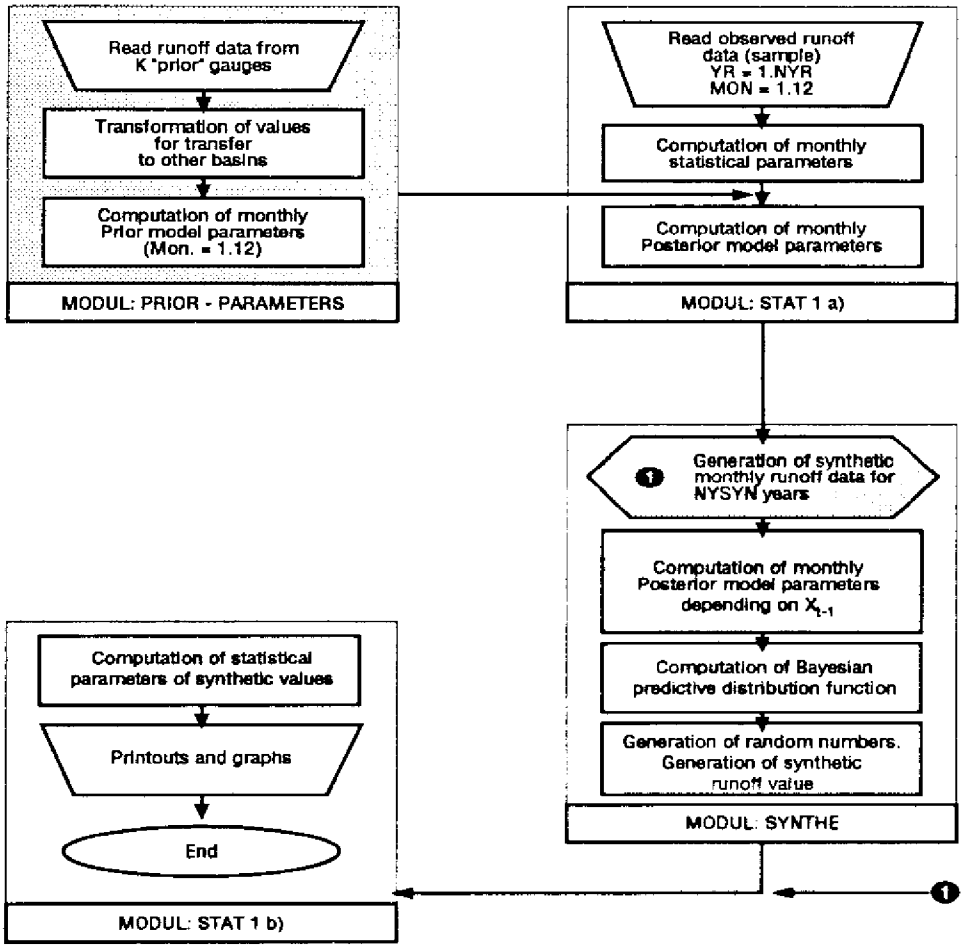

Figure 3 - Bayesian generation of synthetic monthly runoff series

In order to estimate the influence of the information content on the planning results, the Bayes' risk for various information subsystems is computed and the risk values are compared. Two types of information subsystems are considered:

— sample time series of runoff at project site of duration n_1, n_2, ... N;

— prior information observed at neighbouring river gauges in combination with observed (sample) data at project site.

3.2 Simulation Procedure and Evaluation Submodel

The Bayesian data generation submodel (Fig. 3) forms only part of the total simulation model (Fig. 2). The latter simulates the reservoir operation including energy generation, whereas the evaluation submodel allows to analyze and compare various alternative information-decision systems and to compute their risks. The risk is expressed as expected value of annual losses for each possible decision alternative based on the computed values (via simulation) of generated energy and energy deficit. Since the Bayes criteria for optimum decisions is based on minimum risk, this optimum was found by a simple search technique from the computed alternatives. Two loss functions were developed, one economic function, the other a dimensionless loss criteria.

The technique described was applied to the ENDE hydropower system in Bolivia. The risk values or the values of additional information were estimated for various information-decision system. Prior information came from 15 other basins in the central and upper Andes mountains as well as from 3 river gauges within the ENDE system catchment.

4. SIMULATION OF SYSTEM PERFORMANCE AND RESULTS

In order to analyze the influence of additional data (longer data time series at the project site or prior data from other sources) on the performance of the hydropower system expressed by Bayes' risk, many computer simulations have been carried out. The power system chosen was the Corani-Santa Isabel-San José hydroproject which is located in the eastern Andes mountains in Bolivia.

The point under consideration here is a design problem, namely the determination of the required storage capacity of the Corani reservoir. Thirty potential capacities are investigated and for each simulation runs were carried out. The optimum reservoir capacity for each simulation is found as that value which yields the minimum expected loss (or risk according to Bayes minimum risk criteria.

The procedure for the various simulations based on synthetically generated data (Fig. 3) is as follows: the length of the observed runoff time series for the project site was 29 years of monthly data. For comparison purposes it seemed desirable to have a population of data available instead of the sample. A "pseudopopulation" of 1000 years was generated with the aid of an AR-1 model. It could be expected that the choice of this model may influence the simulation results. Since, however, later the value of additional information is estimated on the basis of *relative* risk values this influence will become very small or eliminated.

The next step consists in the selection of many partial time series of duration n (e.g. 4 years) from the pseudo population series. Each partial series of n years then forms the basis for the generation of many synthetic time series of 20 years duration (project contract horizon).

For each synthetic series the systems simulation was carried out and from the results the expected value of Bayes risk was computed. This procedure was repeated for n = 4, 5, 7, 10, 12, 15, 17, 20, 30, 40 and 50 years of length of partial series taken from the pseudo-population series. This way one obtains many Bayes risk values for each length of original data series, i.e. 4, 5, 7, 10, etc., years of "pseudo-sample" lengths.

The objective function for reservoir operation in the simulation was either maximum energy production or meeting the demand. Both alternatives have been investigated.

After the simulations were carried out by some special averaging procedure the Bayes risk value was obtained for each time series length of pseudo-sample' time series (4, 5, 7, ... 50 years). The risk was expressed both, in the conventional dimensionless form and as a monetary value in Mio $ representing a loss in power production.

The procedure was done -as described above- for increasing amounts of information at project site, i.e. increasing length of hydrologic observation time series (4, 5, 7, ... 50 years) as well as for this type of information extended by prior information obtained from 15 river gauges at neighbouring catchments.

The results obtained show two interesting and for planning purposes important tendencies:

— increasing length of observed data series leads to a decrease of losses (or Bayes risk), or in other words: the value of additional information decreases with observation time;

— the availability of prior information leads to a decrease of losses (or risk).

Figure 4 show a typical example of the results obtained in a hydropower system and Figure 5 the results in a flood-protection system.

From Figure 4 it can be seen that additional information (longer time series or prior information) reduces the losses or risk considerably in only a short observation period exists. If e.g. the observation period of 4 years is increased by only 1 year to 5 years the risk will be reduced by 10 percent or -in the Corani project- by 211.000 $.

If a longer data series is available, e.g. 20 years, then the value of additional data is very low (Figure 4).

The fact that the Bayes risk is reduced by 23% if the observation series is increased by 3 years (from 4 to 7) and reduced by 46% if increased by 8 years (from 4 to 12 years) shows the significant value of additional data.

It can also be seen in Figure 4 that regional prior information reduces the risk significantly if only short data series are available. If 15 or more years of data exist prior information has almost no value.

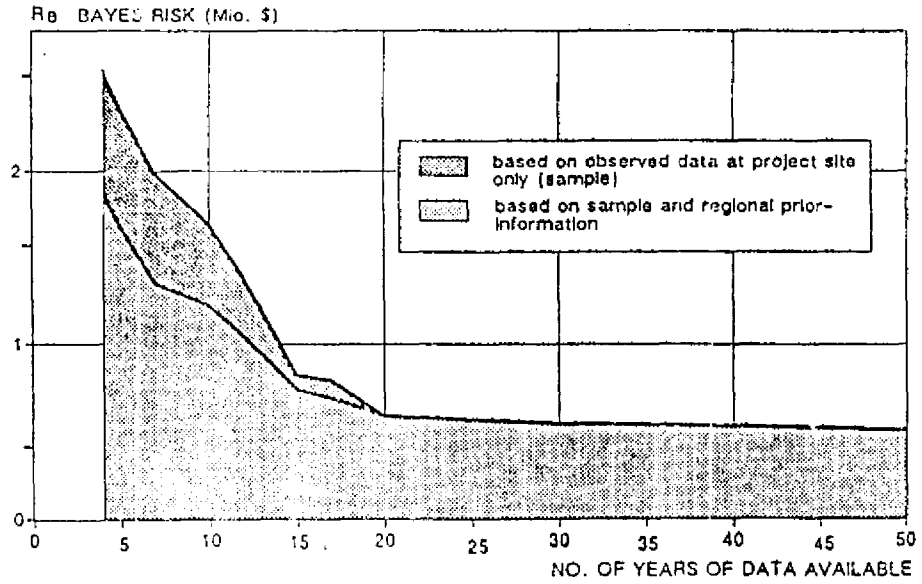

Figure 4 - Bayes' Risk vs. No. of years of Data. Hydropower System ENDE (partial System), Bolivia.

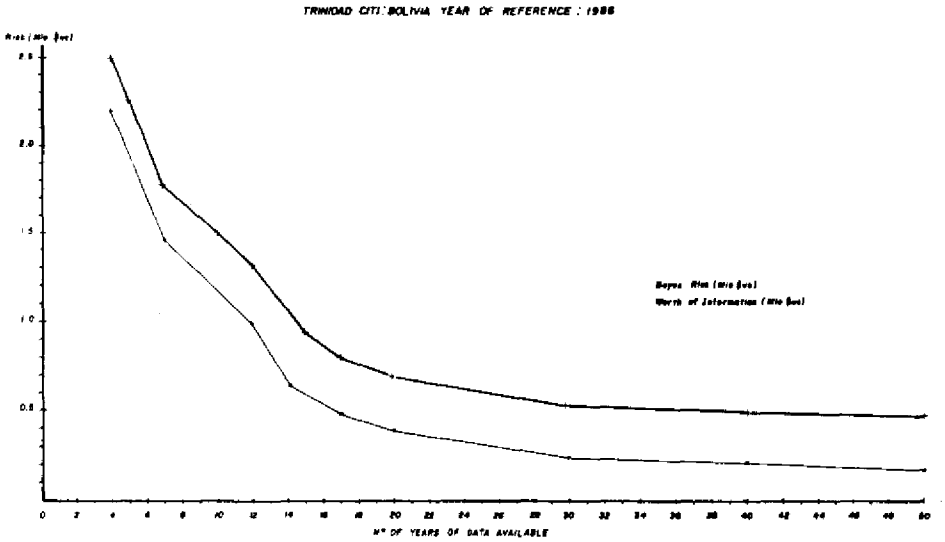

Figure 5 - Bayes risk and worth of information

The above investigations were carried out for different reservoir operating rules and for differents types of loss functions. The results of all alternatives (Salas, 1989) show the same tendency as the curves in Figure 4. It is worth mentioning that there was always onwards additional data which has almost zero value.

Additional information can be obtained in three ways:

— waiting until more data are observed;

— using prior information from other source, e.g. regional data;

— computation of runoff data with the aid of satellite data (Schultz, 1988)

Unfortunately computing time for the above Bayesian analyses as described in this paper is very high — even on larger mainframe computers. Nevertheless results as given in Figure 4 represent a valuable decision support for decision makers faced with planning problems in the field of water resources management.

REFERENCES

Berger, James O. Statistical Decision Theory Foundations. Concepts and Methods. Springer-Verlag, New York, 1980.

Krzvstofowicz, Roman; Davis, Donald R. A. Methodology for Evaluation of Flood Forecast-Response Systems. Water Resources Research, 1983, Vol. 19, No. 6.

Salas, E. A. Anwendung der Bayesischen Theorie auf Wasserwirtschaftliche Planungen mit kerzen hydrologischen Detenreihen (Application of Bayes theory to the design of water resources systems if only short series of hydrologic data are available - in German). Schriftenreihe Hydrologie/Wasserwirtschaft (Ed. G. A. Schultz). 1989, Ruhr University Bochum, Germany.

Schultz, G. A. Remote Sensing in Hydrology. Journal of Hydrology. Elsevier Science Publisher. Amsterdam. Vol. 100 (pp. 239-265), 1971.

Zellner, Arnold. An Introduction to Bayesian Inference in Econometrics. John Wiley & Sons. Inc., New York, 1971.

ANALYSIS OF INTEGRATED WATER RESOURCES MANAGEMENT: SOME EXPERIENCES RELEVANT FOR THE AMAZON BASIN

J. G. S. Smits, J. G. Grijsen and J. P. M. Dijkman *

ABSTRACT

Planning for water resources development and management has evolved into a complex multi-disciplinary activity. As a consequence, analysis to support water resources planning has changed as well. The first part of this paper develops the concept of a *Framework for Analysis* and a *Computational Framework* to structure the analysis and to make optimal use of modern computational techniques. Parts of the computational framework dealing with storage and analysis of hydrological data, river basin simulation, and water quality modelling will be highlighted. The second part of this paper focuses on an important element of the analysis and of the computational framework, dealing with the water quality and ecological consequences of reservoir development. To investigate the possible effects of future large-scale projects, mathematical ecological models have been developed. An application of these models, specifically dealing with water quality in relation to stratification and decomposing drowned vegetation, is presented for the Tucurui and Balbina reservoirs in the Amazon basin. Conclusions are drawn with respect to the biological productivity of the reservoirs.

1. INTRODUCTION

Water resources play an important role in human activities. Due to the growth of population and economic activity the demand for water has increased while the quality of water often has deteriorated. Good quality water has become a scarce resource in most countries. In many cases local systems are no longer sufficient. Consequently more comprehensive, complex schemes for water resources development were designed and are being operated on a scale of a region or a river basin. The rational planning of such schemes has become a complex multi-disciplinary activity.

Analysis to support planning for water resources development and management has a simple aim: to provide (preferably quantitative) information to decision-makers to enable a better selection from alternative measures (strategies). Given the context of water resources planning, the analysis should meet certain requirements:

* *Delft Hydraulics - P. O. Box 177 - 2600 MH Delft, The Netherlands*

— The analysis should be management oriented and aim at the provision of accurate and useful information for the decision-making process.

— An intensive interaction between analyst and decision-maker is required to ensure that the analysis focuses on the important problems, as perceived by the decision-makers, and produces the type of information desired by the decision-makers.

— Besides decision-makers, also implementing agencies and interest groups should be involved in the analysis to promote the acceptance of the analysis results and to produce a successfully implemented policy for water resources development.

— The analysis should be sufficiently flexible. It should allow to examine alternative strategies; to determine the relevant socio-economic and environmental impacts; and to quantify uncertain developments.

— Because water resources planning is a continuous activity, the analysis should be done in such a way that applied analytical techniques fit into a consistent framework for analysis. Such a framework can be gradually expanded and improved, and can be continually used to provide information for decision-making on water resources development and management.

2. ANALYSIS APPROACH TO INTEGRATED WATER RESOURCES MANAGEMENT

Systems analysis is an analysis approach which can meet the above mentioned requirements. It incorporates a framework for analysis, which structures the analysis process and allows the integration of the contributions of various disciplines. It also provides a computational framework containing a consistent set of mathematical models, databases and computational procedures. The use of these analytical techniques promotes the execution of an efficient quantitative analysis.

The Framework for Analysis, depicted in Figure 1, can be divided into three phases:

— **Inception phase**, in which the problems are identified, objectives, constraints and criteria are defined, an inventory of possible measures is made, and analysis conditions are specified. The findings of this phase are summarized in an inception report.

— **Preparation phase**. In this phase, characterized by data analysis and model development, a detailed analysis is made of the water using activities and the water resources system. The computational framework is developed in this phase.

— **Analysis phase**, in which alternative strategies for water resources management are analyzed and their impacts assessed and evaluated.

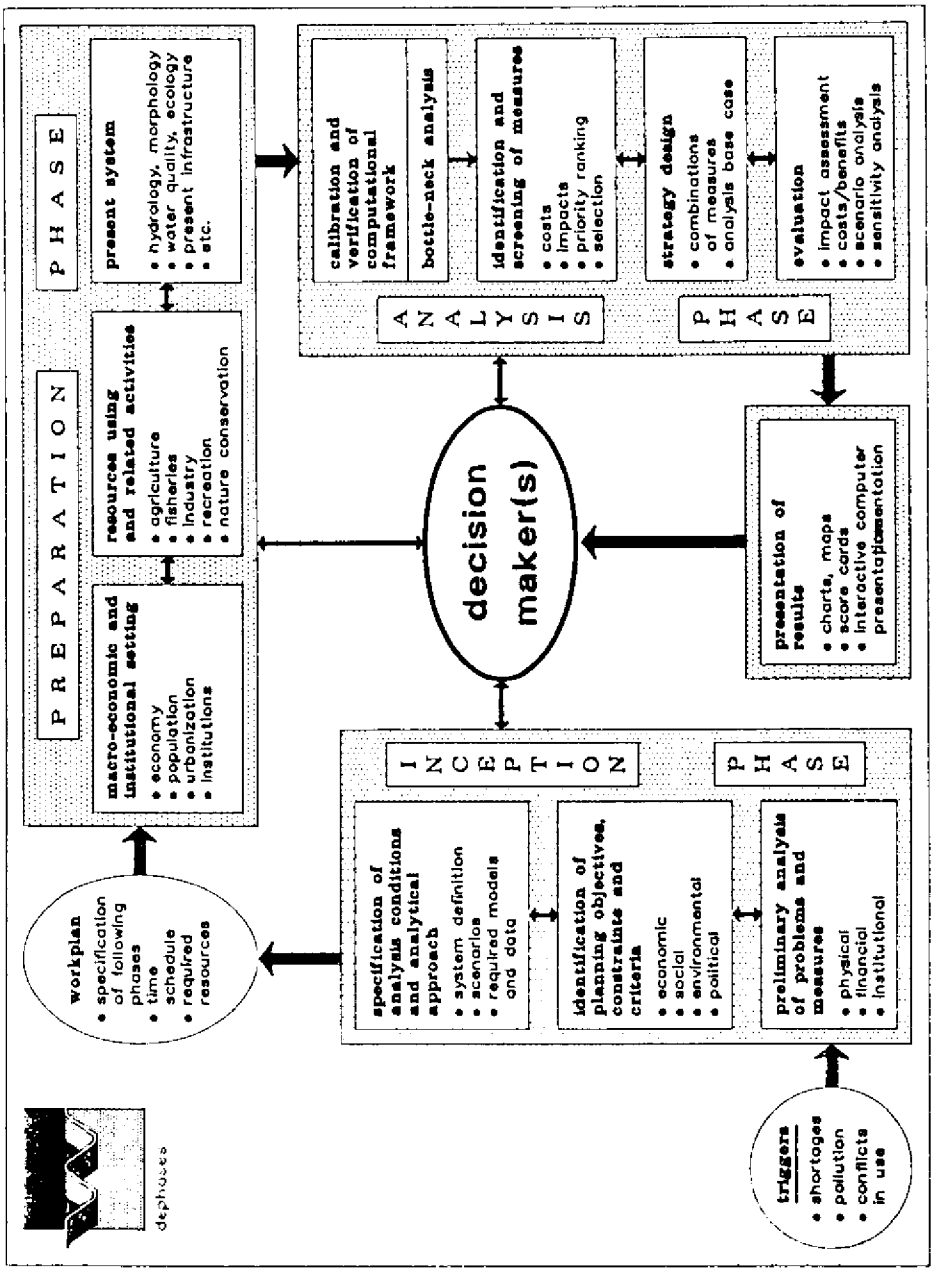

Figure 1 - Framework for Analysis for Water Resources Management studies

3. COMPUTATIONAL FRAMEWORK

The computational framework to be developed during the preparation phase comprises a set of models (economic, physical, ecological, etc.) and databases, which are well tuned to each other. The computational framework assists in the quantitative evaluation of alternative measures and strategies.

The models should be simple in view of the often global character of the evaluation and the large uncertainties in data, process parameters and scenario variables. They should be 'transparent', allow interactive use and be well documented. For example, it makes no sense to use a complicated dispersion model if the underlying processes are not very well known or the values of pollutant loads have a large range of uncertainty. The selection of the type of model is a difficult choice, which requires experience to obtain proper balance between simplicity and credibility or completeness.

Figure 2 presents the main components of the computational framework as developed by DELFT HYDRAULICS for the simulation of the water resources situation in river basin systems.

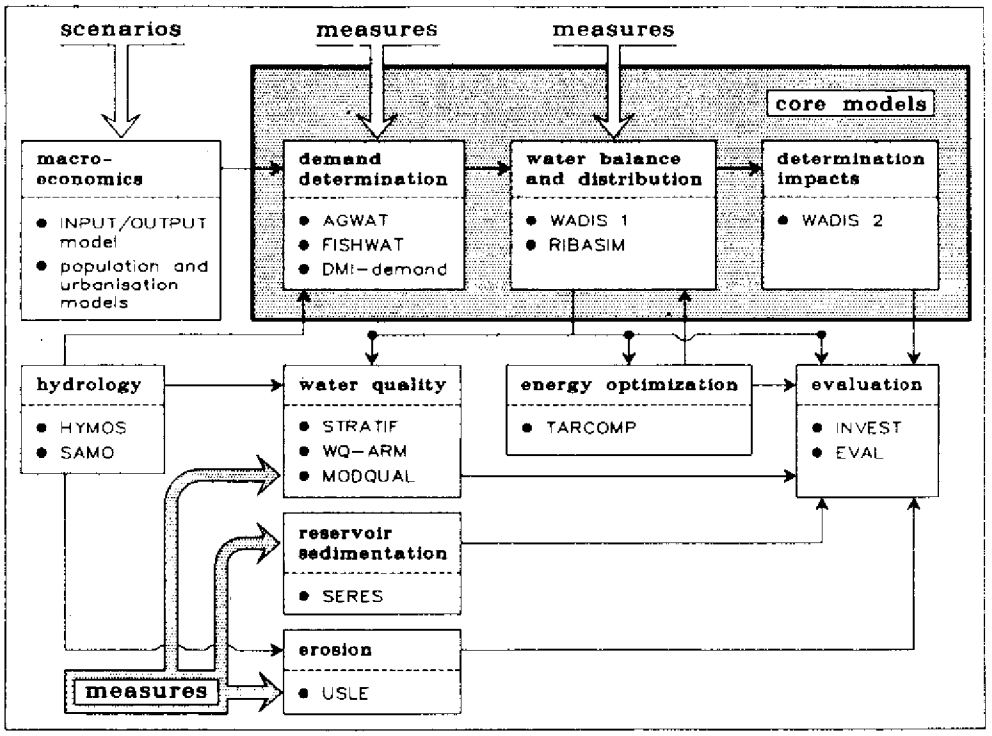

Figure 2 - Main components of computational framework

The computational framework will integrate both the supply of water as well as the demand for water. Models representing the water demand side (agriculture, public water supply, hydropower generation, etc.) and the supply side (rainfall-runoff, sediment supply, etc.) are integrated with the help of a riverbasin model which calculates the allocation of water over the users and regions given a certain infrastructure and management strategy.

The RIver BAsin SIMulation program, RIBASIM, provides the backbone of the computational framework by covering the simulation of the water distribution in the network. The supply side of water is represented by HYMOS (acronym for HYdrological MOdeling System), while the water requirements by the various water using sectors is covered by a set of designated models. After RIBASIM established the water distribution in the network (based on the "physics" of the river basin system, but also based upon the operational management of the control points like reservoirs, diversion weirs and pumping stations), the effects of the water distribution is covered by a set of so called "post-processing" programs. WADIS2 calculates the agricultural production (both expressed in quantities as well as in financial and economic terms) as a function of the allocated amounts of irrigation water. Other post-processors deal with the generation of hydropower, the reliability of the drinking water supply, and other aspects. All these models operate on-line, hence providing and integrated modelling of the various phenomena of interest in river basin development studies.

The development, calibration and verification of a computational framework and the related data collection often consumes a considerable amount of time. It proves very helpful, however, in understanding the system and the interactions between the various subsystems. Moreover, it is a necessity to be able to carry out a comprehensive analysis, including many alternative measures, strategies and scenarios. To serve this purpose, the computational framework will enable the evaluation of a wide variety of potential measures, including:

— physical/infrastructural projects (for example construction of additional reservoirs, canals, etc., or changes in waste or sediment loads);

— operational measures (for example changes in operation of reservoirs, diversion weirs and canals); as well as

— incentive and institutional oriented measures (for example aimed at deriving allocation priorities over water using sectors and over regions, or quantifying the expected effects of possible legislation with respect to water use.

Application of the computational framework basically consists of:

— a first simulation of the water resources system *without* taking into account the measure or project under consideration; and

— a second simulation run for the same water resources system *including* the measure of project under consideration.

Differences in results of these two runs can directly be attributed to the measure under study. Such differences between the runs may comprise differences in water flows, hydropower generation, water supply to water using activities, etc. Depending on what models are linked to RIBASIM, these differences may also include differences in production, in agriculture and aquaculture (expressed in both tons/year and financial terms).

RIBASIM could be considered the core-model in studies focusing on river basin development. Other models will either provide input to RIBASIM, or use the output for further processing. Such links between programs can either be on-line or off-line, indicating the level of interaction between the programs.

The following models are considered of prime importance for comprehensive modelling of the most important aspects of water resources development, with RIBASIM and related water demand models covering the modelling of the physical main system (including reservoirs) and its operation:

— a sub-basin (sometimes called district or water-district) model;

— water demand models (agriculture, public water supply);

— water quality models;

— a reservoir sedimentation model;

— economic evaluation models; and

— an energy sector model, that determines the hydropower generation requirement.

Sub-basin model WADIS1

Districts are defined as part of the basin that drain water and are supplied with surface water in a well defined fashion. In the upper part of a river basin, districts will generally coincide with sub-catchments, while in the downstream part districts may coincide with individual irrigation schemes. This approach allows *full coverage* of the surface area of the river basin under consideration.

The district model WADIS1 is on-line connected to RIBASIM and performs the following tasks:

— Calculation of the run-off of the district, for example using a Sacramento model approach (see section 5).

— Calculation of the water demand in the district for all water using sectors, comprising irrigated agriculture, aquaculture, domestic, municipal and industrial water supply. This can be performed by specific programs, like for example the programs AGWAT for irrigation, FISHWAT for aquaculture. Alternatively, water requirements expressed in tabular form can be applied. In case interaction with groundwater resources is relevant, this can be incorporated in the district model as well.

— Calculation of the water balance at the district level: determination of the water supply (drainage) from the district to the network and of the water demand asked by the district from the network, specified for the various water uses. For example: part of the irrigated area is to be supplied from within the district, another part has to be supplied by the network.

Both the drainage amounts and the water requirements are passed on to RIBASIM, which in turn solves the water balance for the network and allocates water to the district.

Water demand models

The computational framework offers a wide variety of possibilities to reflect the water demand at the demand nodes of the networks. These alternatives range from a simple to a more sophisticated approach:

— In case of a cyclical but otherwise fixed demand, the water demand can be specified as a series of numbers that describe one cycle. During the simulation, the model repeats the cycle. Example: seasonal fluctuations of the drinking water demand of a city.

— In a more detailed approach, the water demand at a node can be calculated for each timestep. This calculation is performed as part of the RIBASIM simulation. For example: one way to use the irrigation node in RIBASIM is to use a time series of actual rainfall at the irrigation scheme, and to calculate the irrigation water demand using a fairly simple representation of the irrigation process. This way, for each timestep a water demand at the irrigation node is calculated by RIBASIM.

— In a detailed analysis, the water demand at a node is calculated by a separate simulation model, on-line connected to RIBASIM. The separate model may include an assessment of the consequences in case water shortages occur. In this set-up, other programs serve as on-line pre- and post-processors linked to RIBASIM. For example: RIBASIM allows a flexible interaction with the program AGWAT, that calculates irrigation water demands in a very detailed fashion. Each timestep, the irrigation water demand in irrigation schemes is calculated and transferred to RIBASIM. In turn, RIBASIM allocates water over various water using activities in the basin, and determines how much water is available for the irrigation scheme. The water availability is passed on to AGWAT. In case of water shortage, AGWAT determines the consequences of that shortage in terms of an increase in irrigation water demand for the next timestep, and in terms of possible yield reduction due to water stress.

Water quality models

Water quality aspects can be taken into account in two ways:

— Assuming *no direct link* between water quality and water quantity, or in other words: assuming that a certain water quality situation does not determine the water quantity distribution. In this case, the water quantity distribution that is determined by RIBASIM and related pre- and post-processors is conveyed to a water quality model, that determines the consequences of the water management in terms of water quality parameters.

— Assuming a *direct link* between water quality and water quantity. In this case, a full interaction between water quality and quantity is assumed: the water quality distribution determines the water quality situation, but in turn a certain water quality situation will create boundary conditions for the water quantity distribution. For example: if the concentration of a certain pollutant exceeds the standard, then a larger discharge has to be realized at that location to create dilution or transport and hence a lower concentration.

A wide variety of water quality simulation programs is available today. One of these programs, STRATIF/WQ-ARM, focuses on water quality aspects of reservoirs. STRATIF/WQ-ARM will be discussed in section 6.

Reservoir sedimentation model

Due to sedimentation, the storage characteristics of reservoirs will change with time, gradually reducing the capability to control the river flow and to generate hydropower. In some cases, sedimentation of reservoirs forms an important phenomenon in river basin management. For such cases, the reservoir sedimentation module SERES will assist in answering the following questions:

— how much sediment enters the reservoir, depending on river flow and entrapment in upstream reservoirs;

— how much sediment is trapped within the reservoir, depending on hydraulic characteristics, inflow of water and sediment, sediment characteristics, and the reservoir operation policy; and

— how is the deposited sediment distributed in the reservoir and how does it affect the active storage, depending on the size and shape of the reservoir.

The calculations are based on the Churchill trap-efficiency curve, that outlines an empirical relation between the percentage of sediment passing the reservoir and the so called sedimentation-index.

Economic evaluation models

Output of the RIBASIM program and related post-processing programs can be made directly available to economic evaluation models. For example, simulation data with respect to hydropower generation and crop production in (irrigated) agriculture and aquaculture can directly be fed into an economic evaluation model. The program also makes use of construction, maintenance and operation costs and performs an economic evaluation of the projects under investigation.

By generating a timestream of expected benefits and costs, the economic evaluation program determines for each project economic as well as financial indicators, comprising the internal rate of return, total investment costs, employment effects, etc. The program finally generates the regional distribution of benefits of projects under investigation.

Energy sector model

Policy decision with respect to how to distribute the total power requirement of the region over each of the hydropower generation facilities in a basin and over non-hydropower facilities (coal, oil, gas, nuclear, etc.) can be addressed by the optimization program TARCOMP. This program starts off with the power requirements of the region, and distributes the production over the available generation facilities by establishing the least-cost alternative. This distribution is based on a formal optimization, that minimizes the maximum deviation from the power requirements. The solution of the TARCOMP

optimization serves as a boundary constraint for the RIBASIM simulation. The programs are coupled on an on-line basis.

Application of the computational framework

The following types of studies can benefit from application of the computational framework described above:

— (pre-) masterplan studies, in which generally large sets of alternative projects and strategies have to be analyzed;

— feasibility studies, in which a more detailed evaluation of some alternative water resources development schemes is carried out; as well as

— (real-time) operation studies, in which details on the operation procedures are determined.

Typical issues that can be addressed include:

— Screening of water resources implications of (large sets of) alternative water resources developments.

— Selection of reservoir capacity and operation rules.

— Trade-off between planning targets, for example irrigation versus drinking water supply versus hydropower generation.

— Trade-off in reservoir operation for different objectives, for example the intrinsic difference between operation for flood control purposes ("keep the reservoir level as low as possible") and operation for hydropower generation ("keep the reservoir level as high as possible for maximum head").

The flexibility of the computation framework not only allows the efficient evaluation of large sets of alternative options for water resources development, but also allows quick sensitivity and scenario analysis to determine the robustness and resilience of the conclusions.

5. MODELLING THE WATER SUPPLY: THE SAMO MODEL

Rainfall, evaporation and, most important, runoff data are required to assess the water availability at the RIBASIM for irrigation, hydropower, public water supply, etc. Runoff records of sufficient length are often not available and rainfall-runoff models have to be used to bridge the gap. Various options exist with respect to the type of model to be used, ranging from simple black box models to very sophisticated ones. Whereas the former lack any physical basis, the latter require too many data to be generally applicable. The SAMO model based on the well known Sacramento model offers a good compromise between the desired physical basis of the model, its complexity, the amount of basic information required to run the model, and the computed time required to simulate the runoff process in a water district for a large number of years.

Basically, the model consists of a system of interconnected parallel and serial reservoirs. Flow components discerned in the model range from very rapid direct runoff to slow base flow. Hence, flow conditions ranging from wet season peak discharges to dry season low flows, can be simulated with one set of parameters. The catchment area can be divided into a number of segments. Hence, in case the catchment upstream of a gauging station consists of a group of water districts, it is possible to include each district separately with its own parameter set and rainfall and potential evapotranspiration time series in one model run. This greatly enhances the flexibility of the model in its application, in particular during the calibration and verification of the model.

Prior to the use of the model a thorough validation of the data is required. For that purpose the data are stored in a data base structured and processed by the HYMOS data base management and processing system for hydro-meteorological data. HYMOS provides an extensive set of tools for data entry, validation, completion, analysis, retrieval and reporting. To calibrate and verify the SAMO models for the various water districts the model is linked to the HYMOS data base.

Recently, the SAMO model was used in the Cisadane-Cimanuk Integrated Water Resources Development Project in Indonesia to determine the water availability. This Project aimed at the optimization of the utilization of water resources in the Northern part of West Java.

The study area covers some 28.000 km^2, consisting of lowlands being a relatively flat coastal plain where the major irrigation areas and population centres are located, and uplands, representing the hilly and mountainous areas. The rainfall varies from less than 2000 mm per annum in the lowlands to over 4000 mm in some parts of the uplands. The seasonal rainfall distribution is mainly affected by the monsoons, wet from November to April and relatively dry in the rest of the year. The annual catchment evapotranspiration is rather constant and amounts approx. 1100 mm.

For purpose of water resources simulation 141 water districts were discerned, which required water supply data for a representative period of 29 years (1951-1979). Only at 18 locations for about 11 years discharge series were available, hence with the SAMO model, to a large extent, series had to be completed for the existing and had to be created for the ungauged sites. The model was calibrated first on two sub-catchments with respectively moderate and high rainfall. The same set of parameters could be used for it. Subsequently, with this set of parameters the remaining 16 sub-catchments were run with good results. Figure 3 illustrates the results of the validation for one of these 15 sub-catchments. Hence, the whole of Northern West-Java could properly be simulated with only one set of model parameters. The differences between the long term annual observed and computed flows appeared to be less than 5% of the long term annual rainfall, which was considered sufficiently accurate for the purpose of the study also in view of the various inaccuracies and uncertainties in the records. Hence for the ungauged water districts the same parameter set with the local rainfall and evapotranspiration series were used to estimate the water availability.

In the SAMO and RIBASIM computations half-monthly time steps were used. In the RIBASIM simulations these values were adapted at the water intake sites. Half-monthly flow values give a too optimistic picture of the total amount that can be diverted at the intakes due to the daily variation of the flow. Divertible flow curves were derived assuming gaussian distributed instantaneous flows. The curves could be described as a function of the mean half-monthly river flows (Q_a), the intake capacity at the site (Q_m) and the coefficient of variation (C_v) of the instantaneous river flows. Figure 4 illustrates this curve.

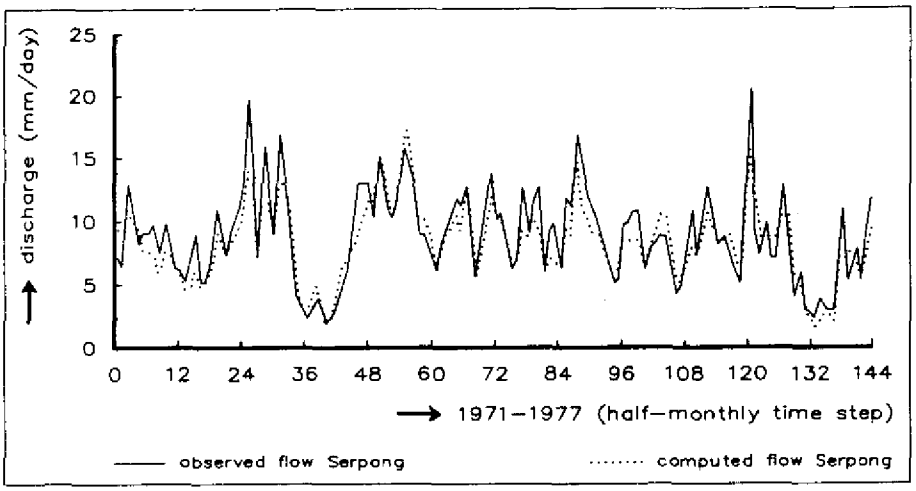

Figure 3 - Observed and computed flows at Serpong

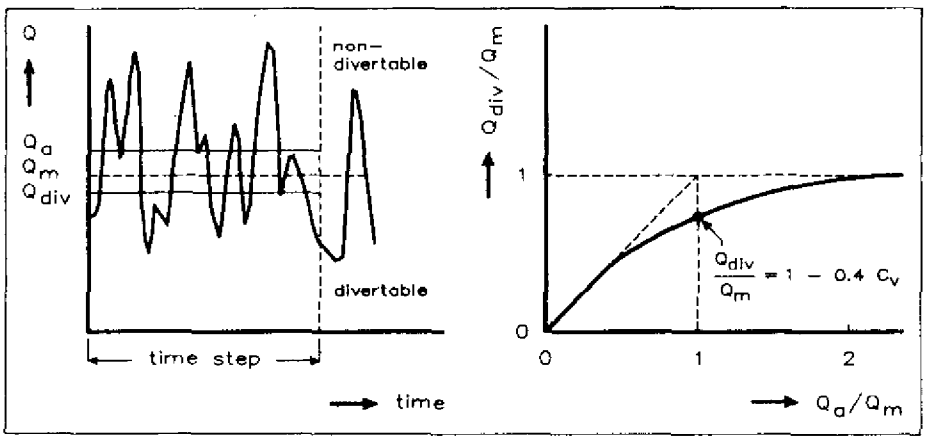

Figure 4 - Definition sketches divertible flow curve

6. CHARACTERISTICS OF THE RESERVOIR WATER QUALITY MODELS STRATIF/WQ-ARM

Water quality problems of reservoirs

Water quality deterioration in reservoirs can result from two types of causes:

— decomposition of drowned vegetation; and

— pollution from upstream sources

Only the former is relevant in the case of Amazonian reservoirs. Poor water quality may arise from the decomposition of large quantities of organic matter from vegetation, floating aquatic weeds and phytoplankton. The decomposition withdraws oxygen from the water, which may lead to anaerobic conditions in the lower water layers. Toxic and corrosive substances like sulphide are produced under such conditions.

The production of organic matter (detritus) by phytoplankton is stimulated by ample availability of nutrients such as phosphate, ammonium and nitrate. The nutrients are imported by a river and released from decomposing vegetation. A certain productivity of phytoplankton is desirable since higher organisms benefit from it as phytoplankton constitutes the basis of the food chain. However, enrichment with nutrients (eutrophication) may reach a point at which the growth of phytoplankton (and aquatic weeds) becomes excessive, leading to deterioration of both water quality and aquatic ecosystem.

The consequences of poor water quality may have adverse effects on several functions of reservoirs, among which in the case of the Amazon area are:

— power production, corrosion of turbines and piping;

— ecological function, reduced stability and diversity in both the reservoir and the downstream river; and

— fish production, reduced productivity and mortality.

Background of the model package

The model package WQ-ARM/STRATIF was developed for the study of water quality and related problems of Amazonian reservoirs. The development took place within the framework of a recent cooperation project with Eletronorte and Instituto National de Pesquisas da Amazonia. The coherence of the individual models can be seen in Figure 5.

WQ-ARM (Water Quality Analysis for Reservoir Management) consists of submodels for the reservoir and the downstream river. The reservoir is schematized in horizontal layers as depicted in Figure 6. The river is divided in subsequent compartments. WQ-ARM simulates dissolved oxygen, various organic detritus components, phytoplankton, phosphate, ammonium, nitrate, sulphate, sulphide and methane. These substances are subject to a substantial number of processes, among which are

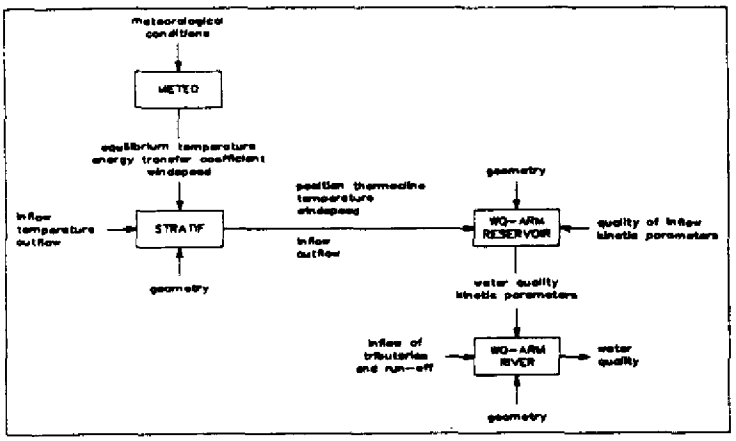

Figure 5 - Relations between WQ-ARM, STRATIF and METEO

primary production by phytoplankton, microbial decomposition, oxidation, reduction, adsorption, sedimentation, advection and dispersion. Figure 7 shows the relations between processes and concentrations in the oxygen budget.

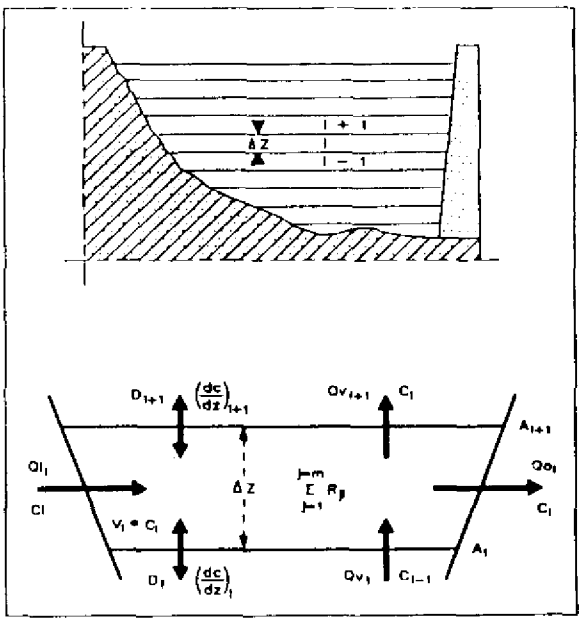

Figure 6 - Schematization of a reservoir for WQ-ARM

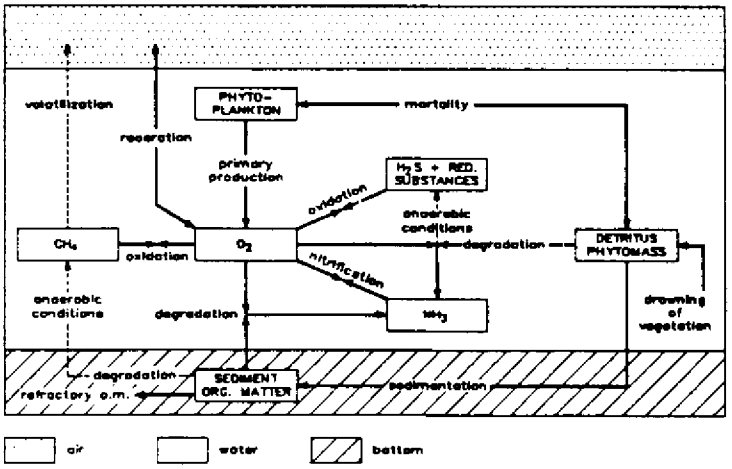

Figure 7 - The dissolved oxygen budget in WQ-ARM

WQ-ARM solves time-dependent mass balances for each substance and each layer (or compartment). The input consists of geometrical, hydrodynamical, meteorological and water quality data as well as process parameters. The concentrations of the substances as functions of time and depth (or distance) constitute the output.

The stratification model STRATIF with preprocessor METEO is needed because vertical mass transport slows down in stratified water to an extent, at which large differences arise between the water qualities of the warm, upper layers and the cool, lower layers. STRATIF simulates the thermal stratification influenced by solar radiation, wind and throughflow in a two-layer system. WQ-ARM uses the position of the thermocline and the temperatures of both layers to calculate the vertical, dispersive mass transport.

The model package was calibrated using water quality data of the Tucurui reservoir. An extensive set of data was prepared for this reservoir under the supervision of Eletronorte. From the comparison of calculations and observations appears that the models are capable of sufficiently accurate reproduction of the observed water quality (Figure 8).

Applications of the model package

The models were used to simulate the long-term behaviour of the Tucurui and Balbina reservoirs, built for the purpose of power production (Figure 9). The production of fish may be considered as an interesting side-goal. The Tucurui reservoir (2430 km^2) was filled in 1984 with relatively nutrient-rich water of the Tocantins river. The filling of the Balbina reservoir (2360 km^2) with very nutrient-poor water of the Uatuma river started in November 1987, when the water quality simulations had been completed already. The reservoirs differ greatly with respect to their hydrological and hydrodynamical features. The average depth of the Balbina reservoir is smaller and its average residence time is much longer; 7.5 versus 19 meter, and 1 year versus 40 days.

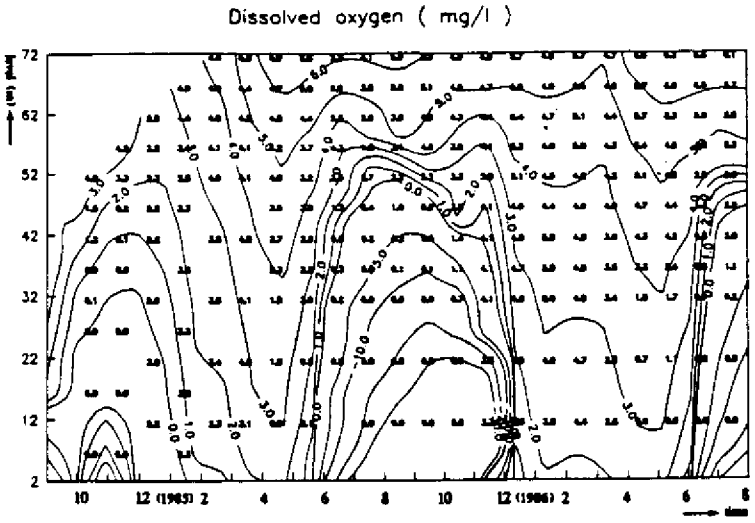

Figure 8 - Calculated (-) and observed dissolved oxygen concentration in the Tucurui reservoir.

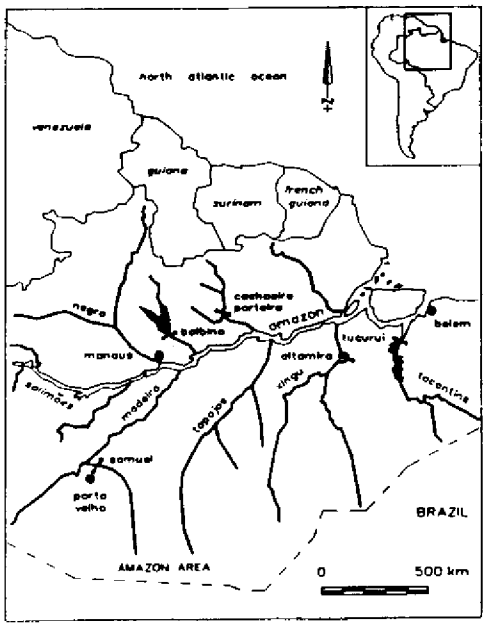

Figure 9 - Location of the Tucurui and Balbina reservoirs

The results for the Tucurui reservoir reflect destratification during the wet season and gradual disappearance of nitrogen nutrients as a consequence of flushing. The concentrations are reduced by a factor of 2-10 within a ten years period, whereas phosphate remains present in hardly reduced concentrations. Phosphate is obviously retained in the reservoir because it adsorbs onto suspended solids and accumulates in the bottom under the prevailing aerobic conditions. Release from the bottom maintains rather constant concentrations in the water column. The accumulation of phosphate infers that the primary production of phytoplankton can be maintained on a relatively high level. Consequently there is ample food supply to higher organisms. It is therefore expected that the commercially important fish will develop in large numbers.

The predicted water quality of Balbina reservoir contrasts strongly with this picture. Permanent stratification causes persistent anaerobic conditions at depths greater than 4-5 meters during a period of more than 10 years (Figure 10). The Balbina reservoir will discharge anaerobic water into the downstream river leading to the removal of most of the organisms from the river in a reach of over 50 km. Moreover, the water passing the turbines may be corrosive.

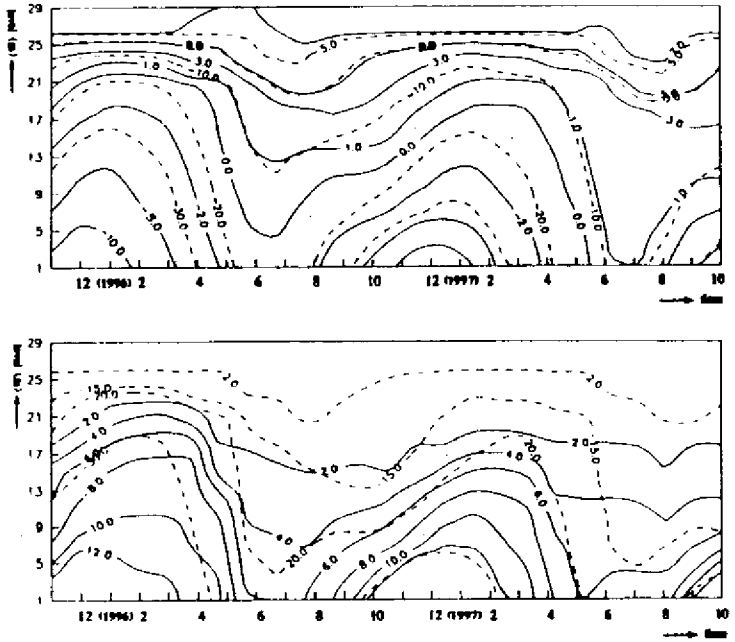

Figure 10 - Concentrations of dissolved oxygen (mg/l) and inorganic phosphate (μgP/l), predicted for the Balbina reservoir for periods of 8-10 year (-) and 4-6 year (—) after the filling.

Phosphate will not accumulate in the bottom of Balbina reservoir because of the prevailing anaerobic conditions. However, sufficient flushing occurs to remove this nutrient from the reservoir. The growth of phytoplankton will be more and more phosphated-limited, leading to very low phytoplankton concentrations. It seems therefore justified to expect that commercial fish production will not develop at Balbina reservoir.

FINAL REMARKS

The combined use of a consistent framework of analysis and the application of analytical techniques (computer models) has become a necessity in the analysis of complex integrated water resources development and management issues. The paper has highlighted a few aspects of such approach which can be of interest for the Amazon basin.

It should be borne in mind that the development of a computational framework is a time and money consuming activity. Although there are ample general computer programs available, experi-

ence shows that each application (model) requires adaptation of the programs for the particular local situation under investigation. Moreover, the quality of the model results will depend to a large extent on the quality of the input data. The expression "garbage in, garbage out" certainly holds. Hence, ample attention is required for the generation of an appropriate set of input data, comprising sets of hydrological data reflecting the supply of water, data sets of required water quantities for water using activities, sets of parameters for water quality models, but also data sets describing the physical system and its operation.

The application of described approach and models require a high level of experience and (multi-disciplinary) skills. In many cases training will have to be a major part of projects of this kind. Given the fact that in most cases important issues are at stake (high investments, ecological impacts, public health, etc.) it still can be concluded that the ultimate results in terms of quantitative and reliable information on which decision makers can draw their conclusions, justify the efforts of following such approach.

REFERENCES

Smits, J. G. C. Ecological modelling for reservoirs in the Amazon Area, Volumes I and II, Delft Hydraulics, March 1988, T102/T333.

Smits, J. G. C. Formulation and calibration of WQ-ARM, a water quality model for reservoirs, Publication, Delft Hydraulics, 1990.

DELFT HYDRAULICS. June 1989. Resources Development Planning, Framework for Analysis, Publication, Delft Hydraulics.

DELFT HYDRAULICS and Puslitbang Pengairan. September 1989. Cisadane-Cimanuk Integrated Water Resources Development (BTA-155). Volume II: Main Report; Volume VII: Hydrology; Volume VIII: Water Quality. Delft Hydraulics, T136.

DELFT HYDRAULICS. March 1989. HYMOS, System for Storage and Processing of Hydrologic Data, Delft Hydraulics, Computer Model Description, Version 2.1.

WATER QUALITY SIMULATION IN RESERVOIRS IN THE AMAZON BASIN: PRELIMINARY ANALYSIS

Carlos Eduardo Morelli Tucci *

ABSTRACT

Rational development and occupation in Amazon basin is a challenge for the countries in the region. Brazil covers the greater part of the basin and has planned and constructed most of the Amazonas reservoirs for hydropower generation. Evaluation of the impact on the aquatic environment is based on the behavior of physical, chemical and biological processes of the system. Mathematical models have been used to represent these processes, and as tools in the evaluation of planning and operation alternatives. In this paper, we present the standard sequence of studies adopted for the hydropower sector, a summary of mathematical models characteristic for water quality in reservoirs, some data of planned and operating hydropower, recommendations regarding the use of mathematical models in the sequence of studies, and research requirements.

INTRODUCTION

The construction of a reservoir and its support structure has positive and negative impacts on the environment, due to the artificial lake created upstream, and changes the hydrological regime downstream

The reservoir modifies natural flow conditions with small width and high velocity, into a slow longitudinal flow with great depth and large width. These flow conditions change the water quality conditions and the environment.

The water quality of a reservoir is a function of external and internal factors. The external factors are inflows, nutrient concentrations and other substances from the tributaries, climatic conditions and volume and quality of rainfall contribution. The internal conditions are physical, chemical and biological interactions with the environment.

The implementation of reservoirs in the Amazon region basins results in the flooding of nutrient-rich forests which tend to eutrophicate the lake. The climatic conditions in a tropical region with high temperatures the year round establish favorable conditions for the development of macrophytes, gas formation and other problems which may be harmful to the environment and the project itself.

* *Professor - Institute of Hydraulic Research - Federal University of Rio Grande do Sul, Brazil*

The planning of development phases used by ELETROBRAS (Holding of the Brazilian Electrical Companies) and the general characteristics of environmental analysis for each phase are presented below. A brief review of water quality models and their main features is shown subsequently. The choice of these models during the different phases of the study is discussed, taking into account the main characteristics of general conditions in the Amazon basin.

PLANNING PHASES

The choice of hydropower development sites was based on regulated flow and hydraulic head.Taking into account, in design, the environmental impact which may be caused by reservoir construction, the number of variables and restrictions relating to the problem will be increased.

ELETROBRAS (1986) defines the planning phases for hydropower development as Estimation of the Hydropower Potential: Inventory , Feasibility, Basic Design, Executive Design, Construction and Operation. In table 1 a summary of the contents of these phases. is seen . The River Basin is evaluated in the first two phases, and each project is analyzed as to feasibility. The last two phases are executed after the final decision to build a specific project.

ELETROBRAS prepared a Handbook for the Study of the Effects of Electric Systems on the Environment, in which it defined, generally, the environmental studies for each phase of design (table 2).

In August 1981, a national law was passed concerning the environment, which was then regulated in 1983 by an act. CONAMA, established by this act, presented some normative resolutions in 1986. Some of the important points are:

1) Hydropower developments above 10MW are obliged to present a RIMA(Environmental Impact Report); 2) The authorization given by the State Environmental Agency comprises the following licences: a) LP-Preliminary Licence- During the preliminary phase of planning of activities; b) LI-Licence to Set-up - this authorizes the beginning of implementation; c) LO-Operation Licence- authorizes the beginning of activities. The LP is required to begin the feasibility study, when the RIMA is presented. The LI must be obtained before building, and the LO before the dam is finally closed.

Table 1 - Hydropower planning phases

Phases	Characteristics
Estimation of hydropower potential	First evaluation (done in the office) of the hydropower potential. Definition of priorities schedule and cost of inventory studies.
Inventory	Determination of the hydropower potential for the basin through the best division of hydraulic heads and cost estimation of each hydropower development.
Feasibility	Definition of the comprehensive conception of each hydropower, including design and infrastructure requirements for its implementation.
Basic Design	Definition of civil works and permanent equipment, for bids and hydropower construction.
Executive Design	Detailed study of basic design used for construction and setting up equipment.

Table 2 - Environment studies in the planning phases

Phases	Characteristics
Estimation of hydropower potential	Identification of general environmental characteristics of the basin.
Inventory	Analysis of environmental effects of selected dams and indication of specific recommendations for feasibility studies.
Feasibility	Detailed analysis of the environmental effects of a given development,and evaluation of the cost of actions relating to the environment.
Basic Design	Detailed studies of environmental aspects of design and preparation of Master Plan for reservoir use.
Executive design	Operationalization of environmental aspects of design and preparation of a Master Plan for reservoir use.
Operation	Implementation of the Master Plan for reservoir use.

WATER QUALITY SIMULATION IN RESERVOIRS

The choice of a mathematical model to simulate water quality conditions in a river and reservoir system depends on the characteristics of the system to be simulated, the desired level of precision, and the available data. Flow conditions in the system, in general, determine the basic types of model structure due to advective and diffusive processes. The water quality standard level is evaluated based on the parameters defined in the legislation, which identify general conditions of quality and pollution, and show the main processes occurring in the system.

Generally, the types of models may be classified according to flow conditions, mass transport and chemical-biological processes. Due to flow conditions in a free flowing river and in reservoirs, the models have different formulas. In a reservoir, flow velocity is low and the depth great. The main processes usually take place vertically. In a river there is greater velocity than in the reservoir and mass transport is produced predominantly in the longitudinal direction, with less influence from the transverse and vertical directions.

Reservoir model classification may be performed according to different criteria. The classification based on spatial discretization is as follows:

concentrated model - (zero dimension). This considers a mixed reservoir. These models use mean constant concentration or a time variable one. The Vollenweider model (1968) is an example of this type of model.

one-dimensional models - They simulate the processes taking into account only one dimension in space. Usually longitudinal or vertical one-dimensional models are used in the studies. The former takes into account the velocity and level of concentration variation in the longitudinal direction, ignoring transverse and vertical variations. The vertical models are more often used when the reservoir may present thermal stratification and has a long residence time, since most of the energy and mass transfer processes occur on the vertical. Some of the vertical one-dimensional models are described in Orlob(1983).

two-dimensional models - These are models which ignore one of the directions. The model may be two-dimensional: on a plane (longitudinal and transverse directions); in profile (longitudinal and vertical directions). The former allows simulation of velocity and concentration on the plane formed by the reservoir. In the second type it is possible to obtain the result of vertical and longitudinal variation of concentration in the reservoir when it has short residence time and is long.

three-dimensional models - These models represent all directions. A large amount of data is required to estimate the parameters involved, besides numerical difficulties. In this class Thoman(1972) presented a three-dimensional model which simplifies the dynamic flow equations.

The models may also be classified, regarding time variation, as steady and non steady. In the first case the change in time is not considered.

As to water quality parameters, the models initially used a simplified simulation of Dissolved Oxygen (Bella, 1970). The models which followed them included nitrification processes and phytoplankton dynamics. Formulae for specific problems have been developed to consider forest flooding, gas formation and some types of macrophytes. The main difficulties in these methodologies have been to identify the parameters involved and the reliability of the mathematical formulae used.

CHARACTERISTICS OF THE HYDROPOWER DEVELOPMENTS IN THE REGION

The characteristics of some developments which already exist, or are being planned in the Amazon region, are presented in table 3. At the time this article was prepared, some information was not available. As can be seen, the basins involved cover large drainage areas to allow energy

production, since the heads are usually not significant. Of this group of eleven reservoirs, four are already operating and seven are in the planning phase.

The main impacts of the water environment due to the implementation of reservoirs in this this region are:

— flooding of the forests and lake eutrophication;
— gas formation and turbine corrosion;
— water quality downstream from the dams.

The upstream load is usually the natural pollution of the basin. In some basins, upstream pollution is important due to changes in basin vegetation and discharges from gold mining.

In table 4 are presented some indicators of environmental conditions in reservoirs, as follows:

Residence time - This is the ratio between reservoir volume and inflow. This factor allows the identification of mean time of renewal of the reservoir volume.

Densimetric Froude Number - (Orlob,1983) indicates whether stratification will occur in mean terms. Thermal stratification worsens water quality conditions in the lower strata of the reservoir, from which water for the turbines is usually taken. It increases equipment corrosion and decreases the water quality of the downstream reach.

$$Fd = (L.Q) / (H.V) [i/ (g.e)]^{1/2} \quad (1)$$

where Fd= densimetric Froude number ; L= reservoir length (m); H= height in m; V= reservoir volume in m3; Q=streamflow in m3/s; g=gravity acceleration; e= mean gradient of the specific mass. When Fd < 0,32 there will be strong stratification; 0,1< Fd <1,0 small stratification gradient and mixed. This equation is based on the comparison between the inertial force of the flow through the reservoir and the gravitational force which tends to maintain stability.

Table 3 - Hydropower characteristics of reservoirs in the Amazon region

Reservoir	Basin area Km²	Mean flow m³/s	Volume Hm³	Flooded area km²	Project phase	Installed capacity MW
Tucurui	767.000	10.400	45.500	2.635	operation	4.000
Balbina	18.450	578	17.533	2.360	operation	250
Samuel	15.280	350	3.250	560	exec.design	217
Ji-Parana	47.300	900	11.950	957	basic design	512
B.Peixe	17.310	310	23.430	1.020	feasibility	450
Brokopondo		362	9.400	880	operation	
C.Nunes	24.200		138	23	operation	40
B.Monte	477.000		14.600	1.225	basic design	11.000
C.Magalh.	5.170		651	53	basic design	260
Manso	9.364		7.337	387	exec.design	210
S.Quebr.	229.750	4.630	3.190	370	inventory	1.450
C.Porteira	50.650	1.739	12.200	912	basic design	700

* Some information was obtained from ELETRONORTE (1989). This information may be updated.

Table 4 - Water quality indexes

Reservoir	Residence ime days	Fd	Total load(1) dry vegetal matter 10**(6) t	O2(2)	N(3)	P(4) mg/l
Tucurui	50	0.58	6.324	176	2.03	0.281
Balbina	351	0.46	5.050	365	4.21	0.583
Samuel	107	0.58	1.198	467	5.38	0.746
Ji-Parana	154	0.15	2.048	217	2.50	0.347
B.Peixe	875	0.03	0.925	50	0.58	0.080
Brokopondo	300	0.04	4.700	238	2.73	0.374
S. Quebrada	8	2.34	0.370	147	1.69	0.235
C. Porteira	81	0.23	1.952	203	2.33	0.324

(1) Load estimated based on values used in previous studies for Tucurui, Brokopondo and Barra do Peixe (Hohannes,1988;DHL,1981 and Engevix,1988)

(2) Total Oxygen Demand required for degradation of carbon from vegetal matter;

(3) Total Nitrogen concentration from the Carbon degradation of vegetal matter;

(4) Total Phosphorus concentration from the degradation of vegetal matter.

Vegetal matter load - Due to the climatic characteristics of the Amazon region which is warm throughout the year, forest flooding exerts a heavy impact on the reservoir water quality.

The forest density can be given in kg of wet matter/m2. Of this total, leaves and dead vegetation are the parts which represent the phytomass load. Each of these parts has a proportion of dry matter. The amount of rapidly degradable dry matter is the sum of these parts.

According to Meyer et al. (1958) there is about 44% of carbon in vegetal matter. The amount of oxygen required for organic matter degradation is obtained by a factor of 1.88 according to Meyer et al. Therefore, the amount of oxygen required for carbon oxidation, in rapidly degradable matter, is

$$D = 1.267\ Dr\ .\ A/V \qquad (2)$$

where Dr= density of of rapidly degradable dry matter; A= area of the utilized density; V= volume; The coefficient for Nitrogen in equation 2 is 0.0146 and for Phosphorus, 0.002.

Maximum concentration - The relation between maximum concentration and total load is obtained for Nitrogen and Phosphorus by the following equation

$$Cm/D = K/(r - K)\ [\exp(-aK) - \exp(-aK)] \qquad (3)$$

where $r = 1/td + Ks$ for the total phosphorus equation and $r = 1/td$ for total nitrogen; $a = \ln(K/r)/(K-r)$; K = coefficient of Nitrogen or Phosphorus transference for the water (1/day); td= residence time in days.

The following simplifications were adopted to obtain equation 3:

— total load at t=0 ;

— inflow equal to outflow;

— Zero inflow concentration for total Phosphorus and

Nitrogen and DO;

— mixed reservoir;

— only rapidly degradable load.

Using K=0,005/day and Ks=0,0074/day this ratio is related to time of residence (fig. 1). For the analysed reservoirs, the values are presented in table 5. The DO expression is excessively long and the required result shows a negative concentration. Recovery time is the period of time, in which the reservoir shows negative mean concentration of DO, after its filling until the recovery of positive concentration.

The favorable aspects for a development would be low residence time, mixed unstratified reservoir and low organic matter load due to vegetation.

Table 5 - Maximum concentration and recovery time

Reservoir	Maximum concentration		Recovery time
	P	N	month
Tucurui	35	321	7
Balbina	144	2.000	25
Samuel	133	1.402	13
Ji-Parana	70	802	15
B. do Peixe	22	375	19
Brokopondo	90	1.213	21
Serra Quebrada	8	59	1
C. Porteira	51	510	10

* These values should be used in a relative analysis since they were obtained from many simplifications and represent only the load of vegetal matter.

In these overall indicators, Tucurui has a short stratification residence time. The total load of dry matter is high due to the surface, but corresponds to a total concentration of parameters below those of the other projects. Barra do Peixe has a high residence time, stratification conditions, 19 months of recovery, but a smaller load value due to the smaller surface and plant vegetal matter density. Balbina presents an unfavorable residence time condition, vegetal matter load and recovery time.

These values vary throughout the year, according to hydrological conditions. Since, in the Amazon region, the temperature does not vary significantly, the stratification conditions depend on the state of the reservoir and inflow. For high residence time and low inflow conditions, stratification increases and the oxygen in the lower strata is reduced.

Streamflow impact over the year may be observed at two points in the Tucurui reservoir (points shown in figure 1). At point M1, when there is less flow in the lower levels, the reservoir becomes anaerobic and recovers during the wet season (figure 3). In this specific case it should be considered that filling took place in 1984, and that, therefore, the result is influenced by a higher load in 1985. At point C1 (figure 4), which has a much longer residence time, it is observed that there is much less recovery with a permanently anaerobic hypolimnio (Johanes,1988). This part of the reservoir is outside the main flow and receives the discharge of the direct contribution from a small basin, or when the reservoir becomes greater. It is also observed that at M2 the temperature is slightly lower than at C1.

The impact of vegetation density is linearly proportional. Therefore, a site with less density may produce a smaller amount of flooding with the same density ratio.

CHARACTERISTICS OF THE MODELS WHICH MAY BE USED DURING THE PLANNING PHASES

The proposal presented here should be understood as general advice concerning the use of water quality models, subject to change according to specific problems and further information regarding the behavior of these systems.

In this context, the model should be seen as a support tool, which requires: reliable information to provide reliable answers; formulations which are consistent with the behavior of the physical processes of the system; representativeness of the parameters and variables involved.

Usually, to evaluate the positive and negative environmental impacts of a development, it is necessary to analyze the scenarios of present and future conditions without the development, and future conditions with the development, considering:

- natural loads and those which are due to human action in the basin;
- oad from flooded vegetal matter in the reservoir;
- haracteristics of the planned reservoir;
- hydrogeological and hydrological conditions in the basin;
- meteorological conditions.

For this purpose, it is necessary to represent the aquatic system upstream from the reservoir, the reservoir itself and the river reach downstream. The delimitation of river reaches is in direct proportion to the influence on the reservoir and of the latter on the river.

Estimation of the hydropower potential

This phase corresponds to a preliminary evaluation of the basin as to hydropower availability. The surveys will identify local potentials.

The identification of environmental conditions in the river basin corresponds to a general description of natural and evolutionary conditions regarding the different disciplines which are involved in the environment.

Water Quality conditions in the river basin are evaluated taking into account the location of possible sources of pollution in the basin: domestic, industrial and agricultural effluent loads; spatial distribution of these sources, critical hydrologic conditions, natural nutrient concentration conditions; the interaction of sources of pollution with the existing uses in the basin. At potential dam sites, besides physical information, surveys or estimates of the density of flooded vegetation.

This diagnostic phase is based on the available descriptive information and on indicators such as those decribed in the previous item, which will allow the identification of the most favorable sites and predict problem areas, by comparative tables of existing and planned developments in the region.

For future studies, projections should be made of sampling and monitoring of the sites identified as the most appropriate for developments.

Inventory

The inventory is divided into two phases.The preliminary phase during which different alternatives for developments are formulated, to be detailed in the final studies.

In the preliminary phase several alternatives for development will be established. Therefore, in order to study the river basin as whole, the combination of concentrated models in reservoir and uniform or non-uniform steady flow models in rivers, can be used as a function of the available data. The combination of these simple tools with load estimations of the basins and reservoir allow a preliminary evaluation of some basic alternatives such as:

— Recovery capacity during the reservoir filling;
— Impact of the upstream loads from the basin;
— Downstream effluent in the cascade system.

The load data and parameters of this phase will be obtained from literature, preliminary estimates or regional values.

In the final phase, one-dimensional vertical models may be used, for the development alternatives chosen. In this case the model would provide a better evaluation of the downstream reaches and specific conditions of filling and recovery.

Feasibility

In this phase the analysis is made for a specific dam. In the evaluation of a development, the characteristics of the model to be used depend on the reservoir characteristics identified in the earlier phase and on the enviromental problems to be investigated. The main aspects are:

— impact of forest flooding and recovery time;
— flow condition of the turbines, as to concentration and gas formation;
— eutrophication

Normally, under these circumstances, the effect of inflow is small and the longitudinal and transverse variations in temperature and concentration are not significant, and a vertical model may well represent the processes. However, an effort must be made to improve the ecological aspects trying to estimate, besides the Nitrogen and Phosphorus cycles, also gas formation and macrophyte development.

For developments with a short residence time, longitudinal variability may prove important, since it allows the identification of reservoir areas in more critical condition. Longitudinal variability may also be important for the evaluation of selective deforestation. In this case, two types of models may be used:

— one-dimensional longitudinal model combined with a vertical model, when longitudinal flow is significant and depths are not as great. The vertical model is normally used near the main body where the depths are great.;
— two-dimensional longitudinal and vertical models for a reservoir with a short residence time and great depth. The tendency of energy developments is to present this characteristic, due to the heavy impact of environmental and

social factors, when large areas are flooded. Since the volume and residence time are small, the height of the dams should be significant for economical energy production.

The models used during this phase should be based on data collected during the inventory, and even at this stage.

Basic design

In this phase, a large part of the problems have been analyzed and detailed. However, specific aspects may remain regarding the details of the work, refering to minimization of environmental consequences. Some of these aspects may be:

— the evaluation of outflow mechanisms from the reservoir for the improvement of corrosion and flow mixture conditions downstream from the turbine and spillway;
— artificial reaeration or aeration caused by downstream turbulence;
— lateral areas with a long residence time.

The simulation of each case involves specific problem formulations with the support of models developed during the previous phases.

In this phase, monitoring to be carried out during the operation should be planned, taking into account the conclusions which were forecast during this and previous phases.

Operation

After the development has been built, and has begun to operate, it is necessary to check previous models forecast. With the data collected in this phase the parameters can be calibrated. During this phase an effort should be made to improve the models, reassess the forecast of development of water quality conditions in the reservoir,and the use of data as a laboratory for other projects.

CONCLUSIONS AND RECOMMENDATIONS

The main characteristics of the Amazon region reservoirs are:

— small temperature variation throughout the year;
— high temperatures;
— thermal stratification with small gradients;
— main loads resulting from forest flooding, with the consequent critical situation in reservoir filling;
— the main impacts are eutrophication, gas formation and corrosion of equipment and worsening water quality downstream;
— the reservoirs will tend to have a short residence time.

Therefore, it is necessary to improve and develop the following aspects which help in studying these conditions:

- quantification of vegetal matter density, based on remote sensing;
- improvement of the mathematical functions and parameters which deal with the pollution caused by flooded vegetation;
- design hydraulic equipment to increase reaeration of the dam effluents;
- quantitative evaluation of economic and technical feasibility of selective deforestation and its impact on the reservoir environment;
- evaluation of the use of aeration for some areas of the reservoir;
- review and consolidation of studies performed on the Amazon region reservoir, as a foundation for future studies;
- general basic criteria for water quality monitoring during the different phases of project planning and operation;
- sensitivity analysis of the parameters of some models chosen for use in the region.

REFERENCES

Bella, D. Dissolved Oxygen Variations in Stratified Lakes, ASCE, Journal of Sanitary Engineering Division, Vol 96, SA5, October. 1970.

DHL. Environmental Impact of the Kabalebo Project, Volume III, Water quality, Delft Hydraulics Laboratory. 1981.

ELETROBRAS. Manual de Estudos de Efeitos Ambientais dos Sistemas Eletricos, Eletrobras. 1986.

ELETRONORTE. Cadastro de reservatorios em Operação, Eletronorte. 1989.

ENGEVIX S.A. and THEMAG ENG. UHE Tucurui, Monitoramento de Qualidade da Agua. Apresentação e Discussão dos Resultados dos Ensaios Limnologicos Rel 1,2 and 3 TUC-10-26835/261841/26848-RE. 1986.

Johannes, S. Ecological modeling for reservoirs in the Amazon area. Delft Hydraulics, T 102/T 333. 1988.

Meyer, B. S. and Anderson, D. N. Plant Physiology. Van Nostrand Co. 1958.

Orlob, G. Mathematical Modelling of Water Quality: Streams, Lakes and Reservoirs, John Wiley & Sons. 1983.

Vollenweider, R. Scientific Fundamentals of the Eutrophication of Lakes and Flowing waters with particular reference to Nitrogen and Phosphorus and factors in Eutrophication, Organ. Econ. Coop. Dev. Paris Report M. DAS/CSI/68.27. 1968.

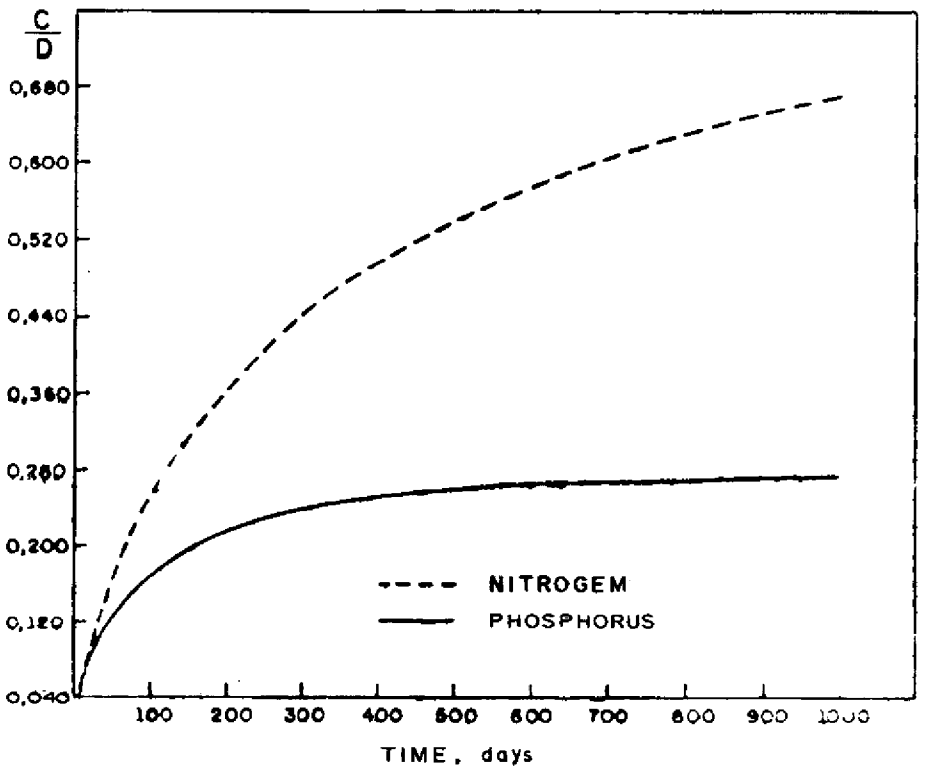

Figure 1 - Ratio of Maximum concentration and N and P loads as a time function

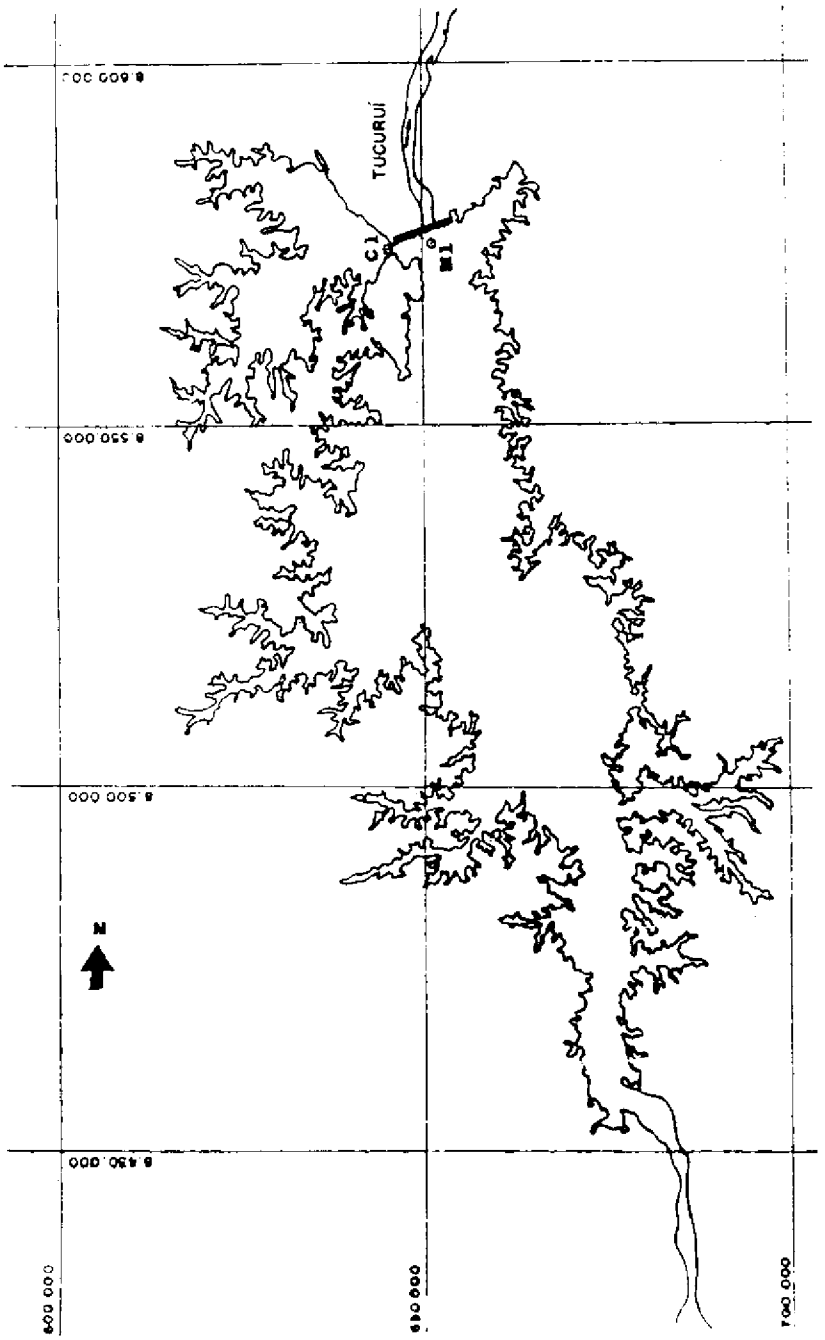

Figure 2 - Tucurui Reservoir

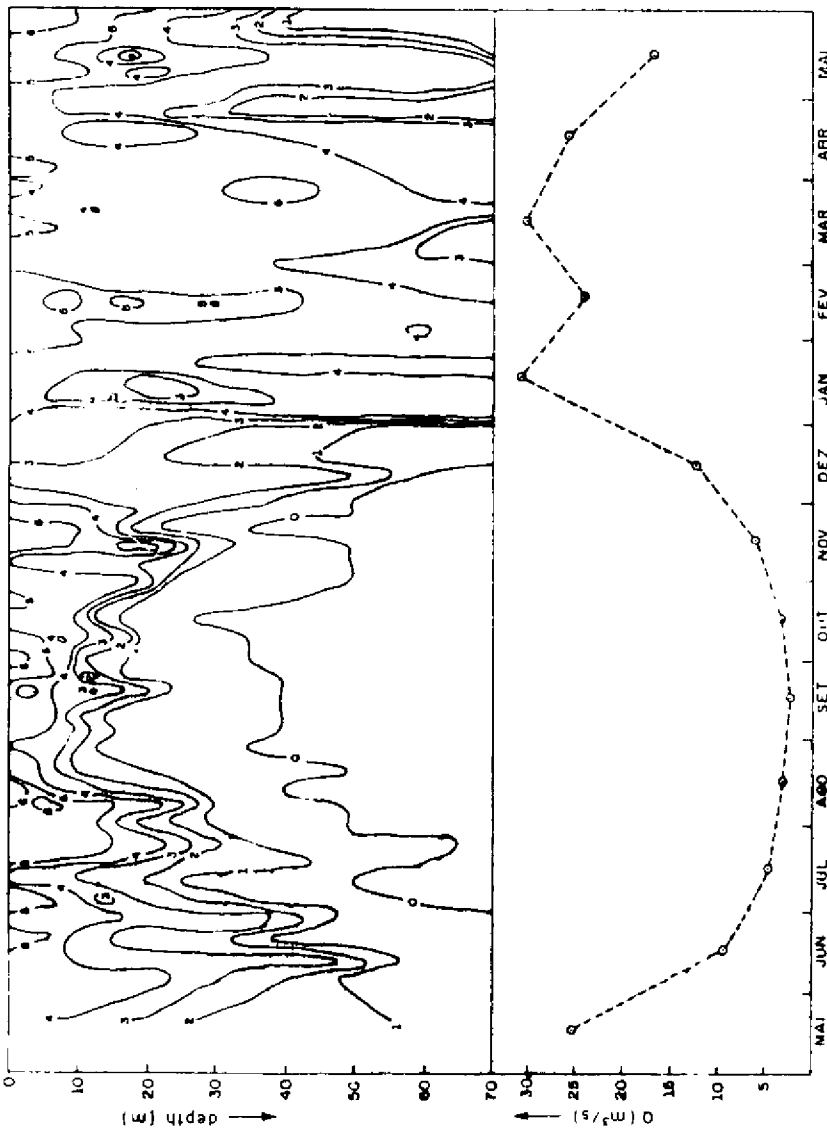

Figure 3 - DO (mg/l) at M_1 and Tucurui inflow

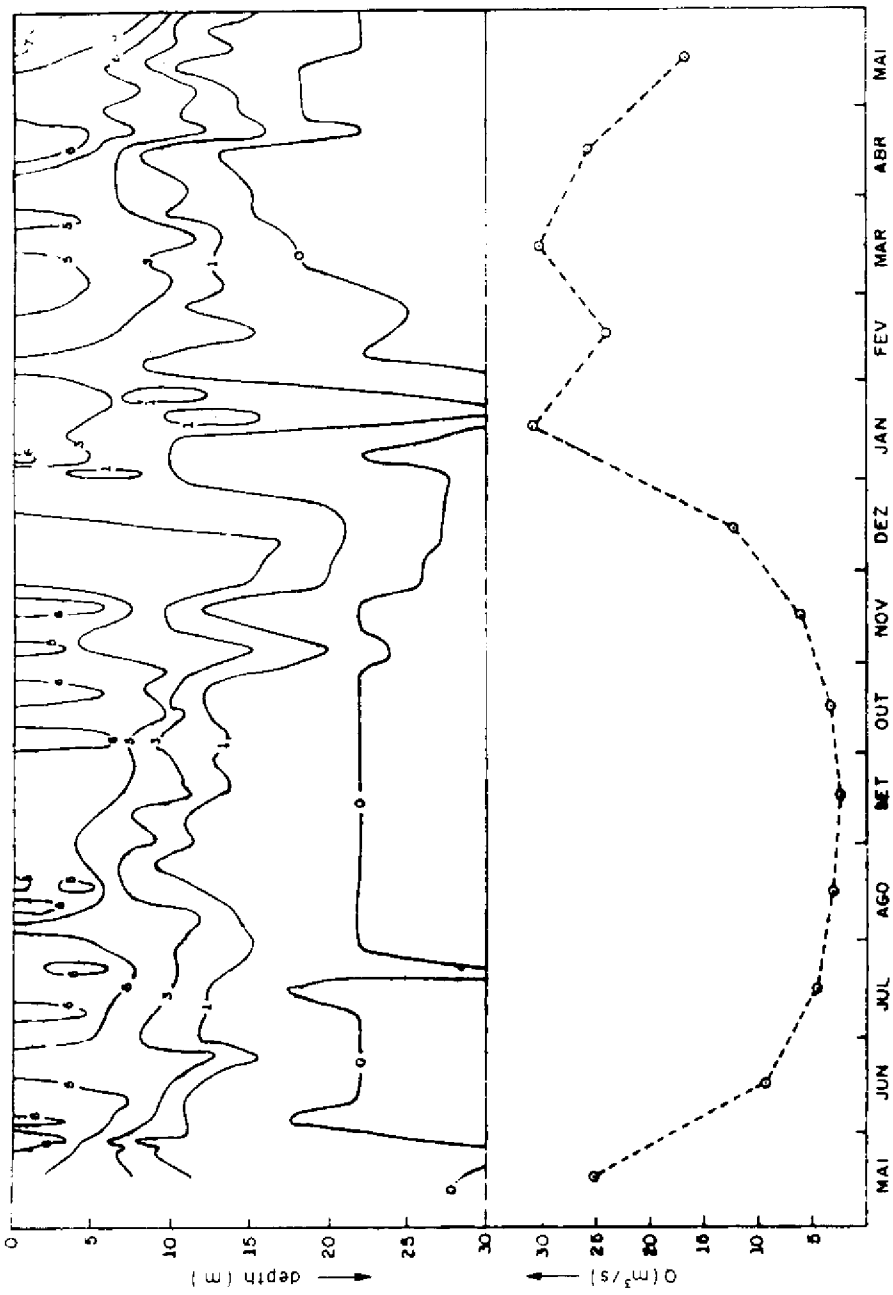

Figure 4 - DO (mg/l) at C_1 and Tucurui inflow

NUMERICAL SIMULATION OF THE UNSTEADY DENSITY CURRENT IN THE RESERVOIR

*Young Der-Liang**
*Lin Quain-Hsin***

ABSTRACT

This paper simulates and discusses the propagation of the density current of underflow in a reservoir. The method is based on a finite element scheme of the movable mesh technique dealing with the variation of free surface. Two case studies will be performed to examine the model feasibility. The model is first applied to simulate the density current of the Generalized Reservoir Hydrodynamics Flume designed by the U.S. Corps of Engineers, where the density current is generated by thermal stratification. Comparison of the physical characteristics of measured and calculated results reveals that this model is able to predict the salient feature of the structure of density current very well. Secondly the model is used to simulate the density current in the Te-Chi Reservoir at the middle of Taiwan. In this case, the density current is caused by the heavy sediment-laden suspension of inflow discharge. Again, the transport of the density current with a underflow type is vividly simulated.

1. INTRODUCTION

In reservoir dynamics, the density current may occur and behave in terms of three characteristics depending on the density difference between the ambient reservoir water and river discharge. These characteristics are overflow, interflow and underflow. Underflow occurs when the density of river discharge is greater than that of the ambient. When the density of river discharge is lesser than that of the ambient, overflow occurs. Interflow occurs when the density of river discharge is greater than that of the epilimnion while smaller than that of the hypelimnion. In this paper by the numerical analysis, we will simulate and discuss the transport phenomena of the density current due to the underflow in the reservoir.

The density difference of river inflow and reservoir ambient is attributed to thermal stratification and concentration of sediments in the reservoir environment. When the complete mixing process is not possible due to the entrainment of buoyancy force, the motion of density current is inevitable. The density current is vital to the understanding of the basic physics of the transport feature of sediment, temperature, pollutants, etc. Therefore, study of density currents has drawn a lot of investigators [1, 10].

* *Professor of Department of Civil Engineering, and Director of Hydraulic Research Laboratory, National Taiwan University - Taipei, Taiwan, 10764, R.O.C.*

** *Graduate Student of Department of Civil Engineering - National Taiwan University - Taipei, Taiwan, 10764, R.O.C.*

Due to the complex system of the subject, early research of density currents concentrated on the field observations and laboratory experiments [10]. Theoretical analysis seemed almost impossible owing to the mathematical difficulty. The advent of new numerical techniques has enabled us to look at this old subject one more time. This study will make use of the mathematical models to simulate the physical characteristics of unsteady density currents in reservoirs. The mathematical model is established as a vertical-horizontal two-dimensional profile, where the lateral direction of the reservoir is averaged. Both the temperature and the concentration of suspended sediment will be considered as contributors to the density current.

In consideration of its versatility in dealing with irregular topography and variable parameters, the finite element method is adopted to solve the governing equations of the density current. Two case studies will be used to illustrate the model applications. For first example, the Generalized Reservoir Hydrodynamics (GRH) Flume measured by the U.S. Corps of Engineers is simulated to demonstrate the density current caused by thermal stratification. The second case simulates the density current of Te-Chi Reservoir in central Taiwan. The reservoir is characterized by a very high sediment concentration of river inflows. The formation of the reservoir density current, the movement of density front, and the occurrence of plunging phenomenon were vividly simulated in this study.

In the case of GRH Flume, the density currents generated by laboratory experiments were used to verify the accuracy of present numerical scheme. In the case of Te-Chi Reservoir, qualitative prediction of density currents in a sub-tropical climate is performed. The more comprehensive studies of this sub-tropical Reservoir are in progress and will be reported later.

2. MATHEMATICAL MODEL

The mechanics associated with the density current in reservoir are governed by the basic conservation laws of fluid mass and momentum, and the transport process of heat and suspended sediments. To simplify the problem, some assumptions can be employed as far as the mathematical modeling is concerned. First, since the reservoir is very long and narrow and the characteristics of the hydrodynamics vary in the longitudinal and vertical directions, the vertical 2-D model with lateral average was chosen. Second, in the vertical momentum equation, the advection and diffusion effects may be neglected in comparing the gravity acceleration. The hydrostatic pressure assumption can be used, because the aspect ratio is very large, it can be considered as a shallow water problem. Furthermore, for this stratified flow of density current, the Boussinesq approximation is suitable, where the buoyancy effect is considered in the gravity acceleration term only [2]. After these simplifications, the governing equations can be expressed as following:

a. Continuity equation

$$\frac{\partial (uB)}{\partial x} + \frac{\partial (wB)}{\partial z} = 0 \qquad (1)$$

b. Longitudinal momentum equation

$$\frac{\partial u}{\partial t} + u\frac{\partial u}{\partial x} + w\frac{\partial u}{\partial z} = \frac{1}{\rho o}\frac{\partial P}{\partial x} + \frac{1}{B}\frac{\partial}{\partial x}\left(BK_{xx}^{M}\frac{\partial u}{\partial x}\right) + \frac{1}{B}\frac{\partial}{\partial z}\left(BK_{xz}^{M}\frac{\partial u}{\partial x}\right) \quad (2)$$

c. Hydrostatic pressure (Vertical momentum equation)

$$\frac{\partial P}{\partial z} = -\rho g \quad (3)$$

d. Heat transport equation

$$\frac{\partial T}{\partial t} + u\frac{\partial T}{\partial x} + w\frac{\partial T}{\partial z} = \frac{1}{B}\frac{\partial}{\partial x}\left(BK_{xx}^{H}\frac{\partial T}{\partial x}\right) + \frac{1}{B}\frac{\partial}{\partial z}\left(BK_{xz}^{H}\frac{\partial T}{\partial z}\right) \quad (4)$$

e. Sediment transport equation

$$\frac{\partial C}{\partial t} + u\frac{\partial C}{\partial x} + (w - w_3)\frac{\partial C}{\partial z} = \frac{1}{B}\frac{\partial}{\partial x}\left(BK_{xx}^{C}\frac{\partial C}{\partial x}\right) + \frac{1}{B}\frac{\partial}{\partial z}\left(BK_{xz}^{C}\frac{\partial C}{\partial z}\right) \quad (5)$$

where t = time; x = longitudinal coordinate; z = vertical coordinate; u = longitudinal flow velocity; w = vertical flow velocity; P = hydrostatical pressure; B = lateral width; ρo = a referential fluid density; ρ = the ambient fluid density; K_{xx}^{M}, K_{xz}^{M} = horizontal and vertical eddy viscosity; T = temperature; C = concentration; w_s = the settling velocity of suspended sediment; K_{xx}^{H}, K_{xz}^{H}, K_{xx}^{C}, K_{xz}^{C} = eddy diffusivities.

Because suspended sediment can settle in water, in equation (5), the w_3 term serves this phenomenon [3[. To compute the density in the fluid, the equation of state can be expressed as the function of temperature and concentration:

$$r = f(T,C) \quad (6)$$

The density currents that occur in reservoirs are turbulent flows. One of the principal difficulties in modeling the density current is the choice of suitable turbulent exchange coefficients. Higher order turbulent model, such as the k-ε model [4], may be more suitable for the developing flow

and associated recirculation. For the sake of economical computation, this study adopts the eddy viscosity and diffusivity model, with the vertical turbulent exchange coefficients K_{xz}^{M}, K_{xz}^{H} and K_{xz}^{C} taken from the semi-empirical formula of turbulent closure models for stable stratified flows, such as the Munk-Anderson formula [5].

The nonlinear equations 1 to 6 are solved by the numerical method. Although many numerical methods can be chosen, for the purpose of easily and directly describing the complex irregular reservoir topography, the finite element method are employed to discritize the space. The Eulerian forward explicit scheme, with adding the artificial blancing tensor viscosity [6] in order to increase accuracy and stability, is used to do the time discritization. The moving mesh technique can be applied to eliminate the difficulty of numerical scheme to satisfy the kinematic boundary condition of flow with free surface.

3. MODEL APPLICATIONS

Two cases of density current are simulated in this study:

3.1 Generalized Reservoir Hydrodynamics Flume

The Generalized Reservoir Hydrodynamics (GRH) flume, maintained by the U. S. Corps of Engineers, is designed to test reservoir hydrodynamics. This flume has been used to compare a number of models [7, 8]. The length of the flume is 24.39 m and it varies in depth from 0.3 m at its inflow end to 0.91 m at its outflow end. It has two different cross sections. The upper section 1 which is 6.1 m long, has a horizontal bottom and linear variation in width from 0.3 m to 0.91 m. The lower section 2 has a constant width of 0.91 m and a bottom which drops 0.61 m over its 18.29 m length.

To simulate the density current due to the inflow temperature of lower than the initial temperature of the flume, the flume is filled with water at a uniform temperature of 21.44°C. Inflow water at 16.67°C is introduced under a baffle and allowed to flow into the system over the lower 0.15 m. Outflow is removed from outlet located on the dam 0.15 m from the bottom. The inflow rate of 0.00063 m^3/sec is the same with the outflow rate.

The GRH flume geometry is discritized by the finite element mesh containing 612 linear triangular elements and 342 nodes as shown in Figure 1. Because the inflow temperature is lower than the ambient temperature, the underflow type of density current occurred. At time $t = 4$ min, the model results of both the velocity and temperature field are shown in Figure 2. The salient feature is the faster velocity and recirculation gyre in the inflow region as compared with the other homogenous region where the velocity is lower. As the time goes by, the density current advances along the bottom with the recirculation gyre moving rapidly toward the dam.

Figures 3 and 4 depict the transient processes of the structures of density current at $t = 14$ and 20 min respectively. Because the vertical turbulent mixture is reduced by the buoyancy effect, the temperatures vary in the region near the bottom. After the current arrives at the dam at $t = 50$ min, the flow field becomes more stable and the recirculation gyre occupies the entire region, as shown in Figure 5.

Figure 6 shows the progress of the density current front for calculated and observed results. It is interesting to notice that the simulation and the measurement are very consistent. The comparison of the computed and measured horizontal velocity at the vertical line near the center of the flume is shown in Figure 7. Although the model result is more smooth than the measurement, the general form is similar in each.

3.2. Te-Chi reservoir in central Taiwan

Te-Chi reservoir, located in the middle of Taiwan, suffers form over development in its watershed. The major dimensions of the reservoir are as follows: 11 km long, 20 m and 120 m deep in upstream and downstream location, inflow rate 220 cms and outflow rate 250 cms. To simulate the density current due to the sediment-laden inflow, the initial ambient water is clear in the reservoir and the inflow concentration is 100 ppm with suspended particle setting velocity of 0.0001 m/sec.

Figure 8 shows the modeling results of velocity and concentration field at t = 667 min. It appears that the plunging phenomenon [9] occurs near the inflow end and results in a recirculation gyre. Due to the high concentration and density in this current, under the effect of gravity acceleration in the direction of the bottom slope, the density moves rapidly along the bottom and its front forms a "noise" shape, at t = 1000 min, as shown in Figure 9. Figure 10 shows the results at t = 1333 min, the density current arrives near the dam and the "noise" becomes bigger. However, due to the settling behavior of suspended particles, the thickness of density current enhances as shown in Figure 9 and 10. After the density current strikes the dam, under the effects of strike and selective withdrawal, the flow condition becomes more complex with two circulation gyres and high concentration in the dam bottom region, as shown in Figure 11, at t = 1667 min.

4. CONCLUSIONS

The salient characteristics of density currents, either caused by the thermal stratification or the over concentration of suspended sediments, are simulated by a two-dimensional (vertical-horizontal) mathematical model using the finite element analysis. Two case studies were performed to demonstrate the capability of the numerical methods. The structures of density current caused by the thermal stratification of the Generalized Reservoir Hydrodynamics Flume and the density current of Te-Chi Reservoir caused by heavy sediment-laden suspension of inflow discharge are both well simulated by a finite element scheme with the movable mesh technique. The model can be used as a prediction tool for the simulation of reservoir dynamics.

REFERENCES

[1] Graf, H. W. "The Behavior of Silt-laden Current", Water Power and Dam Construction, Sept. pp. 33-38, 1983.

[2] Gray, D. D. and Girgini, A. "The Validity of the Boussinesq Approximation for Liquids and Gases", Int. J. Heat Mass Transfer, Vol. 9, pp. 545-551, 1976.

[3] DeVantier, B. A. and Larock, B. E. "Sediment Transport in Stratified Turbulent Flow", J. of Hy. Eng., Vol. 9, No. 12, ASCE, pp. 1622-1635, 1983.

[4] Rodi, W. "Turbulent Models and Their Application in Hydraulics", IAHR Publication, Delft, The Netherland, 1980.

[5] Munk, W. H. and Anderson, E. R. "Notes on a Theory of the Thermocline", J. of Marine Research, Vol. VII, No. 3, pp. 275-295, 1948.

[6] Gresho, P. M.; Chan, S. T.; Lee, R.L. and Upson, C. D. "A Modified Finite Element Method for Solving the Time-Dependent, Incompressible Navier-Stokes Equations, Part 1: Theory", Int. J. for Num. Meth. in Fluids, Vol. 4, pp. 557-598, 1984.

[7] Johnson, B. H. "A Review of Numerical Reservoir Hydrodynamic Modeling", Tech. Rep. E-81-2. Prepared for Office, Chief of Engineers. U.S. Army, Washington, D.C., 1981.

[8] King, I. P. "A Three Dimensional Finite Element Model for Stratified Flow", 4th Symp. FEM in Fluids, Tokyo, Japan, 1982.

[9] Farrell, G. J. and Stefan, H. G. "Mathematical Modeling of Plunging Reservoir Flow", IAHR, J. Hy. Res., Vol. 26, No. 5, pp. 525-537, 1988.

[10] Vanoni, V. A. editor. Sedimentation Engineering, American Society of Civil Engineers, 1975.

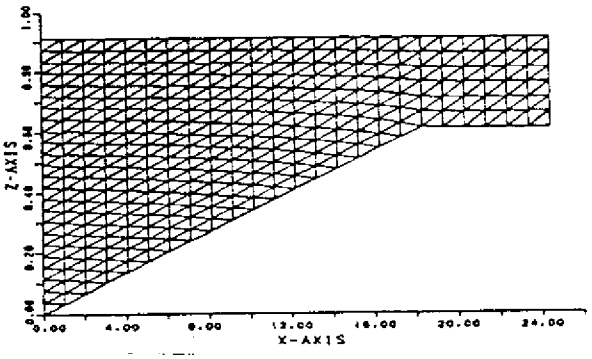

Fig. 1 - Finite Element Mesh of GRH Flume

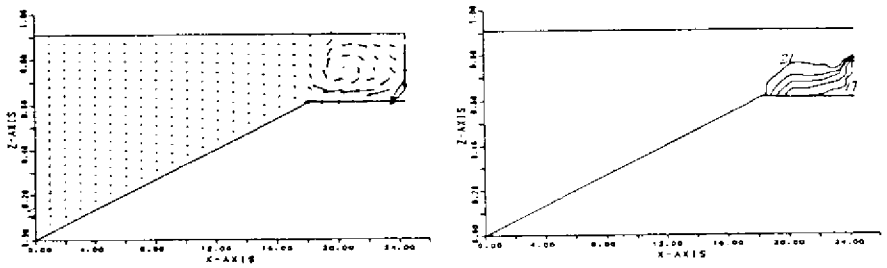

Fig. 2 - Structure of Density Current (Left) and Temperature Distribution (Right) of GRH Flume, at t = 4 min.

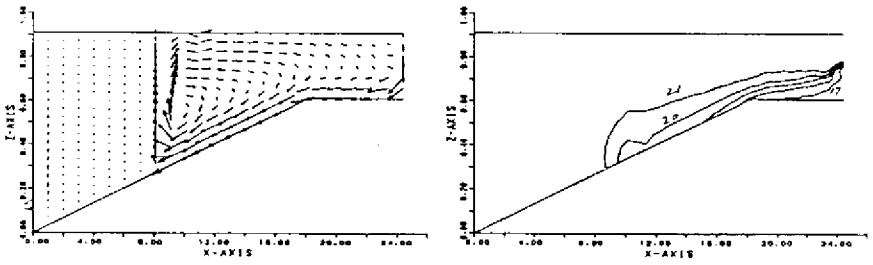

Fig. 3 - Structure of Density Current (Left) and Temperature Distribution (Right) of GRH Flume, at t = 14 min.

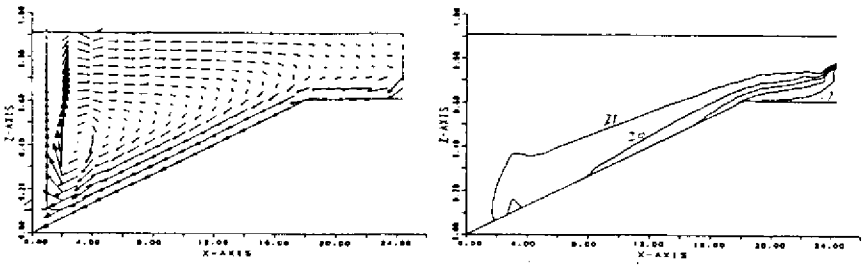

Fig. 4 - Structure of Density Current (Left) and Temperature Distribution (Right) of GRH Flume, at t = 20 min.

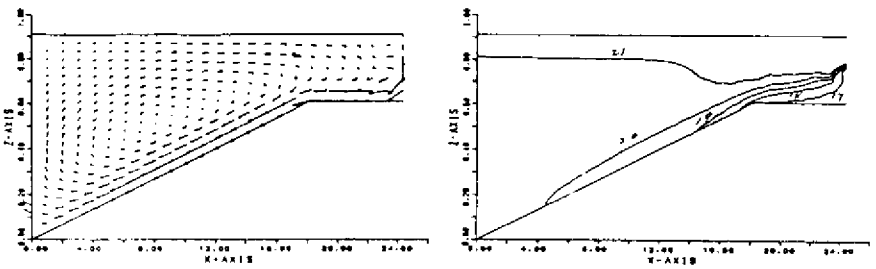

Fig. 5 - Structure of Density Current (Left) and Temperature Distribution (Right) of GRH Flume, at t = 50 min.

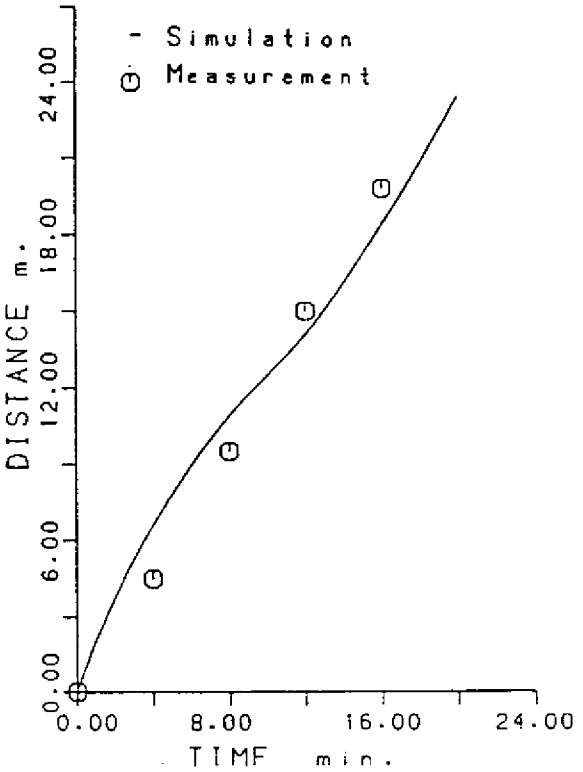

Fig. 6 - Comparison of Propagation of Density Current Front of GRH Flume

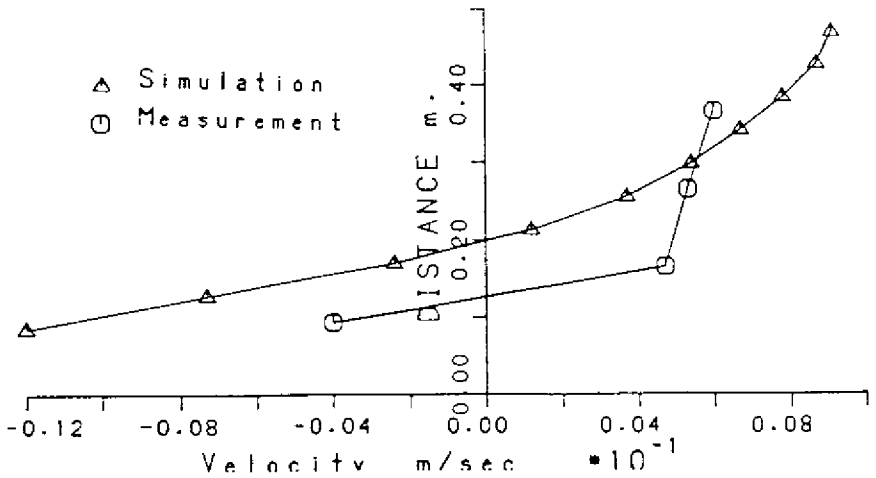

Fig. 7 - Comparison of Horizontal Velocity Distribution at the Central Section of GRH Flume.

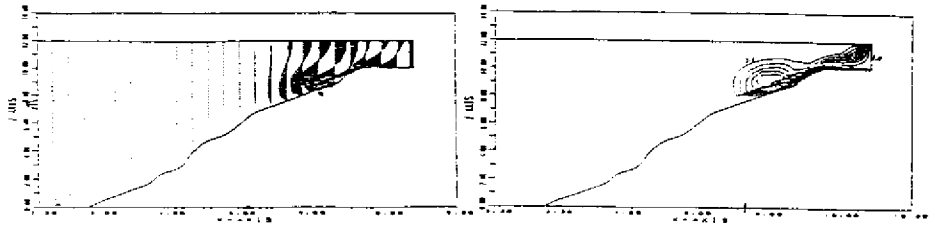

Fig. 8 - Structure of Density Current (Left) and Concentration Distribution (Right) of Te-Chi Reservoir, at t = 667 min.

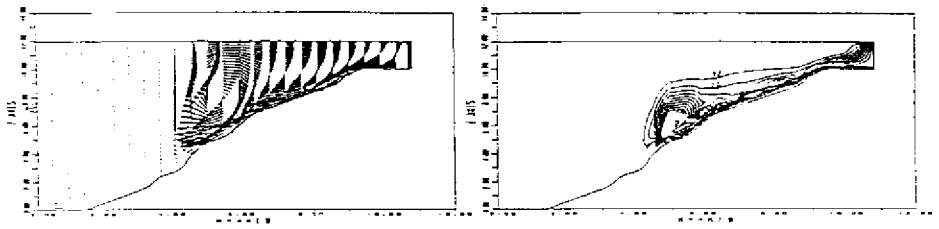

Fig. 9 - Structure of Density Current (Left) and Concentration Distribution (Right) of Te-Chi Reservoir, at t = 1000 min.

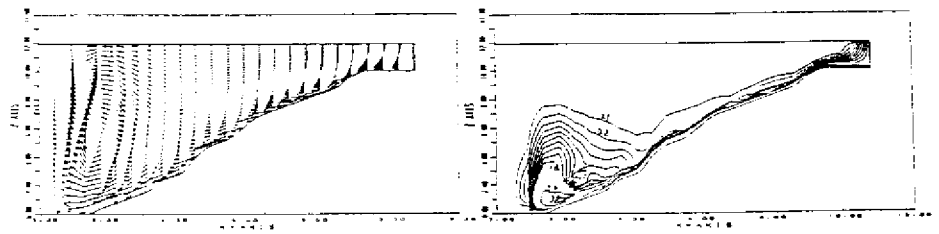

Fig. 10 - Structure of Density Current (Left) and Concentration Distribution (Right) of Te-Chi Reservoir, at t = 1333 min.

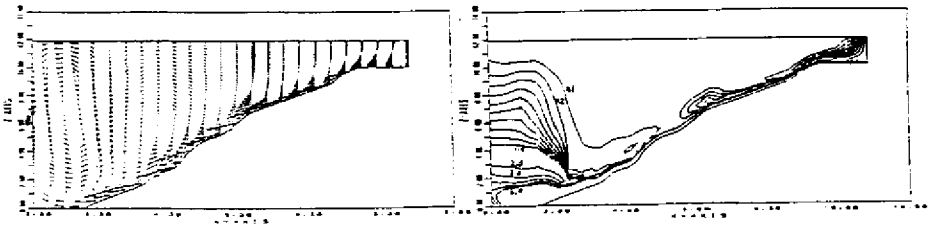

Fig. 11 - Structure of Density Current (Left) and Concentration Distribution (Right) of Te-Chi Reservoir, at t = 1667 min.

WATER QUALITY MODELING IN TROPICAL RESERVOIRS *

L. W. Canter **

ABSTRACT

The planning, design, construction, and operation of surface water reservoirs in tropical areas has typically been accomplished with only minimal attention given to water quality considerations. This historical practice has occurred because the primary focus of attention has been on water quantity management. Within the last two decades attention has been increasingly given to water quality issues derived as natural consequences of reservoir construction and operation. Accordingly, this paper has been prepared to summarize water quality concerns and modeling opportunities for reservoirs, with particular attention given to such engineering works in tropical areas. Topics to be addressed include: (1) background information; (2) timing of water quality modeling; (3) examples of types of water quality models; (4) interpretation of modeling results; (5) monitoring as a supplement to modeling; and (6) other related issues. Finally, several conclusions will be drawn.

BACKGROUND INFORMATION

An initial issue for consideration related to reservoirs created as a result of hydropower, water supply and flood control projects is the impacts of such projects on water quality. Some reasons for concern related to water quality include: (1) the increasing use of multipurpose reservoirs; i.e., reservoirs for hydroelectric power, flood control, and/or water supply; (2) the increasing adoption and enforcement of water quality standards in relation to in-reservoir and downstream water uses; and (3) the documentation of water quality changes based on information collected over the last 25 years (Canter, 1977). Since water quality changes are often rate and temperature dependent, they are of increased concern in tropical reservoirs due to higher temperatures and larger rate constants.

A number of key processes within a reservoir can influence water quality. These processes include thermal/density stratification, sedimentation, evaporation, chemical and/or biological cycling, bacterial die-away, and gas or nitrogen supersaturation. Summary points regarding these processes are as follows:

---

* *Presented at International Conference on Hydrology and Water Management of the Amazon Basin, August 5-9, 1990, Manaus, Brazil*

** *Sun Company Professor of Ground Water Hydrology and Director, Environmental and Ground Water Institute, University of Oklahoma, Norman, Oklahoma, United States*

(1) Thermal/density stratification and resultant epilimnetic and hypolimnetic processes (aerobic processes in epilimnion and anaerobic processes in hypolimnion).

- (a) The density of water varies with the temperature of water — see Figure 1 (Smalley and Novak, 1978).
- (b) As a result of density differences, can have density induced flow anomalies in reservoir (for example, warmer water flowing over colder water, colder water flowing under warmer water, or cooler water flowing between warmer and colder water).
- (c) Because of the layering effect can get reservoirs which thermally stratify and thus an epilimnion, thermocline, and hypolimnion can form — see Figure 2 (Smalley and Novak, 1978).
- (d) Epilimnion characterized by good oxygen transfer, good mixing and diurnal temperature fluctuations; the thermocline is the transition zone; and the hypolimnion is characterized by low oxygen to anaerobic conditions, limited mixing, and nearly isothermal conditions.
- (e) Stratification can lead to both lateral and vertical water quality changes within a reservoir.

(2) Sedimentation of suspended materials (sediments) which flow into the reservoir; suspended materials inputs are a function of drainage area size, characteristics, rainfall, and other factors:

- (a) Sedimentation rate varies as a function of sediment size and other factors such as temperature and turbulence; sedimentation will increase with temperature and decrease with turbulence.
- (b) Excessive sedimentation can cause reservoir filling.
- (c) Sediments can adsorb dissolved constituents and transport them to the reservoir benthic zone.
- (d) Sediments can disrupt benthic organisms and cover previously deposited pollutants.

(3) Evaporation of water from the reservoir will lead to higher concentrations of dissolved constituents; evaporation rates increase with increases in temperature.

(4) Chemical and/or biological cycling of water quality constituents; numerous examples and processes can be cited:

- (a) Nitrogen — inorganic and organic chemical forms, nitrification/denitrification, and biological uptake.
- (b) Phosphorus — inorganic and organic chemical forms, adsorption, ion exchange, precipitation, and biological uptake.
- (c) Iron and manganese — oxidation and precipitation, and reduction and dissolution.
- (d) Chromium — chemical forms, adsorption, oxidation and reduction.
- (e) Other metals — adsorption and/or precipitation.
- (f) Hydrogen sulfide — chemical forms, adsorption, biological uptake, and stripping (due to anaerobic conditions and decaying vegetation).
- (g) Oxygen — used in decomposition, produced by algae photosynthesis, and reaeration.

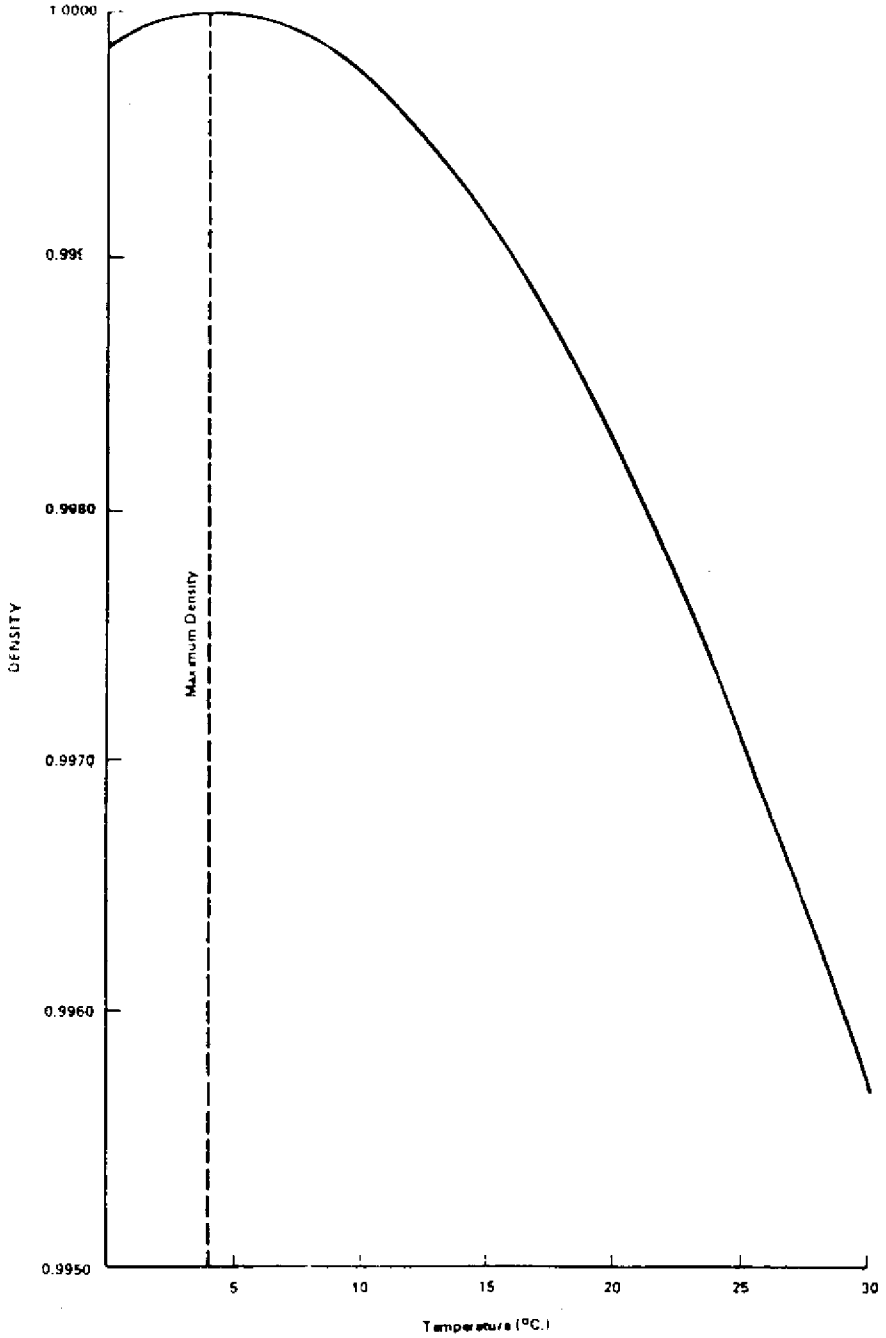

Figure 1 - Temperature Versus Density for Water (Smalley and Novak, 1978).

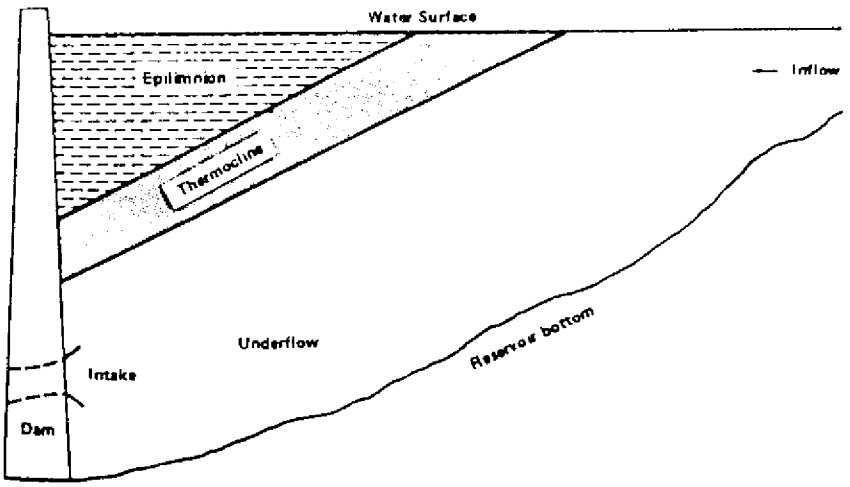

Figure 2 - Representation of Epilimnion and Thermocline Tilting Due to Inflow Displacement (Smalley and Novak, 1978).

(h) Carbon — inorganic and organic forms, and biological uptake.

(i) Methane — may be formed from decaying vegetation under anaerobic conditions; can be stripped to atmosphere over spillway or by passage through dam and/or turbines.

(5) Bacterial die-away which is a function of temperature and residence time.

(6) Gas or nitrogen supersaturation due to air entrainment in stilling basins; high nitrogen gas concentration can cause fish impacts (Legg, 1978).

Another basic issue related to water quality impacts of reservoirs involves the consideration of reservoir input loadings of different potential pollutants. Key water pollutant sources and consequent loadings include the following:

(1) Point source discharges upstream of the reservoir, these can include treated and/or untreated discharges from urban areas and industrial activities.

(2) Nonpoint source discharges upstream of the reservoir; these include runoff from urban, industrial, agricultural, and undeveloped areas; some key pollutants include sediment, nutrients, organics, and pesticides (note — river basin deforestation may exacerbate these discharges).

(3) In-reservoir decomposition of terrestrial flora left in place during reservoir filling; anaerobic conditions near the bottom or in the hypolimnion can cause problems with methane and hydrogen sulfide formation and then their subsequent release.

(4) Uses of water in the reservoir and resultant quality changes; could be concerns regarding organics, nutrients, and bacteria.

(5) Direct precipitation and/or dry deposition into reservoir; nutrients and metals as well as acid rain may be of concern.

(6) Ground water flow into reservoir.

Finally in terms of background considerations, it is pertinent to consider which water quality parameters should be modeled. Typical parameters or characteristics subject to modeling include:

(1) Dissolved oxygen and biochemical oxygen demand.

(2) Nutrients.

(3) Temperature.

(4) Others (pH, iron, solids, pesticides, fecal coliforms, methane, hydrogen sulfide, etc.).

(5) "Waste assimilative capacity" of the reservoir.

TIMING OF WATER QUALITY MODELING

Water quality modeling should be done during several phases over the project life. Different purposes may be associated with modeling for a given phase. The phases can be considered in terms of pre-construction planning, construction, transition years, and continued operation.

Pre-construction Planning Phase

Modeling should begin prior to the finalization of the reservoir design and the initiation of the construction phase. This modeling would typically be included in an environmental impact statement (or environmental impact assessment). The purpose should be to predict potential problems and then develop mitigation measures to minimize these problems (the measures could include reservoir design changes and/or selective removal of terrestrial flora in the area to be inundated). The modeling should anticipatorily address the construction phase, transition years, and continued operation of the reservoir.

Construction Phase

Real-time modeling should be done during this phase, with several-fold purposes to be achieved. Several years might be required for construction, and most of the terrestrial flora in the inundated area is typically left in place and is in various states of decomposition. A water quality monitoring program should be conducted during this phase. The monitoring program would allow the calibration/verification of the water quality models used during this phase. In addition, the modeling should facilitate the implementation of positive environmental management (water quality manage-

ment) programs. Examples of such programs include the planning of specific construction activities for specific seasons, and adjustment in selective removal of terrestrial flora in the area being inundated.

Transition Years Phase

Real-time modeling should be done during the transition period between the completion of the filling of the reservoir and a point in time when the reservoir water quality exhibits repeatable patterns. This period would typically encompass the time of the most rapid decomposition of the terrestrial flora in the inundated area. While no specific time can be identified, periods in the order of 5 to 10 years might be a good estimate. Again, it is assumed that a water quality monitoring program is in place. As noted earlier, the monitoring program would allow the calibration/verification of the utilized water quality models. The modeling could also be used to evaluate and facilitate the implementation of positive environmental management (water quality management) programs. Examples of such program include the use of artificial aeration at selected locations within the reservoir, and the use of water level drawdown to expose and allow the selective removal of decaying terrestrial flora from the fringes of the inundated area.

Continued Operation Phase

This phase represents the long-term operation of the reservoir. It could extend for several decades and even beyond. Water quality modeling during this phase is important in that longer time periods are involved and greater opportunities exist for the planning and implementation of positive water quality management programs. Monitoring could continue to be used for calibration/verification of utilized water quality models. It is assumed that more sophisticated models would be selected/developed/used during this phase. Potential water quality impact mitigation measures which could be used during this phase include the design and use of in-reservoir artificial aeration measures, and the planning and implementation of land use controls and watershed management measures.

EXAMPLES OF TYPES OF WATER QUALITY MODELS

There are numerous water quality models that exhibit a wide range of technical sophistication and input data requirements (Canter, 1985). Three key points are revelant to the selection and usage of these numerous models: (1) simple models should be used in the case where water quality and flow data is minimal; (2) qualitative models can be useful for planning monitoring programs and anticipating impacts in the absence of site-specific data; and (3) sophisticated multi-dimensional models should only be used when the available data is sufficient to justify the usage of such models. Accordingly, consideration should be given to the selection of appropriate models for each of the temporal phases mentioned earlier. Four types of models to be briefly summarized herein include physical models, qualitative models, simple quantitative models; and quantitative models.

Physical Models

Physical models can be built and used to enable the physical measurement of water quality changes. Examples include:

(1) Scale models of segments of a reservoir — 10 meter diameter and 10 meter deep tanks are an example — can use to determine important processes and develop rate information.

(2) Laboratory microcosms to focus on understanding specific processes and developing rate information — 0.5 to 1 meter cubes or rectangles to simulate reservoir conditions.

Qualitative Models

Qualitative predictions of water quality changes in a proposed reservoir can be based on using data on experienced changes from nearby projects of similar type ("look alike" projects). It would be best to look at common patterns of change from several studies. Expert (professional) judgment must be used to qualitatively infer changes in water quality; this can be best done by using several pertinent professionals, examples include environmental engineers, chemists, and aquatic biologists.

Simple Quantitative Models

There are several simple models and relationships which can be used to estimate water quality changes in reservoirs. Examples include:

(1) Calculate mass balances of chemical inputs and outputs to reservoir; based upon calculations related to reservoir size (volume) and flow rate, and assumptions related to in-reservoir processes, average in-reservoir concentrations of specific water quality constituents can be calculated; an example of the major nutrient inputs and exports for a reservoir include (Interim Mekong Committee, 1982):

   (a) inputs from five sources — watershed surface drainage, ground water inflow, reservoir sediments, atmospheric precipitation and dry fallout, and direct lakeside introductions;

   (b) exports from water phase via three routes — movement through reservoir and to downstream, sedimentation, and harvesting of biomass.

(2) Can express pollutant loading from various point and nonpoint sources via calculation of population equivalent (Canter, 1977).

(3) Utilize densimetric Froude number to anticipate the propensity of the reservoir to thermally stratify (Canter, 1985).

(4) Can use simple mixing model for entire reservoir or for segments of reservoir, in this case uniform mixing of all constituents is assumed to occur, could then account for various reservoir processes described earlier.

(5) Based on rational assumptions related to reaeration in a reservoir versus a flowing stream, could calculate the change in waste assimilative capacity by assuming certain organic matter decomposition rates (Canter, 1977).

(6) Can account for bacterial die-away by using Chick's law and adjusting the die-away rate for reservoir conditions (Canter, 1977).

Quantitative Models

Quantitative models typically involve the consideration of multiple influencing factors and processes in a reservoir. Quantitative models also typically consider reservoir dynamics in lieu of steady state conditions; models for transient conditions can be for continuous time or discrete time. To serve as an example, the oxygen relationships in a reservoir can be modeled by considering decomposition, reaeration, benthic oxygen demand, and photosynthesis.

Quantitative models can be one-dimensional (x direction), two-dimensional (x and y directions), or three-dimensional (x, y and z directions); the multi-dimensional models are more complicated from a mathematical perspective. In addition, they are more data intensive. Table 1 summarizes the key characteristics of several quantitative models which can be used for reservoir water quality studies (U.S. Army Corps of Engineers, 1987).

INTERPRETATION OF MODELING RESULTS

The results of reservoirs modeling studies must be interpreted from a professional perspective. The following approaches can provide a basis for such interpretations; they should be used collectively (if possible) and not singularly:

(1) existing water quality standards or criteria (either in-country or WHO or UNPE standards or criteria);

(2) case study comparisons which are focused on experienced consequences of other reservoir projects;

(3) changes in parameters or characteristics when compared to baseline conditions; need to consider natural variability of parameters and characteristics; could calculate percentage changes from baseline conditions; and

(4) aquatic ecological consequences of water quality changes; examples include implications for algae, rooted or floating plants, benthic organisms, and fish.

Table 1 - Summary Comparisons of Several Water Quality Models (U.S. Army Corps of Engineers, 1987).

Model Name	Description	Major Features	Data Requirements	Output
CE-THERM-1	1-D vertical reservoir model for temperature	Temperature total dissolved solids (TDS), suspended solids (SS) coupled to density Specify outflow ports or ports based on temperature objective Reregulation pool, pumped-storage, and/or peaking hydropower options	Inflow rates and constituent values Outflow rates/operations Structural configuration and hydraulic constraints of outlets Initial constituent profiles Morphometric data Meteorological data Process and rate coefficients Release flow and temperature targets if using outflow-port decision routine	Vertical profiles and outflow values for constituents over time (printed and/or plotted) Statistics of predicted and observed values Flux information Operations schedules for multilevel outled configurations
CE-QUAL-R1	1-D vertical reservoir model for water quality	All CE-THERM-R1 features Allow simulation of most major physical, chemical, and biological processes and associated water quality constituents Simulates anaerobic processes Monte Carlo simulations	Same as CE-THERM-R1 plus additional water quality data and coefficients	Same forms as CE-THERM-R1

WESTEX	1-D vertical reservoir model for temperature and conservative constituents	Simulate temperature and conservative water quality constituents Optimal design or operation of multilevel outlets for temperature objective Reregulation pool operation under generation and pumpback conditions	Same as CE-THERM-R1 plus optimization parameters if optimization routines are used	Vertical profiles of constituents over time Release quality over time Optimization results such as multilevel outlet port selection Operations schedules for multiple outlet configurations
CE-QUAL-W2	2-D longitudinal, vertical, hydrodynamic and water quality model for reservoir, estuarine, and other 2-D waterbodies	Solves 2-D hydrodynamics Head of flow boundary conditions Allows multiple branches Simulates temperature, salinity and up to 19 other water quality variables	Basically same as CE-QUAL (THERM)-R1 Tidal boundary conditions for estuarine applications Morphometric data including widths for each cell	Velocities and water quality constituents at all points on 2-D grid (printed) 2-D vector plots and 2-D constituent concentration contour or shading plots Time series data and plots Statistical output Restart files for subsequent hot restart simulations
SELECT	1-D vertical steady-state model of selective withdrawal from a reservoir	Computation of withdrawal zone distribution from a density-stratified reservoir Release temperature, density, conservative constituents computed Multiple outflow types (spillway, water quality gate, flood-control outlet, etc.) handled internally User specifies ports operating or selects ports internally based on quality objective (e.g., temperature) Reaeration of hydropower and flood-control releases computed	Reservoir profiles for temperature (density) and conservative constituents Outflow rate/operation Structural configuration and hydraulic constraints of outlet(s) Quality targets if deciding port operation	Vertical profile of withdrawal zone Release qualities Appropriate port operations to meet quality targets
WESSEL	2-D laterally averaged stratified flow model	2-D hydrodynamics coupled to density Nonhydrostatic Irregular geometry	Geometric data and grid Flow rates and boundary conditions Initial density profile	Velocities, densities and pressures printed and plotted
STEADY	1-D longitudinal steady-state stream temperature and DO model	1-D steady-state Steady flow Allows branches, loops, and lateral inflows and withdrawals Flow can be piecewise nonuniform	Flows, depths, and velocities Average equilibrium temperature and heat-exchange coefficient temperature and DO Rate coefficients	Printed output for predicted temperature and DO at each node

QUAL-IIE	1-D longitudinal stream water quality model	Simulate up to 11 (+4 arbitrary) water quality constituents -state or time-varying water quality Steady or slowly varying flow Flow augmentation Allows branching lateral inflows and withdrawals Can specify or roughly simulate hydraulics	Reach ID and riverine data Flow augmentation data (optional) Flag field data Hydraulic or channel data Reaction rate coefficients Initial conditions Inflow data Meteorological data	Input data echo Tabular output of hydraulic data, meteorologic data, fluxes, productivity data and concentrations Longitudinal graphical profiles for constituents
CE-QUAL-RIV1	1-D, dynamic flow, time-varying streamhydralic (RIV1H) and water quality (RIV1Q) models	Simulates dynamic (highly unsteady) flows Simulates up to 10 time-varying water quality constituents Allows branching systems Allows multiple control structures Stream, structural and wind reaeration options Direct energy balance or equilibrium temperature approach for temperatures	Physical data, cross-section geometry, elevations, and locations of nodes; lateral inflows and tributaries; control structures Initial conditions Boundary conditions for flow and water quality Rate coefficients and other parameters Meteorological .data or equilibrium temperatures and exchange coefficients	Hydraulic information and water quality constituent values printed for all nodes at specified print intervals. Time-series plots of selected variables at selected nodes
HEC-5Q	Reservoir system simulation/optimization model for multiple water-resource purposes including water quality, water supply, hydropower, and flood control	Balanced reservoir system regulation determination Optimum gate regulation for multiple water quality constituents	Inflow quantity and quality Initial water quality conditions System configuration and physical description Reservoir Regulation Manual Op System diversions Water quantity and quality targets at system control points Coefficients	Reservoir and river water quantity profiles Reservoir and river discharge rates, elevations, and travel time

MONITORING AS A SUPPLEMENT TO MODELING

In order for water quality modeling efforts to be successful, water quality monitoring should be considered as a required supplement. As noted earlier, monitoring is needed in order to calibrate/verify the modeling efforts at various times in the life cycle of a project. Planning a water quality monitoring program can be complicated due to the large number of items to consider. Examples of items which must be addressed during the planning and operation of a monitoring program include:

(1) Delineation of monitoring objectives.

(2) Selection of water quality parameters to be monitored (including the possible use of algae bioassays).

(3) Monitoring station location and depth of sampling.

(4) Frequency of sampling.

(5) Operational consideration for monitoring (including sample storage, field testing, laboratory analytical methods, and data storage and retrieval).

(6) Preparation of monitoring reports and the usage of the information.

OTHER RELATED ISSUES

In addition to direct water quality changes within tropical reservoirs used for hydropower, water supply, and/or flood control, there are other related issues associated with general water resources concerns. These related issues include health impacts, changes in reservoir biology, alterations in the local microclimate, and downstream effects.

(1) Health impact concerns (disease transmission) are a result of construction worker influx, people relocation, and the reservoir serving as a breeding place for mosquitoes and other disease factors. Water-related diseases can be classified into water-borne diseases, water-based diseases, water-related diseases, and water-washed diseases. Table 2 summarizes some characteristics of these four groups, and Table 3 lists some important disease vectors associated with water (World Health Organization, 1983).

(2) Changes in reservoir biology as a result of water quality changes; these biological changes can occur on phytoplankton, aquatic plants, benthic organisms, and/or fish.

(3) Microclimate effects of the reservoir; these effects are largely dependent upon the size of the reservoir.

(4) Downstream effects of the reservoir on water quality and stream biology; downstream effects can also occur on estuaries as a result of flow decreases, water quality changes, and stream biology changes.

Table 2 - Categories of Water-related Diseases (World Health Organization, 1983)

Water borne diseases are caused by highly infective organisms, only a small number of which are needed to cause disease. The diseases are transmitted by contamination of water supplies by faeces from a human carrier of the infective organism. The two classic examples of waterborne disease are typhoid and cholera. In addition, diarrhoea and dysentery may be caused by waterborne organisms, including protozoa (for example giardiasis), amoebae (such as Entamoeba histolytica) and enterobacteria (especially the Shigella genus).

Water based diseases are infections by worms, including flukes and trematodes. Most depend on aquatic crustacean hosts (called intermediate or secondary hosts) for their transmission. Faeces from infected humans contain worm eggs, which enter the secondary crustacean hosts through contamination of water. Parasite larvae emerging from the snails are able to bore through human skin, and thus are transmitted to humans by direct skin contact with water. The most important water based disease, schistosomiasis, is dependent on Bulinid snails as the main secondary host. Another water based disease, guinea-worm infection, is transmitted by ingestion of water containing the microscopic crustacean secondary host of the disease (Cyclops spp.). The disease organism leaves the secondary host once it is inside the primary host, the human body.

Water related diseases are transmitted by insect vectors that breed in or around water. Mosquitoes, tsetse flies (Glossina species) and Simulium species are the most important vectors of water-related diseases; they carry a wide range of infections including malaria, sleeping sickness, onchocerciasis and viral diseases. The diseases are transmitted when the insect bites an infected human host followed by an uninfected human.

In contrast to the other types of water related disease, the transmission of water washed disease is reduced, not aided, by water. This group includes diseases where the level of infection may be reduced by provision of more abundant or more accessible water supplies. The diseases are transmitted from one person to another when personal hygiene is poor due to lack of adequate water supplies. The most important water washed diseases are diarrhoeas transmitted by a faecal-oral route; others include skin ulcers, scabies, skin fungus infections and trachoma.

Table 3 - Important Disease Vectors Associated with Water (World Health Organization, 1983)

Culex quinquefasciatus, which breeds in organically polluted water and is associated with bancroftian filariasis and arbovirus transmission;

Culex tritaeniorhyncus, the rice-field breeding mosquito known to be a vector of Japanese B encephalitis;

Aedes aegypti, the container breeding mosquito vector of dengue and urban yellow fever;

Aedes simpsoni, breeding in banana, Colocasia and pineapple leaf axils and incriminated in the sylvatic yellow fever cycle;

Aedes africanus, a tree-hole breeding mosquito also incriminated in the sylvatic yellow fever cycle;

Mansonia spp., breeding in ponds with Pistia, Salvinia, Eichornia, etc., whose roots provide its substrate; associated with brugian filariasis and Spondweni arbovirus transmissions.

Anopheles, breeding mostly in less polluted still or slowly moving water with or without vegetation and shade; responsible for malaria and bancroftian filariasis transmission as well as Chikungunya arbovirus;

Cyclops, the tiny fresh water crustacean that thrives in ponds and is the intermediate host of dracontiasis (Guinea worm infections);

Glossina, the tsetse fly, associated with light forest type vegetation zones, certain species (*G. palpatis*) are even riverine, and responsible for the transmission of African trypanosomiasis or sleeping sickness;

Simulium, the blackfly, breeding in fast flowing clear waters attached to any suitable substratum; it is the vector of onchocerciasis and capable of long distance migration.

Aquatic snails: bulinids — *Schistosoma haematobium* transmission; planorbids — *S. mansoni* transmission; and *Oncomelania*, the amphibious species — *S. japonicum* transmission. All these are aquatic snails found in still or very slow moving waters and often associated with certain types of aquatic vegetation and muddy soil and capable of aestivation.

CONCLUSIONS

Several conclusions can be drawn from this brief review of water quality modeling for tropical reservoirs. These conclusions include:

(1) The purposes of water quality modeling can include the development of an understanding of the reservoir processes; and the development of information which can be used to plan, design and manage (environmentally) the project.

(2) A selection process should be used for models so as to match the model with data availability and phase of study. The assumptions and limitations of any selected model should be considered in interpreting the results of modeling efforts.

(3) The most effective modeling requires a long-term commitment to both modeling and monitoring efforts.

(4) Modeling can be used to establish linkages to watershed management, operational controls, and downstream developments.

SELECTED REFERENCES

Canter, L. W. *Environmental Impact of Water Resources Projects*, Lewis Publishers, Inc., Chelsea, Michigan, Ch. 2, pp. 77-110, 1985.

Canter, L. W. *Environmental Impact Assessment*, McGraw-Hill Book Company, Inc., New York, New York, Ch. 5, pp. 86-119, 1977.

Interim Mekong Committee. *Environmental Impact Assessment—Guidelines for Application to Tropical River Basin Development*, 1982, Mekong Secretariat, c/o ESCAP, United Nations Building, Bangkok, Thailand.

Legg, D. L. "Gas Supersaturation Problem in the Columbia River Basin", in *Environmental Effects of Large Dams*, American Society of Civil Engineers, New York, New York, pp. 149-164, 1978.

Smalley, D. H. and Novak, J. K. "Natural Thermal Phenomena Associated with Reservoirs", in *Environmental Effects of Large Dams*, American Society of Civil Engineers, New York, New York, pp. 29-50, 1978.

U. S. Army Corps of Engineers "Water Quality Models Used by the Corps of Engineers", Vol. E-87-1, Information Exchange Bulletin, Waterways Experiment Station, Vicksburg, Mississippi, March 1987.

World Health Organization "Environmental Health Impact Assessment of Irrigated Agricultural Development Projects — Guidelines and Recommendations", Regional Office for Europe, Copenhagen, Denmark, 1983.

MEASURING FRESH WATER FLOWS IN LARGE TIDAL RIVERS

Michael B. Amphlett and Thomas E. Brabben *

ABSTRACT

A numerical model developed by Hydraulics Research for the estimation of fresh water flows in the tidal reaches of rivers is described. The computational method is based on a system requiring synchronous water level records at both ends of a suitable tidal reach. Sequential values of instantaneous discharge through a tidal cycle are computed and then integrated to obtain the fresh water component. Application of the technique on a tidal reach of the Berbice River, Guyana is described with good agreement between model results and field observations.

1. INTRODUCTION

The tidal influence in estuarine rivers of the world can extend for many hundreds of kilometres inland from the mouth, particularly where they flow through coastal areas of low relief. For example, the Gambia River in West Africa has a tidal excursion of 526 km and the Amazon River in Brazil 735 km. Usually associated with the tidal excursion in the river is the intrusion of a tidal salinity front. How far the tidal salinity penetrates inland will be a balance between fresh water flow in the river and the tidal influence. If the fresh water flow component is reduced by upstream abstractions and river regulations then this balance is disturbed and the tidal salinity front can migrate landward. With any movement of the tidal salinity front landward the danger of damage to cultivable land and even pollution of the abstracted water may arise. These problems are more acute in tropical climates which have pronounced wet and dry seasons and hence a greater seasonal variation in fresh water flow. Even with no water regulation or abstraction upstream, a fluctuation in the intrusion distance of the tidal salinity front will normally occur between seasons. For example in the Gambia River, the discharge can vary between 2 m^3/s and 2000 m^3/s from the dry to the wet season and at low flows salinity intrusion can penetrate from 200 km to 250 km of its 526 km tidal reach [1]. In other major rivers such as the Congo, Mississippi and Columbia salinity intrusion distances are of the order of 40 km, 100 km and 40 km respectively. In the Amazon River however, the flows are significantly large even during the dry season so that at present no salt water intrusion occurs [2]. This situation could change with future water resources development activities within the Amazon Basin.

* *Overseas Development Unit - Hydraulics Research, Wallingford - United Kingdom*

Research undertaken by the Overseas Development Unit (ODU) of Hydraulics Research (HR) has focused on the problem of salinity intrusion in tropical estuaries. A predictive model has been developed and applied to the Gambia estuary [3], the Guayas estuary in Ecuador [4], the Arbary estuary in Guyana [5], the Kuantan estuary in Malaysia [6] and the Nilwala Ganga in Sri Lanka [7]. These studies have assessed the likely effects of planned water abstraction or regulation on long-term salt movement in the estuaries where agricultural land or intakes would be threatened if the salinity front were to ingress beyond acceptable limits. Such information is required both at the planning stage and for subsequent operation of control works.

A dominant factor in the reliable prediction of saline intrusion is an accurate knowledge of the fresh water flow, and in particular the minimum dependable flow. Obtaining reliable and accurate estimates of fresh water flows in the tidal reaches of large rivers can however be problematic. In reversing tidal flow, conventional flow measuring techniques which depend upon routine measurement of water level alone and which deduce the water flow from this by the application of a rating curve, will not work. Such flow gauging stations that do exist have to be upstream of the tidal limit and this can be some considerable distance from the area of concern. In such situations, if existing flow records are to be utilized then allowance has to be made for any tributaries entering the tidal reach further downstream, which may or not be gauged, and for evaporation losses or groundwater inflows. For measuring flow in the tidal reach itself, the most commonly employed method in large rivers is continuous gauging using boats equipped with current meters. Measurements over a full tidal cycle can then be analysed to remove the reversing tidal component of flow to deduce the residual uni-directional fresh water flow. Such exercises of this scale are time-consuming, laborious and costly to conduct and can thus only be mounted occasionally and are therefore insufficient to indicate the statistics of flow and so ascertain a reliable minimum flow. A need thus exists for a better method for measuring the net river flow at sites where there is a tidal reversal of flow. One such technique is the stage computational method.

2. STAGE COMPUTATIONAL METHOD FOR LOW FLOW ESTIMATION

A technique particularly suited for low flow estimation in tidal reaches, but one which is not widely used, is the stage computational method. This method is based on a system developed by the United States Geological Survey (USGS) in the 1950's and 60's and requires synchronious stage records at both ends of a suitable tidal reach [8]. A computational model is then used to analyse the stage records. The computational method relies on obtaining sequential values of instantaneous discharge through a tidal cycle and then integrating to obtain the uni-directional fresh water flow component. Proving of the numerical model is necessary and this is achieved through comparison of observed and computed tidal hydrographs. When relevant parameters in the model have been optimised to give acceptable correspondence between computed and observed data it can then be routinely applied. Its main advantage therefore is that once the stage recording stations have been set up a continuous record of fresh water flows can be obtained which will enable the statistics of the flow be deduced.

There are, however, two principal sources of error in the method. Firstly, how accurately the fresh water flow can be estimated will depend on how well the model replicates the instantaneous tidal

flood and ebb discharges. Secondly, having obtained the flood and ebb discharges, the differences between these two, normally quite large, quantities have to be evaluated in order to obtain the much smaller uni-directional fresh water component. The accuracy of estimation can thus be expected to decrease as the fresh water flow rate decreases. This latter source of error is of course also applicable with conventional flow gauging techniques for flow estimation. Despite these deficiencies, the stage computational method does have distinct advantages over other methods provided that the errors implicit in the method are recognised and quantified.

3. LOW FLOW ESTIMATION IN THE BERBICE RIVER, GUYANA

In Guyana, where all major rivers have long tidal reaches due to low coastal relief, salinity intrusion can be a major constraint on agricultural development. The higher fertility alluvial soils, which offer the potential for development are found in a narrow coastal strip, some 10 km wide, whereas further inland the soils are white sands of lower agricultural potential.

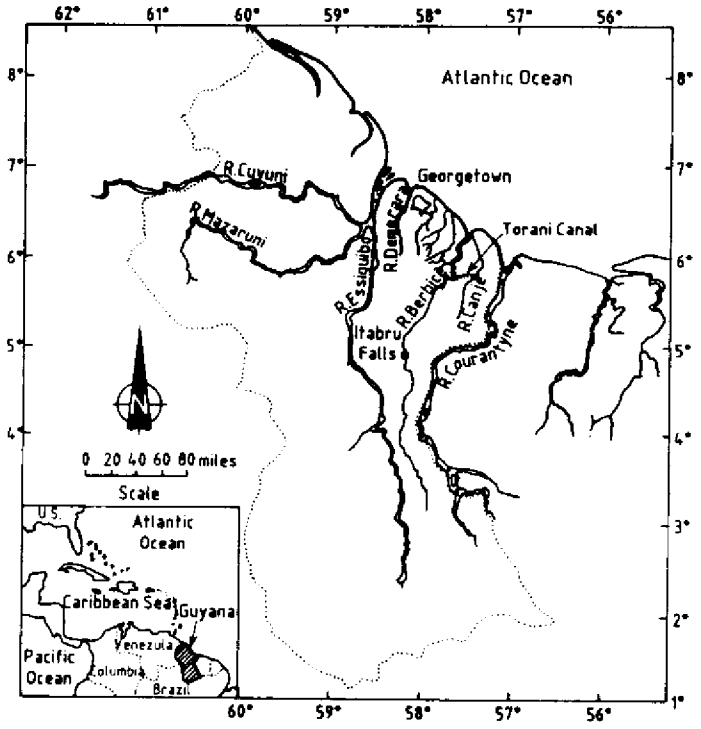

Fig. 1 - Map of Guyana

Development of an area bounded by the Berbice River and its tributary the Canje is dependent on how much fresh water can be safely abstracted. In the Berbice estuary itself, saline intrusion already extends beyond the best agricultural areas and so it is difficult to use the river directly for irrigation. The main focus of attention is an old canal, the Torani, which was constructed to transfer water from the Berbice to the Canje. The canal inlet is located some 80 km from the sea where, although subject to tidal influence, flow is presently fresh throughout the year. Saline intrusion also occurs in the Canje but extends less distance inland due to its smaller dimensions. By passing water to the Canje, its flow is augmented and so suitable irrigation water can be brought nearer to the good coastal lands. Development of the Berbice-Canje area is reliant on maintaining a flow in the Canje in excess of irrigation needs so that there is a residual seaward flow to prevent ingression of the tidal salinity front.

Abstraction of water at the Torani canal naturally increases salinity intrusion in the Berbice estuary, but as there are no significant offtakes downstream of the canal inlet this is not a problem at present. However, the upper limit on development of the entire Berbice-Canje system is set by the constraint that saline intrusion in the Berbice must never reach the Torani intake. Knowing how much water can be safely abstracted requires a knowledge of the fresh water flow in the Berbice River at the intake point.

The Berbice drainage basin is long and narrow and stretches southward from the Atlantic Ocean for a distance of 644 km. The tidal limit is between 160 and 320 km from the sea. The nearest conventional flow gauging station is at Itabru Falls, some 336 km from the sea, at which point the contributing basin area is around 5040 km^2. At the Torani canal inlet, the contributing area is about 11.520 km^2. Thus the fraction of the catchment that can be measured by conventional means at Itabru Falls is only 44%. Furthermore, recorded dry season flows at Itabru Falls drop to as low as 2 m^3/s when abstractions from the Torani canal at around the same time have exceeded 30 m^3/s. This suggests that the unmeasured lower 56% of the basin yields a significant amount of water. The large number of short tributary rivers entering the Berbice are difficult to measure. So in the circumstances it is not possible to adjust the Itabru Falls data to estimate what is available at the Torani canal. For this reason a stage record computational method was employed.

To support an earlier study Fisher and Porter digital stage recorders were installed on the Berbice River at Hoffwerk and Fort Nassau, approximately 6.5 km apart, in a suitable tidal reach upstream of the Torani canal inlet. A digital computer model, based on a USGS power series method, was developed and worked on the assumptions of uniform cross-section for the channel over the reach, uniform Mannings 'n', uniform bed slope and a homogenous estuary. There were significant errors between the observed and computed instantaneous discharges and due to deficiencies in the model. It was decided not to pursue further development of the power series model but to adopt an improved modelling technique. A tidal model developed at HR for simulating tidal propagation in narrow, partially mixed, single channel estuaries was used.

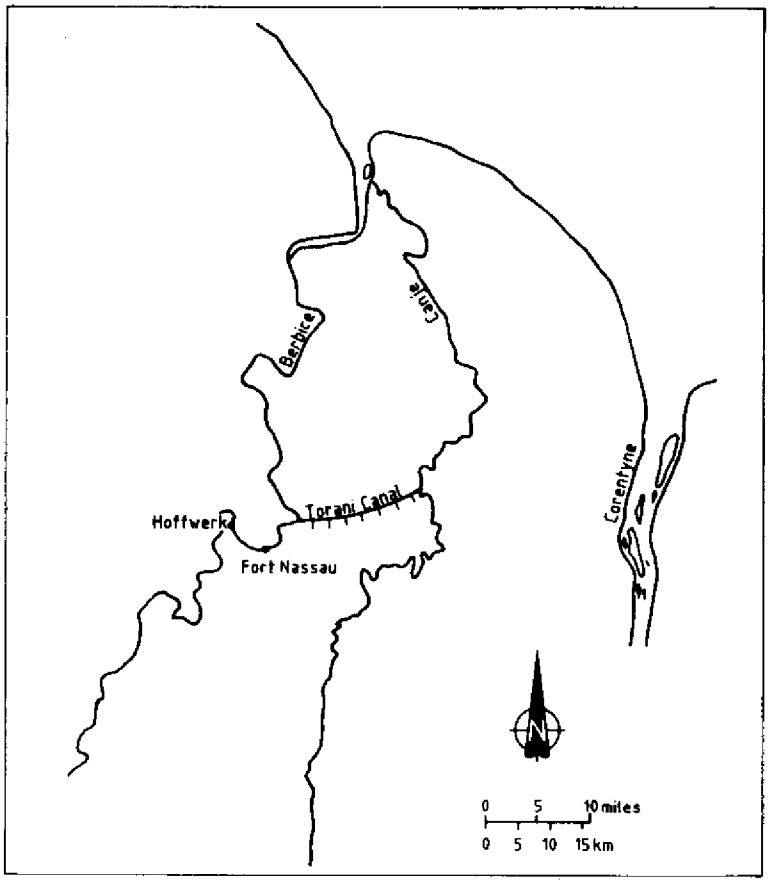

Fig. 2 - Berbice and Canje river systems

4. HR NUMERICAL MODEL

The HR tidal model works on a one-dimensional implicit numerical scheme and is based on the principles of conservation of mass, or volume and momentum [9]. To apply these physical laws in the model, the channel is divided into a series of storage (continuity) elements which overlap a similar set of flow (conveyance) elements. The schematised elemental representation of the tidal reach between Hoffwerk and Fort Nassau, selected for the model is shown in Figure 3. Flow through storage (continuity) elements and flow (conveyance) elements is governed by the following partial differential equations:

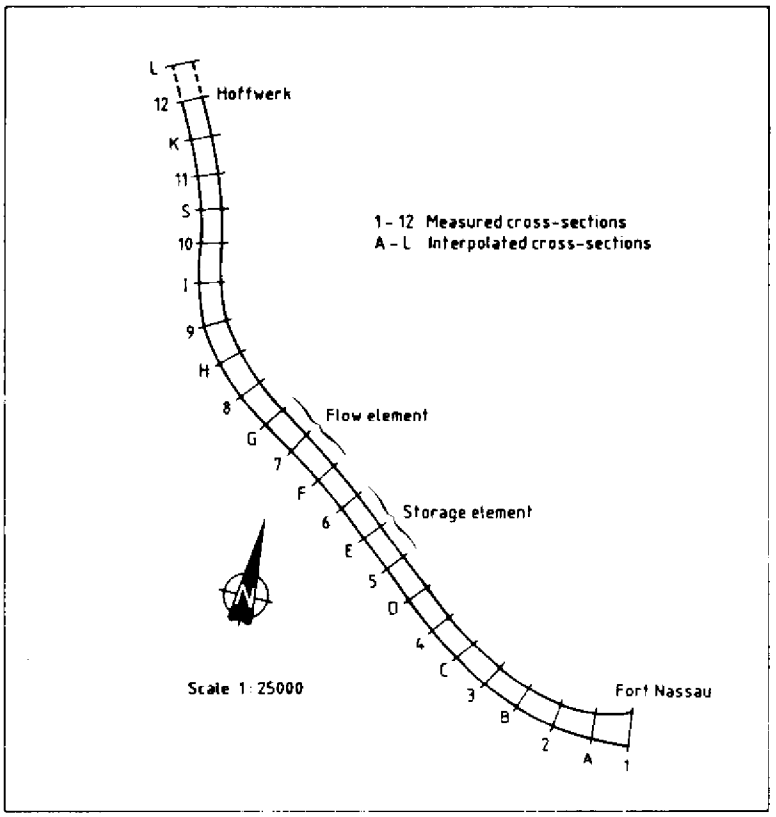

Fig. 3 - Channel reach showing cross-sections and schematised model elements

Storage element,

$$\frac{w\partial h}{\partial t} + \frac{\partial Q}{\partial x} = 0 \qquad (1)$$

Flow element,

$$\frac{\partial Q}{\partial t} + gA\frac{\partial h}{\partial x} + \xi'\left(\frac{\bar{u}\partial Q}{\partial x} + \frac{Q\partial \bar{u}}{\partial x}\right) + \frac{\xi f|Q|Q}{8RA} \qquad (2)$$

where

w = water surface width (m)
h = water surface height (m)
Q = discharge into the element (m^3/s)

A = cross-sectional area of the element (m^2)
R = hydraulic radius (m)
f = friction factor
ξ ; ξ' = correction coefficients
$\bar{u}$ = area mean velocity (m/s)

In the model these equations are solved by means of an implicit finite difference scheme. Channel geometry was represented by assuming that individual element boundaries have equivalent trapezoidal flow cross-sections of variable depth, width and side slope. Tidal stage records obtained from the automatic gauges formed the landward and seaward boundary conditions necessary for solving the equations; model output being instantaneous tidal discharges at the upstream and downstream boundaries. A detailed description of the model together is given by Amphlett & Makin [10]. To obtain the uni-directional fresh water flow component, a separate computed program was written which simply integrates the computed instantaneous tidal discharge results.

5. MODEL APPLICABILITY

Model applicability depends initially on how closely the numerical model will replicate field conditions. Reasonable correspondence between computed and observed tidal discharge measurements can be achieved with limited optimisation of gauge data and friction parameters. Exact correspondence can never be expected as the final choice of model parameters is a compromise to obtain an acceptable fit over the range of measured flows.

The magnitude of the errors depends on how accurately the numerical model predicts tidal discharges for conditions other than those used for verification.

Within the range of flows tested (i.e. observed) errors were within $\pm$ 40%. Even if exact replication of tidal discharge is achieved an error in computed fresh water flow is still inherent due to the period over which the tidal results are integrated. As described below a $\pm$ 10% error in computed flows is possible for flows down to 150 m^3/s when a 24.8 hour integration period is used.

6. VERIFICATION OF THE HR MODEL

Parameters that can be optimised in the model are water level recorder (gauge) reference levels, roughness, channel geometry and lateral velocity distribution correction coefficients. Gauge datum and channel geometry should not require optimisation if they have been accurately measured in the field. However the stage computational method was found to be very sensitive to gauge datum, and because of likely errors in levelling in difficult terrain gauge datum points were included in the optimisation procedure. With the lateral velocity distribution correction coefficients being taken as a unit, model parameter optimisation was thus confined to roughness 'f' and gauge data. For the optimisation exercise, the five periods when synchronous stage records and instantaneous tidal discharge measurements were available were used. The synchronous stage records were at 15 minute intervals but to overcome some instability in computed discharges in the model the computational

timestep had to be reduced to 1 minute; a simple linear interpolation being applied to obtain estimated stage values between those measured. Furthermore, it was assumed that roughness was constant in all model elements along the reach. The best fit with measured data was found with a roughness of 0.05 (equivalent to a Manning's 'n' of 0.025). Although measured gauge datum levels were supposedly the same for both Hoffwerk and Fort Nassau it was necessary to adjust the datum at Hoffwerk by +0.017 m. This sensitivity to gauge datum is shown in Figure 4, where observed and computed tidal discharges are compared using the measured gauge and the datum at Hoffwerk adjusted for one of the available dates. A similar result was obtained for the four other time periods of tidal discharge measurements; in all cases a consistent correction having to be made to the Hoffwerk datum. This figure shows the very good fit to the measured tidal discharge records that was obtained with the optimised HR model.

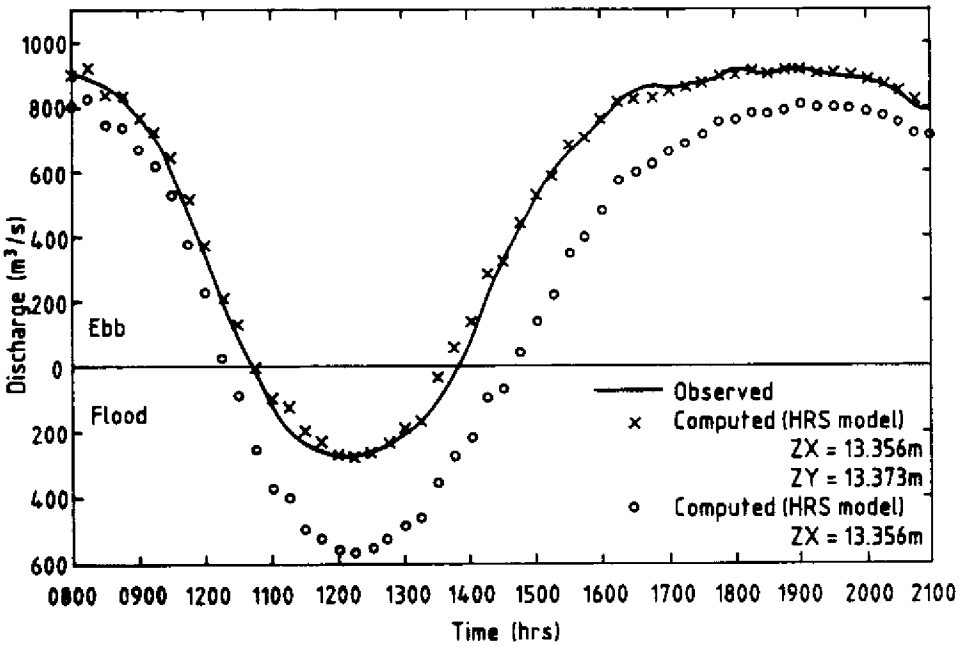

Fig. 4 - Observed and computed discharge at Hoffwerk for 11 August 1974.

7. FIELD STUDY

Fresh water flows for the five periods of measurements varied between 157 m³/s and 462 m³/s. However, the problem in the Berbice estuary is whether flows of the order of 30 m³/s at the Torani canal intake can be relied on throughout the year. To investigate whether the HR model would work as well for lower flows, an intensive field survey was undertaken in October 1981, timed to coincide with the period of expected dry season low flow.

Over a 15 day period beginning in October 1981, tidal velocity measurements were taken spanning a spring to neap cycle. Twenty six hour continuous velocity measurements at 9 verticals at Hoffwerk were taken every 2 days. It was unfortunate that during the survey period the Fort Nassau stage recorder malfunctioned and records from this were unusable. However, gauge boards had been installed as a back-up and manually read every 15 to 30 minutes during the survey period. The HR model, using these gauge board records again gave very good correspondence between computed and observed instantaneous tidal discharges. The objective of the October 1981 survey, that of obtaining proving data for flows below that observed between 1972 and 1976, was unfortunately not achieved; the lowest recorded flow during the period being 164.2 m³/s compared to 157.3 m³/s in October 1972.

8. FRESH WATER FLOWS

To obtain the uni-directional fresh water flow component the instantaneous tidal discharge results have to be integrated over a full tidal period, or some multiple of it. The likely error in computed fresh water discharge using either one tidal period (12.4 hours) or two tidal periods (24.8 hours) was investigated. The results of this analysis are shown in Figure 5. It can be seen that there is two large quantities, namely flood and ebb discharge, in order to obtain the much smaller uni-directional fresh water flow component. Errors associated with the a significant improvement in computed fresh water flow using the double tide integration period although errors increase rapidly as the fresh water flow component decreases. For example, with the 24.8 hour integration period the error increases from ± 10% at a fresh water flow of 150 m³/s to ± 30% at a fresh water flow of 50 m³/s. Errors, due solely to the tidal integration period, are however implicit in both computations for measured and computed flows.

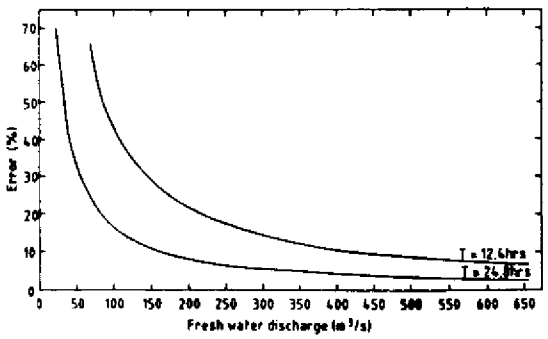

Fig. 5 - Error bounds associated with tidal integration period

Table 1 - Comparison between measured and computed fresh water flows

Date	Mean measured flow Hoffwerk (m^3/s)	Mean computed flow Hoffwerk (m^3/s)	Mean computed flow Fort Nassau (m^3/s)
14.10.72	157.3	102.5 (-35)	-
30.06.73	305.5	333.8 (+9)	-
10.08.74	462.5	480.3 (+28)	-
11.08.74	268.6	276.3 (+3)	-
31.07.76	452.5	623.4 (+38)	-
15/16.10.81	275.1	308.5 (+12)	308.5
17/18.10.81	266.6	206.7 (-22)	207.4
19/20.10.81	259.5	231.5 (-11)	231.5
21/22.10.81	244.2	247.9 (+2)	246.6
23/24.10.81	206.6	150.5 (-27)	149.1
25/26.10.81	164.2	119.2 (-27)	115.7
27/28.10.81	214.3	120.9 (-43)	116.5
29/30.10.81	238.2	167.1 (-30)	166.4

Figures in ( ) are percentage errors in mean computed flows

To determine fresh water flows for the model proving data, observed and computed tidal discharge results were integrated over a 24.8 hour period for the October 1981 survey and over a 12.4 hour period for dates prior to this when measurements only spanned one full tidal period. The results, given as mean measured flow and mean computed flow at Hoffwerk, are given in the table. For the model proving data fresh water flow estimated for computed instantaneous tidal discharges were within $\pm$ 40% of measured values. The errors depend on the magnitude of the measured flow. The numerical model tends to progressively overestimate fresh water flows for flows greater than 275 m^3/s and to underestimate below this value.

9. CONCLUSIONS

The numerical model reproduces tolerable well observed instantaneous tidal discharge measurements that were taken in the tidal reach of the Berbice River. However, use of the stage computational method is dependent on the evaluation of methods that depends not only on the model's ability to replicate instantaneous tidal discharges but also on the tidal integration period used to evaluate the food and ebb flow volumes. Analysis of available field data for the Berbice River has shown that fresh water flow estimates are very sensitive to the integration period used and that the errors associated with a particular integration period increase significantly as the fresh water flow component decreases.

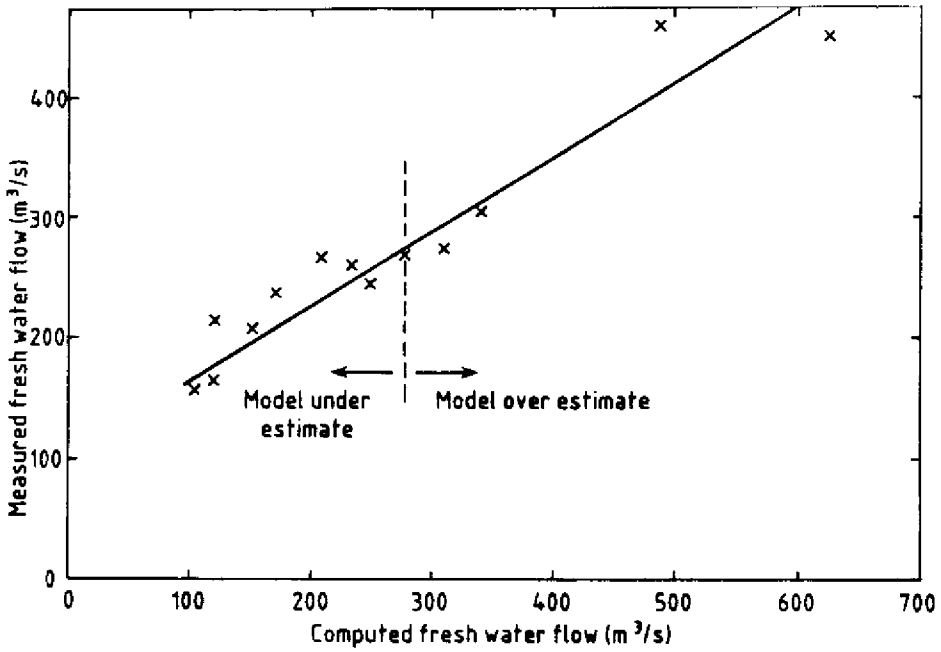

Fig. 6 - Relationship between measured and computed fresh water flows for Hoffwerk

The errors discussed do not negate the usefulness of the method as a means of estimating fresh water flows. In the absence of any other suitable technique for measuring river flow at sites where tidal reversal of flow occurs, such a model will at least give a reasonable indication of river flow statistics provided that the limitations of the method are appreciated and account of this taken in interpreting results. The linear relationship between measured and mean computed flows can be used to correct model results at least within the range of proving data.

This paper has used a case study from the Berbice River, Guyana to demonstrate a technique that the authors believe could be used on many of the sub-basins of the Amazon River. The application of this model to use water level information (which is often the only data that is collected) in assessing, planning and controlling water resources in the lower reaches of large tidally affected rivers is recommended as a practical technique.

10. ACKNOWLEDGEMENT

This paper has been prepared in the Overseas Development Unit of Hydraulics Research using research funds provided by the British Overseas Development Administration.

11. REFERENCES

[1] Sanmuganathan, K. and Waite, P. J. Analysis of the discharge measurements carried out at Bansang, The Gambia, during March 1974, Hydraulics Research, United Kingdom, Report No. OD3, July 1975.

[2] Gibbs, R.J. Circulation in the Amazon River estuary and adjacent Atlantic Ocean, Journal of Marine Research, 28(2), 1970.

[3] Sanmuganathan, K. One dimensional analysis of salinity intrusion in estuaries, Hydraulics Research, United Kingdom, Report No. OD2, April 1977.

[4] Waite, P. J. Rio Guayas, Ecuador. Field data for estuary salinity study, Hydraulics Research, United Kingdom, Report No. OD8, September 1976.

[5] Waite, P. J. Abary River, Guyana. Salinity prediction model, Hydraulics Research, United Kingdom, Report No. OD20, March 1979.

[6] Hydraulics Research, Juantan River, Malaysia. Prediction of salinity intrusion, Report No. EX814, April 1978.

[7] Waite, P. J. and Amphlett, M. B. Matara water supply scheme, Sri Lanka salt water intrusion in the Nilwala Ganga. Hydraulics Research, United Kingdom, Report No. OD34, March 1981.

[8] Davidson, J. Computation of discharge in tidal reaches. United States Department of the Interior Geological Survey. Book 1, Chapter 2, 1964.

[9] Maskell, J. M. A one-dimensional implicit numerical tidal model incorporating species analysis, Hydraulics Research, United Kingdom, Report No. INT 145, June 1976.

[10] Amphlett, M. B. and Makin, I. W. Estimation of fresh water flow in the tidal reach of the Berbice River, Guyana. Hydraulics Research, United Kingdom, Report No. OD43, June 1982.

AN OUTLINE OF HYDROSEDIMENTOLOGICAL ZONES IN THE BRAZILIAN AMAZON BASIN

Marc Pierre Bordas *

ABSTRACT

Between 1986 and 1988, ELETROBRAS (Brazilian Power Authority) sponsored a preliminary study throughout the whole of Brazil of the liability to erosion and sedimentation risk. For this purpose, all data on solid discharge were examined from rivers within the responsibility of 23 private organizations and government agencies, and spatial variability of parameters in the Universal Soil Loss Equation (USLE) was assessed. Data were also collected on problems caused by sediment in the operation of hydraulic structures and in the maintenance of rivers, canals and highways, since these data could confirm the risk zones defined by analysis of solid discharges and soil erosion. The results led to the identification of 19 homogeneous regions of hydrosedimentological behaviour, of which 8 lie in the Amazon basin and also, to elucidate the sedimentological regime of the Amazon river.

INTRODUCTION

In 1985, Centrais Elétricas Brasileiras S. A. (ELETROBRAS) asked the Institute of Hydraulic Research (IPH) at the Federal University of Rio Grande do Sul (UFRGS) to prepare a preliminary hydrosedimentological diagnosis of the main Brazilian rivers. ELETROBRAS was already concerned as to the possible effects of intensified agriculture and land use on the life of hydropower reservoirs and, above all, at the sedimentological impacts which might be caused to or by new small and medium-sized dams. Therefore, tendencies to erosion and sedimentation risks in water were to be assessed for the whole of Brazil. The results for the Brazilian Amazon basin are presented here.

METHODOLOGY

1. Fundamentals

The methodology used in preparing this zoning is based on the premise that river regimes governed by the same factors generally present similar hydrosedimentological behaviours, characterizes by typical hydrosedimentological cycles (some examples of which are shown in Figure 1), or at

* *Full Professor — Institute of Hydraulic Research (IPH) — Federal University of Rio Grande do Sul, Porto Alegre, Brazil*

least by similar solid loads expressed by a liquid flow/solid discharge (relationship ($\bar{G} = a\bar{Q}^b$ for example) or, ultimately, by an annual mean concentration of solids (AMC) or specific sediment yield ($\bar{GM}$) in similar-sized basins. Figure 1a illustrates the different ways of describing a hydrosedimentological cycle and shows the loss of representativeness associated with each of them. Among the most important factors influencing the hydrosedimentological regime of a river are annual rainfall distribution, relief, soil distribution and land cover, together with the two anthropic factors which usually have opposite effects: land cover changes and building dams across river beds.

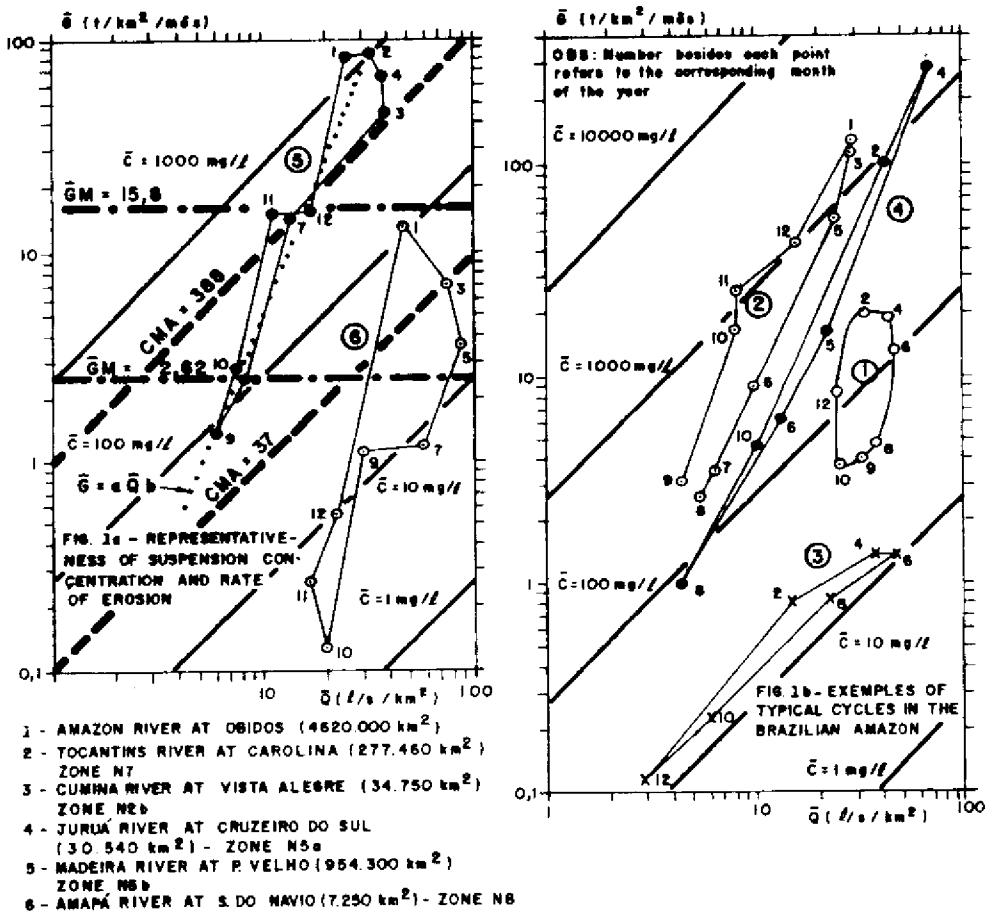

Fig. 1 — Description of the hydrosedimentological cycle

2. Strategy

For zoning purposes an attempt was made to group rivers with the same hydrosedimentological characteristics and to identify associations of control factors which might explain and distinguish these groups. The strategy included five steps:

2.1 Description of the hydrosedimentological cycles by monitoring solid discharges at the river gauging stations;

2.2 Zoning of four of the five factors which govern sediment production at interfluves: rain erosiveness, soil erodibility, relief and plant cover;

2.3 Survey of problems involving sediment (silting up of dams and rivers, unusual water or road maintenance costs, frequency of dredging, ...);

2.4 Comparison of the zoning resulting from 2.1 and 2.2;

2.5 Use of the information (2.3) to solve doubts arising during the foregoing comparison (2.4).

This strategy was initially tested for validity using the annual mean concentration of suspension to describe the hydrosedimentological cycles (Bordas *et al*, 1987). The results obtained were surprisingly favourable considering the quality of the data used and simplifications required: the first two zonings (2.1) and (2.2) were almost completely superposable, and the survey (2.3) helped corroborate this result instead of raising the doubts they were intended to solve. Therefore it was decided to begin zoning, based on the other sedimentological data.

3. Information used

3.1 Hydrosedimentological cycle — Information on solid discharge in rivers was identified in 23 Brazilian agencies, only three of which had data about the Amazon basin. Of the 472 sediment measurement stations surveyed, 83 were located in the Amazon basin and corresponded to 70 stations. (One station may have equipment operated by different agencies). Table 1 provides essential information on the functioning of and data collected by this station network, and it can be compared to the Eastern region (Basins of rivers which flow out between the mouths of the Paraíba do Sul river and the Amazon) and South (river Prata, Paraíba do Sul and other rivers south of the latter).

This Table summarizes the difficulties encountered in following the hydrosedimentological cycles and even in computing specific sediment yield: scarce bed load and grain size data, lack of systematic streamflow and solid discharge measurements.

Table 1 — Brazilian sediment measurement network (September 1986)

Region			North	East	South	Total
Structure	N° of stations surveyed		70	102	269	441
	Stations operating in 1986		54	62	148	264
	Density (p/100.000 km^2)		1,43	5,3	15,8	5,2
Type of data collected	Unit.: N° of stations	Suspension concentration	61	91	201	353
		Liquid flow	46	85	161	292
		Bed load	17	1	19	37
		Bottom grain size	15	64	43	122
		Suspension grain size	43	82	14	139
Functioning	Sampling frequency	Daily	0	21	49	70
		Sporadic	70	91	210	371
	Period of operation	1 year	7	2	17	26
		1-4 years	16	27	59	102
		5-8 years	25	33	89	147
		9-12 years	19	25	77	121
		> 12 years	0	16	11	27

A substantial amount of data was raw and had never been analyzed, much less tested for consistency. They were used all the same, since it was a comparative study, and it was likely that the same errors and inadequacies would be repeated in almost every case. Two kinds of hydrosedimentological information could be obtained from these data:

a) Annual mean concentration (AMC) of suspended material at 59 sites (see Figure 4). The values used are obtained from an average of 12 monthly concentrations, computed from the means of all concentration measurements performed during the same month.

b) Specific annual suspended sediment yield ($\bar{G}$) taken as the annual mean weight of suspended sediment, produced or stored per unit basin surface during one year.

This yield was found in 51 basins, and sediment budgets were calculated according to the methodology described by Bordas *et al.* (1988). The basic aspects of the methodology are:

— Annual yield is obtained from the sum of monthly measured yields, this is done only when they are available for at least 5 out of 12 months of the year. Therefore stations which had data for 4 months only were not included.

— The monthly yields are a result of the difference in the weights of sediments entering and leaving the basin during that month, and they are computed from the mean daily concentration of suspension averaging the liquid flows measured during the whole period of sampling. When this flow is unknown, mean daily flow at the station is used.

— Mean daily concentration is the average of suspension concentrations obtained using all the sporadic measurements performed during the month concerned, since the station began to operate. When stations have daily sampling, control measurements made by the hydrometry staff are used.

Therefore, no preliminary selection was done. The only critical study of the data was performed when the yield value was abnormal or did not make sense. In these cases data compatibility, number of samplings used in calculation, and flood discharges at a station were examined...

3.2 Interfluve erosion — The quality of information used to zone the four main factors governing sediment production in interfluves is variable. The circumstances under which the study was carried out made it impossible to gather all the initially intended data. However the distribution of these factors could be outlined (Figures 2 and 3).

a) Soil erodibility (Figure 2). Thanks to the cooperation of SNLCS/EMBRAPA and ORSTOM, Brazilian soils were grouped in three large erodibility classes: weak $K < 0,15$; average $0,15 < K < 0,30$ and high $K < 0,30$ plus a few other special associations found in the Amazon Basin (K is the Wischmeier erodibility factor).

b) Relief (Figure 2). Since there are no clinometric maps of the Amazon basin, relief zoning was based on hypsometric maps.

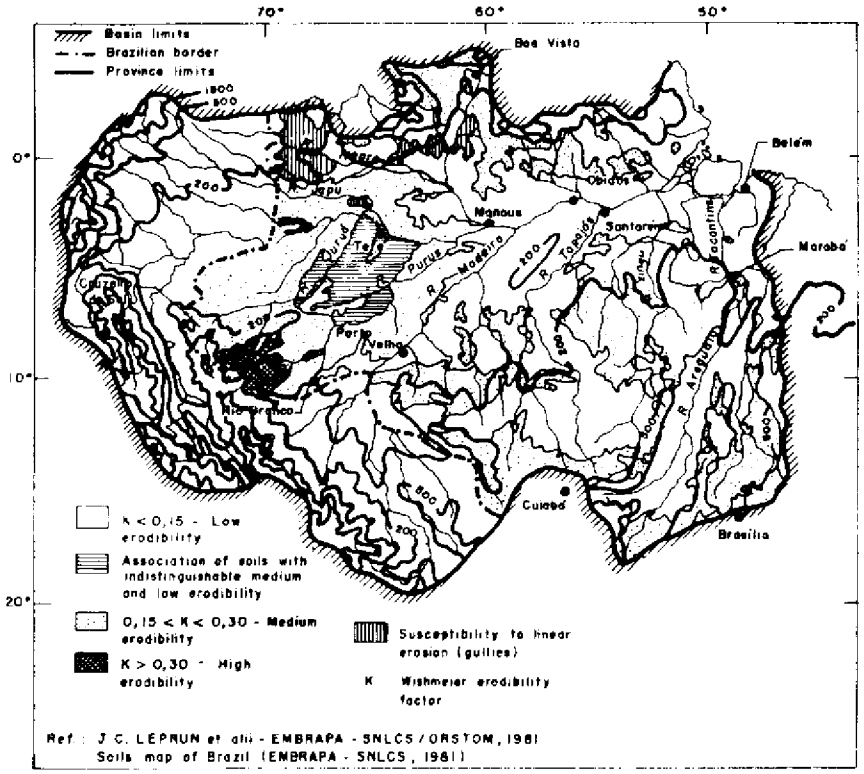

Fig. 2 - Zoning of erosion factors: a) Soils; b) Relief.

c) Rain erosivity (Figure 3). Information on the Wischmeier factor R of erosivity collected by SNLCS and ORSTOM indicated only that it was higher than 1000 $t.ha^{-1}.mm.h^{-1}$ throughout the Amazon basin. To differentiate this information within the basin, annual isohyets were used. They had been published by DNAEE (1984) based on WMO/UNESCO studies performed using data of the 1931/1960 period.

d) Land cover (Figure 3). Since there is no practical possibility of updating the cover surveyed by RADAMBRASIL to the time of hydrosedimentological monitoring, it was chosen to use plant cover maps.

3.3 Miscellaneous — During and after the research proper, data from several studies on Amazon sediment yield and transport were examined, compared and sometimes included (Ref. 5 to 10).

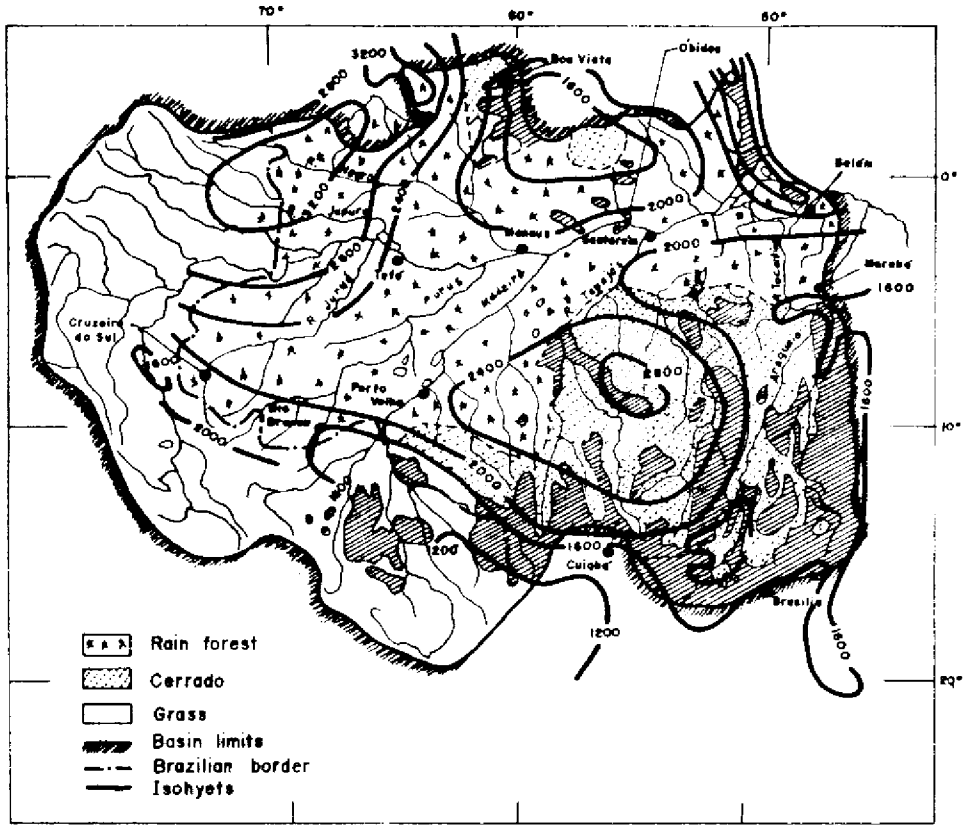

Fig. 3 - Zoning of erosion factors: a) Rainfall; b) Land cover.

4. Outline of hydrosedimentological zoning

A new analysis of zoning previously performed using mean annual concentrations of suspension, which took into account values of annual specific sediment yield and erosion factor distribution in interfluves, indicates that there are 8 homogeneous sedimentological behaviour zones in the Brazilian Amazon basin, to which should be added the Amazon river channel whose hydrosedimentological behaviour differs from the others. According to the situation at the beginning of the 1980's (most solid load data is from 1977-1985) it is possible to distinguish nine 'hydrosedimentological provinces' by mean values of specific fine sediment yield (suspension $\widehat{G}$) and their annual mean concentration (AMC) in rivers. A more precise description based on a liquid flow/solid discharge ratio or on the shape of the hydrosedimentological cycle could not be obtained due to lack of information, although it was possible to indicate the feature of these parameters general outline.

Before describing these provinces it should be reminded that the values used in describing hydrosedimentology are merely indicative: suspension concentrations are subject to broad local and temporal variations and the specific yields are usually underestimated, due to the method used to determine them. Therefore, these values cannot be utilized in solving specific problems.

N1 — Amazon River — It is not precisely a hydrosedimentological province as defined in this study. Because of its size and type of sediment problems it may not be included among the other zones. The AMC ranges from 260 to 100 mg/l, from upstream to downstream, around a mean value of 220 mg/l. Specific yield when entering Brazil is approximately 470 t/km^2/year, but the most important feature of this zone is that it is a deposition area throughout this long river reach. The only budget study which could be carried out indicates that deposition would occur at a rate of 180 t/km^2/year between Obidos and the border. These data agree with those presented by Gibbs (1967) and Meade *et al*, (1979): the specific yields of 307 to 251 t/km^2/year in the Uyacali and Marañón river basins indicated by the former do not disagree with the 470 t/km^2/year recorded here, nor with the 489 and 527 t/km^2/year presented by Guyot *et al*. (1988) for the Madre de Dios and Beni river basins, respectively. The concentrations found by all these authors also agree with those of WMO-UNDP (1980), indicating an average of 300 mg/l at the Brazilian border and a decrease along the river until Obidos.

N2 — Northern Amazon — This zone includes the headwaters of the Branco river and most of the other tributaries on the left bank of the Amazon between the Branco and Jari rivers. Annual precipitations in the region range between 1500 and 2000 mm and are higher in the western part; the region is covered mainly by forest but large areas are occupied by 'cerrado' or grasses. Two sub-regions can be distinguished mostly based on soil erodibility:

- N2a Rougher relief than the other one, soils with more homogeneously mean erodibility: it includes the basins of the Branco, Uatumá and Mapuera rivers, which suffer more anthropic action. MAC is 65 mg/l and specific degradation of 50 t/km^2/year for basins around 20,000 km^2.
- N2b All other basins in the western part of the region. The soils are more heterogeneously erodible, human interference appears negligible, therefore AMC are lower than 15 t/km^2/year and a degradation of 4,5 t/km^2/year occurs for basins with 30,000 km^2.

This subdivision is apparently confirmed by different types of sedimentological cycle which were traced for this region.

N3 — Central Amazon — Vast low-lying zone (< 100 m) completely covered by rain forest, with high pluviosity (annual average 2000 mm): it may be divided into two sub-regions characterized by different soil erodibility;

- N3a Low erodibility — in the lower basins of the Madeira and Tapajós rivers, and other less important tributaries on both banks of the Amazon river downstream from Manaus.
- N3b Low or medium erodibility, but subject to erosion (gully formation) in the Negro river basin.

The CMA is the same in both sub-regions (15 mg/l). The few sediment yield data indicate rates of 23 t/km^2/year for the basins of medium-sized basins of Madeira and Negro river tributaries (1000 to 50000 km^2) and 2 t/km^2/year for similar plains rivers. There are indications that the rates for the larger basins lying on the plain are even lower (0,15 for Negro river) which might be explained by the fines that are retained on the flood plains, as inferred by the sediment budget of the middle basin of the Negro river. These values are compatible with those presented by other authors, especially the value of specific yield for the joint Negro/Branco rivers basins (10 t/km^2/year (Gibbs)), which corresponds approximately to a 4 t/km^2/year rate for the lower Negro river basin.

N4 — Western Amazon — This region covers the area between the Amazon and Madeira rivers, but the upper basins of the river systems of Juruá and Purús are excluded. Heavy rainfall (> 2000 m), mean soil erodibility, flat relief rain forest which cover them are typical of the region. The few sediment measurement stations located there indicate a AMC around 150 mg/l and a specific degradation of 100 t/km^2/year in a 125,000 km^2 basin. The two sedimentological stations in the region indicate AMC values and production rates similar to those pointed out by Gibbs, except for the Juruá river, where the highest rates may be explained by basin shape and heavy erosion at the headwaters. Mean values 70 mg/l and 60 t/km^2/year appear adequate to estimate AMC and mean rate of erosion at a first approach.

N5 — Southwest Amazon — The area is formed by the Madeira river basin upstream from Porto Velho and by the upper basins of the Purús and Juruá rivers. It is the site of one of the highest rates of erosion in Brazil. Rainfall is above 2000 mm/year and the topography does not vary much, although higher in the Madeira basin (800 m instead of 500 m). Forest covers the region but the intense deforestation in Rondônia and greater soil erodibility in the state of Acre led to distinguishing two sub-regions:

- N5a Acre — these rivers have a higher AMC (500 mg/l) and specific degradation reaches 250 t/km^2/year in a 30.000 km^2 basin.
- N5b Rondônia — (Precisely the Madeira river basin). With a widely varying AMC (25 to 400 mg/l) around an average of 170 mg/l, and erosion rates which behave similarly 14 to 1800 t/km^2/year, for an average of 455 t/km^2/year. The latter rate (1800 t/km^2/year in a 54.000 km^2 basin) is the highest found in Brazil and almost equals the rates recorded by Guyot *et al.* in similar sized basins in the Bolivian Andes.

These values are practically identical to those presented by Guyot *et al.* (1988) in their study of the hydrosedimentology of the Madeira river on the Bolivian side (AMC = 363 mg/l; $\widehat{G}$ = 527 t/km^2/year). They are also compatible with the data of Gibbs and Meade (AMC = 330 mg/l; $\widehat{G}$ = 290 t/km^2/year).

This sub-division is apparently confirmed by the differences between hydrosedimentological cycles found in this case (see Fig. 1, examples 4 and 5).

As in the Northern Amazon (N2), it is to be expected that additional complementary data will show that these sub-regions should be considered distinct hydrosedimentological provinces.

N6 — Tapajós — This zone, formed mainly by the middle basin of the Tapajós river, also includes the upper basin of the Xingú river. Pluviosity is high (2000/2500 mm/year), soil erodibility low and the relief is hilly. 'Cerrado' covers the region. There are practically no sediment measurement stations. The two found indicate a AMC of 20 mg/l and specific sediment yield about 10 t/km^2/year, in 15,000 km^2 basins. This corresponds to an average of 4 t/km^2/year for the whole basin (Gibbs indicates 1,2 t/km^2/year).

N7 — Eastern Amazon — This area consists almost completely of the Xingu and Araguaia river basins and the middle/lower basin of the Tocantins river. The pluviosity is lower than in the other areas mentioned previously (1500/2000 mm/year); soil erodibility is medium or low; relief is hilly and land is covered by 'cerrado'. The remarkably homogeneous AMC is around 65 mg/l and mean specific degradation is 65 t/km^2/year, for 120,000 km^2 basin. Sediment budget surveys indicate deposition at the points at which the Xingu and Tocantins rivers enter the Amazon plain.

N8 — Amazon Coast — This region is formed by the basis of the rivers which flow into the Amazon river estuary or enter the ocean north of the Amazon mouth; it includes the island of Marajó. High pluviosity (> 2000 mm/year), low soil erodibility, flat relief and rain florest are typical features of this region. The AMC is 27 mg/l and the specific sediment yield 16 t/km^2/year for 26.000 km^2 basins (Gibbs gives a rate of 7 t/km^2/year for the Araguari basin which has a 45,200 km^2 area).

00 — Backbone or Southern Headwaters — This region is identified in a different manner, since it also extends into river basins of the East and South hydrographic regions. In the Amazon basin it includes the headwaters of the Tapajós, Araguaia and Tocantins rivers. It coincides approximately with the 1000 erodibility line and is a transition zone with a marked erosivity gradient and mean annual rainfall around 1500 mm. The soils generally present a mean erodibility (0,15 > K > 0,30), altitude ranges from 200 to 800 m and the plant cover is mainly 'cerrado'. The average AMC is 260 mg/l. Mean degradation (specific sediment yield) was estimated at 146 t/km^2/year, for medium-sized basin of 17.000 km^2.

RESULTS

The limits of the hydrosedimentological provinces identified are outlined in Figure 4, and their main features are covered again in Table 2.

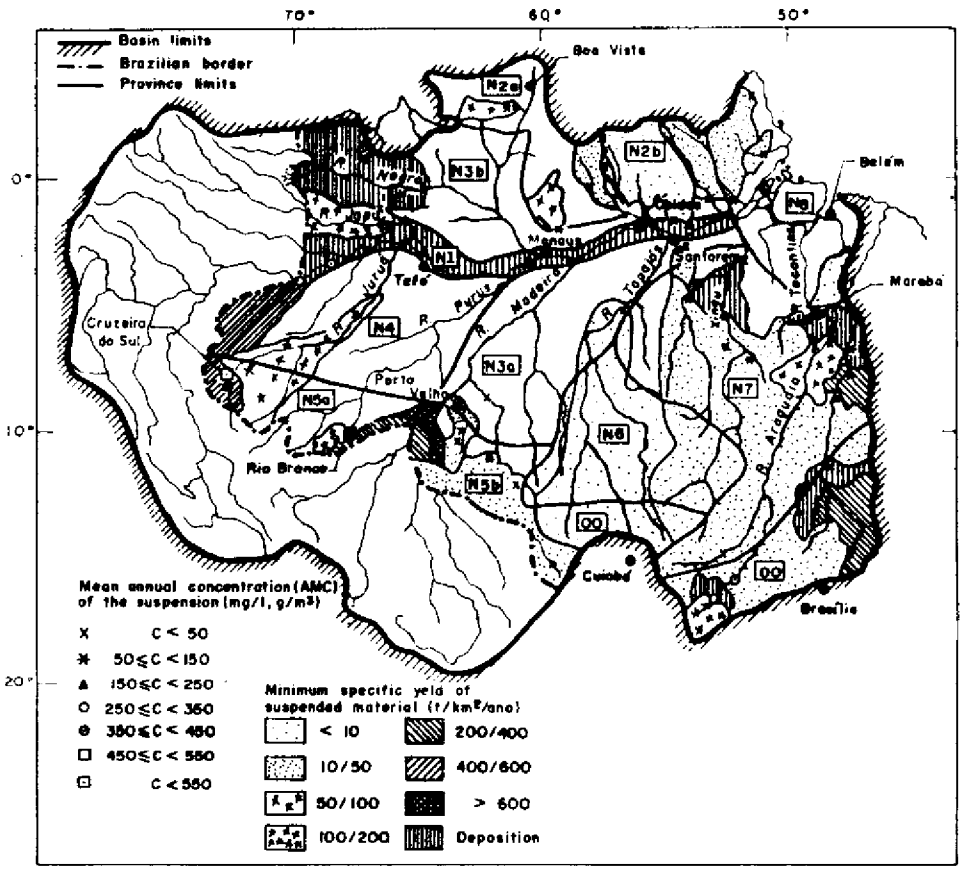

Fig. 4 — Outline of hydrosedimentological zoning of the Brazilian Amazon basins (Hydrosedimentological provinces)

In Table 2 is included the specific suspended sediment yield extrapolated to a 15.000 km^2 basin. This parameter was introduced to help rank risks or erosion in the different regions. Its values corresponds to the yield averages calculated for 15000 km^2 with the help (for lack of a better instrument) of the formula $\widehat{G} = K A^{0.24}$ used in the United States, from the solid discharges measured at all sediment measurement stations in the region under study. (In this formula, A represents the basin area and K a typical coefficient). The 15.000 km^2 basin was used as a reference, since it was the only on e which occurred with the same frequency (20%) in all three large hydrographic regions into which the study has divided Brazil. Thus, predisposition to erosion/sedimentation risks in the Amazon basin may be compared to those in the rest of the country.

Table 2 — Main features of hydrosedimentological provinces of Brazilian Amazon basin

Table 2 — Main features of hydrosedimentological provinces of Brazilian Amazon basins

						Mean concentration of suspended material (mg/l)			Specific production of suspended material (t/km²/yea)	
Ref.	REGION	Rainfall *	Relief **	Soil erodibility	Plant Cover		During high flow	During low flow	Average of basins in region $\hat{G}_M$	Average of projections for 15000 km² basins $\hat{G}_M$
N1	Amazon River Bed	NA	NA	NA	NA	220	324	112	$G_M < 0$ (depositions)	NA
	Northern Amazon									
N2a	Roraima	1	1	2	1/2	65	94	46	50	50
N2b	Guianas Shield	3	2	2/3	1/2	15	20	13	4,5	7,5
	Central Amazon									
N3a	Amazon Plain	2	3	3	3	15	25	8	2,5	2
N3b	Negro River	1	3	3***	3	15	15	14	-	23
N4	Western Amazon	1	3	2	3	70	107	58	60	100
	Southwest Amazon									
N5a	Acre	3	2	1	3	500	830	140	250	350
N5b	Rondônia	3	1	2	1/2	170	340	61	455	245
N6	Tapajós	1	2	3	1/2	20	23	11	-8	-10
N7	Eastern Amazon	3	2	2/3	1	65	78	34	65	50
N8	Amazon Coast	1	3	3	3	27	28	17	16	17
00	Backbone	3	1	2	1	260	380	150	146	145

* The degree of susceptibility is evaluated of a decreasing scale of 1 to 3.

** Preliminary appreciation subject to review after more appropriate data is collected.

*** Risk of gullying.

Table 3 — Predisposition to sediment risks in Brazil at the beginning of the eighties

Class of risk	Erosion rate $\hat{G}_R$ (t/km²/year) *					Hydrosedimentological province
Erosion I			$\hat{G}_R$	>	300	N5a ; N5b
Erosion II	150	<	G_R	<	300	Minas Gerais (E6)
Erosion III	100	<	G_R	<	150	00 ; N4
Erosion IV	75	<	G_R	<	100	South Atlantic Façade (S1) Argentine border (S4)
Erosion V	50	<	G_R	<	75	N2a ; N7 ; E3 ; E5
Erosion VI	25	<	G_R	<	50	N3b ; S2 ; S5
Erosion VII	5	<	G_R	<	25	N2b ; N6 ; N8 ; E2
Erosion VIII	0	<	G_R	<	5	N3a
Sedimentation IX			G_R	<	0	N1 ; Pantanal

* Rate of erosion (suspension only) for river basins between 2500 and 30000 km²

** The letter E identifies a province in the East and S in the South. Further details in Bordas *et al.* (1988).

CONCLUSIONS AND RECOMMENDATIONS

Nine classes of sediment risks were tentatively defined for all of Brazil, based on the specific suspended sediment yield. In this classification (Table 3), some of the hydrosedimentological provinces of the Amazon basin presented a very high predisposition both to risk of erosion (N5: Acre, Rondônia) and sediment deposition (N1 Amazon flood plain bed) in which the mean deposition rate 180 t/km²/year appears to be higher than that of the Pantanal (140 t/km²/year maximum, upstream from Cuiabá)). Risks are ranked in Table 3, but it may be generally stated that most of the Amazon basin did not present any special risks in the situation, as observed around 1980.

The precision of this classification and the outline of the hydrosedimentological provinces still leave much to be desired. Solid discharges are systematically underestimated, and do not include solid bed load. Zoning of most erosion factors in the interfluves requires higher precision with frequent updates concerning plant cover. Finally, erodibility studies of soils under different plant cover management conditions should be encouraged, in order to establish maximum allowable critical erosion rates. Despite these deficiencies, the zoning described here is sufficiently precise to guide the implementation of a more appropriate sediment monitoring measurement network and to make an initial assessment of the risks and impacts of soil and water use in the Amazon basin.

ACKNOWLEDGEMENTS

This study could not have been done without the support of ELETROBRAS/SNCLS/EMBRAPA, ORSTOM, (particularly Dr. J. C. Leprun), and of the many organizations which allowed us to consult their files. We therefore wish to thank them all on this occasion.

BIBLIOGRAPHY

[1] Bordas, M. P.; Lanna, A. E.; Leprun, J. C. and Semmelmann, F. R. Diagnóstico preliminar dos riscos de assoreamento no Brasil. Anais do 7o. Simpósio Brasileiro de Hidrologia e Recursos Hídricos. Salvador. Nov. 1987, Vol. 3, pp. 223/235, 1987.

[2] Bordas, M. P.; Lanna, A. E. and Semmelmann, F. R. Evaluation des risques d'érosion et de sédimentation au Brésil à partir de bilans sédimentologiques rudimentaires. Proceedings of the Porto Alegre Symposium. IAHS Publication No. 174, pp. 359-368, 1988.

[3] Centrais Elétricas Brasileiras S.A. (ELETROBRAS). Diagnóstico das condições sedimentológicas dos principais rios brasileiros. Relatório final. IPH/UFGRS. 2 volumes. Maio de 1988.

[4] DNAEE. Inventário das estações fluviométricas, 1987.

[5] Gibbs, R. J. The Geochemistry of the Amazon River System: Part I. The factors that control the salinity and the composition and concentration of the suspended solids. Geol. Society of America Bulletin. V. 78 pp, 1203-1232, October 1967.

[6] Graham Jr., D. H. The Samuel dam: Land use soil erosion and sedimentation in Amazonia. M. A. Thesis — University of Florida, USA, 1986.

[7] Guyot, J. L.; Bourges, J.; Hoorelbecke, R.; Roche, M.A.; Calle, H.; Cortes, J.; Barragan Guzman, M. C. Exportation de matières en suspension des Andes vers l'Amazonie par la Beni, Bolivie. Sediment Budgets - Proceedings of the Porto Alegre Symposium, IAHS Publ., No. 174, December 1988.

[8] Meade, R. H.; Nordin Jr., C.F.; Curtis, W. F. Sediment loads in the Amazon river. Nature. Vol. 278, pp. 161-63, 1979.

[9] SNLCS/EMBRAPA. A situação da conservação do solo e da água no Brasil. Relatório interno. (Comunicação dos autores), 1988.

[10] WMO-UNDP. Hydrology and climatology of the Brazilian Amazon River: Sediment studies in the Brazilian Amazon River Basin. Technical Report 6 of project BRA/72/010. Geneva, 42 p., 1980.

WATER DEFICIT DISTRIBUTION IN THE BARRA DO GARÇAS REGION, MT

Antonio Eduardo Lanna *
Lawson F. S. Beltrame *
Elvio Giasson **

ABSTRACT

This study presents the irrigation needs of the region of Barra do Garças, located between the Araguaia and Coluene rivers which form the Xingu. In this area are 81,622 km² of soil appropriate for irrigation purposes (Beltrame et alii 1989). With these results it is possible to know the annual variability of irrigation requirements and confront them with the rainwater available, in mean values for the 1970-1986 period. It was found that, to the contrary of what is normally expected, considering that this is the Amazonian region,there is considerable need for irrigation particularly during the dry period, from May to October. Even during the other times of the year, with very intense rainfall, it is observed that the effective rainfall is often insufficient to satisfy agricultural demands. These results do not show water scarcity problems in the region, since water resources are relatively abundant in the water courses. However they do prove the need to use the river water, if it is intended to eliminate or attenuate the commonly observed agricultural deficits.

1. INTRODUCTION

This paper presents the partial results of a study which was carried out to assess the feasibility of introducing irrigation in the Amazonian region of Barra do Garças, state of Mato Grosso. The irrigation requirements were estimated using a daily crop water balance model, based on the precipitations observed in the town of Nova Xavantina, during 1976-1984. Two alternatives were adopted: one a mesophytic crop which presented a demand profile similar to maize or soy bean. Under these circumstances, sprinkler irrigation was considered the technique of choice. The other alternative was flood irrigated rice. It was found that, to the contrary of what is normally expected, considering that this is the Amazonian region, there is considerable need for irrigation, particularly during the dry period from May to October. Even during the other times of the year, with very intense rainfall, it is observed that effective rainfall is often insufficient, from the agricultural point of view, to satisfy demands. These results do not show water scarcity problems in the region, since water resources are relatively abundant in the water courses. However they do prove the need to use the river water, if it is intended to eliminate or attenuate the commonly observed agricultural deficits. The economic attractiveness of eliminating agricultural deficits is analyzed in Lanna et alii (2).

* *Associate Professors - Institute of Hydraulic Research - Federal University of Rio Grande do Sul, Brazil*

** *CNPq fellow - Institute of Hydraulic Research - Federal University of Rio Grande do Sul, Brazil*

2. ESTIMATION OF IRRIGATION REQUIREMENTS

The estimation of irrigation requirements in an agricultural plan is a water balance problem, in which the crop water needs are compared to the natural water availability. The crop water requirements depend on different factors including plant variety, stage of vegetative cycle, soil and climate. The water availability results naturally from rainfall. In case of agricultural deficits, i.e. when needs are greater than availability, irrigation should be used until they are cancelled or attenuated.

A mathematical water balance model, used under these conditions, involves simulation of hydrological processes and soil-water-plant-climate relationships. The hydrological process determines separation of rainfall into a portion which infiltrates and another which runs off on the surface, water movement, and evaporation from the soil. The soil-water-plant-climate relationship is a result of the plants' water needs and their capacity to extract water from the soil and release it by means of transpiration. It should be noted that, considering the present state of art, the mathematical simulation of the former process, although it can only be carried out in an extremely simplified manner as compared with reality, is still much more precise than the simulation of the latter process.

Nevertheless, in this paper a simplified mathematical model of these processes is used as an approach to estimate irrigation needs. The model, called BALHIDRO, was presented by Lanna et alli (3), and is a generalization, adapted to 16 bit microcomputers, of a program originally developed by HIMAT(4).

3. DESCRIPTION OF BALHIDRO

Model aplication assumes that there is an Agricultural Development Plan for given area constituted by different types of land use, represented by plant varieties, cultivated at specific time periods previously established by agricultural zoning. This representation allows great flexibility in the Devolopment Plan and may simulate the situation of a succession of crops, including the practice of leaving certain sub-areas fallow each year. The water needs for each type of soil use are estimated by multiplying a cultivation coefficient Kc, by potential evapotranspiration, ETP, at ten-day intervals. The cultivation coefficient Kc is a function of the crop and its vegetative stage, obtained from regional agricultural experiments.

It is assumed that the irrigation needs are fully supplied. Two irrigation methods are foreseen: sprinkler irrigation of the mesophytic crop, such as soy beans or maize, and flood irrigation of rice. The water balance is estabilished taking into account the humidity exchanges in the soil profile. For mesophytic crops, irrigation is determined by the state of humidity of the upper horizon and the water applied to maintain it between the humidity corresponding to field capacity and a lower level of humidity which prevents crop stress. In the case of flood irrigated rice, it is assumed that a water layer will be established on the soil surface after saturation. This layer must lie between two limits, which are a function of the rice variety and terrain microrelief.

The water balance performed at daily time intervals assumes that two forms of water supply exist: rainfall and irrigation. The total daily rainfall is distributed among an initial loss, a part which runs off superficially and another which is infiltrated. The latter part is of greater agricultural interest and is called effective rainfall. The partition method used is that proposed by the United States Soil Conservation Service and adapted to Brazilian conditions by Setzer and Porto, Porto (5).

The effective rainfall increases humidity in the upper zone of the soil. Irrigation is added to this term. The withdrawal of water from this zone may be performed by evapotranspiration and by infiltration to the deep soil horizon. This horizon, fed by percolation from upper layer, loses water to deep percolation.

When the irrigation method used is continuous flooding, both soil zones will be saturated down to the impervious horizon. Percolation will be estimated by a previously sized value, a function of the physical and water characteristics of this impervious layer.

The irrigation will be introduced into the model with an addition Ad(t) of humidity to the water balance of the upper soil zone. This addition will be defined daily by two humidity limits according to the irrigation method used and mentioned previously. The daily irrigation water is also limited by the maximum capacity of the pumping equipment.

The humidity of the upper soil layer is calculated by:

$$H(t) \cdot R(t) = H(t-1) \cdot R(t-1) + Hp(t-1) \cdot (R(t) - R(t-1)) +$$

$$+ Ex(t) + Ad(t) - Ap(t)$$

where H(t) is the percent humidity of the upper soil zone at the end of day t, limited to the Useful Volumetric Reserve (RUV).

RUV specifies the amount of water stored in the soil when it is at field capacity, in percentage of soil depth. Ex.: if RUV is 20% and the soil depth is 100cm, the water content at field capacity is equivalent to 20cm.

R(t) is the root depth at the end of day t in mm;

H(t) . R(t) is, therefore, the water content in the upper soil layer at the end of day t;

Ex(t) is the agricultural excess or deficit during day t, supplied by the difference between infiltrated rainfall and evapotranspiration, i.e.:

$$Ex(t) = Pe(t) - Kc(t) \cdot ETP(t)$$

where:

Pe(t) effective rainfall during day t (mm),
Kc(t) cultivation coefficient during day t (mm) and
ETP(t) potential evapotranspiration during day t (mm)
Ad(t) rrigation water applied on day t (mm),
Ap(t) percolation during day t (mm).

If the humidity in this layer is greater than the soil Useful Volumetric Reserve, percolation will occur (AINFD) to the lower zone as the excess of H(t) over RUV. If no irrigation occurs, resulting in H(t) less than zero, its final value will be nil, and real evapotranspiration will be less than the potential one by a difference given as the original negative value of H(t).

The water balance of the lower soil zone will be given by:

$$Hp(t) \cdot (Rmax - R(t)) = Hp(t-1) \cdot (Rmax - R(t-1)) + H(t-1) \cdot (R(t-1) - R+t)) + Ap(t) - App(t)$$

where:

Rmax total depth of the lower zone (mm)
Ap(t) percolation from the upper zone (mm) and
App(t) deep percolation (mm)

The first term of the sum, in the equation above, is the water content of this zone at the end of day t-1. Addition or subtraction to this content are performed depending on the sign of R(t-1) - R(t), the humidity which belonged to the upper zone during the time interval t-1 and, due to root growth or retraction now belongs to the lower one. Finally, the percolation from the upper zone is added to the result and deep percolation is subtracted.

The percolation value will usually be nil, unless the resulting humidity in one of the zones is greater than the Useful Volumetric Reserve, in which case the excess will percolate. When percolation occurs in the upper zone, it will feed the lower one. If it occurs in the latter, it will reach even deeper soil layers.

When the flood irrigation method is used, both zones will be saturated. RUV will be the water content found in the saturated soil as percentage of depth. Rmax will correspond to depth down to the impervious soil layer. Percolation will be estimated by a previously sized value, a function of the physical and water characteristics of the impervious horizon.

4. APPLICATION

The input data used in applying model BALHIDRO were:

— Daily rainfall - refering to the raingauging station of Nova Xavantina, code 01452000 of the Brazilian National Department of Water and Power, 1970-1986.

— The potential evapotranspiration at 10-day intervals calculated for the region using the Penman method as informed by the Climatology Sector of Federal University of Mato Grosso.

According to the Agricultural Development Plan, two situations were simulated: Plan A with two rice crops irrigated by continuous flooding and Plan B with two crops of grains belonging to mesophytic species, irrigated by sprinkling. The cultivation periods in each case were: Irrigated rice: from December 20 to the end of February and from the beginning of June to the end of August.

This is a situation of fully irrigated agriculture based on agricultural and climate zoning.

Maximum root depth taken is 300 mm. In the case of continuous flood irrigation, a depth of 1 m was stipulated, limited by the impervious soil layer.

The minimum and maximum humidities which define the irrigation plan were established respectively as 60% and 100% of the Useful Volumetric Reserve of soil, in the case of mesophytic crops, and as 50 and 100 mm of water depth, in the case of flood irrigation.

Percolation during rice flooding was estimated at 4 mm/day, based on field experiments performed by the Institute of Hydraulic Research, Federal University of Rio Grande do Sul, reported by Fietz(6).

The soil characteristics represented by Useful Volumetric Reserve (RUV) and Curve Number (NC) of the Soil Conservation Service were established at 20% and 78 respectively.

5. RESULTS

Figures 1 and 2 present variability of 10-day totals of observed and effective rainfall, irrigation water applied, potential and real evapotranspiration, and percolation in terms of mean values during the 1970-1986 period. It may be noted that non-nil values for irrigation needs occurred for both crops even during the wet season. The maximum irrigation needs for the mesophytic species were 32.5 mm at the beginning and end of the dry season. For rice it was 270 mm at the beginning of the dry season. The maxima, which occur at the beginning of the dry season, arrived from the need to wet the soil up to the established levels. It is observed the irrigation requirement for mesophytic species is low during the wet season, meaning that rain almost covers agricultural demands. These accumulated values attain 27 mm. However, in the case of rice, a large amount of water is required, both in the beginning, to saturate the soil, and throughout cultivation, reaching a total of 328 mm. During the dry season the accumulated needs are 271 mm and 1194mm for mesophytic species and rice, respectively.

6. CONCLUSION

The analyses performed, based on the results of water balances, indicate that agricultural development in that region, with two crops a year, requires irrigation. The system will be used intensively in the case of rice, and only during the dry season in the case of mesophytic species. However, irrigation may be useful to the latter species during some dry periods which occur in the wet season.

7. REFERENCES

[1] Beltrame, L.; Lanna, A.; Kaiser, P.; Oliveira, J.; Giasson, E. Estudo de Viabilidade Técnica para Irrigação na área. Programa de Barra do Garças, CONSPAGRO (Out. 1989).

[2] Lanna, A.; Beltrame, L.; Giasson, E. Análise Econômica Pre-liminar da Viabilidade de Irrigação na Região de Barra do Garças, MT. Trabalho apresentado no "Hydrology and water Management of the Amazon Basin", Manaus (August 1990).

[3] Lanna, A.; Beltrame, L.; Aguinsky, S. Estimativa de Necessidades de Irrigação por Balanço Hídrico: Programa BALHIDRO - Manual do Usuário (IPH/URGS, Porto Alegre, 1989).

[4] HIMAT Cálculo Estadístico de Requerimientos de água de Riego - Memoria de Utilización (Instituto Colombiano de Hidrología, Meteorología y Adecuación de Tierras, Bogotá, 1985).

[5] Porto, R. Bases Hidrológicas para Projetos de Irrigação. In: PRONI, Curso de Elaboração de Projetos de Irrigação (PNI/ Fundação CTH, Brasília, 1986).

[6] Fietz, C. Demanda Hídrica em Lavoura de Arroz Irrigado (Oriza sativa L.) em Planossolo, Diss. Mestr. Engenharia Civil, UFRGS (1987).

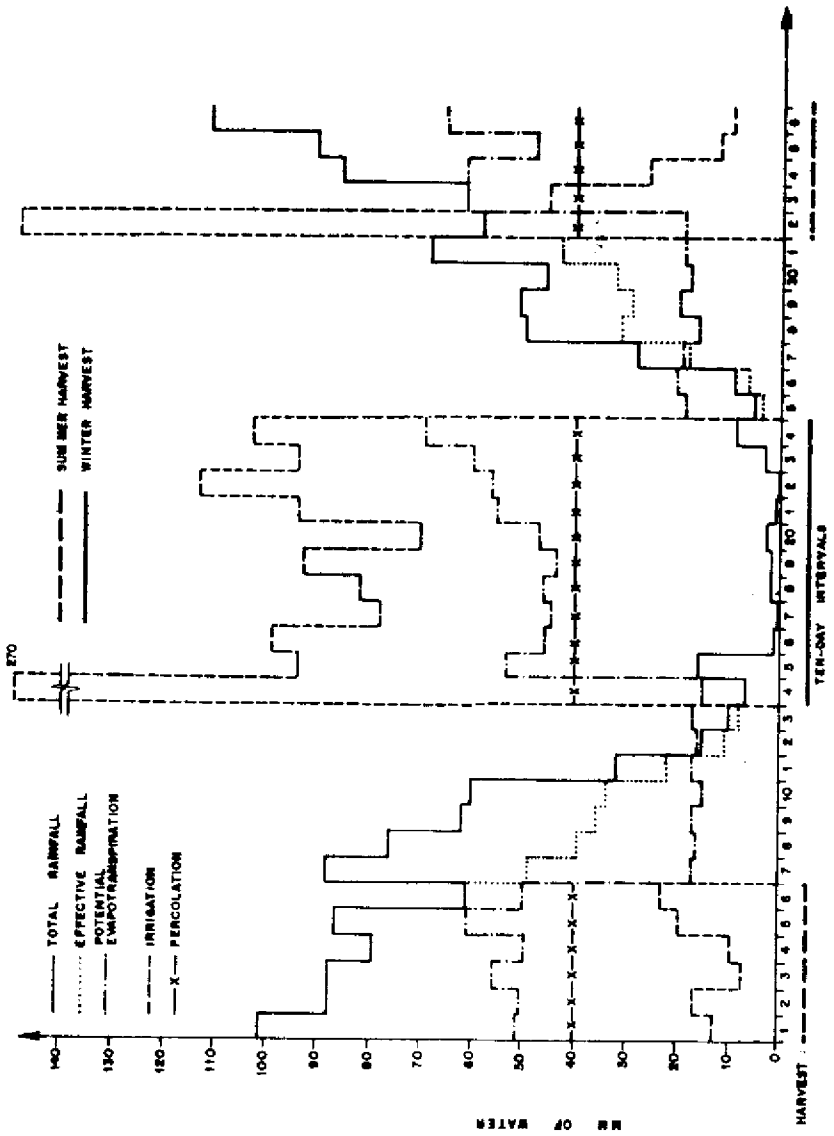

Figure 1 - Irrigation needs of mesophytic crops

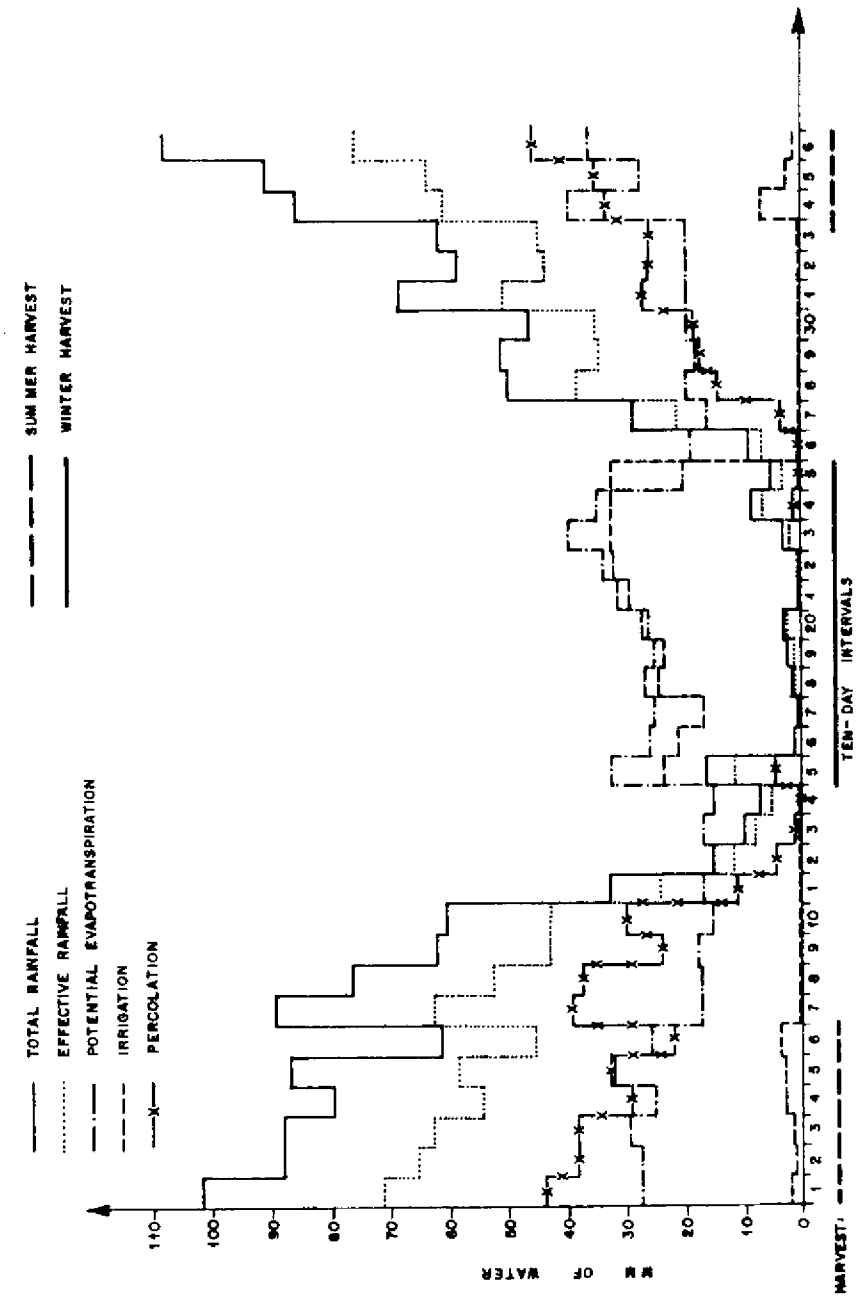

Figure 2 - Irrigation needs of rice

THE MECHANISMS OF OVERLAND FLOW GENERATION IN A SMALL CATCHMENT IN WESTERN AMAZONIA

*H. Elsenbeer**
*D.K. Cassel***

ABSTRACT

Overland flow was found to be a common phenomenon in a first-order rainforest catchment of Western Amazonia. A very pronounced decrease in soil saturated hydraulic conductivity at a very shallow depth results, under the prevailing rainfall intensities, in the formation of a perched water table. This water table may result in widespread saturation overland flow upon reaching the surface, or in return flow from soil pipes where it is tapped by an ubiquitous macropore network.

1. INTRODUCTION

The traditional classification of runoff-generating processes according to their environmental controls emphasizes the importance of saturation overland flow (SOF) and subsurface stormflow (SSF) in humid climates with dense vegetation (see, e.g. [2]). With respect to the humid tropics, SSF is considered the dominant process, mainly based on the assumption that such environments are characterized by deep, permeable soils (see, e.g. [9]). This had led to the belief that overland flow (OF) is not a widespread or frequent phenomenon in natural ecosystems of the humid tropics, notwithstanding the documentation of widespread SOF from tropical Australia [1].

The absence of OF, except for SOF in valley bottoms, was also postulated by Nortcliff et al. [7] who worked in the Amazon Basin near Manaos. Besides their study, few, if any, detailed investigations of runoff processes were conducted in Amazonia.

2. THEORY

Three mechanisms of OF generations are generally distinguished:

The *Horton mechanism* requires rainfall intensity to exceed saturated hydraulic conductivity of the surface soil. OF occurs once rainfall amount exceeds depression storage.

* *University of Bern, Switzerland*

** *North Carolina State University, United States of America*

- The *Dunne mechanism* requires surface saturation due to, e.g., the rise of a perched water table. Any precipitation will run off as SOF regardless of its intensity.
- Return flow (RF) to the soil surface of SSF due to, e.g., soil hydraulic characteristics and/or hillslope topography.

Thus, it is mainly the interaction between soil and rainfall variables which determines the predominant mechanism.

3. THE RESEARCH SITE

The research catchment (1 ha) is situated in the Selva Central of Perú in the Río Pichis valley (75°5'W, 10°13'S) which belongs to the Ucayali drainage. It is located on the highest and most dissected of three geomorphic surfaces that can be distinguished in this valley. This surface is characterized by steep, convexo-linear sideslopes reaching 35°, by narrow valley floors, by flat interfluves in places reduced to narrow ridges, and by abundant rills and gullies around stream heads.

A dense network of pipes and macropores is found at a shallow depth.

Tertiary red beds consisting of sandstones, siltstones, and shales are the dominant parent materials from which mainly Ultisols developed.

Mean annual temperature for the area is 25.5°C, and mean annual precipitation if about 3300 mm [8]. Monthly precipitation is highest from December through March (up to 900 mm), and lowest from June through September when it may drop below 100 mm. Daily rainfall amounts rarely exceed 100 mm.

4. METHODOLOGY

The spatial and temporal frequency of OF occurrence was determined by means of detectors similar to those described by Kirkby et al. [5]. Seventy-two of these devices were installed throughout the catchment (see Fig. 1) to cover all possible configurations of slope profile and contour line curvature. The occurrence of OF was verified after 187 precipitation events.

OF was monitored continuously for a period of two years at three sites (S1, S2, and S3 in Fig. 1).

Soil saturated hydraulic conductivity (Ksat) was determined on undisturbed soil cores by the constant-head method [6]. Two sampling approaches were employed: random sampling throughout the catchment and stratified sampling according to landscape position or slope unit (see Fig. 2) from four depth intervals: 0-0.1, 0.1-0.2, 0.2-0.3, and 0.3-0.4 m.

Soil water pressure potential, as a proxy for soil moisture conditions, was monitored by means of 15 tensiometers installed at depths of 0.1, 0.3, 0.6 and 0.9 m, respectively, and read every 24 hours for a two-year period.

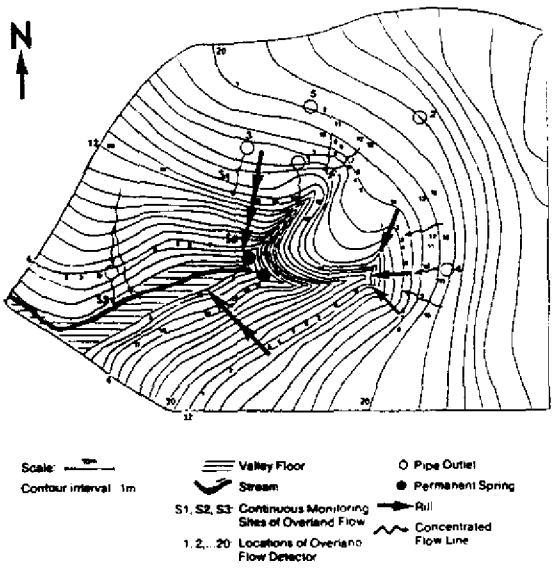

Fig. 1 - The research catchment at "La Cuenca"

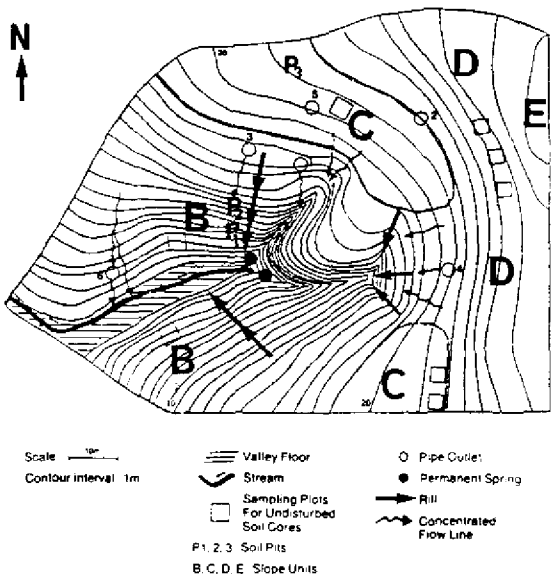

Fig. 2 - Landscape positions in the research catchment. B: lower sideslope, C: intermediate terrace, D: upper sideslope, E: interfluve.

Rainfall intensities were obtained from a recording rain gauge which was installed in a nearby clearing.

5. RESULTS

Frequency of overland flow occurrence

Table 1 shows that OF is a frequent and widespread phenomenon. Every third precipitation event produced OF at 50% or more of the 72 sites. An arbitrary critical duration of one hour between two events was employed to define these events as independent.

Table 1 - Frequency of occurrence of overland flow, based on 187 storms between September 1986 and January 1988

Spatial frequency (% of sites)	Temporal frequency (% of events)
≥ 25	74
≥ 50	33
≥ 75	4

The continuous monitoring of OF at sites S1, S2 and S3 (see Fig. 1) confirms the high temporal frequency (Table 2). It must be emphasized, however, that a higher frequency does not also imply a higher volumetric contribution. For instance, those events that resulted in OF in both S1 and S2 usually produced higher volumes at the upslope site, S1, than at the downslope site, S2. In this case, it could be established that outflow from pipe 3 contributed to the runoff intercepted at site S1.

Table 2 - Frequency of overland flow at continuous-monitoring sites

Year	1987	1988
Site No. of events > 0.2 mm	291	270
S1	84	71
S2	244	221
S3	150	146

Evidence for the Horton mechanism

Table 3 shows that the maximum rainfall intensities exceed the surface Ksat occasionally in some places. For instance, the maximum 30 min intensity, I30, of 25% of the events analyzed, exceeded surface Ksat in 16% of the random samples. Stratified sampling (see Methodology) revealed, however, that Horton OF occurs preferentially in slope unit B (see Fig. 2 and Table 4). Here, the 25% quartile of I30 exceeded surface Ksat in 38% of the samples, quite in contrast to the other slope units (see [3] for details). Landscape position B, the steep valley sideslopes, is characterized by a poorly developed or missing A-horizon, and a patchy and sparse litter layer. From this, a positive feedback loop may be inferred: erosion - low surface Kst - OF - erosion.

Table 3 - Comparison of soil saturated hydraulic conductivities and maximum rainfall intensities

Soil		I_{60}			I_{30}			I_{15}		
depth	quartiles:	25	50	75	25	50	75	25	50	75
- m -		- exceedance probability (%) -								
0-0.1		15	13	9	16	13	9	16	13	9
0.1-0.2		56	49	39	60	49	38	63	54	39
0.2-0.3		71	59	55	76	61	55	80	63	55
0.3-0.4		93	89	85	93	89	81	93	89	85

Table 4 - Comparison of surface soil saturated hydraulic conductivities and maximum rainfall intensities

Landscape		I_{60}			I_{30}			I_{15}		
position	quartiles:	25	50	75	25	50	75	25	50	75
		- exceedance probability -								
B		36	30	22	38	30	20	42	32	22
C		5	3	0	5	3	0	8	4	0
D		4	4	4	4	4	4	8	4	4
E		2	0	0	4	0	0	4	0	0

Evidence for the Dunne mechanism

It is obvious from Table 3 that a hydraulic discontinuity exists at a very shallow depth. Roughly speaking, 50% of all events analyzed had maximum intensities that exceeded Ksat of the 0.1-0.2 m depth interval in 50% of the samples: for the 0.3-0.4 m depth, the latter percentage reached about 90. This discontinuity is conducive to the formation of a perched water table. SOF is generated when and where this water table reaches the surface. It may be inferred from Figure 3 that surface saturation is easily achieved since the frequent precipitation in this environment causes almost perennial near-saturation of the soils. Except for a period of a few weeks towards the end of that year's (1987) dry period, and occasional dry spells throughout that year, even the surface soil is at or close to saturation. SOF is likely to occur in a 'widespread', rather than 'localized' fashion, because of the predominant importance of soil hydraulic over topographic characteristics in this environment, similar to the situation in Queensland [1].

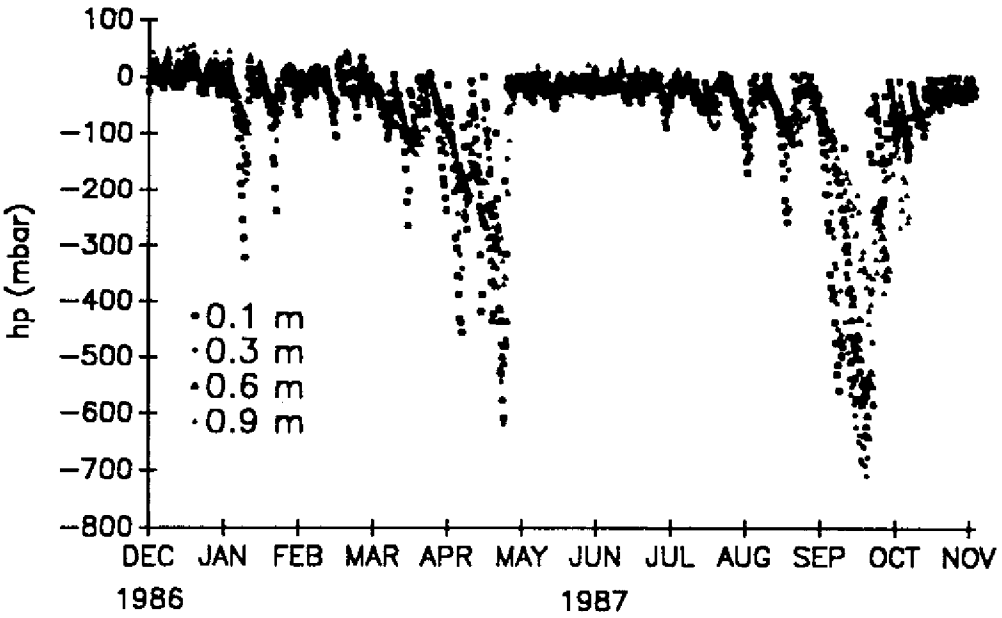

Fig. 3 - Time series of soil water pressure potential at four depths.

Evidence for return flow

Several pipe outlets were identified in the field (see Fig. 1) by tracing concentrated-flow lines during precipitation events. In particular, it was ascertained that outflow from pipes 3 and 6 (see Fig. 1) contributed to OF monitored at sites S1 and S3, respectively. The existence of a dense network of pipes and macropores at a shallow depth was also demonstrated in soil pits (see Fig. 2). It is conceivable that such a network taps a perched water table, which may form due to the observed hydraulic discontinuity, even before it reaches the soil surface. Details about return flow monitored at pipe 1 (see Fig. 2) were reported elsewhere [3].

CONCLUSIONS

All three described mechanisms of OF generation—Horton, Dunne and return flow—operate in this tropical rainforest environment. The generation of HOF is most likely on the steep, eroded valley sideslopes, whereas SOF and RF may occur anywhere. The generation of OF in this environment can be explained by the interaction of rainfall variables, notably intensity and frequency, and the Ksat-depth function and its spatial distribution. The occurrence of RF renders a distinction of the various forms of OF in the field nearly impossible.

REFERENCES

[1] Bonell, M.; Gilmour, D.A. and Sinclair, D.F. Soil hydraulic properties and their effect on surface and subsurface water transfer in a tropical rainforest catchment, Hydrol. Sci. Bull. 26(1), 1-18, 1981.

[2] Dunne, T. Field studies of hillslope processes, in: Kirkby,M.J. (ed.), Hillslope Hydrology, Wiley, New York, 1978.

[3] Elsenbeer, H. and Cassel, D.K. Hydrological and hydrochemical characteristics of pipeflow: a case study from a humid tropical environment. Agronomy Abstracts, Madison, Wisconsin, p. 183, 1988.

[4] Elsenbeer, H. and Cassel, D.K. Spatial distribution of hydraulic conductivity in a tropical rainforest environment. Agronomy Abstracts, Madison, Wisconsin, p. 186, 1989.

[5] Kirkby, M.J.; Callan, J.; Weyman, D. and Wood, J. Measurement and modeling of dynamic contributing areas in very small catchments. University of Leeds, School of Geography, Working Paper No. 167, Leeds, United Kingdom, 1976.

[6] Klute, A. and Dirksen, C. Hydraulic conductivity and diffusivity: laboratory measurements, in: Klute, A. (ed.), Methods of Soil Analysis, Part 1, 2nd edition, Agronomy 9, 687-734, 1986.

[7] Nortcliff, S.; Thornes, J. B. and Waylen, M. J. Tropical forest systems: a hydrological approach. Amazoniana 6(4), 557-568, 1979.

[8] ONERN, Inventario y Evaluación Semidetallada de los Recursos Naturales de la Zona del Río Pichis. Proyecto Pichis-Palcazu, ONERN, Lima, Perú, 1981.

[9] Walsh, R. P. D. Runoff processes and models in the humid tropics. Z. Geomorph. NF Suppl. 36, 176-202, 1980.

SURFACE RUNOFF ON A TROPICAL TURFED SLOPE

*Yee-Meng Chiew**
*Soon-Keat Tan***

ABSTRACT

This paper presents results obtained from a field monitoring project of surface runoff from two turfed slopes on the campus of the Institute. The results show that the structure of the vegetation cover has an important influence on the characteristics of surface runoff. It also affects the frictional resistance to flow. Field data show that the ratio of the effective over total precipitation is related to the rainfall intensity.

1. INTRODUCTION

Most information relating to the topic of Hydrology is derived from studies and researches conducted in a temperate environment, where the pattern of precipitation, evapotranspiration, infiltration, etc., may differ substantially from that in the tropics. The characteristics of surface runoff is dependent on the amount of runoff losses as well as the type of vegetation cover. While there are abundant published data on surface runoff in temperate regions, there are comparatively little data, especially field data obtained in the tropics. In order to understand the characteristics of surface runoff from a tropical catchment, it is imperative to understand the differences between flows in these two climatic conditions. Information such as frictional resistance on turfed slopes derived from a temperate region may not be appropriate for use in a tropical catchment.

The surface runoff in a temperate region may be viewed as a shallow sheet flow, where the water flows over the vegetation cover. The grass bend over as water flows over them. In the tropics, the grass are, in general, much stiffer and they are less likely to bend under the shear stresses exerted by flowing water. The stiffness of the grass stalks causes the water to flow through and around the grass and the resulting surface runoff resembles that of inter-flow, normally associated with conditions where there are thick mulches or in forests. The difference in these two types of flow is the thickness of surface water trapped within the turf. As a result, the retention period of rain water on land is longer in the latter, leading to more losses of surface water.

* *Lecturer - Nanyang Technological Institute - Singapore*

** *Senior Lecturer - Nanyang Technological Institut - Singapore*

Infiltration is not always constant. The rate is highest at the beginning and approaches a constant but much lower rate after the soil layer saturates. In addition, it appears that the rate of infiltration increases with rainfall intensity. Wilson (1983) stated that the final constant rate of infiltration is higher for higher rainfall intensity. Likewise, Akan & Yen (1983) show that while the rate of infiltration increases with rainfall intensity at the beginning of a rainfall event, the final constant infiltration rate remains the same.

This paper describes findings from a field monitoring project of surface runoff on a turfed slope in Singapore. The amount of rainfall is measured using a tipping bucket rain gauge installed on site. The surface runoff is measured at the main entrance to the storm drains. The results show that the mechanics and amount of flow on turfed area in the tropics is closely related to the types of vegetation cover that exists in the catchment under considerations.

2. EXPERIMENTAL SLOPES

Two small plots within the campus at the Nanyang Technological Institute are selected for the study. Table 1 summarizes the characteristics of the two experimental slopes. These two slopes are within 100 meters of one another. As such they are experiencing the same rainfall most of, if not all the time.

Table 1 - Characteristics of experimental slopes

	Characteristics	Slope (A)	Slope (B)
a.	average slope	0.5 (30°)	0.35 (20.5°)
b.	paved area of catchment	238 m^2	0
c.	turfed area of catchment	1017 m^2	2056 m^2
d.	general vegetation	turf	turf, low bushes
e.	typical soil porosity	49%	49%
h.	base flow	nil	nil
i.	f_o	420 mm/hr	480 mm/hr
j.	f_c	72 mm/hr	90 mm/hr

Plot A is the smaller of the two plots and consists of a uniform slope covered with grass similar in nature to that shown in Fig. 1a. The grass are sparsely located and their stalks are coarse and stiff. Plot A is a filled slope and turfed after landscaping work has been carried out. The slope is terraced with a concrete pavement with open drains on the flats of the terraces. The drains run across the slope. They join the main terrace drain at the center of the plot, which eventually drains into the main storm water system. The terrace and drain system define the catchment area.

Plot B is covered with its natural vegetation of turf and low bushes. The grass (see Fig. 1b) is thick and springy with thick undergrowths. This catchment is defined in the north by the divide at the top of the slope which curves to enclose the western side of the basin and a storm drain at the toe of the slope. The eastern side contains a uniform slope. The end of the drain marks the catchment boundary.

The surface runoff measurements in both plots were made at the end of the surface drains before the system joins the main storm water system. The infiltration constants in Table 1 were measured using an infiltrometer.

3. DATA COLLECTION

Tropical rains usually have high intensity but last for a comparatively short time. As such, infiltration and surface retention of water on land surface would account for most of the losses from a rainfall. Surface runoff would then be the difference between the total rainfall and surface retention and infiltration losses. This method of accounting for the volume of water is essentially a water budget method, similar to that used by Davis & Hollis (1981).

In using the water budget method to account for the amount of water involved during a rainfall event, four terms need to be considered. They are: total precipitation, surface retention, infiltration and surface runoff. The first and last parameters are determined through direct measurement. The second and third parameters need to be assessed with skill and sometimes it is just not possible to separate the two.

The following describe the procedure adopted to determine each of the four terms in this study.

Total Precipitation

Tipping bucket rain-gauge with mercury contact switch is used to measured the depth of rainfall received at the site. Each tip corresponds to 0.2 mm depth of water. The mercury switch is connected in series to a 3 V dry cell and a chart recorder with pre-set speed of paper feed. In this way, not only the quantity of precipitation but the temporal distribution of the rainfall are also recorded. As the experimental plots are small, it is reasonable to assume that rainfall distribution over the area is uniform. Therefore, the total precipitation in a given rainfall event can be estimated readily.

Total Surface Runoff

A v-notch weir is set up at the entry point to the storm drain. The water level upstream of the weir is measured by using a twin wire conductivity probe. The stage-discharge relationship of the v-notch weir and the probe has been previously calibrated on the actual site. The D.C. voltage output from the probe is directed to a different channel of the same chart recorder used for rainfall recording. As a result, the surface runoff hydrograph can be obtained directly. The total volume of runoff is obtained from integration of the hydrograph with respect to time.

Surface Retention and Infiltration

These two terms are not easily separated. However, the sum of these must equal the difference between total precipitation and total surface runoff, since there is no base flow involved. In this context, all other losses such as evaporation and transpiration loss are lumped together with the term for surface retention. By plotting total precipitation against total surface runoff, the intercept of the fitted curve should yield the amount of water due to surface retention and infiltration.

Regression analysis using LOTUS 1-2-3 package yields the following regression equations:

Plot A:

$$\log_{10}(\text{Total Rainfall}) = 0.784 \log_{10}(\text{Effective Rainfall}) + 0.707$$
$$R^2 = 47.0\%$$

Plot B:

$$\log_{10}(\text{Total Rainfall}) = 0.404 \log_{10}(\text{Effective Rainfall}) + 0.866$$
$$R^2 = 48.3\%$$

where both total and effective rainfall are measured in mm.

A more tedious alternative would be to make actual site measurement of moisture infiltrated into the soil during the rainfall event. This method is not tried.

4. RESULTS AND DISCUSSION

The type of turfs grown in a tropical country like Singapore differs from those grown in temperate countries because of the different climatic conditions and amount of rainfall. In the tropics, both the temperature and humidity is high and this is conducive to plant growth. In general, the grass stalks in both the experimental plots in this study are coarse and the two types of grass are commonly found in the island republic. Thick undergrowths, in the form of fibrous roots grow loosely for up to 4-5 cm from the soil level above which the leaves are seen (see Fig. 1b), are found in plot B. The total height of grass above the ground level is approximately 7 cm. These undergrowths create large air voids within which water can flow. Besides this, the coarse grass stalks tend to 'block' the flow of water, thus creating a head as the water flows through the grass.

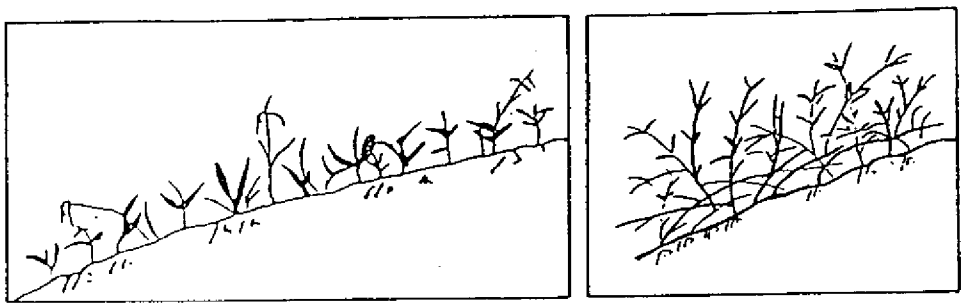

(a) (b)

Figure 1 - Grass Types Found in (a) Plot A: (b) Plot B

1. Infiltration rate is controlled, among others things, by the surface pores of the soil grains. An increase in the hydrostatic head over these pores results in an increase in the flow through the soil surface, thus increasing the infiltration rate. Hence, it is envisaged that the infiltration rate will be greater for water flowing through grass as compared with that flowing above it.

2. The blockage of the water by the grass tends to increase the retention time of flow over a given path length. This increases the opportunity for infiltration.

The higher rate of infiltration for water flowing through the grass is substantiated by conducting an experiment in experimental plot A where a constant rate of water is supplied to two strips of grass. The area of both strips were constant at 3 m x 0.5 m. The two strips were formed by hammering galvanized iron sheets into the soil. The grass on one of the strips was left untouched whereas the grass on the second strip was trimmed to a bare minimum such that the water was flowing through the grass on the first strip and over it on the second. The resulting hydrographs for a constant volume of discharge were measured and are shown in Figure 2. For comparison purposes, the two hydrographs have been shifted such that their origins coincide. The results show that the volume runoff associated with the first strip is about 10% lower than that associated with the second strip. It may be inferred from this simple experiment that the infiltration rate associated with flow through grass is higher than that associated with flow over grass.

The ability of a tropical grass to resist bending under the influence of surface runoff also has an important effect on the frictional resistance to flow. Because of their rigidity, the grass stalks deflect the flow of water over and around them, generating high levels of turbulence and drag. The result is the occurrence of a turbulent flow even though the flow Reynolds Number suggests otherwise. In a separate study, the writers (1990) measured frictional resistance to flow on a typical grass type in Singapore and analyzed the frictional resistance in terms of both the Darcy-Weisbach friction factor, f and the Manning n. Their results confirmed the reasoning stated above. They found that the Manning n values range from 0.19-0.26 for the type of vegetation cover tested in their study. The grass cover in both plots A and B are different from that tested by Chiew and Tan (1990).

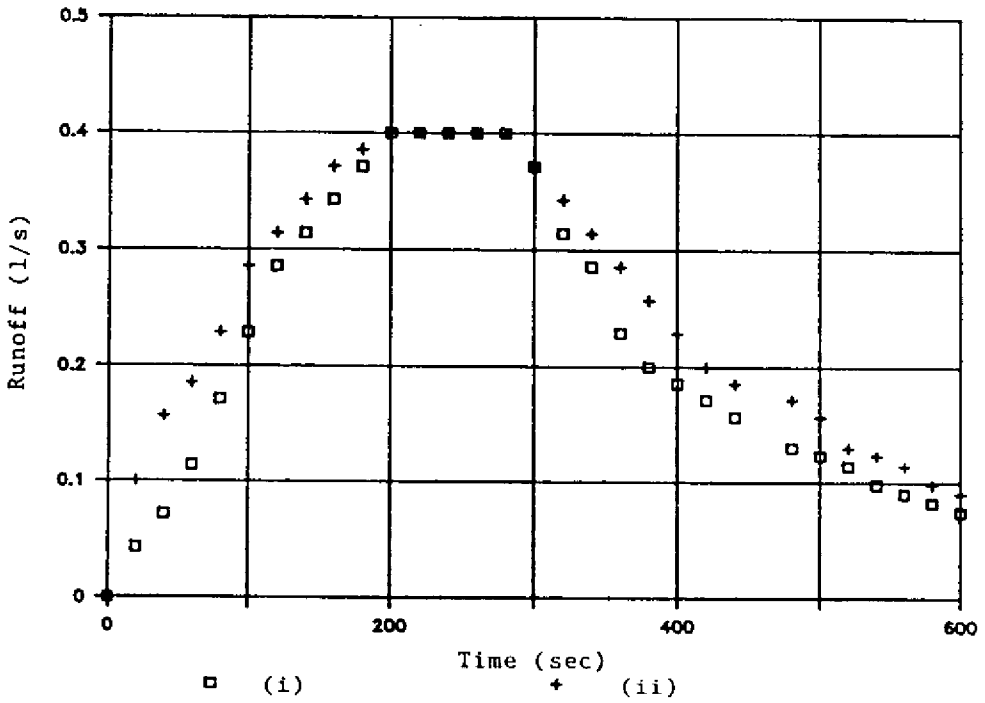

Figure 2 - Runoff Hydrographs for Turfed Slopes with (i) Grass Intact; (ii) Grass Trimmed

The rainfall intensity in tropical regions is generally higher than that in temperate countries. Findings from this study confirm results reported by Wilson (1983) and Akan & Yen (1983) that infiltration rate is related to the rainfall intensity. Figure 3 contains the plot of the ratio of runoff volume (or effective rainfall) over total rainfall, P_e/P_T as a function of rainfall intensity, i. The rainfall intensity was computed using a constant duration of 5 minutes. The curve shows a rapid increase in the ratio of P_e/P_T with increase in rainfall intensity until a maximum is reached at about i = 5 mm/hr. Thereafter the values of P_e/P_T decreases until a constant is reached when i reaches approximately 50 mm/hr. The initial increase is because of the need to completely wet the surface cover before runoff can take place. Thereafter, the amount of runoff is the difference between the total precipitation and losses. The results in Figure 3 shows that losses increases as rainfall intensity increases and it may be inferred that this increase in loss of water is caused by the increase in filtration rate as rainfall intensity increases, as was reported by Wilson (1983) and Akan & Yen (1983).

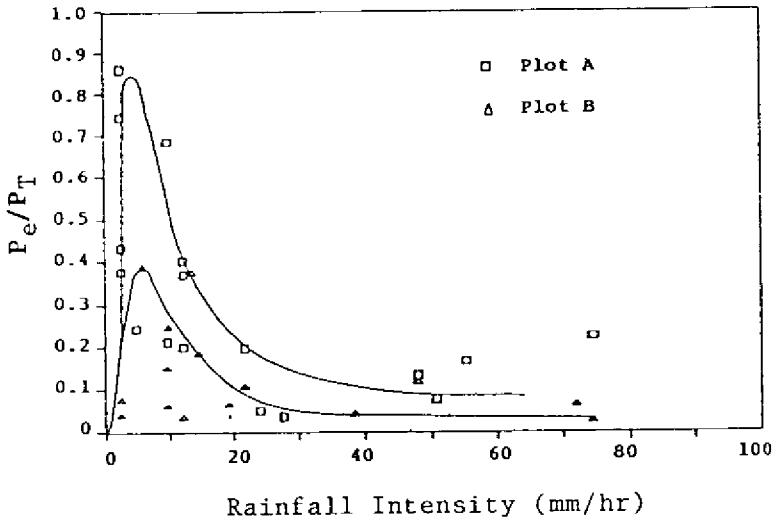

Figure 3 - Ratio of Effective Rainfall Over Total Rainfall (P_e/P_T) versus Rainfall Intensity (i) with 5 minutes duration

5. CONCLUSIONS

Results from this study show that the amount of surface runoff over a turfed slope is different for water flowing through and over the grass. In a tropical country like Singapore where the grass stalks are coarse and the undergrowth are thick, rain water is likely to flow through the grass whereas in temperate countries, the grass are a lot finer where rain water is likely to flow over the grass. The coarse grass and thick undergrowth tend to block the flow of water, thus creating a relatively large hydrostatic head which increases the rate of infiltration. The study also found that the ratio of the effective over total precipitation is related to the rainfall intensity. The writers infer that this is caused by the increase in infiltration rate for large rainfall intensity.

6. REFERENCES

Akan, A. O. and Yen, B. C. "Effect of Rain Intensity and Surface Runoff Rates", *Advances in Infiltration*, Proceedings of National Conference on Advances in Infiltration, December 12-13, 1983, Chicago, Illinois: 324-331, 1983.

Chan, C. P. and Ding, K. L. "Frictional Resistance of Overland Flow", *Final Year Project*, Civil & Structural Engineering, Nanyang Technological Institute, 1988.

Chiew, Y. M. and Tan, S. K. "Frictional Resistance of Overland Flow on Tropical Turfed Slopes". Submitted to *Journal of Hydraulic Engineering*, A.S.C.E., 1990.

Davies, H. and Hollis, T. "Measurements of Rainfall-Runoff Volume Relationships and Water Balance for Roofs and Roads", *Second International Conference on Urban Storm Drainage*, Urbana, Illinois, United States, 434-443, 1981.

Hawkins, R. H. "Interpretations of Source Area Variability in Rainfall-Runoff Relations", *Rainfall-Runoff Relationships*, Proceedings of the International Symposium on Rainfall-Runoff Modeling, Mississippi State University, Mississippi State, Mississippi, United States, May 1981, 303-324.

Wilson, E. M. *Engineering Hydrology*, 3rd. edition, MacMillan Press Ltd., London & Basingstoke, 1983.

REMOTE SENSING OF THE PRECIPITATION BY RADAR AND SATELLITE HYDROLOGICAL APPLICATIONS IN THE AMAZON BASIN

Roberto Vicente Calheiros *
Marlene Elias Ferreira **

ABSTRACT

Remote sensing of the precipitation by radar and satellite is focused under the viewpoint of hydrological applications in the Amazon Basin. The respective techniques of rainfall estimates, currently in use, are presented and new techniques under consideration are mentioned. Alternatives involving radar only, satellite only, and a combination of both sensing systems are suggested for areal rainfall estimation over the Amazon region. The previous Brazilian experience, as well as works presently in development abroad, concerning rainfall estimation in the region under consideration and the radar-satellite integration techniques regarding precipitation, are commented.

1. INTRODUCTION

Remote sensing has great potential for obtaining hydrological data, among which stands out precipitation. In this regard, it is verified that the feeling of several hydrologists [1] is that the use of complex models of river basin response will end up being a sterile activity, unless the uncertainties related to the spatial variability of rain - among others - may be reduced by the use of more comprehensive measurements, for which the radar and the satellite have potential. In this context, Schultz [2] comments on the credit that many specialists still seem to give to the possibility of overcoming, through mathematics, the problem of "garbage in - garbage out" instead of looking for input improvements. On the other hand, this author quotes Eammon Nash: "I find it difficult to believe that we should enter the third millennium after Christ measuring rain in little buckets - and guessing evaporation".

The use of radar and satellites has shown to be ever more valuable for estimating precipitation along the times. Specially the radars have proven to be a very promising tool in this regard. The European radar network (Cost-73) and the USA next generation radars (NEXRAD) programs are good

* *UNESP/IPMet, INPE/NPI; Caixa Postal 473; 17033 Bauru SP; Brazil; Fax: (142) 23 36 08*

** *INPE/DAT; Caixa Postal 515; 12201 São José dos Campos SP; Brazil; Fax: (123) 21 87 43*

examples of the remote sensing importance for rain estimation. On the other hand, several techniques using satellite imagery to estimate precipitation are being developed. Of particular interest, mainly when the radar area coverage is limited, is the methodology that combines the two observation techniques - radar and satellite - to estimate precipitation.

For geographic regions with the dimensions of the Amazon Basin and presenting difficulties to obtain in situ measurements the remote sensing techniques are particularly relevant.

This work deals with the problem of estimating rain using radar and satellite, considering the fundamentals of each technique, separately as well as in combination. Their potential and main limitations are discussed. Specially focusing the Amazon region, alternatives for the use of the mentioned techniques to estimate rain in area are suggested. Essentially, the possibilities explored range from a radar network to the use of combined radar-satellite techniques and the sole use of satellite imagery. It is also suggested that the radar network be calibrated by a particular statistical procedure. This allows for the determination of radar reflectivity factor - optimized radar reflectivity-rain rate relationships derived from raingauge point measurements in some sites and from a short time series - up to one year of radar observations in the area.

Finally both completed and ongoing research works on the precipitation estimation with satellite imagery for Amazonia, as well as future developments and applications concerning the techniques treated in this article, are commented.

2. WEATHER RADARS AND RAIN ESTIMATION

In essence, the precipitation measurement with weather radars is made through the echo quantification by the returned power received by the radar, that is:

$$Pr = \frac{C L^2 \sum_{j=1}^{n} \sigma_j}{r^2 V} \qquad (1)$$

where

Pr : power returned to the radar by the precipitation;
C : radar constant;
L : one-way attenuation;
r : distance between the precipitation and the radar;
V : volume illuminated by the radiation related to the cell defined by the radar pulse;
σ_j : radar backscattering, or effective, cross section of the i-th hydrometeor. It is defined through $S_i \sigma 4 \pi r^2 S_r$, that is, it is equivalent to the surface that, intercepting the incident wave at the target (hydrometeors) with power density S_i, returns isotropically to the radar the power density S_r, corresponding to what is effectively received by the radar.

It is frequently used in radar meteorology the so-called radar reflectivity factor, Z, which has specific meteorological meaning and is defined by:

$$Z_{e\ H,\ V} = \frac{\lambda^4}{\pi^5\ |K_w|^2} \frac{\sum_{j=1}^{m} \sigma j H, V}{V} \qquad (2)$$

which is the equivalent reflectivity for the non-Rayleigh scattering and for nonspherical droplets, applicable to the C band and to higher frequencies, where:

$Z_{e\ H,\ V}$: radar effective reflectivity factor,for horizontal (H) and vertical (V) polarization, respectively;

λ: radiation wavelength;

$|K_w|$: complex refractive index of water. $|K_w|^2$ varies between 0.91 and 0.93 for λ between 0.01 and 0.10 m and is practically independent of the temperature for the liquid phase. For ice $|K_w|^2$ is about 0.18 for density of 0.917g.cm^{-3}, and it is practically independent of the temperature in the microwave region.

On the other hand,

$$Z = \frac{\sum_{j=1}^{n} D_j^6}{V} \qquad (3)$$

which is the reflectivity for Rayleigh scattering, thus defined when $D_j < \lambda/10$, applicable to the S band frequencies, where:

Z : reflectivity factor;

D_j : diameter of the equivolumetric sphere correspondent to the j-th particle.

The precipitation intensity R is obtained from Z, through the Z x R relation.

The reflectivity factor Z is empirically related to the rain intensity R by the following expression:

$$Z = A\ R^b \qquad (4)$$

where A and b are constants empirically determined which depend on the type of precipitation being observed.

Several factors may introduce discrepancies between the rain intensity measured by the radar and the rain observed at the surface. A list of these factors, classified into three groups, is presented below [3]:

A) Sources of random errors

1) Drop-size distribution (D_i) variability from storm to storm.
2) Drop-size distribution variability inside each storm.
3) Spatial and temporal variability of the precipitation under the cloud base.
4) Precipitation advection.
5) Radar calibration variability.
6) Signal residual fluctuations.

B) Sources of systematic errors

1) Changes presented by the drop-size distribution from the height of the radar measurement to the surface (coalescence, break-up and evaporation).
2) Attenuation.
3) Wet radome.
4) Temporal sampling by the radar.

C) Sources of errors depending on the distance rain-radar

1) Radar sample volume size (V) coupled with the nonuniformity of the reflectivity field.
2) Sample volume height increase as a function of the distance.
3) Minimum detectable signal.
4) Propagation, shadows.

Some verifications concerning the uncertainty of the radar rain estimates at the surface are presented below.

Figure 1 [4] shows the absolute mean difference (absolute value of the mean error) between the accumulated radar rain estimates using one calibration point and "optimum estimates". The "optimum" estimate is considered as the one resulting from measurements made by a high density raingauges network - for example, between 3 and 7 $km^2.(plu)^{-1}$ - employing the radar gradients to interpolate between the raingauges.

The precision indicated in figure 1 is presented in terms of the rain accumulation time and of the area over which the measurements were made. At each hour a new radar calibration was accomplished.

It is verified that, for a given area the error decreases as the accumulation time increases, as a result of the fact that the weather factors, influencing the calibration area, have the tendency of cancelling out as a function of time.

However, if the calibration relation is to be determined over a longer period, e.g. 6 to 12 hours, and used for adjusting the radar measurements over that period, the error can be larger than that exhibited in figure 1. A bias could happen depending on the type of rain falling over the raingauge used for calibration. Therefore, a significant portion of the precipitation detected by the raingauge, over a long period of time, may be due to a small storm of short duration, while most part of the rain falling over the area of interest may be caused by the widespread rain.

Given that the calibration factors for the two types of rain may differ, it would not be appropriate to extend the calibration to the whole area.

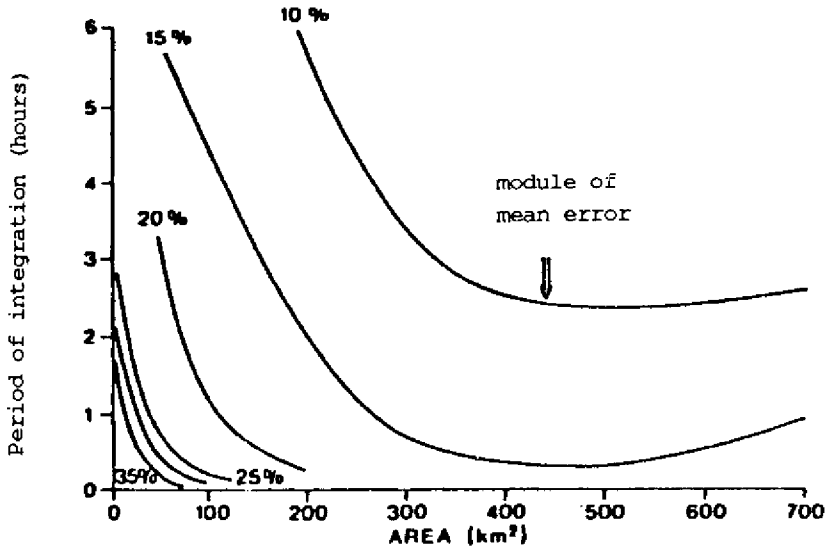

Figure 1 - Absolute mean difference (absolute value of the mean error) between the radar estimates of accumulated rainfall (Collier, 1975).

In figure 1 it is observed that, for a fixed period of integration, the error decreases as the measurement area increases. As this area increases, the errors due to the calibration pluviometer representativeness tend to cancel out but, if the area is so large such that the pluviometer is no longer representative, the error increases.

Figure 2 presents the average difference between the "optimum", or "real", rain estimates computed for Wales (United Kingdom), as a function of the raingauges number [4]. The radar estimates accuracy are presented for sites of calibration (with raingauges) distributed in 1000km² area and for the estimates accuracy determined with the raingauge network only.

It is observed that the radar measurements for this area, calibrated by more than one raingauge, usually have an accuracy within 20%. The radar-raingauge systems are superior to the raingauge network alone, specially in the case of heavy rain occurrences. For typical heavy rains, a radar-raingauge system employing two calibration sites yields the same accuracy as a 50 raingauges network in 1000 km².

The analysis presented in figures 1 and 2 were adapted of [5].

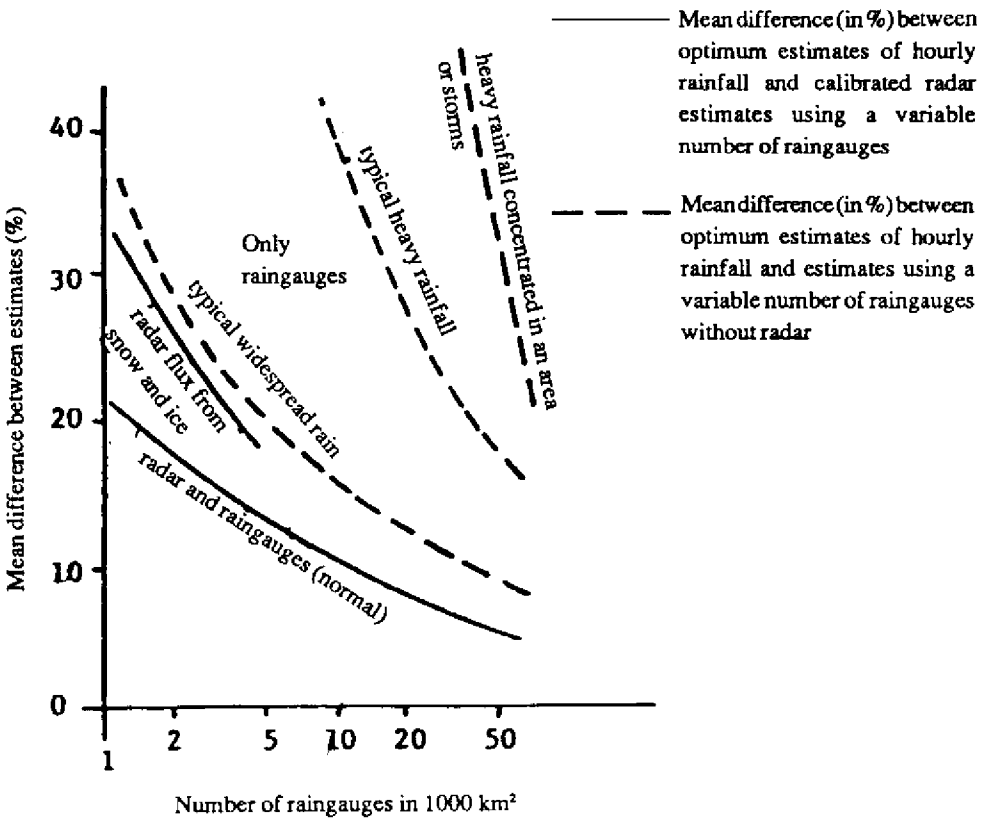

Figure 2. - Difference between hourly rainfall estimates in function of the raingauges network density (Collier, 1975).

Some techniques aiming at improving rain estimation with radar, which only add information to the reflectivity measurements, are mentioned below [6].

Doppler Radar - It is based on the radiation frequency shift that returns to the radar as a function of the hydrometeors radial motion. Probably, the main advantage of the Doppler techniques for precipitation measurements resides in the solution of some problems caused by ground echoes and by anomalous propagation. Among the new radar techniques this is the only one largely accepted by both, users and industry.

Polarization Diversity Radar - The polarization diversity techniques make use of the different polarization states presented by the emitted as well as by the received radiation.

The value of these techniques to improve the rain intensity estimation is widely recognized and the state of the art allows the implementation of reliable equipments, at a reasonable cost. However, some problems concerning long distance observations and the automatic interpretation of the observable parameters remain unsolved; there is also the need for training users and operators.

In the scope of the European radar network (Cost-73) some actions are being taken regarding the additional data obtained by the advanced radars and the industry already started to deal with these techniques.

Dual Frequency Radar - This technique is based on the simultaneous use of two separated radiation frequencies. The radars operating in dual frequency are not adequate for operational purposes when extensive coverage - superior to 100km radius - and stable measurements are required, so the technique gets restricted to research in limited areas of special interest.

Frequency Agility - The frequency agility technique is fundamented in the frequency shifts between pulses providing echoes instantaneous decorrelation. It allows a faster acquisition of echoes independent samples and a high stability of ground echoes maps.

Its use remains restricted to research purposes.

Fast Scanning Radars - This type of radar uses electronic scanning antennas, permitting the fast localization of intense cells and the simultaneous monitoring of various independent cells, through the use of multiple beams.

There are industries developing prototypes but availability and practical use of this type of radar is not expected before the end of the next decade. Besides, cost expectations may restrict their use only to special situations.

In this context, it is also important to consider the area-time integral (ATI) [7] and the vertically integrated liquid water content (VIL) [8] techniques.

The first provides a simple method to estimate, or to verify, the precipitation quantities from a strong relation found between the area covered by rain during its duration and the respective volume; the second uses the vertical integration of the liquid water content and still is to be determined how the VIL can be compared to the rain estimation directly measured from the reflectivity Z.

3. METEOROLOGICAL SATELLITES AND RAIN ESTIMATION

Meteorological satellites remote sense the Earth from two main types of orbit, the quasi-polar sun-synchronous and the geosynchronous, the first promoting global coverage every 12 hours and the second, stationary, always observing the same disc of the planet. Figure 3 presents a geostationary satellite image.

The present operational sun-synchronous satellites belong to the TIROS-N/NOAA series and several advances that may be useful for rain estimation, such as an increased number of microwave channels, shall be introduced in 1992. The quasi-polar orbit makes feasible from the cost viewpoint the on board satellite utilization of heavy equipments as the microwave radars [9].

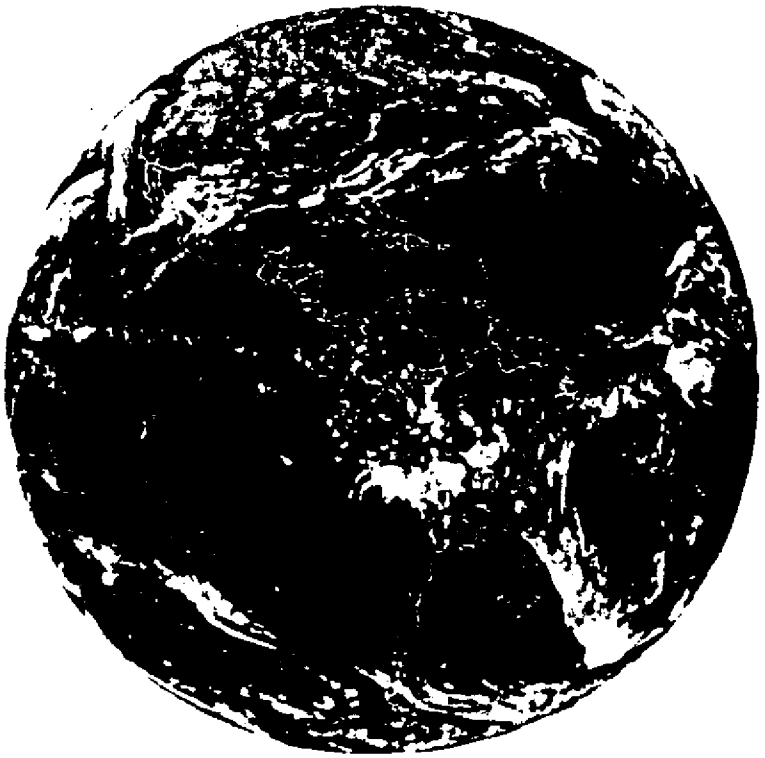

Figure 3 - GOES satellite image transmitted at 09h 47min UT, Dec. 26, 1978, and received at INPE. The sub-satellite point is 75° W.

Of major interest for the South American regions are the GOES series geostationary satellites. The image of figure 3 shows how the GOES satellite, when located in its normal position at 75° W, favors the visualization of phenomena over Brazil, and in particular, over Amazonia. The following series of these satellites, GOES-Next or GOES I-M, will bring important innovations such as a better spatial resolution and a greater number of channels.

Among the future space missions stands out the Earth Observing System (EOS) of the USA agencies NASA and NOAA. EOS, which shall be implemented through polar orbiting and geostationary platforms, is part of the Mission to the Planet Earth. Under this program, the Tropical Rainfall Measuring Mission (TRMM) is of special interest for Hydrology.

Based on previous experiments, TRMM satellite will carry on board three main instruments: a weather radar, a passive microwave radiometer and a visible and infrared imager similar to the AVHRR operating on the TIROS-N/NOAA satellites. Therefore, TRMM will bring in means, never

available before, to validate and calibrate rainfall estimation algorithms based on imagery regularly obtained by the operational meteorological satellites. With launching predicted for 1994 and a useful life of about three years, TRMM will have a circular orbit of 350 km height and 35° of inclination in relation to the equatorial plane [10].

Several rainfall estimation techniques using visible and thermal infrared cloud cover imagery, all of empirical nature, have been conceived since the beginning of the meteorological satellites program in the 60's, and upgraded along the years (Barret and Martin [11]; Wu et al. [12]; Martin and Howland [13]; Adler and Negri [14]; Simpson [10]; França [15]).

Depending on whether a technique is based on geostationary data or on polar-orbiting satellite data, several important facts concerning the nature of rain clouds are used in the estimation scheme (Woodley et al., quoted by Smith [16] and Scofield [17]):

1. Bright clouds in the visible imagery produce more rainfall than darker clouds.
2. Bright clouds in the visible imagery and clouds with cold tops in the infrared imagery that are expanding in areal coverage (in early and mature stages of development) produce more rainfall than those that are not expanding.
3. Decaying clouds produce little or no rainfall.
4. Clouds with cold tops in the infrared imagery produce more rainfall than those with warmer tops.
5. Clouds with cold tops that are becoming warmer produce little or no rainfall.
6. Merging of cumulonimbus clouds increases the rainfall rate of the merging clouds.
7. Most of the significant rainfall occurs in the upwind (at anvil level) portion of a convective system. The highest and highest clouds form where the thunderstorms are more vigorous and the rain heaviest. These cold clouds get thinner downwind and look warmer in infrared imagery as the anvil material blows away from its origin over the updraft.

According to Smith (1985) [16], "from a consideration of the precipitation process in the context of visible/infrared sensing, it is apparent that the primary leverage for the satellite lies in measurements of five cloud parameters: the temperature of the top, the thickness, the phase, the speed of the updraft, and the age of the cloud. Rain has structure. Thus, additional information on the likelihood and intensity of rain can be gained from measurements of gradients, patterns, and textures of brightness about a point for which rain is to be measured".

Therefore, the satellite rain estimation techniques may be of several kinds and present varying degrees of complexity. Some, as the Arkin technique, may be very simple, the fundaments being just the vertical development of convective clouds. As discussed above, the rainfall likelihood generally increases as the cloud top gets higher (and thus colder). The algorithm may be of the type "rain/no rain", according to a threshold established in terms of the infrared imagery digital counts, [14]; [18]. Other techniques are more involved, as the ones which applies pattern recognition to multispectral digital imagery of high spatial resolution [12]; [13]. Or yet, as in the case of the convective-stratiform technique (CST), they may include physical concepts through parameterization based on cloud models, besides discrimination criteria between stratiform and convective rain established with the help of radar data, [14]; [18].

In general, the satellite rain estimation methods may be, on one hand, either automatic or interactive, and, on the other hand, either a life history or a cloud index type. For the interactive techniques implementation, which presumes human intervention, it is essential the availability of working stations which, by the way, is the most appropriate computer environment in the present context. The life history methods, contrary to the indexed methods, take into account the time evolution of the rain systems and, therefore, only make sense if a sequence of images obtained in short time intervals (as, for example, the ones obtained every half hour by the geostationary satellites) is to be employed.

The Arkin and the CST techniques, mentioned above, are examples of indexed automatic methods. The Scofield technique [17], on the other hand, is a typical example of a life history interactive method.

According to the state of the art, the success of satellite rain estimation techniques varies as a function of the objective and of the type of rain to be detected, being possible to distinguish, with high reliability, situations of rain and no rain. However, the rainfall quantification still poses difficulties, calling for more detailed studies and adequate calibration techniques.

On the other hand, the input for the vast majority of river runoff prediction models is the average areal precipitation over the basin. Thus, the parameter of interest is areal rainfall; in this regard, the satellites may be more successful than when point values are required, as discussed by Schultz [2]. According to Strübing and Schultz [19], another promising alternative is the use of satellite data (radiances) directly to determine river runoff, instead of estimating rainfall as an intermediate step.

4. REMOTE SENSING OF RAIN IN AMAZONIA WITH RADAR AND SATELLITE

This article is essentially concerned with the so-called Legal Amazonia, as delineated in figures 4 and 5.

The annual average rainfall is shown in figure 5 [20]. The low lands of the Amazonas state and the Amapá state, on one hand, and the high lands of the Amazonas state and of the Negro river, on the other hand, are included among the main rainfall areas in Brazil [21].

The rainfall distribution in Amazonia may be briefly described as follows:

a) In the Iauretê region (NW) the regime is almost uniform presenting an annual mean above 3500mm, with average frequency higher than 240 rainy days per year. The wettest period extends from March to July. The following approximate numbers for the "maximum rain/minimum rain (mm/mm)" ratio are verified: Iauretê - Cachoeira (450/250), São Gabriel da Cachoeira (300/160) and Fonte Boa (300/135). These are monthly values.

b) In the Amapa coast the annual mean rainfall is higher than 3000mm and the regime is such that the wettest period - January to May - concentrates more than 70% of the annual total and a dry period is from September to November. The average number of rainy days during the year is over 240 and some approximate numbers for the "maximum rain/minimum rain" ratio are: Oiapoque (500/75) and Amapá (650/50).

c) In the areas of intermediate rainfall values corresponding to Central Amazon the annual values are higher than 2000mm and the average number of rainy days is over than 120 days/year. There is a seasonal variation, raining more in the period from December to April. Some approximate numbers for the "maximum rain/minimum rain" ratio are: Porto Velho (300/25), Manaus (350/50) and São Felix do Xingu (340/25).

d) In the areas of low rainfall values, it rains in average less than 1500mm, the annual number of rainy days being inferior to 60. There is a seasonal variation, with dry and wet periods (June-July-August and Dec.-Jan.-Feb., respectively) under the same influence of the air masses displacements verified in the Amazonia central part. As an example, for Cuiabá the approximate number for the "maximum rain/minimum rain" ratio is 200/7.

The convective systems are responsible for large quantities of precipitation in the Amazon Region; studies have shown that, among these systems, the instability lines are responsible for about 45% of the rainfall in the east of the Pará state (Cutrim, cited by Cohen [22]) during the wet period. In addition, according to Cohen [22], Molion and Kousky [23] have indicated that the instability lines are determinant to the rainfall distribution in Amazonia.

Cohen [22] also shows that the majority of the instability lines with intensities varying between average and strong, studied by her, occurred between April and July, the propagation being from the coast to the west reaching up to 2000km inland.

During the GARP (Global Atmospheric Research Program) Atlantic Tropical Experiment (GATE) and the Venezuelan International Meterological and Hydrological Experiment (VIMHEX), it was possible to verify that the observed instability lines cross sections presented radar echoes up to an approximate level of 15km [24].

In the final part of her study Cohen recommends weather radars installation in Amazonia in order to "better understand the structure and quantitatively predict the rainfall produced by the convective systems in the Amazon Region, as well as the displacement speed of the convective cells".

An alternative for rainfall monitoring in Amazonia is the implementation of a radar network, as sketched in figure 4. In this proposed configuration, with average range of 460km, the beam will be illuminating a storm region located over the radar, or adjacent radars, at about 12.5km asl, this contributing to minimize the problems posed by the ground echoes and nearby radar obstacles. The range of 240km considered in figure 4 is the one for which the beam still is below the 0° isotherm, with no interception of the melting layer (brilliant band). The radar positioning was conceived having in mind the minimization of possible terrain obstructions taking into account the large scale topography, and it is only indicative of the location sites based on a 460km grid.

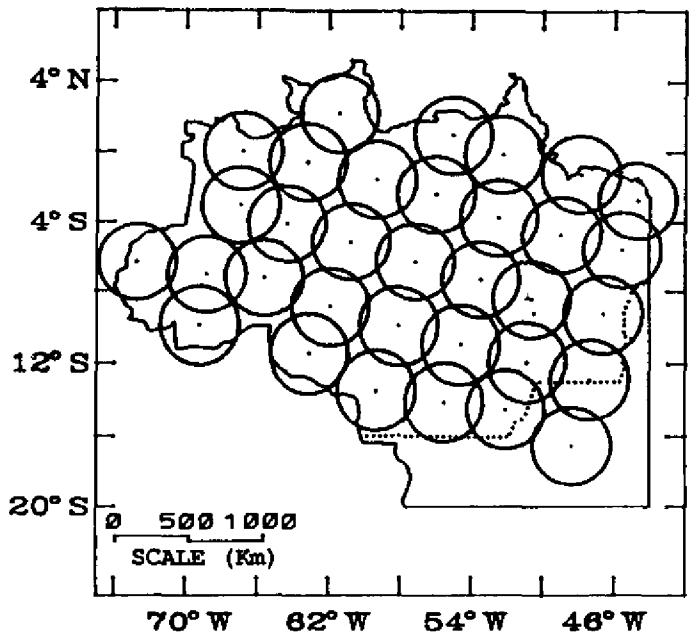

Figure 4 - Radar Network for rain estimation in Amazonia, with registered range of 240km. The dotted line delimitates the Legal Amazonia.

The statistical method proposed by Calheiros and Zawadzki [25], based on the equivalence of the cumulative probability levels of Z and R, that is:

$$\int_{Z}^{\infty} p(Z)dZ = \int_{R}^{\infty} p(R)dR \qquad (5)$$

provides the means to calibrate radars according to the distance for areal rainfall quantification having in mind hydrological purposes after the first year of operation. The corresponding Z x R relations must be stratified as a function of the regional rainfall climatology, as presented above.

In this realm, another possibility that may be considered is to employ the approach proposed by Trovati [26] where the river runoff Q and the reflectivity Z bear a direct relationship.

A second alternative for monitoring rain in Amazonia is the real time composition of radar and satellite imagery. This is based on the procedure adopted by the RAINSAT [27] developed at the McGill University.

The essence of this technique is to compute the rainfall probability distribution:

$$P_{RS}(IV,V) = \frac{R_R(IV,V)}{R_R(IV,V) + R_{NR}(IV,V)} \quad (6)$$

where:

IV and V are the thermal infrared and visible count values in the satellite imagery;
$R_R(IV,V)$ is the number of rainfall events with (IV,V) associated values; and,
$R_R(IV,V) + R_{NR}(IV,V)$ is the total number of points in each (IV,V) interval.

This relation is derived from (IV,V) values within the radar range being used to calibrate the satellite and assumed valid for the whole satellite imagery.

A preliminary proposal for the calibration radars is presented in figure 5, considering the regional rainfall climatology. As in the previous proposition regarding exclusively a radar network, the radar positioning is only approximate.

Finally, the use of satellites alone is another alternative to be considered to monitor rainfall in the Amazon Region.

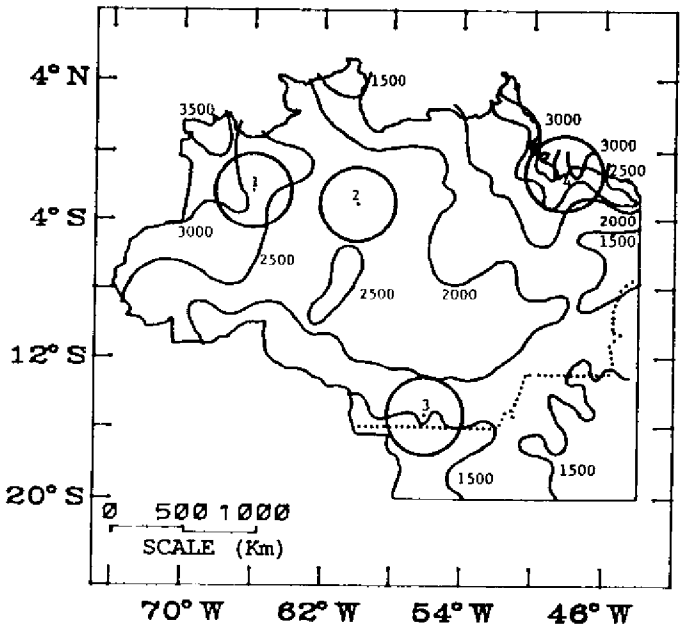

Figure 5 - Radar Network for calibration of satellite imagery in the Amazon Region with the goal of estimating rainfall, and isohyets (annual mean, mm). The numbers are indicative of the radar positions: 1 = Fonte Boa, 2 = Manaus, 3 = Cuiabá, 4 = Belém. The range presented by the radars is 240km. The dotted line delimitates the Legal Amazonia.

5. COMMENTS AND CONCLUSIONS

The works of Brazilian authors on satellite rainfall estimation started with Cutrim [28] with the purpose of computing monthly rainfall values making use of GOES imagery. Presently, it deserves mention the research program being conducted about Amazonia at the University of Wisconsin, in Madison, which includes satellite rainfall studies, among other issues of relevance for the understanding of the hydrologic cycle in this region [29]. Goodman et al. [30], based on previous research works including the one by Cutrim [28], developed the Infrared Power Law (IPL) algorithm that correlates the 3-hour raingauge observed precipitaion with thermal infrared GOES digital imagery counts.

According to Achtor [29] the IPL algorithm is successful in the case of heavy precipitation events (greater than 15mm/day), but is deficient in detecting small precipitation rates and no-rain cases. It also tends to overestimate the rainfall area, pitfall which can only be overcome by the simultaneous use of other channels and/or ancillary information such as radar data.

Out of the three alternatives presented in item 4 for the rainfall remote sensing in Amazonia, the one which combines radar and satellite is possibly the most appropriate, taking into account costs, difficulties regarding the logistics in the region and the requirements posed by the rainfall estimation for hydrological purposes. Regarding radar calibration, the procedure involving the use of pluviometers in real time is problematic, given the rainfall nature and the difficulties presented by the area. However, in any case, the raingauge network support still is fundamental for the remote sensing techniques.

The radars shall operate in S band, being recommended that they are built to easily allow the addition of further techniques, such as the Doppler processing. In this regard, it is important that the equipments present high sensitivity in order to detect the convergence lines from which the storms may develop.

It is important to notice here the possibilities for nowcasting (typical leading times of about 2 hours) which can be made with radars, particularly for weather systems such as the instability lines which develop in the region. A possible stratification of the Z x R relations as a function of the day time shall be investigated.

The effective use of satellite rainfall estimation techniques in Amazonia and the adequate preparation to benefit from future space missions, specially TRMM, are feasible actions which must be implemented in the near future.

6. ACKNOWLEDGEMENTS

The authors wish to thank Dr. Maria Assunção Faus da Silva Dias for the useful discussions about the rainfall mechanisms in Amazonia, Marlene Sueli Moya for typing the text, and the computer software group of IPMet/UNESP for editing the figures shown in item 4.

7. REFERENCES

[1] IAHS. Report on the presentations by the Session Chairman at the Oxford Symp. on Hydrological Forecasting. April, Hydrologial Sciences Bulletin. Vol. 25, n. 4. 1980, 366-8.

[2] Schultz, G. A. Remote Sensing in Hydrology. Journal of Hydrology. Vol. 100, n. 1/3. 1988, 239-65.

[3] Zawadzki, I. Factors Affecting the Precision of Radar Measurements of Rain. In: 22nd. Conference on Radar Meteorology. Zurich, AMS (10-13 Sept., 1984).

[4] Collier, C. G. Rainfall Measurements by Radar. Proceedings, Symposium on Weather Radar and Water Management. Water Research Centre. Medmenham, England. 1975.

[5] Barge, B. L. and Humphries, R. G. Precipitation Measurement by Weather Radar - A Review. Atmospheric Sciences Report 78-1. Alberta Research Council. 1978.

[6] Randeu, W. L. New Weather Radar Techniques: Ready for Operational Use? In: Collier, C. G. and Chapuis, M. (eds.). Weather Radar Networking - Seminar on Cost Project 73 - Brussels (Klumer Academic Publishers, 1990).

[7] Doneaud, A. A.; Ionescu-Niscov, S.; Priegnitz, D. L. and Smith, P. L. The Area-Time Integral as an Indicator for Convective Rain Volumes. Journal of Climate and Applied Meteorology. Vol. 23, n. 4. 1984. 555-61.

[8] Greene, D. R. and Clark, R. A. An Indicator of Explosive Development in Severe Storms. Preprints, Seventh Conf. on Severe Local Storms, Kansas City, AMS. 1971. 97-104.

[9] Hussey, W. J. The TIROS-N Twins are Coming. NOAA Magazine. Vol. 8, n. 2. 1978.

[10] Moura, A. D. and Ferreira, M. E. Meteorologia, as Perspectivas de Plena Capacitação. Revista Brasileira de Tecnologia (MCT/CNPq). Vol. 18, n. 4. 1987. 15-25.

[11] Barret, E. C. and Martin, D. W. The Use of Satellite Data in Rainfall Monitoring. (Academic Press, 1981).

[12] Wu, R.; Weinman, J. A. and Chin, R. T. Determination of Rainfall Rates from GOES Satellite Images by a Pattern Recognition Technique. Journal of Atmospheric and Oceanic Technology. Vol. 2. 1985. 3124-330.

[13] Martin, D. W. and Howland, M. R. Grid History - A Geostationary Satellite Technique for Estimating Daily Rainfall in the Tropics. Journal of Climate and Applied Meteorology. Vol. 25. 1986. 184-95.

[14] Adler, R. F. and Negri, A. J. A Satellite Infrared Technique to Estimate Tropical Convective and Stratiform Rainfall. Journal of Applied Meteorology. Vol. 27, n. 1. 1988. 30-51.

[15] França, G. B. Determinação de áreas de Chuva e Não-chuva na Imagem do Satélite GOES Utilizando Análise de Grupamento. Dissertação de Mestrado em Análise de Sistemas e Aplicações. INPE, São José dos Campos (Jan. 1989).

[16] Smith, W. L. Satellite. In: Houghton, D. D. (ed.), Handbook of Applied Meteorology. (John Wiley, N. Y., 1985).

[17] Scofield, R. A. The NESDIS Operational Convective Precipitation Estimation Technique. Monthly Weather Review. Vol. 115, n. 8. 1987. 1773-92.

[18] Moraes, J. C.; Ferreira, M. E. and Conforte, J. C. Estimativa de Precipitação por Meio de Satélites Meteorológicos: Uma Avaliação das Técnicas GS, NAW e ARKIN. In: Anais, Simpósio Brasileiro de Recursos Hídricos, 8. Foz do Iguaçu, Nov. 26-30. 1989.

[19] Strubing, G. and Schultz, G. A. Estimation of Monthly River Runoff Data on the Basis of Satellite Imagery. Hydrological Applications of Remote Sensing and Remote Data Transmission. (Proceedings of the Hamburg Symposium, August, 1983). IAHS Publ. n. 145.

[20] Ministério do Interior. Atlas Climatológico da Amazônia Brasileira. Belém. 1984.

[21] Ratisbona, L. R. The Climate of Brazil. In: Schwerdtfeger, W. (ed.). World Survey of Climatology. Vol. 12. (Elsevier Scientific Publishing Company, 1976).

[22] Cohen, J. C. P. Um Estudo Observacional de Linhas de Instabilidade na Amazônia. Dissertação de Mestrado em Meteorologia. INPE, São José dos Campos. 1989.

[23] Molion, L. C. B. and Kousky, V. E. Climatologia da Dinâmica da Troposfera Tropical sobre a Amazônia. INPE, São José dos Campos. (Junho 1985).

[24] Garnache, J. F. and Houze Junior, R. A. Mesoscale Air Motions Associated with a Squall Line. Monthly Weather Review. Vol. 110, n. 2. 1982. 118-35.

[25] Calheiros, R. V. and Zawadzki, I. Reflectivity-Rain Rate Relationships for Radar Hydrology in Brazil. Journal of Climate and Applied Meteorology. Vol. 26, n. 1. 1989. 118-32.

[26] Trovati, L. R. and Mattos, A. A Radar Reflectivity-Runoff Model for Use in Flood Warning. In: Collier, C. G. and Chapuis, M. (eds.). Weather Radar Networking - Seminar on Cost Project 73 - Brussels (Kluwer Academic Publishers, 1990).

[27] Bellon, A.; Lovejoy, S. and Austin, G. L. Combining Satellites and Radar Data for the Short-Range Forecasting of Precipitation. Monthly Weather Review. Vol. 108, n. 3. 1980. 1554-66.

[28] Cutrim, E. C. M. Estimating Monthly Rainfall from Geostationary Satellite Imagery over Amazonia, Brazil. Ph. D. Dissertation, University of Michigan, Ann Arbor.

[29] Achtor, T. Investigating the Amazon Hydrologic Cycle. CIMSS View Vol. VI, n. 1. 1990. 1-11.

[30] Goodman, B. M.; Menzel, W. P.; Cutrim, E. C. M. and Martin, D. W. A Power Law Algorithm for Estimating Three-Hourly Rain Rates over Amazonia from GOES/VISSR Observations. To be sumitted for publication in the Journal of Applied Meterology.

POSSIBLE CLIMATIC IMPACTS OF AMAZONIA DEFORESTATION *

Carlos A. Nobre **

ABSTRACT

Large-scale conversion of tropical forests into pastures or annual crops will likely lead to changes in the local microclimate of those regions. Larger diurnal fluctuations of surface temperature and humidity deficit, increased surface runoff during rainy periods and decreased runoff during the dry season, and decreased soil moisture are to be expected. It is likely that evapotranspiration will be reduced because of less available radiative energy at the canopy level since grass presents a higher albedo than forests, also due to reduced availability of soil moisture at the rooting zone primarily during the dry season.

Coupled numerical models of the global atmosphere and biosphere have been used recently to assess the effects of Amazonia deforestation on the regional and global climate. The results from these GCM simulations show that if the tropical forests were replaced by degraded grass (pasture) in the model, there was a significant increase in surface temperature and a decrease in evapotranspiration, precipitation and runoff. There was also an increase in the length of the dry season which can have serious implications for the re-establishment of the tropical forests in the cleared areas.

Global climate changes probably will occur if there is a marked change in rainfall patterns in tropical forest regions as a result of deforestation. It was also seen that tropical deforestation in Southeast Asia is less likely to cause large-scale changes in precipitation of that region. On the other hand, removal of Equatorial Africa's tropical forests might result in equatorward expansion of the semi-arid zones to the north and south of the rainforests.

1. INTRODUCTION

The distribution of global vegetation has traditionally been thought to be determined by local climate factors, primarily precipitation, radiation, and temperature and by soil type, in particular its water holding capacity. For instance, the bioclimatological view held that rainforests would exist in high rainfall tropical areas with short or nonexistent dry seasons where soils physical properties ensue high levels of available soil moisture throughout the year. In turn, the mechanisms giving rise to semi-continuous and high rainfall rates throughout the year for those regions were thought to be solely due

---

* *Parts of this work were based on 'Possible Climatic Impacts of Tropical Deforestation', by E. Salati and Carlos A. Nobre to appear in Climatic Change, and on 'Amazonia Deforestation and Regional Climate Change', by C. A. Nobre, P. J. Sellers and J. Shukla (in preparation).*

** *CPTEC/INPE, Brazil*

to the general circulation of the atmosphere and not dependent on the underlying vegetation. This view has been modified in the last 15 years because controlled numerical experiments with complex models of the atmosphere showed that the presence or absence of vegetation can influence the regional climate, see for example the work of Charney *et al.* (1977), Shukla and Mintz (1982), and a review of GCM experiments of land surface processes in Mintz (1984), and Rowentree (1988). One implication of these results is that the current climate and vegetation may co-exist in a dynamic equilibrium that could be altered by large perturbations in either of the two components.

Deforestation is rapidly progressing in Amazonia. Several sources (Fearnside, 1989; Brasil, 1989; Mahar, 1989; and Setzer *et al.*, 1988) indicate that deforestation rates for the Brazilian Amazonia are between 30,000 and 45,000 km^2 a year. If deforestation were to continue at this rate, most of the Amazonian tropical forests would disappear in 50 to 100 years. One question that arises is whether the large-scale deforestation in Amazonia might affect the regional climate with consequent implications for the biota in the region.

Conversion of tropical rainforests into a different vegetation, most notably pastures or annual crops, inevitably entails major changes in the ecosystem. There appears to be a consensus that this type of conversion changes the flora, the aquatic and land fauna, and the physico-chemical and biological characteristics of the soil and surface waters. There also appears to be agreement that qualitative and quantitative changes are caused in the biogeochemical cycles.

Yet, when analyzing the climatic impacts involved or associated with conversion of tropical rain forests into pastures, the question becomes controversial. This is due to several factors, including in particular the difficulty of quantifying the components of the energy and water balances in the undisturbed and disturbed ecosystems, and the difficulty of developing climate models at the regional level that will permit reliable predictions based on the changes of land use patterns to be introduced.

Quantitatively estimating the effects that large changes in terrestrial ecosystems can have on temperature, circulation and rainfall has been difficult because the equilibrium climate is determined by complex interactions among the dynamical processes in the atmosphere and thermodynamic processes at the Earth-atmosphere interface.

Removal of the Amazonian forest also would have tremendous effects on species diversity and atmospheric chemistry (Houghton, 1985). The Amazon basin is host to roughly half of the world's species, and the intensity and complexity of plant-animal interactions (Mori and Prance, 1987) and the rapid nutrient cycling in the soils (Días and Nortcliff, 1985) makes the region vulnerable to external disturbances. The Amazon is also an important natural sink of ozone and plays an important role in global tropospheric chemistry, including the injection of large amounts of CO_2 into the atmosphere from biomass burning (Fearnside, 1989; Crutzen and Andreae, 1990). The present study is mainly confined to the assessment of the effects of deforestation on the physical climate system.

A number of ecological factors are important in maintaining the forest in place in addition to climatic considerations. These include the complexity and intensity of inter-species relationships (e.g.; association of particular tree species with insect or vertebrate pollen or seed vectors), the dynamics of gap exploitation by young emerging trees and the maintenance of soil microclimate and physical environment (warm, moist well-structured soil) conducive to a dense and active soil fauna population, ranging from bacteria and fungi to earthworms and beetles. All of these ecological factors are vulnerable to changes in climate but they are also very sensitive to the forest patch size; it has been

demonstrated that below a minimum patch size, complex ecological communities rapidly 'lose' species and disintegrate to less diverse and more vulnerable communities. Clearly then it is not only the extent but the geometry of the deforestation that is important in terms of the future of the tropical forest biome.

The rain forest presents unique characteristics, such as low albedo, high rates of evapotranspiration and nutrient recycling, large roughness to the surface airflow, large water holding capacity of soils, in its interactions with the atmosphere above. These characteristics combine to maintain, in principle, a higher level of precipitation than would exist otherwise with a different type of vegetation such as savannah. Considering that evergreen rain forests exist only in places where monthly precipitation is not less than about 100 mm in the driest months (Prance, G., 1986), then this strategy acts like a positive feedback for maximizing the forest's chance of survival, that is, the forest-atmosphere interaction acts in the direction of perpetuating the forest (of course, under the primary control of the general circulation of the atmosphere since there is a limit to the rainforest-induced increase in precipitation; Nobre *et al.* (1990) suggest that this limit is of the order 20% to 30% when compared to a grassy vegetation cover). Now the transition areas (forest to savannah) to the east, south and north of Amazonia, where the dry season is longer and more pronounced, would be the first to be affected by a drier climate following massive deforestation. Those are the areas where intense clearings are taking place in southern and southwestern Amazonia.

Interannual variability of precipitation in Amazonia is large as revealed by the river streamflow record. A large part of this variability is linked to ENSO events (Richey *et al.* 1989; Nobre and Oliveira, 1986). There are also reports showing that during severe dry spells in Amazonia extensive forest fires can occur (ref. cited in Sternberg, 1987). These infrequent, intense and long dry spells are usually linked to the simultaneous occurrence of intense ENSO episodes (Nobre and Nobre, 1990). However, the forest appears to be adapted to withstand these large interannual variations in precipitation and the sporadic occurrence of forest fires. Even at the boundaries of the forest, where the interannual variability is more pronounced, migration of the forest border is not observed.

A question that can be asked is if the meteorological record has shown any changes so far which can be attributed to tropical deforestation. The forest clearings to date are not contiguous but spread over large areas, mostly along the region's roads. Given the yet somewhat small percentage of total deforestation and the fact that it is scattered over a large area, one would not expect large changes in the basin-scale hydrological cycle to have been already detected. Amazon streamflow integrates the effect of rainfall over a large area of tropical forest. It can serve therefore to detected man-induced changes in the hydrological cycle. To date, almost 90 years of riverflow data for a point near Manaus shows only what appears to be natural variability (Richey *et al.* 1989). Even the tendency for higher water levels in the Amazon river from 1964 through 1976, that lead Gentry and Lopes-Parody (1981) to conclude that it was the result of deforestation, was shown to be result of large-scale precipitation changes at decadal time scales (Rocha *et al.* 1989). However, on the local scale, deforestation has shown to cause significant changes in the surface and sub-surface climate for a site in Nigeria (Lawson *et al.* 1981) and Suriname (Shulz, 1960).

2. WATER BALANCE OF THE AMAZON BASIN

The water balance of the Amazon basin is difficult to determine due to the lack of basic data systematically collected over time and space. However, using existing data some attempts have been made to quantify the water fluxes involved.

The observed distribution of precipitation in tropical South America shows broad areas where annual values reach 3 m or more: on the eastern Andean slopes and on the western coast of Colombia annual totals in excess of 5 m are due to the mechanical uplifting of the low level airflow due to the topography; along the Atlantic coast from Guianas to the state of Maranhão, in Brazil, westward propagating sea-breeze squall lines account for the observed large precipitation values (in excess of 3 m annually); the reasons for the broad precipitation maximum found over the western part of Amazonia are not well understood but there has been a suggestion (Nobre, 1983) that the concave shape of the Andes Mountains to the west of the precipitation maximum may favor convergence of the low level, predominantly easterly, moisture-laden flow. Besides these, there is an elongated secondary precipitation maximum, where annual values are above 2 m, extending from southwestern Amazonia toward the southeast and joining with the high precipitation area of the South Atlantic Convergence Zone (SACZ). This secondary maxima marks the northernmost position of frontal systems propagating equatorward from mid-latitudes of the Southern Hemisphere and it is a preferred position for frontal systems to remain quasi-stationary. The dynamics of the interactions between these frontal systems and tropical convection is not well understood.

The mechanisms that explain the various precipitation maxima mentioned above are apparently linked to the general circulation of the atmosphere or other local or mesoscale forcing (topographic uplifting, diurnal land-sea temperature contract) and do not depend to a first approximation on the underlying vegetation cover. It is likely that precipitation maxima would exist in those areas even in the absence of the rainforest (although at a perhaps different intensity and temporal distribution).

This line of reasoning could suggest that the forested surface plays secondary role as a climate forcing factor. However, there is a wealth of observational evidence pointing otherwise. Table 1 summarizes the results of 14 studies dealing with water budget calculations for the Amazon basin: (i) on the basin-wide scale, several independent calculations of real evapotranspiration (see a review of those calculations in Salati and Nobre, 1990) all show that evapotranspiration accounts for more than 50% of precipitation; (ii) evapotranspiration model constructed from measurements at a micrometeorological tower near Manaus, Brazil, for more than 2 years (Shuttleworth, 1988) showed an average flux of water vapor into the atmosphere of 3.6 mm/day whereas the average precipitation was 7.2 mm/day.

Recently, during the Global Atmospheric Experiment - Amazon Boundary Layer Experiment (ABLE-2B), conducted in Amazonia during April-May 1987, upper air data from 6 aerological stations in the Brazilian Amazonia was collected 4 times a day (00, 06, 12 and 18 UT) during a 1-month period (13 April - 13 May, 1987). Based on this data, water balance estimates have been made for the area covered by the aerological stations (approximately 2.2 million km^2). Average precipitation in that area, collected in over 150 raingauges and for that 1-month period, was 290 mm; the calculated convergence of atmospheric water vapor transport was 127 mm. The variation of water vapor in that volume (storage term) during that 1-month period was -6 mm, i.e., there was a slight drying from the

beginning to the end of the period. The area and time averaged evapotranspiration can then be estimated as the residual term in the atmospheric water budget equation (storage term - convergence term - evapotranspiration - precipitation), resulting in 157 mm of evapotranspiration, or about 54% of precipitation, which again shows the importance of water vapor recycling in Amazonia.

Taken together, all the available observational evidence seems to suggest that the Amazonian rainforest is highly efficient in recycling water vapor back into the atmosphere. A different type of vegetation such as degraded pasture might not be as efficient in maintaining high rates of evapotranspiration. That, with other changes, may indicate that the existence of a significant sensitivity of the regional climate to the presence or absence of the tropical forest.

3. MODEL SIMULATIONS OF AMAZONIAN DEFORESTATION

Quantitatively estimating the effects that large changes in Amazonian ecosystems can have on the surface energy and water budgets has been difficult because the equilibrium climate is determined by the momentum and energy exchanges at the Earth-atmosphere interface, interacting with complex dynamical processes in the atmosphere. Results of earlier model studies were generally inconclusive, and sometimes conflicting, about the regional (and global) climate changes following deforestation. The models were of two types: either energy-box models (Lettau *et al.* 1979, Potter *et al.* 1975) or crude resolution GCM's (Henderson-Sellers and Gornitz, 1984). In general, the latter lacked both spatial resolution and an adequate treatment of the land surface processes. For instance, their resolution was typically 10 deg. long. x 5 deg. lat. which would make the whole Amazonia to be represented by a few grid-points. Also their representation of evapotranspiration processes was based on a 'bucket hydrology' parameterization. This parameterization was inadequate to represent evapotranspiration processes over vegetated surfaces (Sellers *et al.* 1986) and makes it difficult to represent the complex changes in soil hydrology following burning and land clearance. Henderson-Sellers (1987, her Table 1, p. 468-469) summarized the main results from these earlier model studies.

Realistic models of biosphere have only recently been developed that can be coupled with realistic models of the global atmosphere (Dickinson *et al.* 1986, Sellers *et al.* 1986). The pioneering work of assessing climate impacts of tropical deforestations using these novel coupled biosphere-atmosphere models was that of Dickinson and Henderson-Sellers (1988), hereafter referred to as DHS. In DHS the National Center for Atmospheric Research Community Climate Model (NCAR CCM), coupled to the Biosphere-Atmosphere-Transfer-Scheme (BATS) of Dickinson *et al.* (1986), was used with a horizontal resolution of 7.5 deg. long. x 4.5 deg. lat. to study the effects of Amazonia deforestation. When the model's rainforests over Amazonia were replaced by degraded pasture, surface temperatures increased by 3 to 5 C and evapotranspiration decreased over the region. The increase in surface temperature was attributed mostly to the decreased roughness length of the grass vegetation compared to that of forest and the reduction of evapotranspiration was mostly due to less absorbed solar radiation for grass given its higher albedo. Some difficulties were reported in the parameterization of incident solar radiation and of interception loss (Shuttleworth and Dickinson, 1989; Dickinson, 1989a and 1989b) that caused unrealistically high net radiation.

More recently two GCM simulations of tropical deforestation were conducted. One at the UK Meteorological Office (Lean and Warrilow, 1989, hereafter referred to as LW) and another at the Center for Ocean-Land-Atmosphere Interactions (COLA) (Shukla, Nobre and Sellers, 1990, hereafter

referred to as SNS). In LW the model's horizontal resolution was 4.5 deg. long. x 3.5 deg. lat. and all the model's vegetation north of 30 S in South America was replaced by grass. Although the total area in which the model's vegetation changed was almost twice that used in DHS and in SNS, their results were similar to those in DHS: increased surface temperature by 2.5 C and decreased evapotranspiration for the pasture scenario compared to the forest one. Additionally, it was found that simulated precipitation was reduced over Amazonia. As in DHS the increase on surface temperature was attributed to the decrease in roughness length. Table 2 (adapted from Table 3 of LW) summarizes the main results of their study. In SNS the COLA GCM, coupled to the Simple Biosphere Model (SiB) of Sellers *et al.* (1986), was used with a horizontal resolution of 2.8 deg. long. x 1.8 deg. lat. —i.e., the simulation with the highest horizontal resolution among the 3 studies— and the model's Amazonian tropical forests were replaced by degraded grass. The main results of SNS are summarized in Tables 3 and 4 for the surface energy and water balances in Amazonia, respectively (adapted from Tables 1 and 2 of SNS) and described below.

Surface and soil temperature were warmer by 1 to 3 C in the deforested than in the control cases. The relative warming of the deforested land surface and the overlying air is consistent with the reduction in evapotranspiration and the lower surface roughness length. The annual mean surface energy budget (Table 3) for Amazonia in the two simulations shows that absorbed solar radiation at the surface is reduced in the deforestation case (186 W/m^2) relative to the control case (204 W/m^2) because of the higher albedo (21.6%) for grassland compared to forest (12.5%). That plus the larger outgoing longwave radiation from the surface due to the higher surface temperature in the deforested case result that the amount of net radiative energy available at the surface for partition into latent and sensible heat flux is smaller in the deforested case (146 W/m^2) than in the control case (172 W/m^2). Also, as remarked in SNS, less precipitation is intercepted and re-evaporated as the surface roughness and the canopy water holding capacity of the pasture are relatively small. Furthermore, the transpiration rates are reduced due to the reduced soil moisture holding capacity for the soils under pasture.

An interesting result was that the reduction in calculated annual precipitation (642 mm) was larger than the reduction in evapotranspiration (496 mm), as seen in Table 4, what suggests that changes in the atmospheric circulation may act to reduce *further* the convergence of moisture flux in the region, a result that could not have been anticipated without the use of a dynamical model of the atmosphere, as noted in SNS. This, in turn, implies that runoff also decreased for the deforested case, a result also found in LW (Table 2), since the decrease in precipitation was larger than the decrease in evapotranspiration.

Taken together the results of these three studies seem to suggest the existence of a significant sensitivity of the regional climate to the removal of the tropical forest. In general, the somewhat short period of integration in these studies precludes drawing conclusions on the significance of global climate changes or even climate changes in regions adjacent to Amazonia.

4. DISCUSSION AND CONCLUDING REMARKS

The conversion of tropical forested areas into pastures or other types of short vegetation will cause changes in the microclimate of the disturbed areas. If the size of the perturbed area is sufficiently large, even the regional climate may be altered. Depending on the scale of these alterations, they may cause climate changes at the global level and affect regions distant from the tropical forests.

4.1 Local changes in climate

Changes will occur in albedo, and energy and water balances. There will be a tendency toward less water infiltration and more runoff during rainy periods and less runoff during prolonged dry periods.

Shuttleworth (1988) suggests that there might be a reduction between 10 and 20% in the evapotranspiration for pastures as compared to the rainforest mostly due to the higher albedo (thus, smaller available energy other things being equal) of grass compared to the albedo of tropical forests. That reduction, in turn, might cause rainfall to decrease by 10%, he suggested. Yet, this hypothetical scenario takes into account only changes in evapotranspiration due to changes in the available radiative energy. Important changes also would occur due to the decrease in surface roughness and at the soil level. Loss of top soil organic matter and soil fauna, compaction due to agricultural practices and overgrazing, and soil erosion may cause large changes in the physical and chemical characteristics of the predominantly clay soils of the Amazonian terra firme forest. Those changes likely would combine to reduce infiltration rates drastically, increase surface runoff during rainy periods, and decrease soil moisture in the shallower rooting zone of the grass vegetation primarily during the dry season. Decreased soil moisture availability also would contribute to reduce evapotranspiration.

Comparative measurements of the diurnal cycle of canopy and subsurface temperature at cleared and forested sites in Ibadan, Nigeria (Lawson *et al.*, 1981) and in Surinam (Shulz, 1960) showed a large increase of soil (> 5 C) and air (> 3 C) temperatures for the cleared areas compared to the forested ones. Not being in the shade of a tall canopy, the diurnal fluctuation of ground temperature and humidity deficit was much larger for the cleared sites in these 2 studies as well. Those changes in soil microclimate will have a profound effect on the biological, chemical and physical processes in the top soil layer. Plant, animal and microorganisms living in that layer will experience temperature, humidity deficit and water stresses not present in the remarkably constant microclimate of the forest floor.

4.2 Regional climate changes

The summation of local climate change over sufficiently large quasi-contiguous areas (say larger than 1 million km^2) might change water vapor transports and the water balance at a regional level with consequent changes in the energy balance. Climatic alterations and the scale at which they occur depend on the geographic location and its geomorphology. For instance, even small changes in the low level wind regime on mountainous areas such as the Andean Cordillera can cause a large change in the temporal and geographical distribution of rainfall. It is not possible yet to predict accurately regional climate changes associated with the observed patterns of deforestation by means of climate model simulations. An important reason for such limitation is that when current climate models are integrated in a control mode, i.e., attempting to mimic the observed climate, they commonly fail to represent important aspects of the regional climate. One problem is, of course, resolution. It is expected that only when model resolution becomes of the order of 100 km (current climate model resolution is typically between 200 and 500 km) will the models probably capture the finer details of the regional climate. Yet, the results of three recent climate model simulations of Amazonia deforestation, reviewed in the previous section, suggest the following changes at the regional level to

be likely following extensive deforestation of tropical forests: increase in surface and soil temperature and in the diurnal fluctuation of temperature and specific humidity deficit, and a reduction of evapotranspiration, precipitation, and PBL moisture. In two of the three studies (LW and SNS), yearly averaged runoff decreased for Amazonia as a whole for the pasture vegetation compared to forest. The annual reduction in rainfall in these two simulations was larger than the corresponding reduction in evapotranspiration, thus explaining the reduction in runoff. It is likely, however, that runoff will increase following rainy periods, that is, runoff (and river streamflow) would be higher after deforestation during the rainy season and decrease during the dry season.

The average low-level airflow over tropical South America east of the Andes shows that moisture flow is directed from Amazonia toward Central Brazil. Thus the water vapor for Central Brazil precipitation comes mostly from Amazonia: any change in the water vapor transports could conceivably affect precipitation in that region, even when one realizes that the main rain-producing mechanism in that area is due to the influence of frontal systems coming from the mid-latitudes of the Southern Hemisphere. The model results in Nobre *et al.* (1990) have shown a smaller decrease in precipitation in Central Brazil. That decrease, however, could to be attributed to smaller southward moisture flux from Amazonia since that flux did not change appreciably: specific humidity decreased but wind speed increased slightly.

Another point of interest is the large precipitation rates of western Amazonia. On average, the atmospheric column in that area has apparently more water vapor than near the Atlantic coast. The Atlantic ocean is, of course, the major supply of water vapor to Amazonia. Considering that western Amazonia is between 2 and 3 thousand km inland from the main oceanic water vapor source, recycling of water vapor through evapotranspiration is clearly very important. A decreased water vapor flux to the west as the model results shows also might imply decreased precipitation in those areas, even in the absence of large scale deforestation there. More locally, it is important to mention that the very high precipitation rates observed on the eastern Andean slopes (up to 5 meter annually in the Peruvian and Colombian Andean slopes) must be somewhat related not only to the mechanical uplifting of the airflow but also to the amount of moisture being transported. The maintenance of these very large precipitation rates and resulting lack of a dry season, is thought to contribute to the tremendous species diversity —reportedly to be the largest in the world— in Colombian Amazonia. Therefore even small changes in precipitation regimes in the eastern Andean slopes could have profound effects on species diversity in that area.

4.3 Global changes

To understand and predict any possible large-scale climate change due to tropical deforestation it is crucial to know to what extent the rainfall patterns will change when rainforests are converted into grasslands. It is well known that the tropical regions function as atmospheric heat sources through the release of latent heat of condensation in convective clouds. The heat so released drives large-scale tropical circulations (of the Hadley-Walker type) with ascending motion over the tropical regions, mostly over Amazonia, tropical Africa and Indonesia-western Pacific region and descending motion over the dry subtropic, primarily over the subtropical oceans. It is conceivable that a significant reduction in rainfall over Amazonia (say, greater than 20% reduction as the model simulations described in LW and SNS suggest) might have an effect in these tropical circulations. However, it is

unclear what these changes would be and how they would manifest themselves in terms of climate changes in the tropics, but away from the perturbed areas, and in the extra-tropics. Regarding the extra-tropics, it is interesting to note the suggestion by Paegle (1987) of a possible link between tropical convection and quasi-stationary features of the large-scale circulation over North America. He suggests that the westward shift of the subtropical jetstream from the east coast of North America in boreal winter to the east coast in spring and a concomitant westward shift of the North American long-wave trough may be linked to the seasonal, northwestward migration of the area of rainfall maxima over tropical South America from Central Amazonia in January-February to Central America in June-July.

Tropical forest areas also have a characteristic energy balance that contributes to the transport of energy as latent heat (water vapor) from the equatorial regions to those of greater latitude. This is particularly conspicuous in Central Brazil, southern Bolivia, Paraguay and northern Argentina where, due to the generally southward low level circulation, most of the water vapor present in those regions comes from Amazonia. Therefore, changes in atmospheric moisture in Amazonia due to deforestation might have an impact on the precipitation of the adjacent regions to the south.

So far we have focused our attention mostly on the Amazonian tropical forest. Can we say anything about climatic impacts arising from removal of tropical forests in Equatorial Africa and Southeast Asia? It is likely that at the microclimate level the effects will be quite similar: higher near-ground temperatures and larger diurnal fluctuations of temperature and humidity deficit, increased runoff during rainy periods and decreased runoff during the dry season, decreased soil moisture and, possibly decreased evapotranspiration. The question whether there would be a significant change in precipitation is a complex one. For Southeast Asia large-scale changes in precipitation are less likely since the precipitation climate of that area of the western Pacific and Indian Oceans is controlled by large-scale features: on one hand, the precipitation distribution responds to the high sea surface temperatures (SST > 28 C) that are conducive to large rates of evaporation besides a tendency for the low level air to converge from areas of lower SST to areas with higher SST; these two factors enable cloud formation and high precipitation. On the other hand, land-sea heating contrast drives the monsoonal circulations of Southeast Asia. The monsoonal circulations account for the copious rainfall observed in that area.

In Africa there is, at least theoretically, the possibility that the removal of the tropical forest might influence the regional climate. A biophysical feedback mechanism as proposed by Charney *et al.* (1977) might cause an enhancement in aridification along the northern and southern boundaries of the forest. For reasons similar to the ones discussed in the earlier session, the changes in albedo, surface roughness and soil moisture caused by replacement of forest by overgrazed pasture would result in decreased precipitation. That could, in turn, induce further clearings deeper into the forest. However, this question is not settled yet because interannual and longer-term rainfall variability in Tropical Africa is apparently also connected to planetary-scale phenomena, notably global SST distributions.

Finally can we say anything on the ecological implications of the possibility of a future drier and warmer climate in Amazonia following extensive deforestation? The decrease in precipitation suggested by the simulation studies for the deforested case is associated with a longer and more pronounced dry season. The authors in SNS remark that "[T]he lack of an extended dry season apparently sustains the current tropical forests, and therefore, a lengthening of the dry season could have serious ecological implications. Among other effects, the frequency and intensity of forest fires

could increase significantly and the life-cycles of pollination vectors could be perturbed... Changes in the region's hydrological cycle and the disruption of complex plant-animal relations could be so profound that *once* the tropical forests were destroyed, they might not be able to re-establish themselves." The authors then conclude that a "complete and rapid destruction of the Amazon tropical forest could be irreversible." Therefore, there might be a tendency of 'savannization' of Amazonia. Two characteristics of such vegetation make it particularly adapted to the foreseeable new climate: they can endure a 6-month dry season and they are fire-adapted (actually fire has played an important role in their ecological evolution as it has done for the savannah vegetation to the north of the rainforest, the Gran Sabana, in Venezuela (Sanford *et al.* 1985, Sternberg, 1987). Amazonia is surrounded to the south, east and north by savanna-like vegetation. Any trend toward 'savannization' in Amazonia would likely be seen first in the transition forests straddled between the rainforest and the savanna because in those areas the dry season is usually longer than in the rainforest. This implies that any increase in the duration of the dry season in those regions might make it unsuitable for the re-establishment of the rainforest.

Table 1 — Hydrological cycle of the Amazon Region

Summary of the results obtained by different studies (Adapted from Salati, 1987).

Research	Rainfall	Transpiration			Evapotranspiration			Runoff	
	mm	mm	%	mm/day	mm	%	mm/day	mm	%
MARQUES *et al.* 1980	2328[1]	-	-	-	1260 (r)	54.2	3.5	1068	45.8
	2328[2]	-	-	-	1000 (r)	43.0	2.7	1328	57.0
	2328[3]	-	-	-	1330 (p)	57.1	3.6	998	42.9
VILLA NOVA *et al.* 1976	2000[4]	-	-	-	1460 (p)	73.0	4.0	540	27.0
		-	-	-	1168 (r)	58.4	3.2	832	41.6
	2101[5]	-	-	-	1569 (p)	73.4	4.3	532	26.6
MOLION 1975	2379[6]	-	-	-	1146 (r)	48.2	3.1	1233	51.8
RIBEIRO *et al.* 1979	2478[7]	-	-	-	1536 (p)	62.2	4.2	942	38.0
		-	-	-	1508 (r)	60.8	4.1	970	39.2
IPEAN 1978	2179[8]	-	-	-	1475 (r)	67.5	4.0	704	32.5
		-	-	-	1320 (r)	60.6	3.6	859	39.4
DMET 1978	2207[9]	-	-	-	1452 (p)	65.8	4.0	755	34.2
		-	-	-	1306 (r)	59.2	3.6	901	40.8
JORDAN *et al.* 1981	3664[10]	1722	47.0	4.7	1905 (r)	52.0	5.2	1759	48.0
LEOPOLDO *et al.* 1981	2089[11]	1014	48.5	2.7	1542 (r)	74.1	4.1	541	25.9
LEOPOLDO *et al.* 1982	2075[12]	1287	62.0	3.5	1675 (r)	80.7	4.6	400	19.3
SHUTTLEWORTH 1988	2636 [13]	992	37.6	2.7	1320 (r)	50.0	3.6	-	-
ABLE - 2B 1987 (1 month)	290[14]	-	-	-	157 (r)	54.1	5.2	-	-

OBSERVATIONS: (r) - real evapotranspiratino; (p) - potencial evap.; (1) aerological method, applied for all Amazon Basin, period 1972/1975; (2) idem, for the region between Belém and Manaus; (3) by Thornthwaite method, for the region between Belem and Manaus; (4) Penman method, mean for the period (1931/1960; (5) idem, for Manaus Region; (6) climatonomic method for all Amazon Region, mean for the period 1931/1960; (7) water balance by Thornthwaite and Mather method for the Ducke Forest Reserve, mean for the period 1965/1973; (8) Thornthwaite method for all Amazon Region and estimated for a period over 10 years; (9) idem, for various periods; (10) water balance estimated by class A pan-evaporation for San Carlos Region; (11) 'Model Basin' water balance and (12) 'Barro-Branco' water balance (Ducke Forest Reserve); (13) Adaptation of Penman-Montheit for the period Sep. 1983-Sep.1985; (14) Aerological method applied to the Brazilian Amazon Basin during ABLE 2B, April 13-May 13, 1987.

Table 2 — Summary of Surface Variables for Control (C) and Deforested (D) Simulations Averaged over 3 years for Amazonia (From: Lean and Warrilow, 1989)

Surface Variable	C	D	
Evaporation (md^{-1})	3.12	2.27	(-27.2%)
Precipitation (md^{-1})	6.60	5.26	(-20.3%)
Soil Moisture (cm)	16.13	6.66	(-58.7%)
Runoff (md^{-1})	3.40	3.00	(-11.9%)
Net Radiation (Wm^{-2})	147.29	125.96	(-14.4%)
Temperature (°C)	23.55	25.98	(+10.3%)
Sensible Heat (Wm^{-2})	57.19	60.15	(+ 5.2%)
Bowen Ratio	0.85	1.50	(+76.5%)

Table 3 — Mean surface energy budget for Amazonia. The data are 12-month mean (January to December) values. Values are in W/m^2, except for B and a which are nondimensional, and T_s which is in °C. S is insolation; a is albedo; L_n is net upward longwave radiation; R_n is available radiative energy; E_t is transpiration plus soil evaporation; E_i is interception loss; E is Evapotranspiration = E_t plus E_i; H is sensible heating; G is ground heat flux; B is the Bowen Ratio (H/E); and T_s is surface temperature (From: Shukla, Nobre and Sellers, 1990)

	S	(1-a) S	L_n	R_n	E_t	E_i	E	H	G	B	a	T_s
Control	233	204	-32	172	91	37	128	44	0	0.34	12.5	23.5
Deforestation	237	186	-40	146	64	26	90	56	0	0.62	21.6	26.0
Difference	+4	-18	-8	-26	-27	-11	-38	+12	0	-0.28	+9.1	+2.5

Table 4 — Mean water budget for Amazonia. The data are 12-month mean (January to December) values. Values E and P are in mm/year; PW is in mm. P is total precipitation; E is evapotranspiration; and PW is precipitable water (From: Shukla, Nobre and Sellers, 1990).

	P	E	(E-P)	E/P	PW
Control	2464	1657	-807	0.67	37.7
Deforestation	1821	1161	-661	0.63	35.4
Difference	-642	-496	+146	-0.04	-2.3
Change (in percent)	-26.1	-30.0	+18.0	-5.9	-6.1

REFERENCES

Brasil, Instituto de Pesquisas Espaciais. Avaliação da cobertura florestal na Amazonia Legal utilizando Sensoriamento Remoto Orbital. INPE, São José dos Campos, SP, Brazil, 1989.

Charney, J. G.; Quick, W. J.; Chow, S. H. and Kornfield, T. A comparative study of the effects of albedo change on drought in semi-arid regions. J. Atmos. Sci., 34, 1366-1388, 1977.

Dias, A. C. C. P. and Northcliff, P. Trop. Agri. 62, 207, 1985.

Dickinson, R. E. Modeling the effects of Amazonian deforestation on a regional surface climate: A review. Agric. and For. Meteorol. (in press), 1989a.

Dickinson, R. E. Implications of tropical deforestation for climate: A comparison of model and observational descriptions of surface energy and hydrological balance. Phil. Trans. R. Soc. Lond. B. (in press), 1989b.

Dickinson, R. E.; Henderson-Sellers, A.; Kennedy, P. J. and Wilson, M. F. Biosphere-atmosphere transfer scheme (BATS) for the NCAR Community Climate Model. Tech. Note TN-275+STR, National Center for Atmospheric Research, Boulder, CO, United States, 1986.

Dickinson, R. E. and Henderson-Sellers, A. Modelling tropical deforestation: A study of GCM land-surface parameterizations. Q. J. R. Meteorol. Soc. 114, 439-462, 1988.

Fearnside, P. M. Amazonian deforestation: A critical review of the 'Our Nature' program estimate (unpublished manuscript), 1989.

Gentry and Lopes-Parody. Science, 210, 1354-1356, 1980.

Henderson-Sellers, A. Effects of change in land use on climate in the humid tropics. In: Geophysiology of Amazonia. R. E. Dickinson (Ed.), John Wiley & Sons, 526 p., 1987.

Henderson-Sellers, A. and Gornitz, V. Possible climatic impacts of land cover transformations, with particular emphasis on tropical deforestation. Climatic Change, 6, 231-258, 1984.

Houghton, R. A. *et al.* Nature, 316, 617-619, 1985.

IPEAN. Zoneamento agricola da Amazonia. Bol. Tec., Instituto de Pesquisas Agropecuarias do Norte, Belem, Brasil, 1978.

Jordan, C. F. and Helveldop, J. The water balance for an Amazonian rainforest. Acta Amazon., 11, 87-92, 1981.

Lawson, T. L.; Lal, R. and Oduro-Afriyie, K. Rainfall redistribution and microclimatic changes over a cleared watershed. In: Tropical Agriculture Hydrology, R. Lal and E. W. Russel (Eds.), John Wiley & Sons, p. 141-151, 1981.

Lean, J. and Warrilow, D. A. Climatic impact of Amazon deforestation. Nature, 342, 311-413, 1989.

Leopoldo, P. R.; Franken, W.; Matsui, E. and Salati, E. Estimativa da evapotranspiração da floresta Amazonia de terra firme. Acta Amazon., 12, 23-28, 1982a.

Leopoldo, P. R.; Salati, E., Matsui, E. and Goes Ribeiro, M. N. Composição isotopica das precipitações e d'agua do solo em floresta Amazonica de terra firme na região de Manaus. Acta Amazonas, 12, 23-28, 1982b.

Lettau, H.; Lettau, K. and Molion, L. C. B. Amazonia's hydrologic cycle and the role of atmospheric recycling in assessing deforestation effects. Mon. Wea. Rev., 107, 227-238, 1979.

Mahar, D. J. Government Policies and Deforestation in Brazil's Amazon Region. The World Bank, Washington, D.C., 1989.

Marques, J.; Salati, E. and Santos, J. M. Cálculo da evapotranspiração real na bacia Amazônica através do método aerológico. Acta Amazônica, 10, 357-361, 1980a.

Marques, J.; Salati, E. and Santos, J. M. A divergência do campo do fluxo de vapor d'água e as chuvas na região Amazônica. Acta Amazônica, 10, 133-140, 1980b.

Mintz, Y. In the Global Climate. J. T. Houghton, Ed., Cambridge Univ. Press, Cambridge, pp. 79-106, 1984.

Molion, L. C. B. A climatonomic study of the energy and moisture fluxes of the Amazonian basin with consideration of deforestation effects. Doctoral Thesis. University of Wisconsin, Madison, WI, United States, 1975.

Mori and Prance, G. T. Species diversity, phenology, plant-animal interaction, and their correlation with climate, as illustrated by the Brazil nut family (Lecythidaceae). In: Geophysiology of Amazonia. R. E. Dickinson (Ed.), John Wiley & Sons, p. 64-69, 1987.

Nobre, C. A. and Nobre, P. A grande seca de 1926 na Amazonia e o fenomeno El Niño. Oscilação Sul. Climanalise (in press), 1990.

Nobre, C. A. and Oliveira, A. S. de. Precipitation and circulation anomalies in South America and the 1982-83 El Niño. Southern oscillation episode. Preprint Vol. at The Sec. Int. Conf. in Southern Hemisphere Meteorology. Publ. by American Meteorological Soc., Boston, United States, 1986.

Nobre, C. A. Amazonia and climate. Proceedings of the Climate Conference for Latin America and the Caribbean. WMO Pub. No. 632, p. 409-413 (Available through World Meteorological Organization, Geneve, Switzerland), 1983.

Nobre, C. A.; Sellers, P. J. and Shukla, J. Amazonian deforestation and regional climate change (in preparation), 1990.

Paegle, J. Interactions between convective and large-scale motions over Amazonia. In: Geophysiology of Amazonia. R. E. Dickinson (Ed.), John Wiley & Sons, p. 347-390, 1987.

Potter, G. L.; Ellsaesser, H. W.; MacCracken, M. C. and Luther, F. M. Possible climatic impact of tropical deforestation. Nature, 258, 697-698, 1975.

Ribeiro, M. N. G. and Villa-Nova, N. A. Estudos climáticos da Reserva Ducke, Manaus, Am. 3. Evapotranspiração. Acta Amazônica, 9, 305-309, 1979.

Richey, J.; Nobre, C. A.; Deser, C. Amazon river discharge and climate variability: 1903-1985. Science, 246, 101-103, 1989.

Rocha, H. R.; Nobre, C. A. and Barros, M. C. Variabilidade natural de longo prazo no ciclo hidrológico da Amazônia. Climanálise, 4(12): 36-43, 1989.

Rowentree, P. Review of general circulation models as a basis for predicting the effects of vegetation change on climate. Proc. of the United Nations University Workshop on Forest, Climate and Hydrology: Regional Impacts. Publ. by United Nations University, Tokyo, Japan, 1988.

Salati, E. The forest and the hydrological cycle. In: Geophysiology of Amazonia. R. E. Dickinson (Ed.), John Wiley & Sons, p. 273-295, 1987.

Salati, E. and Nobre, C. A. Possible climatic impacts of tropical deforestation. Climatic Change (in press), 1990.

Sanford Jr., R. L.; Saldarriaga, J.; Clark, K. E.; Uhl, C.; Herrera, R. Science, 227, 53-, 1985.

Sellers, P. J.; Mintz, Y.; Sud, Y. C.; Dalsher, A. A simple Biosphere Model (SiB) for use within General Circulation Models. J. Atmos. Sci. 43, 505-531, 1986.

Setzer, A. W. and Pereira, M. C.; Pereira Jr., A. C. and Aleida, S. A. O. Progress report on the IBDF-INPE "SEQUE" Project, 1987. Tech. Rep. N° INPE-45-34-RPE/565. Instituto de Pesquisas Espaciais, São José dos Campos, SP, Brazil, 1988.

Shukla, J.; Nobre, C. A. and Sellers, P. Amazonia deforestation and climate change. Science, 247, 1322-1325, 1990.

Shukla, J. and Mintz, Y. Science 215, 1498, 1982.

Shulz, J. P. Ecological studies on rain forest in northern Suriname. North Holland, Amsterdam. 270 p., 70 fig, 1960.

Shuttleworth, W. J. Evaporation from Amazonian rain forest. Proc. Roy. Soc. B., 233, 321-346, 1988.

Shuttleworth, J. W. and Dickinson, R. E. Comments on 'Modelling tropical deforestation: A study of GCM land-surface parameterizations' by R. E. Dickinson and A. Henderson-Sellers. Q. J. R. Meteorol. Soc. (in press), 1989.

Sternberg, H. O'R. Aggravation of floods in Amazon river as a consequence of deforestation. Geogr. Ann. 69A, 201, 1987.

Villa Nova, N. A.; Salati, E.; Matsui, E. Estimativa da evapotranspiração na Bacia Amazonia. Acta Amazon., 6, 215-228, 1976

CLIMATE VARIABILITY AND ITS EFFECTS ON AMAZONIAN HYDROLOGY

Luiz Carlos Baldicero Molion *

ABSTRACT

The hydrologic processes in Amazonia vary widely from year to year due to natural changes in the atmospheric conditions. This paper reviews the dynamic mechanisms that produce rainfall in the Region and their fluctuations due to interannual variability of the large-scale atmospheric circulations, associated with El Niño — Southern Oscillation phenomenon (ENSO), and blocking patterns of the atmospheric flow. It is also hypothesized that the observed trends in precipitation, as well as runoff, reported by Rocha *et al.* (1989), may be related to a higher frequency of positive phases of ENSO and/or the presence of low latitude stratospheric volcanic aerosols over Amazonia, which influence the heating of the Andean Altiplano, thus the seasonal development of the upper tropospheric anticyclone over tropical South America (Bolivian High).

INTRODUCTION

The hydrologic cycle is an integrated product of the climate and of the biogeophysical attributes of the surface. On the other hand, it exerts an influence on climate which goes beyond the interaction between the atmospheric moisture, rainfall and runoff. It is the major single heat source for the atmosphere, in the form of latent heat which is released, mainly in the tropics, through the condensation of atmospheric moisture into clouds and rainfall.

Studies on identification of climatic fluctuations are most of the time inconclusive since the climate, hence the hydrologic cycle, present an intrinsic variability, both in space and time which is not adequately known. At sea level, the climate spatial variability results mainly from the differential absorption of solar radiation by continents and oceans, unevenly distributed on the planet's surface. This, together with its rotation, establish the general circulations of the atmosphere and of the oceans, which redistribute the heat and determine the climates over the continents; the local climate, in turn, is modified through the dynamic coupling between the atmosphere and the biogeophysical characteristics of the underlying surface, particularly the topography and the nature of the surface cover. The temporal variability is more complex since, besides the factors above, it depends on external controls, such as the variation of the solar energy output (solar constant) and Earth orbital parameters, and on

* *Instituto de Pesquisas Espaciais - C. Postal 515 - S. J. dos Campos, SP - Brazil*

internal controls, such as the chemical composition of the atmosphere. In addition, man's actions in changing the environment, which are occurring at unprecedented rates, may be contributing inadvertently to the variability observed today. The anthropogenic contribution cannot be isolated from the natural changes with the present scientific knowledge.

This paper reviews the interannual, i.e., the year-to-year, variability of rainfall in Amazonia and associated physical mechanisms classified by their inherent spatial scales. Rainfall was selected because it is the most significant climatological variable for the tropics and until recently its interannual variability was thought to be negligible. With climatic changes due to man's actions in modifying the environment, this variable is also expected to change; particular attention is given here to the impacts of a large scale deforestation on the hydrologic cycle components.

2. SCALES OF RAINFALL PRODUCING MECHANISMS

The physical mechanisms that produce convection, cloud formation and rainfall in Amazonia may be classified in five broad spatial scales described below.

Continental or large scale

The solar radiation absorbed at the surface is primarily used for evaporating water (latent heat) and for heating the air (sensible heat) near the ground. In Central Amazonia, micrometeorological studies (e.g., Molion, 1987; Shuttleworth, 1988) have shown that 80% to 90% of the available energy is used for evapotranspiration and the rest for heating up the air. Over the continent, the humid warm air is displaced upward (convection) and in its ascent, it expands and cools condensing its moisture and releasing the enormous amount of energy (latent heat) used in the evaporation process. Mass continuity requires the ascending, after drying out, to sink over the adjacent oceans, closing a direct or thermal circulation cell, as shown schematically in Figure 1. The thermal circulation induces low atmospheric pressures (Low) and mass convergence at low level and high pressures (High) and mass divergence at upper tropospheric levels. The High over Amazonia seems to be 'anchored' to the Andean Altiplano, since this is a heat source practically in the middle of the troposphere, hence its denomination as Bolivian High. The seasonal variability of the Bolivian High, both in intensity and position, is linked directly to the spatial and temporal distribution of the rainfall (Kousky and Kayano, 1981). During the Southern Hemisphere summer, the High is well developed and covers practically the entire Amazonas Basin, which, at this time, receives maximum rainfall. When the High weakens and moves progressively northwestward during the winter, the southern and eastern sectors of the Basin experience their dry season, which can last between two (central) to six months (east and south); the northwest, however, is always under the influence of the High and, therefore, does not show a marked dry season. In September, the High starts its way back towards the Brazilian Central Plateau, moving close to the Andes Cordillera, and only in November-December the rainy season is fully reestablished in the whole Basin.

Inspection of satellite imagery suggests that the presence of the High is not continuous but it appears to have a pulsation period of 10 to 15 days. That is, it develops initially due to the surface heating and it is maintained by latent heat release; after 10 days or so, it decays, probably due to the persistent cloudiness cutting off solar radiation, a possible negative feedback.

Another element of the large-scale circulation, which generates rainfall over the northeastern coast of Amazonia and northern coast of South America, is the Intertropical Convergence Zone in the Atlantic (ITCZA). The ITCZA is the confluence of Northern and Southern Hemispheres Trade winds. Hastenrath and Lamb (1977) showed that the ITCZA moves southward progressively from its northernmost position during the Southern Hemisphere winter (July) and reaches its southernmost position by the end of summer (March). Apparently, it follows the relative motion of the Sun with a lag of about three months. The ITCZA is responsible for part of the annual rainfall totals during its passage over the Amazonian coast; there is no evidence of a continental ITCZA during the summer, as reported by some authors (e.g., Trewartha, 1961; Ratisbona, 1976).

Sinoptic scale

The characteristic length of this scale is 1,000 km and the most important dynamic mechanism of rainfall production is the cold fronts or frontal systems. Several authors (e.g., Trewartha, 1961; Parmenter, 1976; Ratisbona, 1976) have described the effects of Southern Hemisphere frontal systems penetration into Amazonia during the winter of that hemisphere. Most of these description emphasized the sharp 15-20°C decrease in temperature, which lasts for 3-5 days, and its consequence to the environment. Frontal systems, however, can penetrate Amazonia any time of the year, organizing convection and rainfall. Oliveira (1986), inspecting ten years of geostationary satellite imagery, showed that many frontal systems, especially during the summer, move equatorward along the Brazilian eastern coast, and organize convection and intensify rainfall over Amazonia. Over the continent, they are generally oriented NW-SE and cross the coast between latitudes 15°-25° S. In some years, these systems remain stationary in this position, establishing a region of convergence with the Trade winds which was denominated South American Convergence Zone (SACZ) and producing high rainfall totals. In these occasions, the Amazonas right bank tributaries are subject to high flooding.

Northern Hemisphere frontal systems may also influence rainfall in Amazonia directly. Molion *et al.* (1987) presented a case-study for February 1980, when the successive passage of frontal systems over the Subtropical Atlantic favoured the penetration of relatively cold and dry air of that hemisphere into Amazonia. The cold and dry air mass helped in organizing an east-west convective cloud band, along latitude 7°S, which was intensified by the merging Southern Hemisphere frontal system. This event produced high rainfall totals especially in Central Brazil, where several stations recorded over 200 mm in 24 hours.

Subsinoptic scale

This scale has typical lengths between 500-1.000 km and the active atmospheric systems are the instability or squall lines and the large Cbs clusters.

In the absence of large-scale forcing, the development of convective cells starts in the mid-morning. These cells undergo a selection process by which the larger ones grow, forming clusters or lines, whereas the smaller ones are suppressed. The formation of a line or a cluster depends on the tropospheric flow pattern. With a moderate wind field, the descending currents (downdrafts) of the original cell act as a mini-frontal zones raising the ambient humid air. The new cell, which originated

from this forced convection, will form in an arched line downwind (Figure 2a.). When the wind field is weak, the new cells surround the mother-cell as a ring or cluster that continues to grow at the expenses of downdrafts (Figure 2b.).

Cavalcanti (1982) demonstrated that the convergence associate with sea breeze circulation organizes convection in a linear fashion over coastal areas near the mouth of Amazonas River. In some occasions, these lines propagate inland, reaching the Andes in about 48 hours (Molion and Kousky, 1985). Recently, Cohen *et al.* (1989) analyzed eight years of geostationary satellite imagery, and with additional surface and upper-air data, were able to identify some of the physical characteristics of these instability lines. The highest frequency of lines occurred in July, when the ITCZA is farther north and a secondary maximum was apparent in April, when the ITCZA is at its southernmost position. Of the total observed coastal lines, only 27% propagated more than 400 km inland and some of these reached over 2.000 km, with typical propagation speeds of about 12-16 ms^{-1} and remaining active some 12-21 hours. The characteristic length and width were 1.500 km and 170 km, respectively. Cohen *et al.* (1989) did not study the contribution of these instability lines to the regional rainfall totals; they only commented that 45% of the eastern Amazonian rainfall may be due to these lines.

The convergence of the sea breeze may not be the only mechanism to give origin to these transient disturbances, since it was observed that some of them develop during the night-time. Some of these lines may be associated with waves in the Trade wind field triggered by frontal systems deep penetration over the subtropical Atlantic, sometimes reaching the geographic equator. In the absence of atmospheric blocking patterns, these deep penetrations occur during the whole year, mainly in periods when the ITCZA is in its extreme positions, particularly the northern position (July).

Meso and microscales

The mesoscale or GCMs grid scale has a typical length of 100 km. The most common weather features in this scale are the convective cell and clusters of Cbs, which produce intense precipitation but of short duration and random distribution. Due to the high instability of the local air masses, most of the times small hills, 100-200 meters high, are sufficient to lift the atmospheric flow to the condensation level; the convective cells, that form in this process, grow selectively.

Molion and Dallarosa (1990) analyzed data of two sets of raingauges, one, with a 11 year record, installed along longitude 56°W and another, with 10 year record, along longitude 60°W and showed that raingauges near the Amazonas River recorded an annual average rainfall 20% to 30% less than the gauges 30 to 100 km away from the large river. During the driest trimester (July-September), the difference was more striking, 97% and 35%, respectively. They attributed the catching reduction mainly to the river breeze circulation, since it can easily develop in areas where the river is sufficiently large, i.e., wider than 10 km. As a matter of fact, inspecting high resolution meteorological satellite visible imagery, one notices that clouds form mainly on the river banks leaving the main channels visible from space. The existence of the river breeze can alter the local convection, hence the rainfall patterns.

The microscale mechanisms have characteristic lengths between 1 to 10 km, and the most commons are the small convective cells, which form during the morning hours and precipitate around 14-15 hs local time. The rainfall from these clouds may not be as important for the local hydrology

as they are for the existence of the tropical forest. The increasing cloudiness in mid-morning reduces the sun radiation load during the time which is more intense and the subsequent light showers wet the canopy which is kept cool through evaporation of intercepted water, so plants are not required to transpire.

3. INTERANNUAL VARIABILITY

The physical causes of the interannual variability of rainfall in Amazonia are not adequately understood yet, but it is surely linked to the spatial and temporal variability of the equatorial latent heat sources. One of the phenomena that greatly modify both the positioning and intensity of the heat sources is the El Niño - Southern Oscillation (ENSO) events. The association of ENSO (negative phase of SO) event and the reduction of rainfall occurs because the ascending branch of the Walker Circulation (east-west component), located over the Amazonas Basin, is displaced westward over the abnormally warm East Pacific ocean and intensified due to strong convection. The descending branch covers the whole Amazonia, the adjacent Atlantic reaching the African continent. The subsidence suppresses convection and thus rainfall is dramatically reduced.

Figure 3 (Kayano and Moura, 1983) shows isolines of deviations of rainfall from the mean, normalized by the standard-deviation, for the period February-May 1958, year when a strong ENSO event occurred. Over parts of Amazonia and West Africa it is noticeable reduction of rainfall in excess of 1.8 standard-deviations. For the period January-May 1983, year in which happened the strongest ENSO of the century, Kousky *et al.* (1984) commented that some selected stations in Amazonia presented over 30% reduction of rainfall. Similarly, Nobre and Renno (1985), using all available station, reported rainfall 70% below normal for January-February 1983, being that the driest February in the last 50 year period.

Figure 4, adapted from Kayano and Moura (1987), shows rainfall reductions in excess of 0.5 standard-deviations for the entire Amazonia during the hydrologic year 1982-83.

If in one hand the negative phase of SO is associated with reductions of rainfall, in the other, during the positive phase of SO, the so called Anti-El Niño, it has been observed an increase of the convective activity and consequent increase of rainfall over Amazonia. Typical Anti-El Niño examples are the hydrologic years 1975/76 and 1988/89 when the Negro River, in Manaus, recorded the second and the third highest levels of the century, respectively.

Figure 5, extracted from Rao and Hada (1987), shows isolines of correlation coefficient between the Southern Oscillation Index (SOI) and precipitation over Brazil during the trimester September-November using 41 year data record. The positive correlation coefficient exceeding 0.6 are found in northeast Amazonia, suggesting strong coupling between the SO and rainfall in that part of the Basin.

The precipitation data point analysis, however, not always reflects the magnitude and extension of the convective activity and associated rainfall, due to inadequate spatial distribution of gauges in the Region. Molion and Moraes (1987) correlated a series of SOI with series of discharge of selected rivers in South America. For the Trombetas River, left bank tributary of Amazonas around longitude 56°W, the correlation coefficients were positive and higher than 0.8, implying that when the SOI are negative (El Niño years) the discharges are below the normal and vice-versa. Just as an

example, one day in February 1983, the observed river discharge near the mouth was 47 m^3s^{-1}, the lowest recorded so far; the long term average discharge for this month is 2.100 m^3s^{-1}. The authors also noticed that there exists a three-month lag between the SOI and the discharge and suggested that, since the SOI is the leader, it might be used for discharge forecasts for this large river.

Other mechanisms besides ENSO may cause variation in rainfall in Amazonia. Moura and Shukla (1981) showed that when the sea surface temperature (SST) in the North Atlantic were above normal and simultaneously the SST in the South Atlantic were below normal, the ITCZA remained northward of its normal position and the descending branch of Hadley Cell was intensified, causing strong subsidence over Central and Eastern Amazonia, reducing convection and rainfall.

As mentioned before, the Southern Hemisphere frontal systems are important large-scale mechanisms organizing convection in Amazonia. This penetration may be affected by atmospheric flow blocking patterns which occur in some years over the southern part of the continent and over adjacent areas of the Pacific Ocean. In years that present high blocking frequency, a smaller number of frontal systems penetrate Amazonia and rainfall is reduced.

It is possible also that precipitation decrease is associated with a reduced heating of the Andean Altiplano, and consequent weakening of the Bolivian High, during periods of strong volcanic activities in the tropics. The presence of volcanic aerosols in the stratosphere reduces the solar radiation during several months. De Luise (1983), for example, observed reductions up to 7% during El Chichón eruption in Mexico in April 1983. With reduced solar radiation, the Altiplano might be cooler, resulting in an increased atmospheric stability, reduction of convection and consequent weakening of the divergence in the upper troposphere; this, in turn would reduce precipitation. This hypothesis, however, is of difficult verification since the stratospheric aerosol concentrations must be, first expressive, and second its positioning must be timed up with the Amazonian rainy season. That is, if the aerosols were not over Amazonia at the proper time, the rainfall would not be affected. Coincidentally, during recent eruptions of El Chichón and Nevado del Ruíz (November 1985), whose effects might well have been added to the ENSO events of those years, reductions of the Amazonian rainfall were observed. On the other hand, if aerosols cover tropical areas distant from Amazonia, the reverse might occur, that is, the Region would be relatively warmer than the surroundings due to higher transparency of the local atmosphere to solar radiation, thus enhanced convection would promote more rainfall, whereas subsiding motion would dominate the areas elsewhere under influence of aerosols. In the literature, other possible climatic effects related to volcanic aerosols have been described. Handler and Andsager (1990), for example, suggested that there is statistically significant relationship between the occurrence of ENSO events and the presence of volcanic aerosols in the stratosphere of low latitudes.

In addition to the observed interannual variation, longer term variations seem to be apparent. Rocha *et al.* (1989) noticed a positive trend of rainfall in several Amazonian stations, which lasted for 10 to 15 years, from the beginning of the 60s until the middle of 70s. There is no adequate explanation for these trends yet. One of the possible hypotheses is that the long term trends may be associated with higher frequency of SO positive phase (Anti-El Niño) events. In the interval 1961-76, in eleven out of sixteen years, the sea surface temperatures of the Central Pacific, between 90°W and 160°W, were below normal (Figure 6). Besides, during this period, the strongest ENSO event occurred in 1972, but in January 1983 the atmospheric circulation had changed already so that the 1972 ENSO event did not affect severely the rainy season as it was evidenced by the excess of precipitation recorded in some stations in Central Amazonia. As it was stated before, the SO positive phase is associated with

precipitation above normal in most of Amazonia. Another hypothesis is that long-term trends might be linked to the variation in heating the Andean Altiplano and the intensity of the high troposphere divergence (Bolivian High) due to the presence of volcanic aerosols in the stratosphere, as mentioned before. During the period 1963-74, higher than normal volcanic activity was observed in equatorial regions distant from Amazonia (see e.g. Handler and Andsager, 1990).

CONCLUDING REMARKS

Changes in rainfall due to man's action in modifying the landscape are controversial issues, mainly due to the difficulty in separating these changes from the natural ones. The effects on small scale apparently are better accepted. For example, it is said that extensive urbanization might have caused increase in rainfall due to enhanced surface aerodynamic roughness and the 'heat island' effect. Introduction of artificial lakes was estimated to have caused increments in rainfall up to 50% downwind, not because enlarged atmospheric moisture content due to evaporation but because of the establishment of an additional rain-producing mechanism, the lake breeze. The large-scale effects, however, have been taken with skepticism. For example, Soviet scientists claimed an increase of 1% to 2% in rainfall due to irrigation of an area of about half million square kilometres. These percentages are within the limits of raingauge detection.

In Amazonia, about half of precipitation depends on local evapotranspiration (Molion, 1975). A large-scale land use transformation, from tropical humid forests to crop or pasture fields, reduces evapotranspiration and, consequently, local rainfall. Climate simulation models (GCMs) were used recently to test the effects of deforestation on the local climate (Dickinson and Henderson-Sellers, 1988; Lean and Warrilow, 1989; Shukla *et al.*, 1990). The results suggested a 20% to 30% reduction in rainfall over the Basin. The evapotranspiration was reduced up to 50% in areas with high rainfall totals. Another important component of the hydrologic cycle, the total runoff, showed reductions between 10% to 20%. The GCMs results also implied that deforestation may change both the spatial and temporal distribution of hydrologic variables and increase the length of the dry season. In addition, reduction of infiltration due to soil compaction, decreases the water availability for crops, increasing the frequency of plant water stress.

Besides these direct effects, removing the forest protective canopy exposes the fragile soils to intense tropical rainfall increasing erosion significantly. Jannson (1982) revised the literature on tropical soil erosion and found erosion rates up to 334 metric tons of soil per hectare per year, that is, a layer of about one inch may be washed away every year. Erosion causes river channels silting, changes the water quality and the aquatic life.

The impacts that deforestation might have on the global climate are controversial issues and they were discussed in more details by Molion (1990). The reduction of rainfall due to deforestation decreases latent heat release in the Amazonian troposphere and, therefore, the power of the heat source. In principle, less heat would be available to be transported to extratropical regions, bringing changes to their present climate.

Some aspects described in this paper resulted from observational studies, others are speculative, due to the lack of more precise information and adequate tools for studying the changes. Considering the influence that Amazonia Forest and its hydrologic cycle might have on local as well

as global climates and the actual difficulty of isolating the anthropogenic effects from the natural climate variability, there is an urgent need to intensify the observational studies on forest-atmosphere interactions and modeling the possible changes that would occur due to large-scale deforestation, particularly the influence of Amazonia on remote extratropical climates.

ACKNOWLEDGEMENT

The author thanks Dr. Nelson de Jesus Ferreira his colleague at Instituto de Pesquisas Espaciais (INPE) for revising the text and for the suggestions to improve it.

REFERENCES

Cavalcanti, I. F. A. Um Estudo sobre Interações entre Sistemas de Circulação de Escala Sinoptica e Circulações Locais. Tese MSc, INPE 2494-TDL/097. São José dos Campos, São Paulo, Brazil, 1982.

Cohen, J. C. P.; da Silva Dias, M. A. F. e Nobre, C. A. Aspectos climatologicos das linhas de instabilidade na Amazonia. Climanalise, 4(11):34-40, CPTEC/INPE. São José dos Campos, São Paulo, Brazil, 1989.

De Luise, J. J.; Dutton, E. G.; Coulson, K. L.; DeFoor, T. E. e Mendonca, B. G. On some radiative features of the El Chichón volcanic stratospheric dust cloud and a cloud of unknown origin observed at Mauna Loa,. J. Geophys. Res. 88:6769, 1983.

Dickinson, R. E. e Henderson-Sellers, A. Modelling tropical deforestation: A study of GCM land-surface parameterization. Quart. J. Roy. Met. Soc., 114: 439-462, 1988.

Handler, P. e Andsager, K. Volcanic aerosols, El Niño and the Southern Oscillation. J. Climat. (in press), 1990.

Hastenrath, S. e Lamb, P. Climate Atlas of the Tropical Atlantic and Eastern Pacific Oceans. University of Wisconsin Press, Madison, WI, United States, 1977.

Jansson, M. B. Land Erosion by Water in Different Climates. UNGI Report 57. Department of Physical Geography, Uppsala University, Sweden, 1982.

Kayano, M. T. e Moura, A. D. O El Niño de 1982-83 e a precipitação sobre a America do Sul. Rev. Bras. Geofisica, 1987.

Kousky, V. E. e Kayano, M. T. A climatological study of the tropospheric circulation over the Amazon Region. Acta Amazonica, 11:743-758, 1981

Kousky, V. E.; Kayano, M. T. e Cavalcanti, I. F. A. A review of the southern oscillation: oceanic, atmospheric circulation changes and related rainfall anomalies. Tellus, 36A: 490-504, 1984.

Lean, J. e Warrilow, A. Simulation of the regional climatic impact of Amazon deforestation. Nature 342:411-413, 1989.

Molion, L. C. B. A Climatonomic Study of the Energy and Moisture Fluxes of Amazonas Basin with Consideration of Deforestation Effects. PhD Thesis, University of Wisconsin, Madison, WI, United States,1975.

Molion, L. C. B. Micrometeorology of an Amazonian Rainforest. In: The Geophysiology of Amazonia, R. E. Dickinson (Ed.): 255-270, UNU, John Wiley and Sons, 1987.

Molion, L. C. B. Amazonia: burning and global climate impacts. In: Proceedings of Chapman Conference on Global Biomass Burning: Atmospheric, climatic and biospheric implications. Williamsburg, VA (in press), 1990.

Molion, L. C. B. e Kousky, V. E. Climatologia da dinamica da troposfera tropical sobre a Amazonia. INPE-3560-RPE/480, São José dos Campos, São Paulo, Brazil, 1985.

Molion, L. C. B. e de Moraes, J. C. Oscilação Sul e descarga de rios na America do Sul Tropical. Rev. Bras. Eng., Caderno de Hidrologia, 5(1):53-63, 1987.

Molion, L. C. B.; Cavalcanti, I. F. A. e Ferreira, M. E. Influencia da circulação do Hemisferio Norte na precipitação pluviometrica da Amazonia: Um estudo de caso. Anais do V Simposio de Hidrologia e Recursos Hidricos, Salvador, BA, Brazil, 1987.

Molion, L. C. B. e Dallarosa, R. Pluviometria da Amazonia: são os dados confiaveis? Climanalise 5(3):40-42, CPTEC/INPE, São José dos Campos, São Paulo, Brazil, 1990.

Moura, A. D. e Shukla, J. On the dynamics of droughts in Northeast Brazil: Observations, theory and numerical experiment with a general circulation model. J. Atmos. Sci., 38:2653-2675, 1981.

Moura, A. D. e Kayano, M. T. Teleconnections between South America and Western Africa as revealed by monthly precipitation analysis. In: Proceedings of the First International Conference on Southern Hemisphere Meteorology, AMS, São José dos Campos, São Paulo, Brazil, 120-122, 1983.

Nobre, C. A. e Renno, N. O. Droughts and Floods in South America due to the 1982-83 ENSO Episode. In: Proceedings of the 16th Conference on Hurricanes and Tropical Meteorology, AMS, Houston, Texas, United States. 131-133, 1985.

Oliveira, A. S. Interações entre Sistemas Frontais na America do Sul e Convecção na Amazonia. Tese MSc, INPE 4008 TDL/239, São José dos Campos, São Paulo, Brazil, 1986.

Parmenter, F. C. A Southern Hemisphere cold front passage at the equator. Bull. Amer. Met. Soc., 57:1435-1440, 1976.

Rao, V. B. e Hada, K. Characteristics of rainfall over Brazil: Seasonal variations and connection with the Southern Oscillation. INPE 4432-PRE/1234, São José dos Campos, São Paulo, Brazil, 1987.

Ratisbona, L. R. The climate of Brazil. In: World Survey of Climatology, Vol. 12. Climates of Central and South America. W. Schwerdtfeger (Ed), Elsevier, Amsterdam, The Netherlands, 1976.

Rocha, H. R.; Nobre, C. A. e Barros, M. C. Variabilidade natural de longo prazo no ciclo hidrologico da Amazonia. Climanalise 4(12):36-42, CPTEC/INPE, São José dos Campos, São Paulo, Brazil, 1989.

Shukla, J.; Nobre, C. A. e Sellers, P. Amazon deforestation and climate change. Science, 247:1322-1325, 1990.

Shuttleworth, W. J. Evaporation from Amazonian rainforest. In: Proceedings Roy. Soc. Lond. B. 233:321-346, 1988.

Trewartha, G. T. The Earth's Problem Climates. University of Wisconsin Press, Madison, WI, United States, 1961.

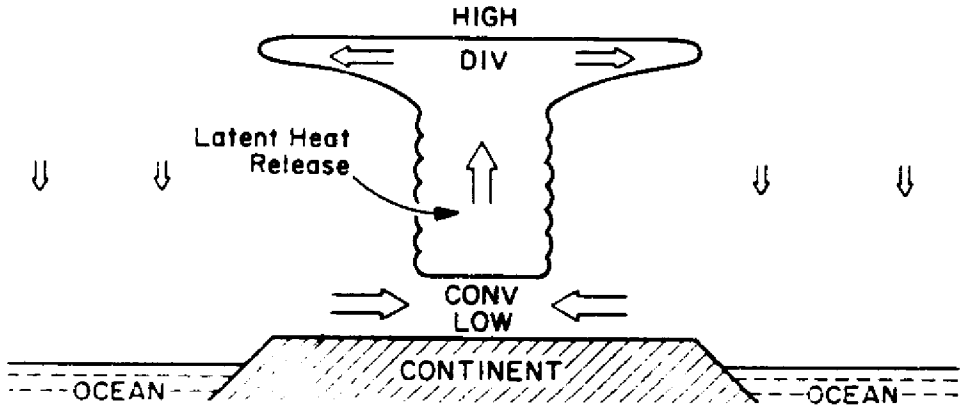

Figure 1 — Schematic representation of the circulation resulting from the differential heating between continent and oceans in the summer.

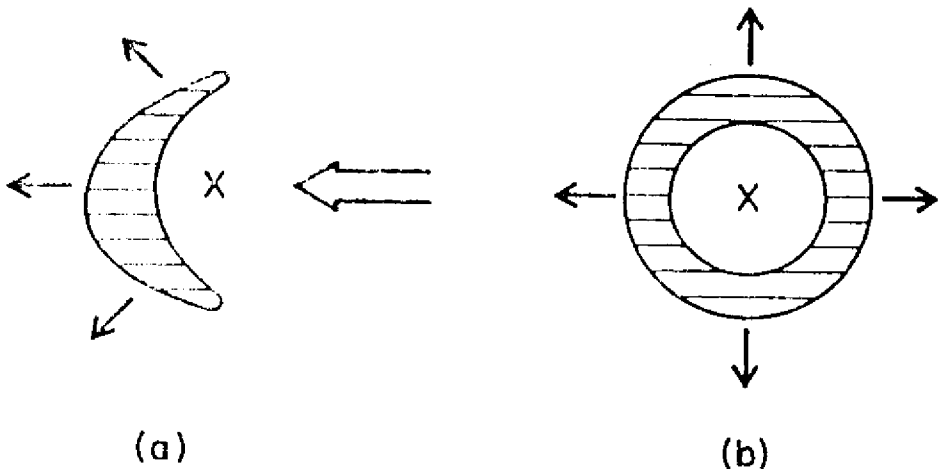

Figure 2 — Schematic diagram showing the formation of instability lines or Cb clusters

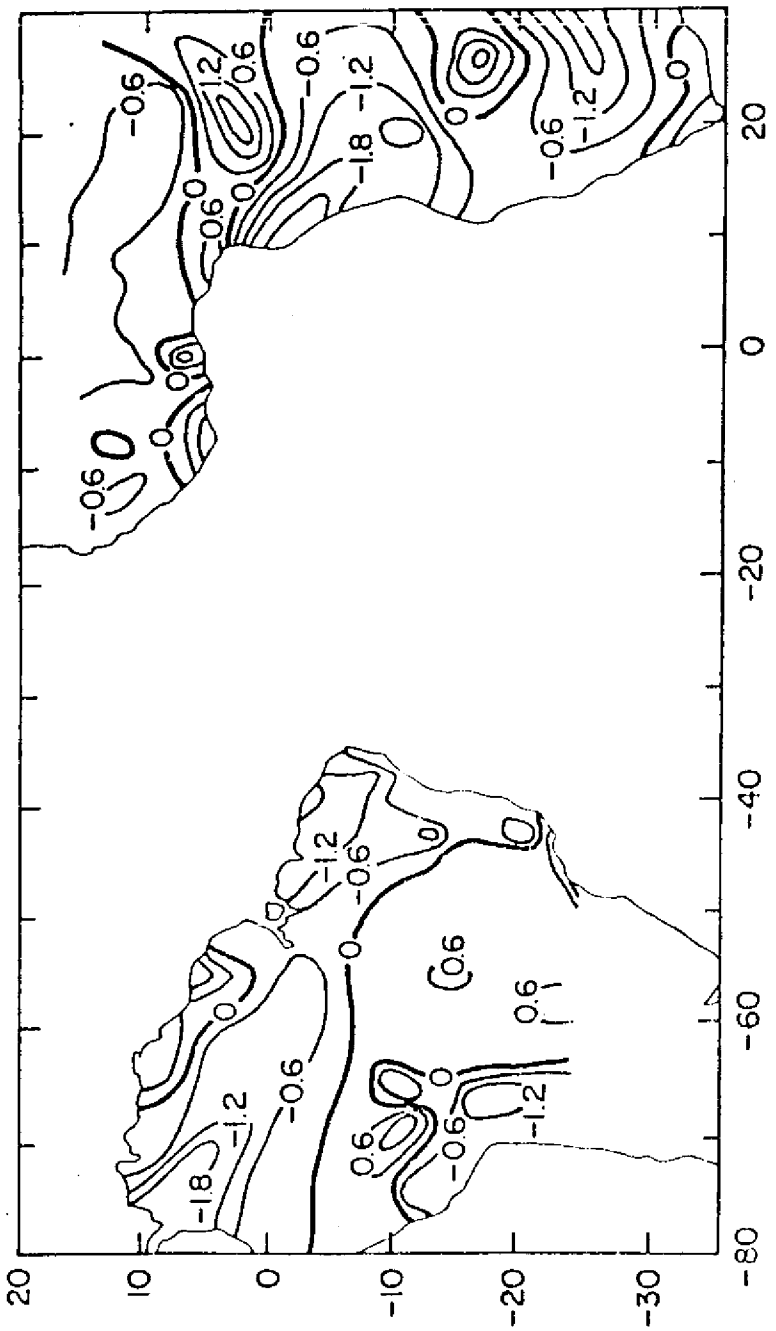

Figure 3 — Isolines of deviation of rainfall from the mean normalized by the standard deviation of the series. Period February-May 1958

Source: Kayano and Moura, 1983.

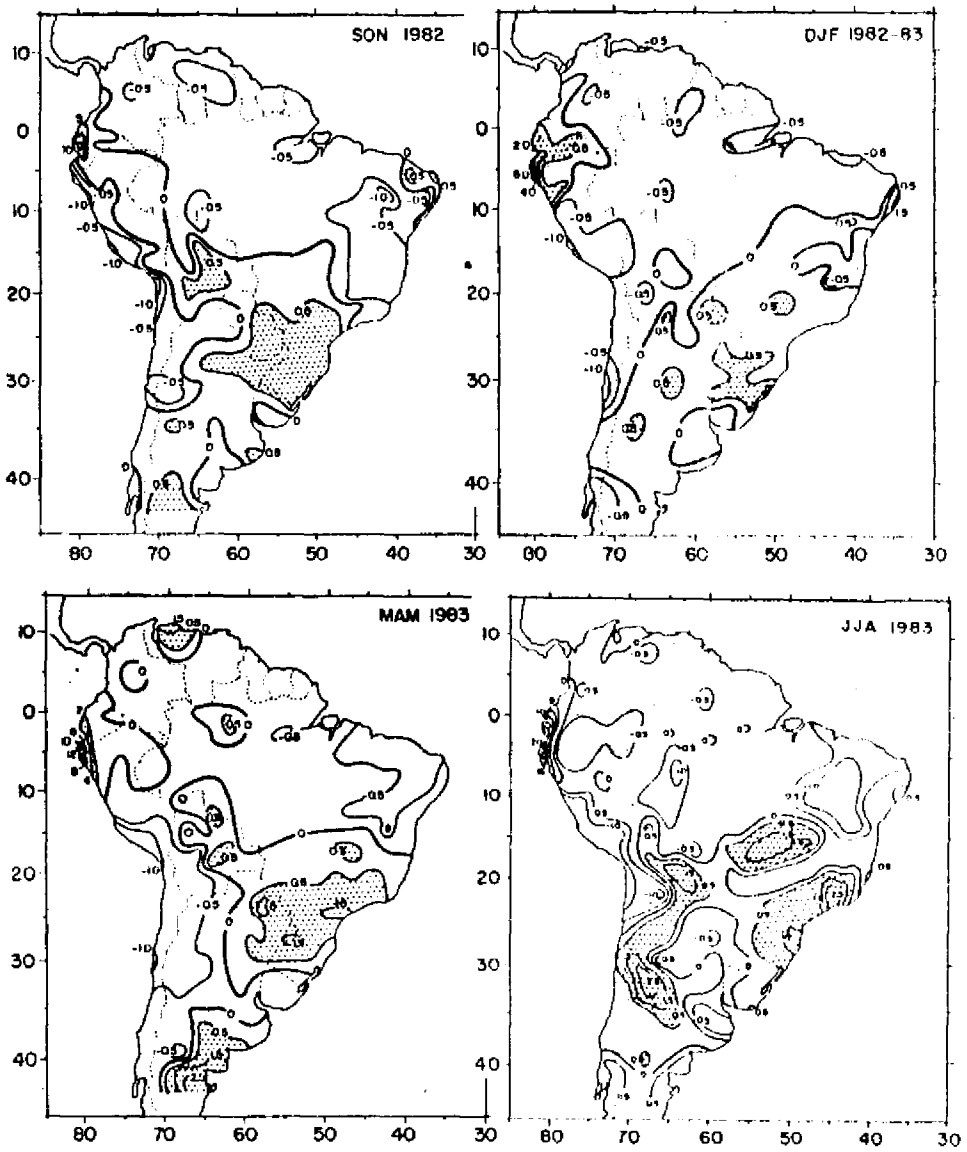

Figure 4 — Trimestral deviation of rainfall, normalized by the standard deviation, for the period September 1982 to August 1983

Source: Kayano and Moura, 1987.

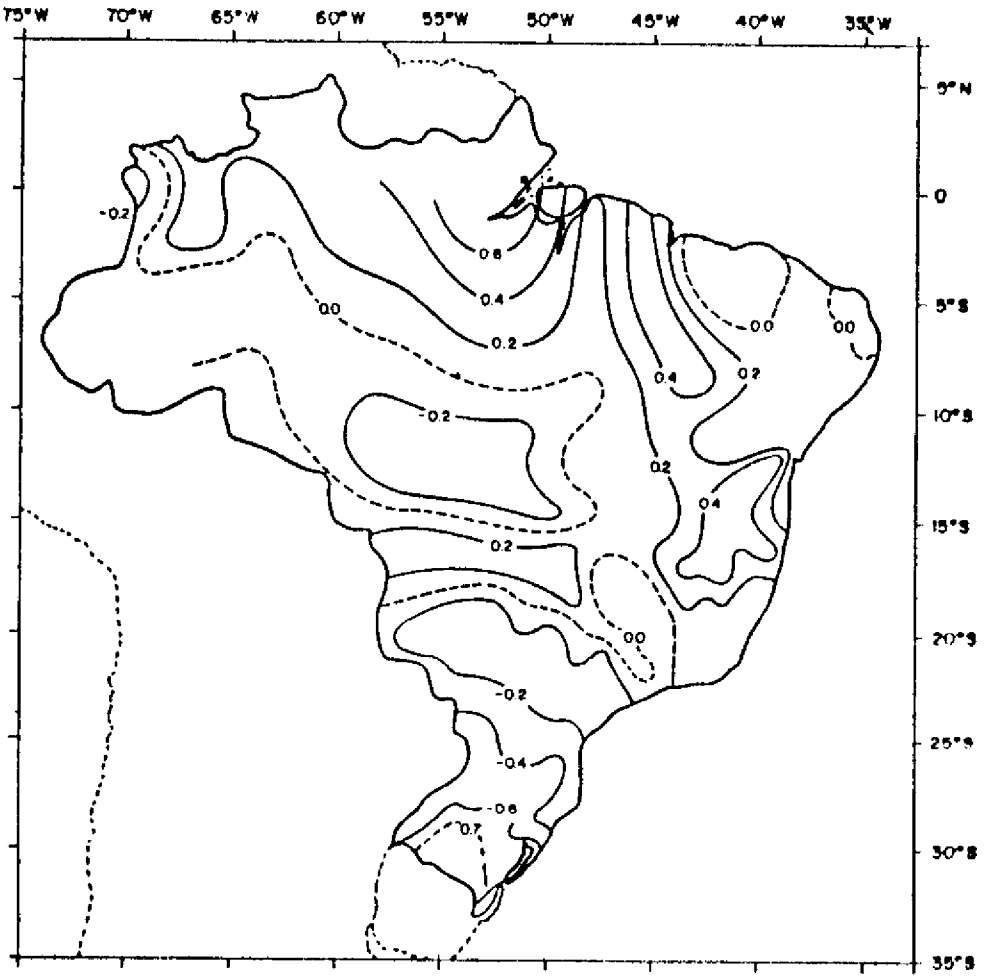

Figure 5 — Isolines of correlation coefficients between SOI and rainfall for Brazil, in the September-November trimester

Source: Rao and Hada, 1987.

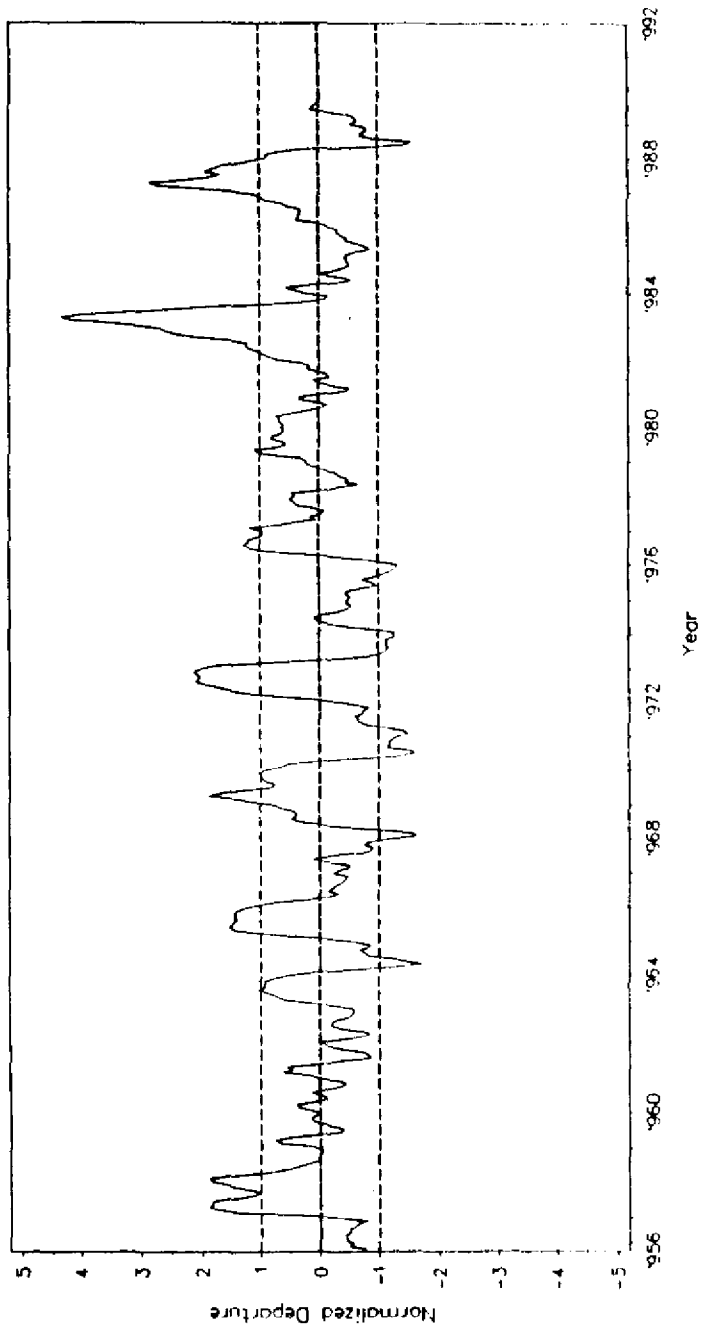

Figure 6 — Deviations of sea surface temperature from the mean, normalized by the standard deviation of the series for Region Niño 3 (90°W to 150°W). The positive (negative) deviations represent El Niño (Anti El Niño) events. The period covered is 1956 to 1989

Adapted from COADS, NOAA Environmental Research Laboratories, March 1990.

POST-DEFORESTATION AMAZONIAN CLIMATE: ANGLO-BRAZILIAN RESEARCH TO IMPROVE PREDICTION

W. James Shuttleworth, John H. C. Gash and John M. Roberts *
Carlos A. Nobre and Luiz C. B. Molion **
María de Nazare Goes Ribeiro ***

ABSTRACT

This paper reviews the experimental activity and primary results of the Amazon Region Micrometeorology Experiment (ARME), and the subsequent impact of these data in improving the prediction of post-deforestation Amazonian climate using General Circulation Models. It previews the new five year programme of collaborative Anglo-Brazilian research which will extend these studies by providing calibration of the land/atmosphere interaction for cleared forest areas, and measurements of the comparative near-surface climatology for large clearings and adjacent areas of undisturbed natural forest. Finally it overviews preliminary plans for a major international study in Amazonia under the World Climate Research Programme and the International Geosphere Biosphere Programme.

1. INTRODUCTION

The possible climatic effects of widescale clearance of tropical forests is a subject of global concern. Prediction of these effects can be made using General Circulation Models (GCMs) but credible predictions require that the models be calibrated against actual field data and their predictions tested against actual climate measurements. Experimental studies carried out near Manaus in Central Amazonia by the UK Institute of Hydrology, INPA and INPE, has improved the representation of the natural rainforest in GCMs and thereby significantly improved their ability to predict post-deforestation Amazonian climate. Future work will extend these experimental studies to give improved representation of cleared forest areas, and by providing actual comparative measurements of near surface climate above forest and adjacent large clearings at sites across the Amazon Basin. In addition, the World Climate Research Programme and the International Geosphere Biosphere Programme, envisage a collaborative international study focussed on a large area (approximately 100 x 100 km) which includes representative cleared and uncleared forest sites.

* *Institute of Hydrology, Wallingford, Oxfordshire, United Kingdom*

** *Instituto Nacional de Pesquisas Espaciais, São José dos Campos, São Paulo, Brazil*

*** *Instituto Nacional de Pesquisas Amazonas, Manaus, Amazonia, Brazil*

2. LAND SURFACE ENERGY BALANCE

The simple observation that climate within continents differs from that of the oceans demonstrates that surface processes influence weather. Moreover, GCM experiments have demonstrated two effects; firstly, that climate, as simulated in the models, is sensitive to large changes in surface properties, such as albedo, roughness and soil moisture [1, 2, 3]. Secondly, that water vapour and energy entering the atmosphere from the ground at one place, can travel large distances before returning to the surface elsewhere [4]. The implication is that changes in atmospheric processes, some generated by human activity on the ground, may have significant and possible detrimental consequences on the climate locally and perhaps at considerable distance.

The reason for such sensitivity is easily understood. Energy drives the atmosphere and it is changes in how and where it enters which cause the difference. Figure 1 illustrates this point. About 30% of the energy from the sun is immediately lost by reflection and some is absorbed in the air and clouds, but about half the original reaches the ground and because of this, our turbulent atmosphere is largely fuelled from below.

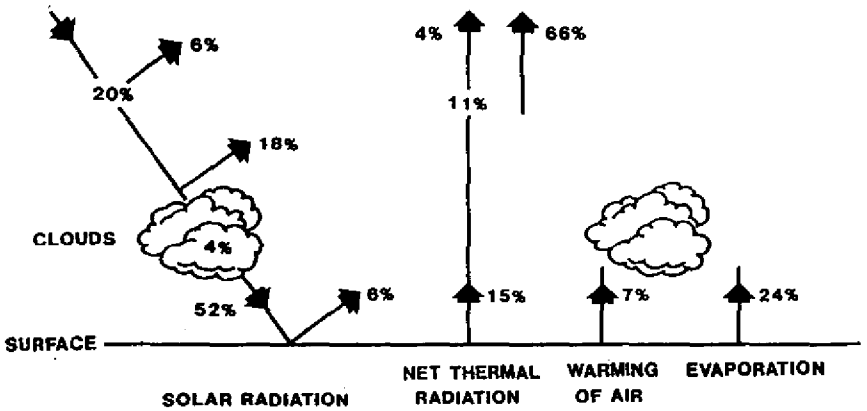

Figure 1 — The schematic diagram of components in the global energy balance

Most of this energy re-enters the air through evaporation, and the 'latent' heat stored in the water vapour can then be transferred over long distances before being released during rain. The energy used to warm the air directly, the so-called 'sensible heat', is only a third as big and is radiated to space more quickly. The remainder — about 50% of the incoming solar radiation — initially leaves the ground as thermal radiation but a great deal is reabsorbed to warm the atmosphere by about 30°C. This is mainly by interaction with water vapour but also with carbon dioxide, ozone and other so-called 'greenhouse gases.

There is a direct link between changes in surface cover and changes in climate because the vegetation covering the ground can directly alter the major inputs of energy/water to the atmosphere above. The size of the vegetation is important — the sun's rays penetrate more deeply into forest and are less likely to be reflected. Pasture or bare soil might well reflect twice as much. Trees also catch, and then re-evaporate, rain better and the wetted leaves dry quickly. Conversely, in dry periods they transpire less water from the soil through their leaves, but in long dry spells they flourish longer and, having deeper roots, lose water after smaller plants have withered and died.

It is certain that there will be some change in local, regional and perhaps even global climate following Amazonian deforestation. Controversy regarding the extent of such change will remain, however, until there is experimental data against which models can be calibrated and which can provide tests of their predictions.

3. THE AMAZON REGION MICROMETEOROLOGICAL EXPERIMENT (ARME)

At the present time, Amazonia largely remains an undisturbed tropical rainforest biome. This being the case, it is possible to make significant progress from a well instrumented single site study providing measurements are sustained for an extended period. Such a study was carried out in the early 1980s at the Reserva Ducke, near Manaus, this being an area of undisturbed forest located in central Amazonia. The experiment is summarized by Figure 2.

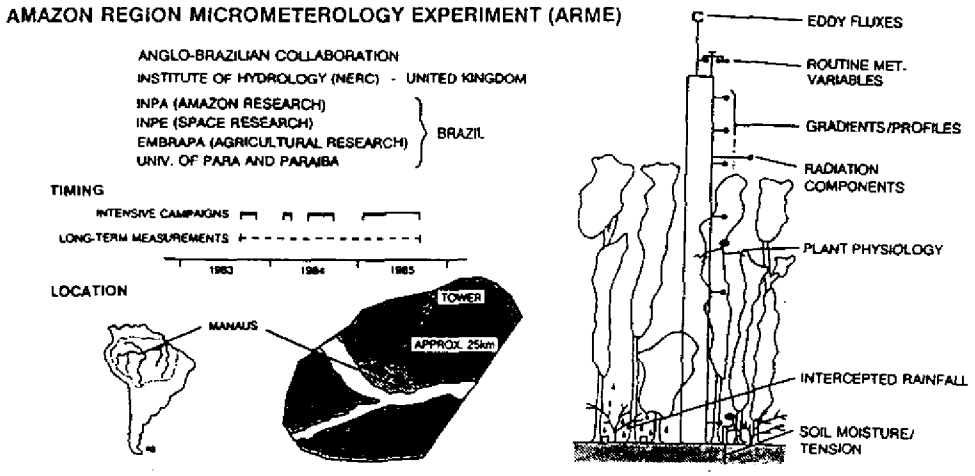

Figure 2 — Overview of the participants, timing, location and experimental systems for the Amazonian Region Micrometeorological Experiment (ARME)

3.1 ARME: Experimental Site and Systems

A 45m scaffolding tower was erected through and above the forest and the near-surface climate, the proportion of rainfall intercepted and subsequently re-evaporated from the canopy, and the soil moisture status were routinely monitored over a 25 month period. Additional measurements were made during four intensive field campaigns. During these campaigns, direct measurements were made of the surface energy exchange both as radiation and as sensible and latent heat, and measurements made to specify the aerodynamic characteristics of forest. The vertical gradients in atmospheric temperature, humidity and windspeed were measured above and through the canopy and detailed studies made on the trees themselves, using plant physiology techniques.

These data have now been used extensively to provide a detailed hydroclimatological description of the forest's interaction at this particular site and also to provide calibration of the best available land surface descriptions in GCMs.

3.2 ARME: Primary Local Results

Arguably the most important aspect of the land/atmosphere interaction for any natural surfaces the proportion of the incident energy from the sun which is adsorbed. The solar radiation reflection co-efficient, or albedo, measured during ARME demonstrated that the Amazon forest is similar to other tropical forests, and indeed forests around the world, in that only about 12% of incident solar radiation is reflected [5]. This is probably significantly less than that for some post-deforestation vegetation types and for bare soil.

A further important result was that the interception loss for the natural forest canopy is less than anticipated being typically 10-15%. Moreover, the experiment suggested that some previous measurements of the interception loss for tropical forests may be prone to significant experimental error. This is a consequence of the extreme spatial variability in the throughfall beneath rainforest. ARME clearly demonstrated that unless there is frequent random relocation of the collection gauges at regular intervals throughout data collection, very significant pseudo-statistical errors can arise, see Figure 3. As important is the possibility that previous investigators have tended to mistrust individual samples of measured throughfall, in their data if they were significantly higher than the average. In practice, such 'drip points' can and do occur giving preferential throughfall and any predisposition on behalf of experimentalists to ignore them will give rise to large and systematic errors in measured interception loss tending towards overestimation of this fraction.

Data from ARME also suggest that the lower portion of the natural forest canopy is in some measure decoupled from the atmosphere above. Figure 4 illustrates this point showing the measurement levels and the specific humidity deficit through the canopy. The temperature, humidity and the specific humidity deficit in the bottom of the canopy differ noticeably from those in the trees and atmosphere above. The specific humidity deficit near the ground is quite commonly only 30% of that in the atmosphere, and is less than this immediately after rainstorms [7].

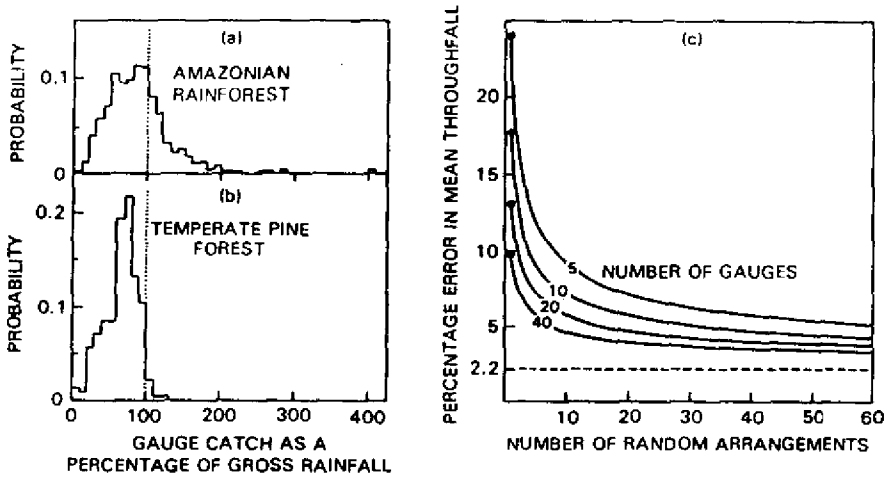

Figure 3 — Typical probability distributions for the throughfall measured at sample points beneath: (a) Amazonian rainforest and (b) temperate pine forest, illustrating the much enhanced spatial variability in rainforest measurements; (c) estimated percentage error in measured throughfall calculated from the probability distribution in (a) for measurements involving a specified number of gauges which are routinely and randomly relocated over a sample grid. Data taken from [6].

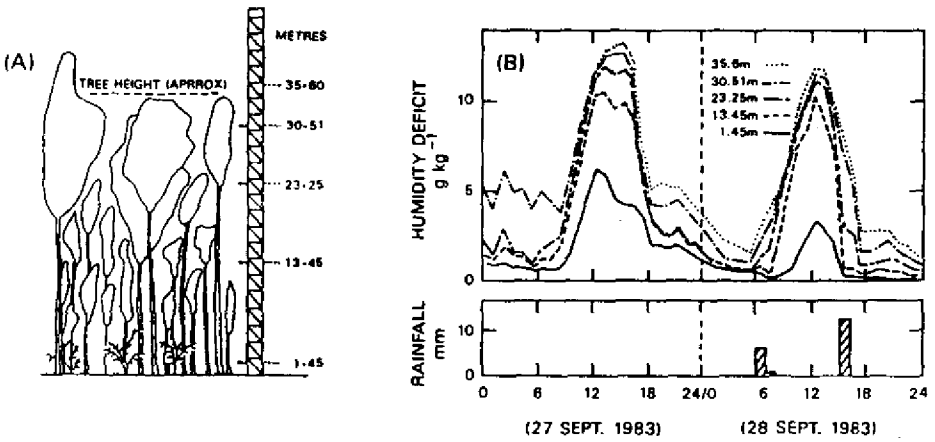

Figure 4 — (a) The heights at which temperature and humidity measurements were made during ARME. (b) The measured variation in specific humidity deficit at these several heights for two successive days. The first was fine while the second had rainstorms at 0600 and 1500 local time. Data taken from [7].

Using the data collected in ARME, it has been possible to build and calibrate a one-dimensional micrometeorological model of the forest/atmosphere interaction for the Reserva Ducke site, and then to use that model to synthesize the net water loss as evaporation at this location. The results are shown in Figure 5, which figure also demonstrates that the 25 month sample period was representative of a longer climatological average. The measured monthly precipitation through the experimental study is consistent with the precipitation pattern measured over a 16 year period at an adjacent climatological station. The calculated evaporation loss given by the calibrated micrometeorological model is therefore representative, and indicates a fairly uniform evaporation rate in the order of 110 mm per month. Over the whole study period it accounts for half of the incoming precipitation. The evaporation largely arises as transpiration: on average the loss due to evaporation of intercepted water is just 25%. About 90% of the measured incoming radiant energy is used for evaporation at this site [9].

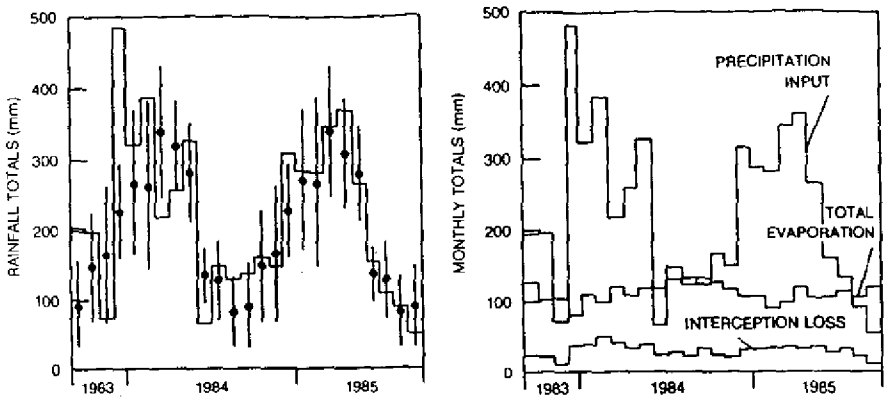

Figure 5 — (a) The monthly average rainfall measured during ARME in comparison with the mean and standard deviation in monthly rainfall over a 16 year period at an adjacent climatological site. (b) The monthly evaporation loss and interception component during ARME, in comparison with the measured precipitation input. Data taken from [8].

3.3 ARME: Impact on Climate Prediction

Perhaps the most significant result from ARME was that it showed that many of the then existing post-deforestation climate predictions had been made with models which were in significant error. In particular, GCMs which use a very simple land surface description, such as a 'bucket model', can dramatically overestimate the evaporation on dry days since they include no representation of the effect of stomatol control.

Figure 6 illustrates a comparison between the results given by a simple bucket model and those obtained with the Simple Biosphere (SiB) model after this last model had been calibrated against the ARME data. It is clear that not only are the surface exchange fluxes poorly represented, but there are ensuing consequences on the simulated near-surface climate. Such consequences necessarily occur because GCMs must preserve energy and mass conservation. In the example given, the near-surface temperature is badly simulated, being at least 2°C less than the actual values, with a reduced diurnal

cycle. There are associated weaknesses in the simulated development of the Planetary Boundary Layer (PBL). With a simple bucket model, the planetary boundary layer remains unrealistically low. With a more realistic description of surface exchange, there is a more realistic description of the diurnal growth in the PBL.

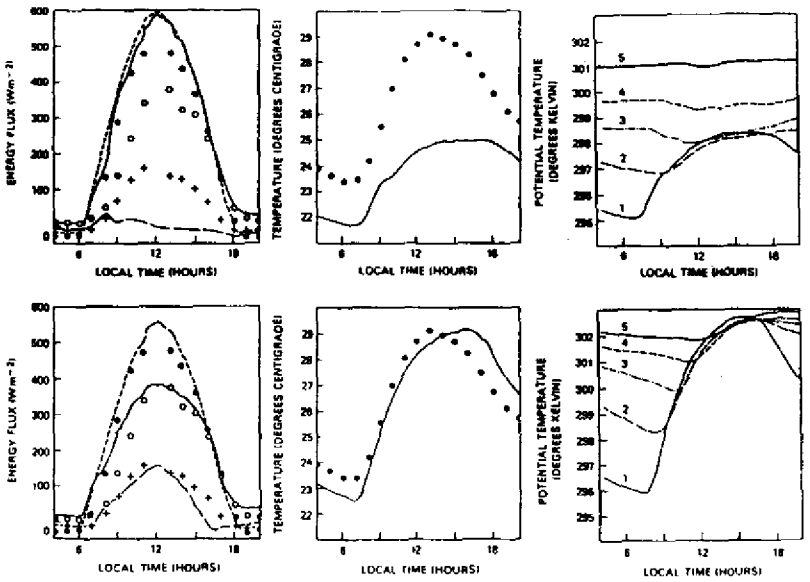

Figure 6 — Comparison between model simulations made with a simple bucket model of land/atmosphere interactions (top row) and those made with SiB (bottom row). Comparisons are against average field data measured for fine days and are made for surface-energy fluxes (left hand side), near-surface air temperature (centre), and air temperature at several levels (right hand side). Data are given as points, model simulations as lines. In the surface-energy diagram the full circles and hashed line are net radiation, the open circles and full line are evaporation, and crosses and broken line are sensible heat. Data taken from [9].

The ARME data has also been useful in demonstrating when other aspects of the GCM simulation required attention. Figure 7 shows the measured monthly average value of certain weather variables compared with simulated values given by NCAR's Community Climate Model (CCM) incorporating a realistic land surface description, the Biosphere Atmosphere Transfer Scheme (BATS), to represent the forest. The very large discrepancies shown have subsequently been identified as arising through weaknesses in the simulation of the extent and duration of convective cloud cover. There is considerable over-estimation of solar, and therefore net, radiation and an ensuing over-estimation in the evaporation. The enhancement in the simulated hydrological cycle then results in increased precipitation.

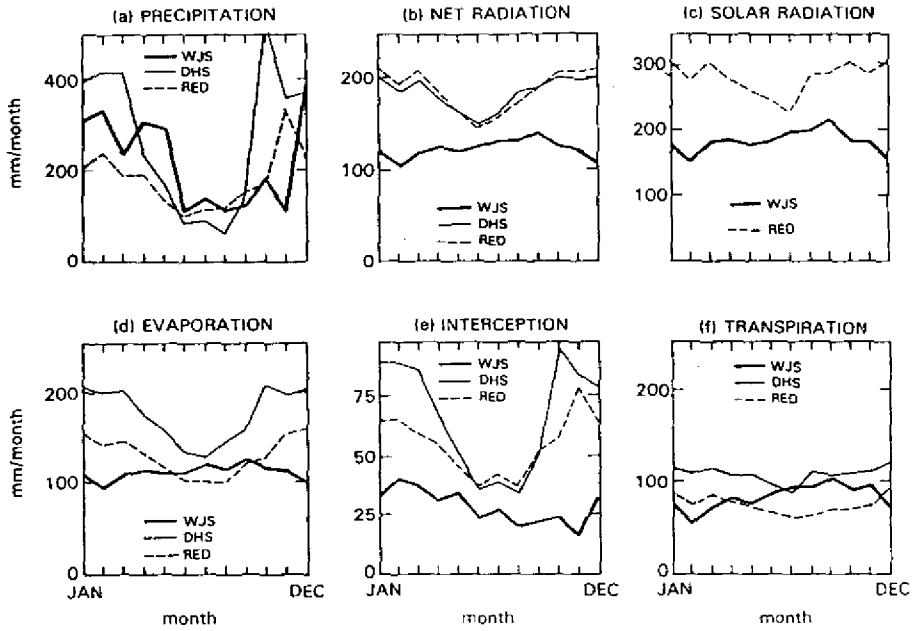

Figure 7 — Comparison for the variables shown between monthly average measured values from ARME (marked WJS) and equivalent values synthesized during two climate simulations (marked DHS and RED) using BATS in the NCAR Community Climate Model illustrating the consequences of poor simulation of convective cloud cover. Data taken from [10].

Once the data from ARME became available, it was possible to calibrate realistic land surface parameterization schemes, such as SiB and BATS, and a much improved simulation of the surface exchange was then possible. Figure 8 shows the level of agreement obtained for the SiB model after calibration.

The present generation of numerical experiments are therefore more realistic and more credible. Figure 9 shows the results of a good recent study of this type [12]. Current predictions are that evaporation will fall by 20% (+/- 10%) with deforestation, that air temperature will rise by 2°C (+/- 1°) and that precipitation will fall by 30% (+/- 20%).

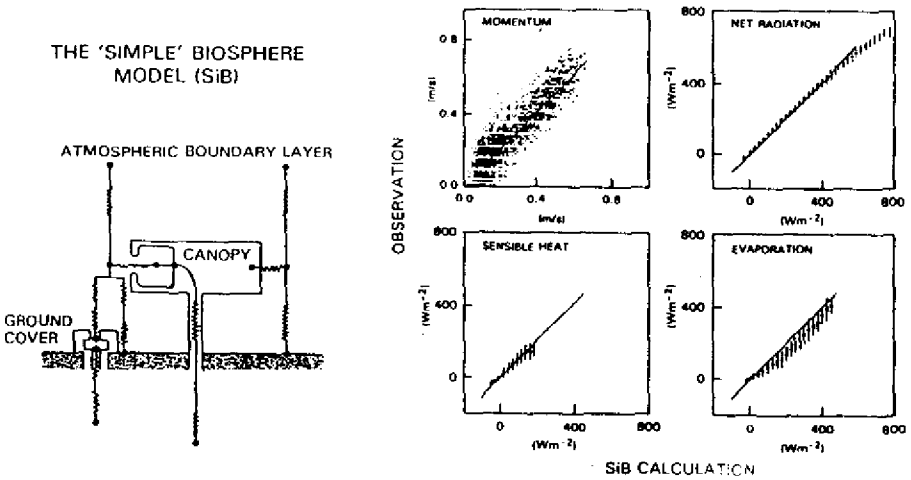

Figure 8 — Illustrating the satisfaction simulation of measurements given by SiB following its calibration against ARME data. Data taken from [11].

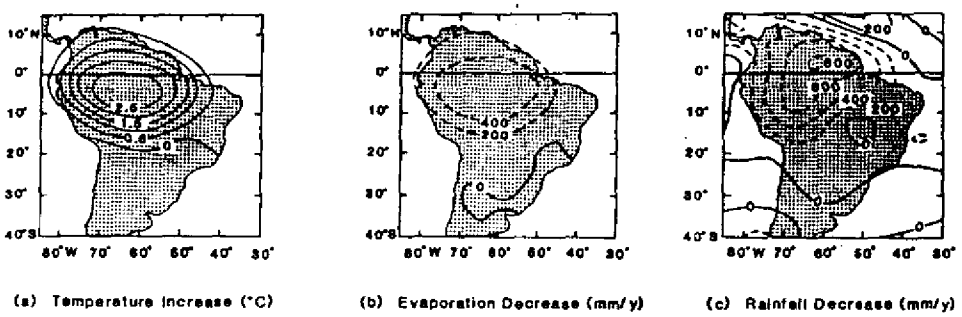

Figure 9 — Predictions of the change in post-deforestation Amazonian climate given by Shukla *et al.* [12] with a GCM which includes the SiB after calibration against ARME data.

4. FUTURE RESEARCH

In a recent review, Shuttleworth [13] defined a research agenda which progressively addresses the priority needs for climate-related, hydrological research in Amazonia. The programme envisages five experimental components: these would investigate:

(i) the atmospheric interaction of cleared forest;
(ii) the difference in near surface climate at adjacent cleared and uncleared sites
(iii) the effect of continental position on the atmospheric interaction of existing forest;
(iv) the aerial distribution of rainfall within Amazonian rainstorms;
(v) the interaction of a post-deforestation land surface with complex mixed cover.

In addition to these hydrological/meteorological priorities, which relate directly to the World Climate Research Programme, there is a clear need in the context of Amazonia to conduct research which addresses the better understanding and description of biogeochemical cycling, and the ecological response of the Amazonian biome to anthropic intervention, both direct intervention in the form of land use change and indirect intervention through the greenhouse effect. These latter priorities receive greater emphasis under the International Geosphere-Biosphere Programme.

4.1 The Anglo-Brazilian Amazonian Climate Observational Study (ABRACOS)

A shared interest in the likely climatic consequences of Amazonian deforestation has stimulated a new Anglo-Brazilian study which seeks to provide more accurate and more credible predictions. The project will address the need to provide data and understanding relevant to items (i) and (ii) in the research agenda defined above and some information relevant to item (iii). The project began in January 1990 with field studies timed to begin in September 1990. Figure 10 summarizes the proposed timing of the experimental activity and the proposed locations at which data will be collected.

The site selected for the intensive measurements of cleared forest interaction is the INPA/WWF study area approximately 80 km north of Manaus. This site was cleared approximately 10 years ago and now is heavily grazed pastureland littered with the still decaying trunks of forest trees. This site will be extensively instrumented with micrometeorological and climatological instrumentation and will also provide the focus for detailed studies of a plant physiological and soil physics nature. Routine monitoring of the near surface climate and soil moisture status will be maintained for at least three years, and will be supplemented by intensive micrometeorological and plant physiological studies carried out in five major missions. The timing of these missions will be selected to allow sampling through the annual precipitation cycle, but with a bias towards the dry season when the vegetation comes under most water stress.

Studies at this cleared site near Manaus will be complemented by further studies over the undisturbed forest at the existing Reserva Ducke site, and with long term climate monitoring both at Reserva Ducke and at an urban site in downtown Manaus. The purpose of this last study is to provide definitive evidence against which to evaluate the hypothesis that there is a systematic difference between the climate of riverside urban developments in Amazonia and that of adjacent forested areas..

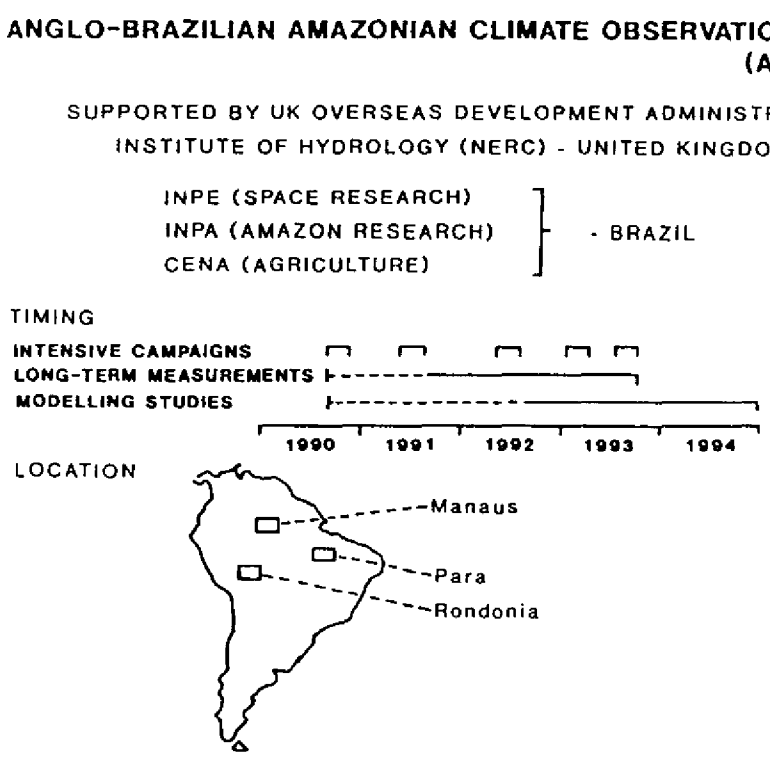

Figure 10 — Overview of the major participants, timing and locations for the Anglo-Brazilian Amazonian Climate Observational Study (ABRACOS)

The second objective of ABRACOS is to provide reliable long term measurements of near surface climate at the centre of large Amazonian clearings and compare these with similar measurements above adjacent uncleared forest areas. Such data will provide validation (or otherwise) of climate model predictions and will, in particular, check the ability of such models to describe ensuing changes in cloud cover. Changes in mesoscale convection and therefore in cloud cover are quite likely to occur with deforestation, and could significantly alter the possible consequences of the change in albedo. In order to test GCMs' ability to simulate a wide range of conditions, these 'paired sites' will be widely separated across the Amazon basin. One site will be in the east, most probably in the state of Pará — the second in the west, most probably in Rondonia. To ensure consistent data quality, the experiment will use remote data capture via satellite, thereby allowing rapid intervention if problems occur. There will be three receiving stations in Brazil and one in the United Kingdom. Figure 11 illustrates the methodology of this paired site study.

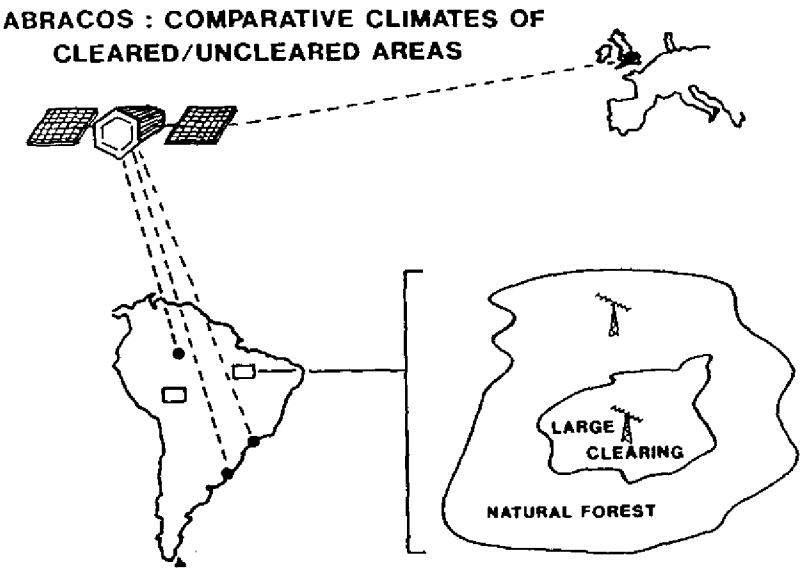

Figure 11 — Methodology and data collection and receiving centres for the ABRACOS 'Paired Site' studies.

An important aspect of ABRACOS is the effective use of these data to better the predictive ability of climate models. The study envisages not only the better definition and calibration of land surface schemes for cleared forest areas, but also the validation of meteorological models operating at both the mesoscale and the regional scale. Brazilian and UK modellers will therefore be actively involved in the research programme.

4.2 International Programmes

International activity in support of better prediction of post-deforestation Amazonian climate over the next decade is likely to occur as co-ordinated initiatives through the World Climate Research Programme, as part of the Global Energy and Watercycle EXperiment (GEWEX) and through the International Geosphere-Biosphere Project. Tentative plans exist for a major multinational experi-

ment to take place prior to the deployment of the Earth Observational System (EOS) in 1997. The outline format for such an experiment was proposed at a meeting of the Joint IGBP/WCRP Co-ordination Committee on Land Surface Experiments which was held in Wallingford, UK in January 1990.

Such an experiment would form part of the 'HAPEX' series and would therefore consider an area approximately 100 x 100 km. It is likely that this area would comprise mixed regions of cleared and uncleared forest. A network of climate stations with remote data capture would be established across and surrounding this study area and a rain radar system installed. It is envisaged that long-term data collection would be made from these systems and that this would be supplemented with routine collection of satellite data for the study area. At least one 'central site' would be established within the 100 km square, this site being a defined hydrological catchment. Long term data collection would be made, not only of hydrological variables, but also direct measurements of surface energy and trace gas transfer above the vegetation, and long term monitoring of ecological aspects of the vegetation itself.

In addition to the central site, other sites would be selected, representative of characteristics vegetation cover. These sites, typically 15-20 km square, would provide the focus of intensive activity during a major study period lasting at least one year. Focussed study would take place within this year as intensive field campaigns with data collection at several surface flux sites within each area, these being overflown by aircraft and boundary layer monitoring systems. Remote sensing data would be collected for each of these intensive study sites and validated against the available ground truth as a means of extrapolating within the 100 km square and beyond.

Clearly such experimental activity would only occur as a Brazilian-led initiative, and there are already plans amongst the Brazilian scientific community to stimulate international participation in a large scale study of this type. Outline plans suggest an early trial study in 1993, possibly centred around the ABRACOS Rondonia site, with the much more substantial experiment taking place in 1995/6.

4.3 Concluding Comments

Past study in Amazonia has demonstrated the value and utility of experimental data in providing enhanced and more credible predictions of post-deforestation climate. The new Anglo-Brazilian initiative which is just beginning will extend this process and yield better understanding of the likely consequences of large scale deforestation in the next five years. The more complex problem of providing prediction for mixed or partial development will necessitate the deployment of very substantial international resources. Preliminary plans exist to allow this.

Notwithstanding the need for more accurate and credible predictions, it is already clear that large scale deforestation which involves replacement of the existing forest with heavily grazed pastureland is very likely to give a significant change in local climate, and that this could propagate to the regional, and possibly even global, scale.

REFERENCES

[1] Charney, J. G.; Quirk, W. J.; Chow, S. H. and Kornfield, J. A comparative study of the effects of albedo change on drought in semi-arids regions. J. Atmos. Sci. 34, 1366-1388, 1977.

[2] Sud, Y. C.; Shukla, J. and Mintz, Y. Influence of land-surface roughness on atmospheric circulation and rainfall: a sensitivity experiment with a GCM. Tech. Mem. 86219, NASA/GSFC, Greenbelt, Md 20771, United States, 1985.

[3] Shukla, J. and Mintz, Y. Influence of land-surface evaporation on the earth's climate. Science, 215, 1498-1501, 1982.

[4] Eagleson, P. S. The emergence of global-scale hydrology. Water Resour. Res. 22(9), 6-14, 1986.

[5] Shuttleworth, W. J. Micrometeorology of temperate and tropical forest. Phil. Tran. R. Soc. Lond. B.324, 299-334, 1989.

[6] Lloyd, C. R. and Marques, A. de O. Spatial variability of throughfall and stemflow measurements in Amazonian rainforest. Agric. For. Meteorol., 42, 63-73, 1988.

[7] Shuttleworth, W. J.; Gash, J. H. C.; Lloyd, C. R.; Moore, C. J.; Roberts, J.; Marques A. de O.; Fisch, G.; Silva Filho, V. de P.; Ribeiro, M. N. G.; Molion, L. C.B.; Nobre, J. C.; de Sa, L. D. A.; Cabral, O. M.R.; Patel, S. R. and Moraes, J. C. Daily variations of temperature and humidity within and above Amazonian forest. Weather 40, 102-108, 1985.

[8] Shuttleworth, W. J. Evaporation from Amazonian rainforest. Proc. R. Soc. Lond. B.233, 321-346, 1988.

[9] Sato, N.; Sellers, P. J.; Randal, D. A.; Schneider, E. K.; Shukla, J.; Hoo, Y-T,; Kinter, J. L. and Albertazzi, E. The effects of implementing the Simple Biosphere Model (SiB) into a GCM. J. Atmos. Sci. 46, 2757-2782, 1989.

[10] Dickinson, R. E. Implications of tropical deforestation for climate: a comparison of model and observational descriptions of surface energy and hydrological balance. Phil. Tran. R. Soc. Lond., B 324, 339-347, 1989.

[11] Seller, P. J.; Shuttleworth, W. J.; Dorman, J. L.; Dalcher, A.; Roberts, J. M. Calibrating the Simple Biosphere Model for Amazonian tropical forest using field and remote sensing data. J. Appl. Met., 28(8), 1989.

[12] Shukla, J.; Nobre, C. and Sellers, P. Amazonian deforestation and climate change. Science, 247, 1322-1325, 1990.

[13] Shuttleworth, W. J. Priorities in Climate-related, hydrological research in Amazonia. Available as IH Report, Institute of Hydrology, OX10 8BB, UK.

Cataloguing:

Braga Jr., Benedito P. F. and
Fernández-Jáuregui, Carlos, edts.
Water management of the Amazon
basin. Montevideo: UNESCO-PHI, UNEP,
ABRH, 1991
288 p.
ISBN 92-9089-017-7
<HYDROLOGY> <WATER RESOURCES MANAGEMENT>
<AMAZON BASIN>

US$ 2.50.
FF 15.-